

University of Szeged  
Albert Szent-Györgyi Medical School  
Theoretical Medicine Doctoral School

**DEVELOPMENT OF NON-TRANSGENIC ANIMAL MODELS OF  
ALZHEIMER'S DISEASE AND INVESTIGATION OF DRUG  
CANDIDATES FOR ITS TREATMENT**

Ph.D. thesis

Emőke Borbély

Supervisor: Livia Fülöp Ph.D.  
Department of Medical Chemistry,  
Albert Szent-Györgyi Medical School,  
University of Szeged

Szeged  
2023

# 1 TABLE OF CONTENTS

1	TABLE OF CONTENTS .....	1
2	LIST OF PUBLICATIONS .....	3
3	ABBREVIATIONS .....	4
4	INTRODUCTION .....	5
4.1	General introduction .....	5
4.2	The AD pathology .....	6
4.3	The central role of medial temporal lobe structures in AD .....	10
4.4	Adult neurogenesis and neuroinflammation.....	11
4.5	Sigma receptors and modulators .....	12
4.6	Animal models and behavior tests in AD research .....	15
4.7	Drug research in AD.....	18
5	AIMS.....	21
6	MATERIALS AND METHODS .....	22
6.1	Animals.....	22
6.2	Synthesis of A $\beta$ <sub>1-42</sub> , and preparation of A $\beta$ <sub>1-42</sub> aggregates.....	22
6.3	Drug candidate (LPYFDa) synthesis.....	23
6.4	Surgery, solutions, and drug administration.....	23
6.5	General description of MWM .....	25
6.5.1	Fixed platform MWM .....	25
6.5.2	Modified MWM (mMWM) .....	26
6.6	Histological examination.....	26
6.7	Quantification of the data .....	28
6.8	Western Blot analysis .....	29
6.9	Statistical analysis .....	29
7	RESULTS .....	30
7.1	IHC experiment .....	30
7.1.1	Injection of fA $\beta$ <sub>1-42</sub> induced deficits of spatial learning and memory in MWM	30
7.1.2	Administration of fA $\beta$ <sub>1-42</sub> decreased dendritic spine density .....	31
7.2	EC experiment .....	32
7.2.1	OA $\beta$ <sub>1-42</sub> impaired, while LPYFDa improved the learning and memory functions when the smaller platform was used .....	32
7.2.2	LPYFDa hindered the oA $\beta$ <sub>1-42</sub> -induced neuroinflammatory processes in the rat brain .....	33

7.3	ICV experiment .....	35
7.3.1	Effects of PRE084 and DMT on adult neurogenesis in oA $\beta_{1-42}$ and vehicle-treated mice .....	35
7.3.1.1	OA $\beta_{1-42}$ and DMT impaired, while PRE084 promoted the survival of progenitor cells in DG. ....	35
7.3.1.2	OA $\beta_{1-42}$ and PRE084 increased the number of premature cells, while DMT did not affect their quantity. ....	36
7.3.1.3	The density of mature granule cells was unaffected by oA $\beta_{1-42}$ or PRE084 administration, while DMT induced a decrease in neuronal density. ....	37
7.3.2	Effects of PRE084 and DMT on neuroinflammation induced by oA $\beta_{1-42}$ .....	38
7.3.2.1	OA $\beta_{1-42}$ stimulated microglia activation, and neither PRE084 nor DMT alleviated this effect, while DMT alone significantly decreased microglial density. ...	38
7.3.2.2	OA $\beta_{1-42}$ stimulated astrocyte reactivation, while the administration of DMT or PRE084 reduced this effect. ....	39
7.3.3	S1R protein level was elevated by oA $\beta_{1-42}$ treatment, as well as by the co-administration of oA $\beta_{1-42}$ and PRE084 or DMT .....	40
8	DISCUSSION .....	41
8.1	Non-transgenic AD rodent models induced by the administration of exogenous A $\beta_{1-42}$ . ....	41
8.2	Application of the traditional and modified MWM protocols to model early symptoms of AD; behavioral and molecular outcomes .....	43
8.3	Neuroprotection with small molecular substances acting on different pathways .....	45
9	SUMMARY .....	48
10	ACKNOWLEDGEMENTS .....	49
11	REFERENCES .....	50
12	APPENDIX.....	66

## 2 LIST OF PUBLICATIONS

- I. **LPYFDa neutralizes amyloid-beta-induced memory impairment and toxicity.** Journal of Alzheimer's Disease 2010 Jan;19(3):991-1005.  
Ivica Granic, Marcelo F. Masman, Cornelius Mulder, Ingrid M. Nijholt, Pieter J.W. Naude, Ammerins de Haan, Emőke Borbély, Botond Penke, Paul G.M Luiten, Ulrich L.M. Eisel. (IF: 4,261)
  
- II. **Simultaneous Changes of Spatial Memory and Spine Density after Intrahippocampal Administration of Fibrillar A $\beta$ <sub>1-42</sub> to the Rat Brain.** BioMed Research International, 2014 June 23; Article ID 345305, doi:10.1155/2014/345305, Emőke Borbély, János Horváth, Szabina Furdan, Zsolt Bozsó, Botond Penke, and Lívía Fülöp (IF: 1,579)
  
- III. **Impact of two neuronal Sigma-1 receptor modulators, PRE084 and DMT, on neurogenesis and neuroinflammation in an A $\beta$ <sub>1-42</sub>-injected, wild-type mouse model of AD.** Int J Mol Sci. 2022 Feb 24;23(5):2514. doi: 10.3390/ijms23052514.  
Emőke Borbély, Viktória Varga, Titanilla Szögi, Ildikó Schuster, Zsolt Bozsó, Botond Penke, Lívía Fülöp (IF: 5,924)



### 3 ABBREVIATIONS

5-HT: 5-hydroxytryptamine	ICV: intracerebroventricular
Ab: antibody	IHC: intrahippocampal
AD: Alzheimer's disease	IP: intraperitoneal
AICD: APP intracellular domain	IRE1: inositol-requiring enzyme 1
ANOVA: one-way analysis of variance	LPYFDa: Leu-Pro-Tyr-Phe-Asp-amide
APP: amyloid precursor protein	MAM: mitochondria-associated ER-membrane
ATF6: activating transcription factor 6	mMWM: modified Morris water maze
A $\beta$ : beta-amyloid, amyloid- $\beta$	MTL: medial temporal lobe
BACE: $\beta$ -secretase	MWM: Morris water maze
BiP: binding immunoglobulin protein	NeuN: Neuronal Nuclei
BrdU: 5-Bromo-2'-Deoxyuridine	NFT: neurofibrillary tangle
CA: Ammon horn	NGS: normal goat serum
C83, 99: 83, 99 amino acid-long C-terminal fragment	NSAID: non-steroid anti-inflammatory drug
CNS: central nervous system	NSC: neuronal stem cell
DAB: 3,3'-diaminobenzidine	oA $\beta$ : oligomeric beta-amyloid
DCX: doublecortin	PBS: phosphate-buffered saline
DG: dentate gyrus	PERK: protein kinase R-like ER kinase
DHEA: dehydroepiandrosterone	PFA: paraformaldehyde
DMSO: dimethyl sulfoxide	PRE084: 2-(4-morpholinethyl)-1-phenyl cyclohexane carboxylate
DMT: N, N-dimethyltryptamine	PS1, 2: presenilin 1, 2
EC: entorhinal cortex	Q1-4: quadrant 1-4
ER: endoplasmic reticulum	ROI: regions of interest
FAD: familiar Alzheimer's disease	ROS: reactive oxygen species
fA $\beta$ : fibrillar amyloid-beta	SR: sigma receptor
GAPDH: glyceraldehyde 3-phosphate dehydrogenase	S1(2)R: sigma-1 (-2) receptor
GFAP: glial fibrillary acidic protein	SAD: sporadic Alzheimer's disease
HC: hippocampus	SGZ: subgranular zone
HFIP: 1,1,1,3,3,3-hexafluoro-2-propanol	UPR: unfolded protein response
iA $\beta$ : intracellular beta-amyloid	WB: Western Blot analysis
Iba1: ionized Ca <sup>2+</sup> -binding adapter molecule 1	

## 4 INTRODUCTION

### 4.1 General introduction

Alzheimer's disease (AD) is the most common type of neurodegenerative disease with wide clinical heterogeneity. It is characterized by deficits in the learning process, severe memory loss, language deterioration, executive and visuospatial dysfunction, as well as complex behavioral (personality and mood) changes such as apathy, agitation, anxiety, and depression [1-4]. AD affects about 35-40 million people worldwide, and it is the leading cause of death in Europe and America [5]. The number of AD patients increases with the growing life expectancy. AD has become one of the most important health and socioeconomic problems, recent studies predict 65 million AD diagnoses by 2030, and 107 million individuals will be presumably affected by 2050 [6].

AD is neuropathologically characterized by severe synaptic loss and the presence of misfolded proteins, forming aggregates in cerebral brain tissue, mainly in the neocortex and in the hippocampus (HC) [7, 8]. The extracellular amyloid plaques composed of  $\beta$ -amyloid ( $A\beta$ ) peptide, and the intracellular neurofibrillary tangles (NFTs) formed by abnormally hyperphosphorylated tau proteins were at first observed postmortem in 1906 by Alois Alzheimer [9-15]. The cerebral presence of these aggregates is considered the main pathological hallmark, and they are still required for the diagnosis of AD [9, 10, 16, 17].

There are two forms of AD: the dominantly inherited, early-onset or familial AD (FAD), which begins typically in the age of forties, and gives less than 5% of total cases, and the non-inherited, late-onset or sporadic AD (SAD), which begins in the age of sixties, being the most prevalent form of age-related dementia with 95% occurrence. FAD has been linked to autosomal dominant mutations in the amyloid precursor protein (APP), presenilin-1 (PS1), and presenilin-2 (PS2) [18]. More than 60 mutations have been identified in APP and around 400 in PSs ([www.alzforum.org/mutations](http://www.alzforum.org/mutations)). However, SAD is linked to other typical mutations, like apolipoprotein E epsilon4, Sortilin-related Receptor 1, Bridging Integrator 1, Clusterin, and Phosphatidylinositol Binding Clathrin Assembly Protein [19]. The principal risk factor of AD is age; the most endangered group is the over-65 population [12, 20]. Aside from age, there are other risk factors: family history with dementia, head injury, genetic factors, being female, vascular disease, untreated high blood pressure, and environmental factors such as stress [9]; their combination enhances the possibility for the development of AD. The clinical and histopathological symptoms of FAD are similar to those of SAD, and presumably, they share common pathomechanistic routes [21, 22].

Accumulation of A $\beta$  is initiated already two or three decades before the onset of neurological symptoms and the diagnosis of AD [22]. The appearance of A $\beta$  deposits is followed by elevated tau level in cerebrospinal fluid, significant brain atrophy, neuronal hypometabolism, and impaired memory function roughly 10-15 years before the expected onset of symptoms [22-26]. According to the results of basic and clinical research, therapeutic interventions may already be late in diagnosed AD patients to alleviate progression. Thus, in the pre-symptomatic stage, new, effective strategies and methods are desperately required to detect, prevent, and treat AD.

## 4.2 The AD pathology

AD was first identified more than 100 years ago, but the intensive research to reveal its basic biological causes and risk factors began only 40-45 years ago. Despite many years of research, the cause of AD is still unknown and there are no prophylaxis or curative treatments available [27]. To date, research is being conducted to clarify the etiology of the disease, so several hypotheses have been proposed to explain the pathomechanism of AD [15]. Some of the main hypotheses are discussed below.

The *cholinergic hypothesis* - created in the 1970s - claimed that degeneration of the cholinergic neurons and the damage of cholinergic neurotransmission in the cerebral cortex and in the HC contributed to the cognitive deficits found in AD patients [28, 29]. The aim of the researchers was, therefore, to increase the level of cholinergic neurotransmitters by cholinesterase inhibitors in order to reverse cognitive deterioration. Although nowadays first and second-generation cholinomimetics are available, these drugs are proven to be suitable only for symptomatic, palliative treatment [30, 31].

In the nineties, after the discovery of AD-associated autosomal dominant mutations in the APP, the  *$\beta$ -amyloid cascade hypothesis* was proposed by John Hardy which claimed that the accumulation of A $\beta$  is a crucial step in the development of AD [32]. APP is a highly conserved protein in different species, and it is expressed in the central nervous system (CNS). APP is a type 1 transmembrane protein with a long extracellular N-terminal and a short intracellular C-terminal domain. It has important physiological functions [33] and it is implicated in cellular processes (e.g., regulation of extracellular protease activity [34], regulation of Ca<sup>2+</sup> level, neuroprotective activities [35], cell growth, and synaptic plasticity [36]). In the so-called amyloidogenic pathway, the proteolytic cleavage of APP by  $\beta$ - (BACE) and  $\gamma$ -secretases results in the formation of A $\beta$  together with other fragments such as soluble APP $\beta$  (sAPP $\beta$ ) and the 99

amino acid-long C-terminal fragment (C99). By the action of  $\gamma$ -secretase on the intracellular part of the APP, another important fragment is formed, the APP intracellular domain (AICD). Only a minor portion of APP (~10%) is processed on this enzymatic pathway, resulting in a heterogeneous mixture of A $\beta$  peptides of different lengths, among which A $\beta_{1-42}$  and A $\beta_{1-40}$  are considered as the most common forms that constitute neuritic plaques in the specific brain regions. The A $\beta_{1-42}$  shows a higher tendency to form toxic assemblies than A $\beta_{1-40}$ . The neurotoxicity of A $\beta$  has been widely acknowledged but this peptide has also been found to regulate the synapses/post-synaptic function in picomolar concentrations, so its physiological role is still not clear [37, 38]. In the non-amyloidogenic pathway, the APP is cleaved by  $\alpha$ - and  $\gamma$ -secretases producing mainly soluble, non-toxic fragments, such as soluble APP $\alpha$  (sAPP $\alpha$ ), the 83 amino acid-long C-terminal fragment (C83), p3, and AICD. The imbalance between the two pathways, as well as between A $\beta$ -production and its clearance may initiate the pathogenic cascade of AD [17, 32, 33] (Fig. 1).

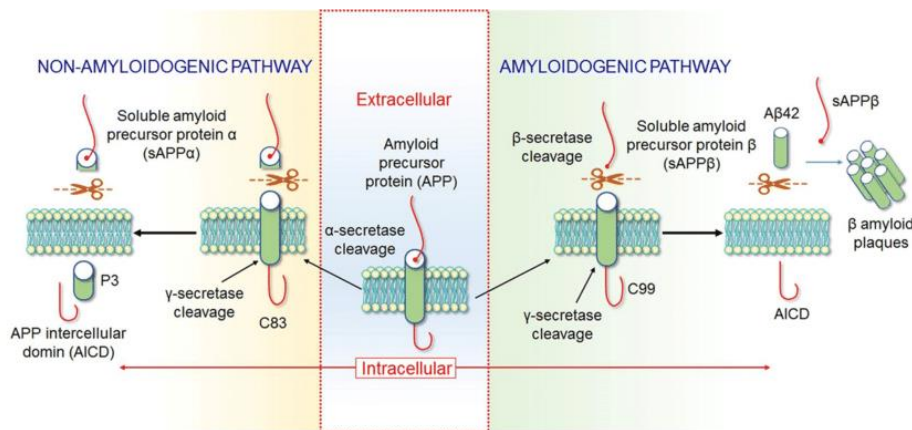


**Figure 1.** Schematic representation of the proteolytic cleavage of APP by  $\alpha$ - or  $\beta$ - and  $\gamma$ -secretases. In the non-amyloidogenic pathway, APP is cleaved by  $\alpha$ - and  $\gamma$ -secretase enzymes producing different fragments such as sAPP $\alpha$ , C83, AICD, and p3. In the amyloidogenic pathway,  $\beta$ - and  $\gamma$ -secretases cleave APP to release sAPP $\beta$ , C99, A $\beta_{1-40}$ , A $\beta_{1-42}$ , and AICD. The image is taken from Ref. [39].

The native peptides produced in the amyloidogenic pathway can misfold by various triggers (e.g., increased temperature, mechanical stress, extreme pH, oxidative stress, glycation, or mutation), which initiate conformational changes. As soon as the misfolded proteins reach a critical concentration, oligomers, then protofibrils, and finally mature fibrils form extracellularly. During this process, the extracellular fibrillar A $\beta$  (fA $\beta$ ) peptide accumulates into plaques which were assumed to be the cause of dementia for a long time. However, analysis of postmortem human brain samples (healthy controls, patients with mild cognitive impairments, and also diagnosed AD cases) has revealed by now, that there is no significant

link between the number of amyloid plaques and the loss of cognitive functions [17], suggesting that the extracellular amyloid deposits alone cannot be responsible for all AD pathologies and symptoms. In 2002, the  $\beta$ -amyloid cascade hypothesis was significantly revised [40, 41]. According to this, besides the extracellular fA $\beta$ , soluble oligomer forms of A $\beta$  (oA $\beta$ ) and protofibrils were also found capable to exert neurotoxicity [41, 42]. The neuronal receptors can bind oA $\beta$  extracellularly, which can initiate aberrant signaling pathways [43-45]. In 2007, it was proposed that A $\beta$  can be formed intracellularly (iA $\beta$ ), and it can accumulate in subcellular organelles (e.g., mitochondria, endoplasmic reticulum (ER), trans-Golgi network, lysosomes, endosomes) [15, 46]. Moreover, the subcellular presence of iA $\beta$  can cause dysregulation and dysfunction of Ca<sup>2+</sup> homeostasis and ER stress, which initiate a series of biological events called ‘unfolded protein response’ (UPR) [47-49].

Many experiments have proved that both the fA $\beta$  and the oA $\beta$  can be synapto- and neurotoxic, activate neuroinflammation, and induce tau-hyperphosphorylation [50-54]. Nowadays it is accepted that A $\beta$  is accumulated both intra- and extracellularly and the two pools have a dynamic connection [15]. Recent results have demonstrated that instead of the extracellular amyloid forms, the amount of iA $\beta$  correlates well with memory declines [15, 55], and synapse damage [56, 57]. Synaptotoxic soluble A $\beta$  oligomers inhibit long-term potentiation of the neurons, thereby influencing memory consolidation [58].

The *tau hypothesis* states that abnormal phosphorylation (hyperphosphorylation) of the tau protein initiates AD pathology by disrupting the microtubule function in the cells so that axonal transport collapses and abnormal synaptic processes can take place [59-61]. Physiologically, tau supports the assembly of tubulin into microtubules to promote the normal structure of the cytoskeletal system, and consequently the morphology of the neurons. To determine the degree of AD, the Braak-staging is used which is based on the localization of NFTs (tau deposits) in the brain structure [11] but this characterization does not always reflect the severity of the disease [62]. Nonetheless, the inhibition of hyperphosphorylated tau seems to be a reliable therapeutic target. Still, currently, there are no clinical studies with successful results in this field [63]. Taking these facts together with the revision of the  $\beta$ -amyloid cascade hypothesis by Hardy and Selkoe, it seems more feasible that A $\beta$  is the synaptotoxic initiator, and tau has only a secondary role. [40, 64].

The *vascular hypothesis* of AD was proposed in the mid-1990s. Vascular risk factors can induce neurovascular impairments and cause endothelial damage by oxidative stress and neuroinflammation, leading to local, cerebral hypoperfusion and ischemia. In this case,

increased A $\beta$  production and reduced A $\beta$  clearance can be observed resulting in the excessive formation of neuritic plaques, and cerebral amyloid angiopathy. The vascular changes are thought to be responsible for cognitive decline and dementia [65-67]. The hypothesis is further strengthened by the finding, that disturbed cerebral blood flow can serve as an important biomarker for the prediction of AD [68].

According to the *inflammation hypothesis*, hyperreactive astrocytes and activated microglia play a key role in AD. Neuroinflammation in CNS is the result of the activation of the immune system as a protective reaction to injuries, infections, and neurodegeneration. One of the most important pathological hallmarks of AD is neuroinflammation, which manifests in the activation of various inflammatory processes involving immune cells, cytokines, and chemokines. Increasing evidence suggests that non-steroid anti-inflammatory drugs (NSAIDs) may alleviate the development of AD. These compounds have an impact not only on the cyclooxygenase system but on the modulation of APP processing as well, whereby A $\beta$  production may be inhibited. Clinical trials were carried out with NSAIDs, but the results remain conflicting [69, 70].

Neurodegenerative diseases, including AD, Parkinson's, and Huntington's disease belong to the family of protein misfolding and protein homeostasis (proteostasis) imbalance diseases, which are characterized by intracellular and/or extracellular misfolded protein aggregates [71]. Factors, like glucose starvation, impairment of intracellular Ca<sup>2+</sup> homeostasis, and failure in protein synthesis, secretion, transport, and degradation can cause ER stress which leads to UPR [72]. An upregulation of proteins involved in the ER stress can be detected postmortem in the AD brain tissue [72]. In mammals, the canonical UPR pathway has three branches, representing key transmembrane proteins: inositol-requiring enzyme 1 (IRE1), protein kinase R-like ER kinase (PERK), and activating transcription factor 6 (ATF6), as proximal stress sensors [73]. If ER stress is prolonged, and cannot be restored, and the misfolded proteins cannot be degraded by common cellular quality control mechanisms, then the UPR may turn into the induction of apoptotic cell death. Maladaptive UPR and ER stress could be reliable therapeutic targets for the treatment of AD [74].

Among several membrane-bound organelles that interact with ER, the membrane connection between ER and mitochondria (so-called mitochondria-associated ER-membrane, MAM) is extensively studied and well-characterized [75]. Several proteins, like APP, PS1-2, and the sigma-1 receptor (S1R), the dysfunction of which is associated with neurodegeneration, are also located in MAM [76, 77]. The altered ER-mitochondria contacts have been proved in both FAD and SAD. The *MAM hypothesis* proposed that the disturbed MAM functions are responsible for

the development of AD [78]. Based on recent results, the utilization of MAM modulators has therapeutic opportunities in this field [76, 78, 79].

Besides the aforementioned hypotheses, several other theories exist, which would explain the origin of AD, such as  $\text{Ca}^{2+}$ -influx into neurons, cell cycle, estrogen, metal ions, lymphatic system, dual pathway [80],  $\alpha$ -Synuclein, free radicals-oxidative stress, autoimmune origin [65], microorganism, microRNA, and prion/prionoid hypotheses [46, 69, 81]. All theories are interconnected and overlapping, using common crucial cellular signaling pathways. Every hypothesis has been proposed to explain the origin of the pathology but none of them can account for every detail of AD. However, for effective therapy, it would be important to identify the starting/most toxic molecular factor(s) in AD. It is very probable, that  $\text{A}\beta$  still plays key roles in the development of AD.

### **4.3 The central role of medial temporal lobe structures in AD**

The medial temporal lobe (MTL) structure, which includes a system of anatomically related areas that are responsible for mnemonic function [82], is the primarily affected brain region in AD [11]. The parts of the MTL are the hippocampal formation (dentate gyrus, DG), HC proper, the subicular complex, and the adjacent cortices [83, 84]. The HC is located medially and ventrally in the inferior part of the lateral ventricle in humans (in rodents, the HC is located dorsally). The HC contains two interlocking parts: the outer domain is the CA region (or Ammon horn CA1, CA2, CA3); and the inner part is DG. The unidirectional transverse loop of excitatory pathways through the DG, CA3, CA1, and subiculum is typical for HC [85]. The pyramidal cell bodies of the 2 major parts of Ammon horn (CA1, CA3) constitute a single continuous layer, the stratum pyramidale. The unique, specialized granule cells of DG can be also located in a separate layer. The dendrites of granule cells project to the molecular layer of DG and constitute synapses with the neurons of the entorhinal cortex (EC). Their axons (mossy fibers) terminate on hilar cells and apical dendrites of neurons of CA3. The collaterals of axons of CA3 pyramidal cells (Schaffer collateral) converge on CA1 pyramidal cells. These collaterals can form synapses at several points of the dendrites of pyramidal cells in CA1. The CA1 pyramidal cells connect to cells of the subicular complex and have projections towards neurons of EC. HC receives inputs from all neocortical sensory regions through the EC, and efferent fibers of HC connect to the neocortex via the subiculum and EC [86]. The perforant pathway, one of the major afferents of HC provides a connection route from entorhinal neurons to granule cells and pyramidal cells of CA3 or CA1. These axons of the perforant pathway are able to terminate not only on the dendritic spines of pyramidal cells to form asymmetrical,

excitatory synapses but also on dendritic spines of inhibitory interneurons [87, 88]. Together the perforant pathway from EC, the mossy fibers, and the Schaffer collateral constitute the glutamatergic, excitatory trisynaptic loop, which is a characteristic feature of the HC.

Generally, most of the synapses are formed on dendritic spines. Dendritic spines are cellular compartments containing the molecular machinery important for synaptic transmission and plasticity [89]. Interestingly, each pyramidal cell of CA1 has only one excitatory synapse while in many brain regions, the spines have two inputs: excitatory and inhibitory ones. In pyramidal neurons of the HC, there is an almost one-to-one relationship between the numbers of dendritic spines and excitatory synapses [89, 90]. The strength, stability, and function of the excitatory synaptic connections constitute the basis of cognitive functions [91]. The progressive loss of dendritic spines and the presence of dystrophic neurites have been reported with aging as well in AD-affected human brain [91-94] and in transgenic mouse models [95, 96], as a hallmark of cognitive decline [1, 97].

At the cellular level, the place cells of HC mediate the allocentric navigation, and form neural spatial maps; moreover, they re-map the place field (update neural spatial maps) in the environment. The place, grid, head direction, and border cells of EC are connected to HC, and they form a system that is able to map the environment with considerable accuracy [98, 99]. These abovementioned cells are collectively responsible for spatial navigation, which is dramatically impaired in AD. The dysfunction or loss of hippocampal and entorhinal cells has been reported in different mouse models of AD [58, 100, 101]. It is proved that the earliest pathological changes typical for AD arise in HC-EC circuits, so these brain structures were targeted with our A $\beta$ -injection experiments.

#### **4.4 Adult neurogenesis and neuroinflammation**

In mammals, new neurons and glial cells continue to be generated throughout life. In adulthood, neurogenesis is derived via mitosis from neuronal stem cells (NSCs). NSCs, which are located in the subgranular zone (SGZ) of the DG in the HC, and the subventricular region of the lateral ventricles, generate neuronal progenitor cells [102-107]. An optimal microenvironment is essential for the division, differentiation, migration, and maturation of NSCs.

After differentiation and migration of the type 2A-B, 3, and immature cells, the newly formed mature granule neurons can integrate into local neuronal circuits of the HC; thus, they might have a significant role in plasticity, cognitive functions, learning, and memory processes [108]. Both extrinsic (stress, aging) and intrinsic (signal transduction pathways, epigenetic modulators, immune system) modulators can influence the whole process of neurogenesis [107-



113]. Physiologically, the activity of adult hippocampal neurogenesis decreases with aging, leading to a usually mild, age-associated cognitive decline [111, 114-117]. However, the results are mainly based on studies conducted with animal models. Because of the problems, which arise upon detecting human neurogenesis processes *in vivo*, it is debated, if the findings are translatable to the human case [118]. Still, the decline of adult neurogenesis in the aging human brain could be detected with careful experimental planning and methodical considerations [119]. It was also proven, that the extent of adult neurogenesis is diminished in the early stages of AD, even before the appearance of senile plaques [115, 120-122]. The findings suggest that the stimulation of neurogenesis might serve as a promising therapeutic target to improve cognitive functions and promote neural adaptability, whereby it might prevent or even treat AD. In recent decades, besides A $\beta$  and NFTs, neuroinflammation has been identified as a third neuropathological hallmark of AD [123, 124]. The neuroinflammatory changes associated with AD have been observed in animal models [125], postmortem human brain tissue [126], and in *in vivo* molecular imaging [127]. Studies have demonstrated that activated microglia or astrocytes that release proinflammatory cytokines and chemokines, support neuroinflammation and they also negatively impact the proliferation and differentiation of NSCs [115, 128-130]. In the early phase, activated microglia and hyperreactive astrocytes probably slow down the progression of the disease by clustering around the plaques and thus exerting a protective effect against the neurotoxic A $\beta$  forms. In later stages of AD, uncontrolled neuroinflammation might enhance A $\beta$  production and plaque formation and it could also be detrimental to adult neurogenesis that may contribute to the onset of more severe neurological symptoms [115, 131]. Therefore, it is hypothesized that reduction of neuroinflammation, possibly together with an intensive stimulation of hippocampal neurogenesis could slow down the decline of cognitive skills in AD.

#### **4.5 Sigma receptors and modulators**

Sigma receptors (SRs) are unique transmembrane proteins, acting as intracellular receptors with chaperone protein functions. Two subtypes of SRs exist, the S1R and SR2 [132-134]. S1R is broadly expressed in the CNS, especially in the DG region of the HC, both in neurons and glial cells. S1Rs are mainly located in the MAM where the ER and the mitochondria establish a tight interplay [76, 135-138].

Without agonists or any other activating stimulus (e.g., cellular stress), the inactive form of S1R binds to the binding immunoglobulin protein (BiP), which initiates the oligomerization of S1R to form low-n oligomers. When the receptor is activated, monomers dissociate from the BiP-

S1R oligomer complex and translocate to various cellular components, such as the cytoplasm, the cell membrane, and the nucleus, where they bind to target proteins and induce a cellular response [136, 138, 139].

S1R, as a pluripotent modulator, can interfere with different ion channels, G-protein coupled receptors (e.g., opioid, dopaminergic receptor, and corticotropin-releasing factor), and cell-signaling molecules, thus it participates in numerous physiological and pharmacological processes [140, 141]. For example, this receptor is thought to play an important role in the modulation of intracellular  $\text{Ca}^{2+}$  levels or in the regulation of phosphorylation of IRE1 [76, 140]. S1R modulates the UPR pathways as its overexpression enhances neuronal survival by decreasing the activation of PERK and ATF6. The low activity of the receptor causes conformational changes in IRE1 and impairs cell survival [76]. The activation of S1R can promote protection from ER stress by defeating reactive oxygen species (ROS) while the low activity of S1R may lead to apoptosis [138, 142]. Besides the neuroprotective role of S1R agonists, peripheral cytoprotective effects of the S1R agonists could also be observed in ischemic hepatocytes and hypertrophic cardiocytes [140, 143]. S1R is known to influence neurite outgrowth, proliferation, plasticity, as well as learning and memory functions [143-147]. Many S1R agonists (sertraline, fluvoxamine, dipentylammonium) improved the nerve growth factor-induced neurite outgrowth in different cell lines [140]. In pathological conditions, e.g., in  $\text{A}\beta$ -induced AD animal models or in neuroblastoma cell lines, the activation of S1R can attenuate ROS production and ameliorate cognitive functions [146-148]. Furthermore, S1R may be essential for modulating neurogenesis in adulthood, which has been already linked to AD. It is proved that in case of S1R deficiency adult neurogenesis is disturbed, as in an S1R knockout animal model, the proliferation of progenitor cells raised but both the neurite growth and the survival of newborn cells significantly decreased [149]. S1R also plays an important role in neuroinflammation. The receptor is expressed in microglia and astrocytes, and it can modulate their activation thus attenuate neuroinflammation [140, 150]. In several animal models of stroke [151-153], amyotrophic lateral sclerosis [154], and AD [155], S1R ligands influenced reactive astrogliosis, thereby modified microglial activity [76]. It is also reported that the expression level of S1R decreases in patients with neurodegenerative diseases like AD [76, 156, 157].

With its unique ligand-binding side, S1R binds a diverse set of molecules with different chemical structures and diverse pharmacological profiles, for example, antipsychotics, antidepressants, and neurosteroids [158-161]. Functional (*in vivo*, *ex vivo*, *in vitro*) and quantitative cell-based assays, methods which measure  $\text{Ca}^{2+}$  levels, receptor fluorescent

resonance energy transfer, and S1R-BiP association enzyme-linked immunosorbent assay experiments help to distinguish between agonists and antagonists - however, none of them are precise. S1R agonists activate S1R and thus support the formation of S1R monomers and dimers, while the antagonists favor the binding to the oligomeric state of S1R [140]. The S1R does not have a well-identified intrinsic activity [162], thus standardized methods in order to characterize the identity and activity of possible intrinsic ligands should be established [140]. Many endogenous (dehydroepiandrosterone (DHEA), pregnenolone, and N, N-dimethyltryptamine (DMT) [144]), and exogenous S1R ligands ((+)-pentazocine, fluvoxamine, ANAVEX2-73, and 2-(4-morpholinethyl)-1-phenyl cyclohexane carboxylate (PRE084), donepezil, cutamesine, haloperidol, NE-100, and sertraline) have been identified [76, 137, 144, 163]. They all can be classified either as agonists (DMT, fluvoxamine, DHEA, donepezil, cutamesine, (+)-pentazocine, fluvoxamine, ANAVEX2-73, PRE084, pregnenolone) or antagonists (NE-100, haloperidol, sertraline) [140, 162]. During our experiments, the impacts of two agonists, DMT and PRE084 were studied.

DMT is a non-specific endogenous ligand of S1R, which is a hallucinogenic agent assumed to be biosynthesized in small quantities and accumulated in the CNS [164-166]. Previous studies have shown that the administration of DMT modulates many ion channels [165], protects against hypoxia-induced damage [167], alleviates neuroinflammation [168, 169], increases the density of dendritic spines [170], as well as promotes neurogenesis and neuritogenesis [171-175]. However, DMT might also exert anxiogenic, neuro-, and cytotoxic effects [173, 176-178]. DMT is known to bind to several receptors with different affinities (5-hydroxytryptamine (5-HT)<sub>1A-B</sub>, 5-HT<sub>1D</sub>, 5-HT<sub>2A-C</sub>, 5-HT<sub>5A</sub>, 5-HT<sub>6</sub>, 5-HT<sub>7</sub> receptors, S1R, serotonin transporter, dopamine 1-5 receptors,  $\alpha_1$  adrenergic receptor, imidazoline 1-3 receptor, trace amine associated receptor, N-methyl-d-aspartate receptor [179-181]). Several adverse effects of DMT are primarily associated with the stimulation of 5-HT<sub>2A</sub> receptors [173, 176, 177, 179, 182], while its positive impact is rather related to the activation of S1Rs [153, 166-170, 172, 175, 176, 178]. However, inflammation regulatory and plasticity-promoting activities of DMT are also considered as results of its binding to both S1 and 5-HT receptors.

The antidepressant and nootropic properties of PRE084 are also recognized [183]. Based on our current knowledge, PRE084 may promote neuroprotection and neurite growth by stimulating the expression of different neurotrophic factors, as well as by activating signaling pathways involved in cell survival [154, 184-188]. Previous studies suggest that this S1R agonist might positively impact learning and memory, as it was demonstrated in animal models of neurodegenerative diseases or of traumatic brain injuries [186, 187, 189]. It is also reported

that after the administration of A $\beta$ <sub>25-35</sub> into the right lateral ventricle of mice, PRE084 treatment moderated the adverse behavioral effects of A $\beta$ <sub>25-35</sub> [147] via reducing neurotoxicity-induced cell death [190]. Moreover, PRE084 may also promote neurogenesis [191] and cell survival by attenuating excitotoxicity and reducing microglial activity, as well as diminishing the expression of proinflammatory factors [192, 193]. Based on the findings detailed above, S1R received considerable attention for its potential role in the prevention of A $\beta$ -induced neurotoxicity, as well as in the regulation of the pathophysiology of AD. Thus, S1R ligands are being recognized as promising therapeutic agents for treating or alleviating AD [53, 76, 194-196].

#### **4.6 Animal models and behavior tests in AD research**

Creating animal models that can recapitulate specific features of AD is of great importance in the understanding of the pathogenesis of the disease and in the development of new therapies [197]. A great variety of models have been developed, invertebrates (*Caenorhabditis elegans*, *Drosophila melanogaster*, and yeast [198, 199]) and vertebrate animals (Rhesus monkey, canine, rodent, and zebrafish models [199]) have been employed to elucidate how the disease is initiated and spread. However, currently, we do not have a single model to mimic the complexity of the disease. Transgenic models (mouse [200] and rat [201], <https://www.alzforum.org/research-models/alzheimers-disease>) express the genetic features of FAD, by applying one or more human mutations of the key proteins (e.g., APP, PS1-2). The possible therapeutic drug candidates are mainly tested on these systems, however, more than 95 % of AD cases belong to the sporadic form [86]. In AD research, a well-established SAD animal model would be urgently needed for the testing of neurocognitive compounds. In the past decades, many SAD models have been generated, based on hypertension, hypoxia, and stroke, lipopolysaccharide-induced neuroinflammation, and the application of neurotoxins or infused A $\beta$  [125, 202, 203]. The main problem with these animals is that they only mimic certain pathological hallmarks of human AD, and none of them can reflect entirely the fundamental pathophysiology of the disease. Nonetheless, nowadays, the non-transgenic rodent models are proven to be cheap, and as they apply young animals, they can serve as a fast and flexible possibility to investigate the etiology, progression, and molecular mechanisms of AD. A non-transgenic model can be obtained by injecting extracellular A $\beta$  peptides directly into the murine brain via intrahippocampal (IHC) [204-215], entorhinal (EC) [203, 216, 217] or intracerebroventricular (ICV) [191, 200, 218-227] administration. In a study, A $\beta$  was administered into different brain areas (olfactory bulb, parietal cortex, striatum, EC, and HC)

[228]. Although A $\beta$  seeds of exogenous origin were detected in all regions, the entorhinal and hippocampal A $\beta$  aggregates were significantly overrepresented and more congophilic compared to those in the striatum. Moreover, the depositions were still present near the injection site even 3 months after the delivery, and their spreading into adjacent brain regions was also detected (e.g., injection into the EC induced the appearance of A $\beta$  deposits in the molecular layer of DG). In another study, it was also proven that the ICV injected oA $\beta$  could enter the brain tissue from the cerebrospinal fluid, inducing widespread changes in neuronal cells [221]. Acute A $\beta$  infusion into the brain rapidly establishes some symptoms of AD, like learning and memory impairments, and a range of AD-associated histopathological hallmarks, such as dendritic spine and synaptic loss, altered neurogenesis, and neuroinflammation are also evincible with varying severity [205]. However, common A $\beta$ -injection experiments widely differ from each other in experimental parameters, such as the type of A $\beta$  (i.e., A $\beta$ <sub>1-40</sub>, A $\beta$ <sub>1-42</sub>, A $\beta$ <sub>25-35</sub>) the aggregation grade (fA $\beta$ , oA $\beta$ ), the concentration of the applied A $\beta$  solution, the duration of infusion (single or chronic treatment), and the site of infusion (ICV, IHC, EC, etc.), which makes the comparison of the results difficult.

In animal research paradigms, behavioral tests are commonly used to assess the effects of neurodegeneration on cognition and behavior. These methods are designed to measure a range of behavioral changes in learning and memory (Morris water maze, Object recognition, Y- and T-maze, Radial arm maze, Hole board, Barnes maze), anxiety (Open field, Elevated plus maze, Light-dark box, Social interaction test), depression (Forced swim and Tail suspension tests), or motor function (Rotarod and Locomotor activity tests) [197, 203, 204, 229, 230]. In AD research, learning and memory are the most studied features. For this purpose, the Morris water maze (MWM) is often used, in which the spatial learning and memory of the rodents are tested. The MWM was developed by Richard G. M. Morris in 1984 [231]. During the test, the rodents navigate in an open swimming arena by using distal cues to find the submerged escape platform in the tank [231, 232]. Several properties of the MWM have contributed to its widespread use such as its reliability despite variable testing procedures, its validity for assessing hippocampal-dependent spatial learning and memory, its sensibility as it is capable to detect subtle differences in learning and memory, and its cross-species applicability (rat, mouse or even human) [232]. Moreover, it can be used to examine versatile research questions related to cognitive functions such as the effects of drugs, aging, and neurodegenerative diseases on learning and memory. Moreover, MWM has further advantages: it requires minimal training of the animals, it is non-invasive, and the rodents possess sufficient motivation to locate the hidden island, moreover, it does not require food deprivation, and complete inactivity of the animals

in the tests is very rare [99, 232, 233]. Still, a few disadvantages are also described [232, 233], e.g., the most common claim is that MWM is stressful to the subjects. The testing procedure increases the level of the stress-related marker, corticosterone, 4-fold in the Barnes maze and 5-fold in MWM, but its influence on the subjects' performance is not yet obvious [234]. Some animals are not motivated to find the platform, they are floating or moving around the perimeter of the arena, and they do not perform an effective searching strategy in the maze. This behavioral phenotype is more characteristic of inbred mouse strains. According to the opinion of certain researchers, the test is not sensitive enough to measure working memory [99].

The most basic procedure of MWM is spatial or place learning. During the learning trials, the rodents must acquire the way to the hidden, escape platform, by using the distal cues, when they start from different points around the perimeter of the arena. At the end of the learning phase, generally within 24 hours, a probe trial is given to assess the reference memory. Several variations of the basic protocol exist that can be used to enhance the evaluation of spatial cognitive functions. The reversal MWM versions ('spatial reversal', and 'spatial double-reversal' ones with a smaller platform), in which the platform is relocated to different quadrants, disclose the learning flexibility of the subjects - that is whether the animals can extinguish their original goal position and acquire new ones. When using a smaller platform, more accuracy is required from the animals to solve the task because the elevated ratio of the search area to target size increases the task difficulty. Consequently, such subtle cognitive deficits and/or effects of drugs may be detected that remain hidden in the learning phase. Another procedure to examine the animals' flexibility and rapid learning ability is the 'matching-to-sample' or 'trial-dependent' protocol. In this procedure, in order to assess the spatial working or trial-dependent learning and memory, (which is primarily affected in AD), a different protocol is required: the platform is relocated every day. Each day, during the first swim, which represents a sample trial, the animals must learn the new position of the island. The second swim on the same day serves as the test or matching trial, in which the performance of working memory is measured. Besides the abovementioned protocols, 'repeated', 'discrimination', 'latent', and 'cued' learning procedures exist, and their application is determined by the goal of the given experiment. During our experiments, the basic and some modified versions of MWM were also applied. We intended to use a modified version of MWM, in which, by combining several protocols (matching-to-sample, basic, and smaller platform), the A $\beta$ <sub>1-42</sub>-injected rodents' learning and memory flexibilities and their subtle cognitive deficits would have become detectable. In human AD, after the impairment of the working memory, other memory types become also affected, like the declarative/explicit/episodic/allocentric one, and the

implicit/procedural/egocentric one. These functions rely mainly on the intact HC and on the parahippocampus. In animal models, it is hard to precisely separate which type of memory is tested. Basic MWM protocols mostly test the allocentric memory that is homologous to declarative memory in humans. In our modified MWM, by applying the matching-to-sample protocol followed by a smaller platform, the spatial accuracy requirements of the animals were enhanced, thus the working memory could be also tested.

Despite many animal models and experiments, currently, there is no cure for AD, and its progression cannot be prevented; at present, only symptomatic treatments with mild to moderate efficiency are available. Several cases reported that drug candidates improved memory functions in a rodent model, but they were ineffective in human clinical trials. There are different theories to explain the negative outcomes. The brains of humans and rodents are structurally and functionally different which can affect information processing. Moreover, artificial rodent models may not reflect accurately the natural progression of the disease. Besides, metabolism and absorption processes in rodents are dissimilar from those in humans, which can influence the efficacy and toxicity of the tested drug candidates. Nonetheless, the importance of animal models and experiments is undeniable. By studying underlying molecular mechanisms and progression of AD in rodent models, potential drug targets and biomarkers for an early diagnosis can be identified. Screening of drug toxicity in animal models helps to reveal safety issues in the early phases of pharmaceutical development. Admitting the fact, that human-rodent comparisons are limited, it seems probable that the exact pathomechanism of AD cannot be elucidated by human experiments alone [235]. Therefore, a methodic selection of translatable experimental paradigms is required, whereby the conversion of basic experimental discoveries into practical applications may considerably improve the diagnosis, prevention, and treatment possibilities of AD [86, 236].

#### **4.7 Drug research in AD**

The expansion of knowledge related to AD pathology, and the dynamical adjustment of theories to the experimental findings constantly influence the directions of AD-related drug research. In parallel with the establishment of the first hypothesis of AD, which was the cholinergic one, cholinesterase inhibitors appeared as potential causative therapeutics [30, 31]. Afterward, the identification of the A $\beta$  peptide provided new possibilities for drug research. At this time, the tau protein also became a potential target, although less significantly, possibly because it is more difficult to create relevant tau-based biological models in which the effects of the compounds could be reliably monitored.

Alforum.org is an internet database, which summarizes the results relating to AD research in a revised form. On this website, discoveries, drug research outcomes, diagnostic procedures, and experimental models are collected (<https://www.alzforum.org/databases>). Analysis of the database related to therapeutics shows that all the main AD hypotheses have already been targeted by pharmaceutical research. Because of the central role of A $\beta$  in AD pathology, one of the largest groups is related to it, with 71 therapeutics being in various phases of clinical testing. A strong candidate among AD therapies is immunotherapy, in which either A $\beta$  antibodies are administered (passive immunotherapy), or a humoral immune response is induced with a proper antigen in the biological system (active immunotherapy). Unfortunately, most of the active immunization trials in humans had to be discontinued, due to severe side effects (encephalitis) [237, 238]. In the last five years, leading pharmaceutical companies (Eli-Lilly, Eisai, Janssen-Pfizer, Hoffmann-La Roche) have focused their efforts on the development of passive immunization therapies [239]. In this procedure, antibodies are produced against A $\beta$  of a specific length or aggregation (monomeric, protofibrillar, and fibrillar) form. Unfortunately, the results revealed problematic efficacy in many cases, e.g., bapineuzumab could not possess any clinical efficacy regarding the cognitive functions, except in the 0.15 mg/kg dose, which caused a significant worsening in cognitive functions [240]. In preliminary experiments, a single administration of solanezumab reduced the amyloid plaques and reversed the memory deficits in a transgenic mouse model, but in human clinical trials, its effects were insignificant [237, 241]. A possible reason for the ineffectiveness of therapies could be the fact that the penetration of the antibodies to the appropriate brain area is limited.

A $\beta$  peptides are produced from sequential cleavage of APP by  $\gamma$ - and  $\beta$ -secretases thus the application of secretase inhibitors or modulators was considered as another promising strategy to treat AD. However, trials with small-molecular  $\beta$ - or  $\gamma$ -secretase inhibitors have also failed because of the negative side effects and the lack of meeting their primary endpoints, i.e., significant improvement of cognitive functions [30, 241]. Secretases act on several biological targets; therefore, they may cause serious adverse effects, e.g., liver toxicity, skin cancer, and decreased resistance to infections [237, 242].

By 2017, the research community was shocked by the negative outcomes of clinical studies applying immunization and secretases. John Hardy summarized the disappointing results and he also attempted to define new therapeutic approaches for the treatment of AD [243]. Systematic and open data analysis at all stages of the disease is a key element for the understanding of AD research. Failed trials still have value, if we learn from them, thus improve our theories and concepts.



Currently, according to the Alzforum.org database, there are 8 therapies available for the treatment of AD in the USA. Five of these therapeutics (Donepezil, Galantamine, Memantine, Rivastigmine, Tacrine) affect the cholinergic system or the level of other neurotransmitters, and they provide therefore only symptomatic treatment. One molecule (Suvorexant) is an approved medication to cure insomnia which became the first drug to be accepted to treat circadian disruption in AD. The two remaining treatments are passive immunization-based monoclonal antibodies, Aduhelm (Aducanumab) and Leqembi (Lecanemab) that are considered to reduce A $\beta$  accumulations. In 2021, the Food and Drug Administration approved the therapeutic use of Aduhelm in the USA after serious professional debates and required further Phase 4 studies to confirm efficacy and to determine appropriate dosages. These investigations are currently ongoing. Leqembi is an approved antibody which selectively binds to soluble A $\beta$  protofibrils, but its Phase 3 studies are currently still ongoing. Although the current results are promising for AD patients, it seems obvious that antibodies possess clinical efficacy only in very high doses. Because of the high costs of antibody production, an effective treatment that is financially affordable for all members of the human community will not be available in a short time. Whether antibody therapies are the right therapeutic approach is also highly debated. All opinions agree that the delivery of antibodies to the target site must be increased, which would possibly enhance the efficacy, and thus reduce the required dose and the costs of the treatments. Therefore, it is worth considering other, less-studied targets of AD pathology. In case of anti-inflammatory drugs, clinical trials have already been carried out aiming their application for AD treatment. The Alzheimer's Disease Anti-Inflammatory Prevention Trial, which examined the effects of naproxen and celecoxib, ended unfortunately with negative results [244]. The reasons for the ineffectiveness may be an insufficient experimental design, a short treatment time, the advanced age of the patients, several comorbidities, genetic reasons, and the inhomogeneity of experimental groups [245]. It can be assumed that by eliminating the errors, the beneficial effects of the anti-inflammatory drugs would be detectable over the course of AD.

One of the targets of our research was the therapeutic application of S1R modulators for AD treatment. Blarcamesine (ANAVEX) which is a mixed S1R/muscarinic agonist [246] is currently being investigated in a Phase 3 clinical trial. Blarcamesine reduced the deterioration of cognitive abilities, although dizziness and confusion occurred in some patients as side effects. Moreover, preclinical studies aiming at the therapeutic expansion of several approved drugs (Fluvoxamine, Donepezil, Citalopram, Dextromethorphan) that bind to S1R, are also underway.

## 5 AIMS

Based on the amyloid cascade hypothesis, our research group aimed to establish such experimental models, in which potential drug candidates, designed and synthesized *in-house*, could be cost- and time-effectively tested *in vivo*. To achieve this, we formulated and validated different treatment protocols applying exogenous A $\beta$ , with the following considerations:

1. In one study, fA $\beta$ <sub>1-42</sub> was administered in the HC of rats. We examined the impact of a single injection of fA $\beta$ <sub>1-42</sub> on spatial memory and on dendritic spine density in the HC of the treated animals. Rats were subjected to standard MWM tests (*IHC experiment*).
2. The effect of Leu-Pro-Tyr-Phe-Asp-amide (LPYFDa), a potential drug candidate molecule was tested in a cooperative project. Our collaborators examined its effect in an injection model, in which oA $\beta$ <sub>1-42</sub> was administered in wild-type mice in the presence of LPYFDa, and the animals were subjected to fear conditioning tests. In parallel with this, we aimed to evaluate spatial memory in a modified version of MWM. Instead of mice, we used rats, which were treated once with oA $\beta$ <sub>1-42</sub>, injected in the EC. The neuroprotective impacts of LPYFDa on cognition and on neuroinflammation were also studied in this model (*EC experiment*).

The change in the leading directions of AD-related drug research made us broaden our portfolio and find possible therapeutics with new pathomechanistic targets. We aimed to assess the role of adult neurogenesis and neuroinflammation in AD, and its connection to S1R-dependent molecular processes.

3. In a third study, oA $\beta$ <sub>1-42</sub> was administered ICV in adult wild-type C57BL/6 mice, in order to induce early acute AD-like impairments in neurogenesis and to reveal its relationship with neuroinflammation. We attempted to restore normal functioning in the A $\beta$ -treated animals by activating S1Rs with two different S1R agonists, PRE084 and DMT (*ICV experiment*).

## 6 MATERIALS AND METHODS

### 6.1 Animals

Male Wistar rats (n=24, Charles-River, Germany), weighing 210-230 g at the beginning of the *IHC experiment*, male Wistar-Harlan rats (n=41, Charles-River, Germany), weighing 250-350 g, and aged 8-10 weeks at the beginning of the *EC experiment*, and male C57BL/6 wild-type mice (n=80) from *in-house* breeding, weighing 23-28 g and aged 12 weeks at the beginning of the *ICV experiment*, were used as subjects.

All animals, divided into groups, were kept under constant circumstances, including constant temperature ( $23 \pm 0.5$  °C), lighting (12:12 h light/dark cycle, lights on at 7 a.m.), and humidity (~50%). Standard rat or mouse chow and tap water were supplied *ad libitum*. All behavioral experiments were performed in the light period. Handling was executed daily, at the same time, started one week before the experiments. All efforts were made to minimize the number of animals used, and their suffering throughout the experiments.

All experiments were performed in accordance with the European Communities Council Directive of 22 September 2010 (2010/63/EU on protecting animals used for scientific purposes). The experimental protocols were approved by the National Food Chain Safety and Animal Health Directorate of Csongrád County, Hungary (project license numbers: XXVI/01699/2010, XXXI/2012., XXVI./3644/2017). Formal approval to conduct the experiments was obtained from the Animal Welfare Committee of the University of Szeged.

### 6.2 Synthesis of A $\beta$ <sub>1-42</sub>, and preparation of A $\beta$ <sub>1-42</sub> aggregates

The iso-A $\beta$ <sub>1-42</sub> peptide, which is a chemically modified form of the natural sequence was synthesized in the solid phase using tert-butyloxycarbonyl (Boc)-chemistry *in-house*, as reported earlier [247]. In the *IHC experiment*, the fA $\beta$ <sub>1-42</sub> was prepared as described by He *et al.* [204]. Briefly, iso-A $\beta$ <sub>1-42</sub> was dissolved in 1,1,1,3,3,3-hexafluoro-2-propanol (HFIP, Sigma Aldrich, Saint Louis, MO, USA) to 1 mM. HFIP was removed *in vacuo*, and the peptide film was suspended in dimethyl sulfoxide (DMSO, Sigma Aldrich Saint Louis, MO, USA) to make a 5 mM solution. The fA $\beta$ <sub>1-42</sub> was prepared by diluting the DMSO stock solution with a 100 mM HEPES buffer to a final concentration of 222  $\mu$ M. The solution was incubated at 37°C for 7 days. After the aggregation period, the sample was centrifuged for 10 min at 15,000 g at RT. The pellet containing the freshly prepared fA $\beta$ <sub>1-42</sub> was resuspended in 100 mM HEPES buffer (pH 7.5) and used in the experiments.

In the *EC experiment*, oA $\beta_{1-42}$  was prepared by applying a modified protocol of Stine *et al.* [248]. According to this, iso-A $\beta_{1-42}$  was dissolved in HFIP and incubated overnight at RT. Aliquots were transferred into Eppendorf tubes, and HFIP was evaporated *in vacuo*. Oligomers were prepared by resuspending the peptide film in NaHCO<sub>3</sub>-buffered saline (20 mM NaHCO<sub>3</sub>, 154 mM NaCl saturated with CO<sub>2</sub>, pH=7.0). Samples were filtered through a syringe filter equipped with a sterile PVDF membrane (pore size 0.1  $\mu$ m, Millipore, Hungary). The peptide content of the filtrate was determined by a bicinchoninic acid assay. The final peptide concentration was adjusted to 75  $\mu$ M. The oligomeric solution was stored at 4°C until further use on the same day.

In the *ICV experiment*, a stock solution of iso-A $\beta_{1-42}$  was prepared using distilled water, to yield a concentration of 1 mg/ml (200  $\mu$ M, pH=7), and it was sonicated for 3 minutes. The solution was incubated for 10 minutes at RT, then the pH level was adjusted with NaOH to pH=11, and it was further incubated for 2 h. After a 3-minute-long sonication process, the oA $\beta_{1-42}$  solution was diluted in phosphate-buffered saline (PBS, 20 mM) to a final peptide concentration of 50  $\mu$ M, verified by a bicinchoninic acid assay. The oligomeric solution was stored at 4°C until further use on the same day.

The fibrillar and oligomeric states of the A $\beta$  aggregates were checked by transmission electron microscopy (Philips CM10, FEI Company, Hillsboro, OR, USA; JEM-1400, JEOL USA Inc., MA, USA) operating at 120 kV. Images were taken by MegaView II Soft Imaging System (Gmbh, Münster, Germany) and an EM-15300SXV system, routinely at a magnification of 25,000 and 50,000, and were processed by the SightX Viewer software.

### **6.3 Drug candidate (LPYFDa) synthesis**

The neuroprotective pentapeptide, LPYFDa was synthesized *in-house* by standard solid-phase peptide synthesis methodologies using Rink-amide resin and fluorenyl-methoxycarbonyl (Fmoc-) chemistry. The pentapeptide was purified on a C18 RP-HPLC column; pure fractions were checked by analytical HPLC, pooled, and lyophilized. Purity control and molecular weight were controlled by mass spectrometry (ESI MS, FinniganMat TSQ 7000) [249, 250].

### **6.4 Surgery, solutions, and drug administration**

Rats and mice were anesthetized by an intraperitoneal (IP) injection of a mixture of ketamine (10.0 mg/0.1 kg) and xylazine (0.8 mg/0.1 kg). The animals were placed into a stereotaxic apparatus (David Kopf Instruments, Tujunga, CA, USA; Stoelting Co., Wood Dale, IL, USA), a midline incision of the scalp was made, the skin and muscles were carefully retracted to

expose the skull, and a hole was drilled above the target area. In all three experiments, Hamilton syringes (32 G) were used for the injections. In each case, the administration started 2 min after lowering the needle, and it was removed very slowly 2 min after the end of the injection. All animals were treated with antibiotics and analgesics after the surgery.

In the *IHC experiment*, the solution was injected into the right HC unilaterally at a rate of 1.0  $\mu\text{l}/\text{min}$ . The following coordinates were used from Bregma point: AP: -3.6; ML: -2.4; DV: -2.8 [251]. Rats were randomly injected either with the fA $\beta_{1-42}$  (222  $\mu\text{M}$  fA $\beta_{1-42}$ ) or with vehicle (physiological saline). Two groups: control (n=12) and fA $\beta_{1-42}$ -treated (n=12) were formed.

In the *EC experiment*, the solution was injected into the EC at three bilateral sites (2.5  $\mu\text{l}$  per site, altogether 15  $\mu\text{l}$ ) at a rate of 0.5  $\mu\text{l}/\text{min}$ . The injection locations were approached at an angle of 15°. The following coordinates were used from Bregma point: AP: -6.4, -6.7, -6.8; ML:  $\pm 4.0$ ,  $\pm 2.4$ ,  $\pm 3.5$ ; DV: -8.2, -7.8, -7.4, respectively [251]. The rats were randomly assigned to groups and subjected to injections with the following solutions: **1.** PBS (20 mM), n=10; **2.** LPYFDa (375  $\mu\text{M}$ ), n=10; **3.** oA $\beta_{1-42}$  (75  $\mu\text{M}$ ), n=10; and **4.** oA $\beta_{1-42}$  and LPYFDa (for oA $\beta_{1-42}$  75  $\mu\text{M}$ ; for LPYFDa 375  $\mu\text{M}$ , 1:5 molar ratio), n=11.

In the *ICV experiment*, a single intracerebroventricular injection of either oA $\beta_{1-42}$  (50  $\mu\text{M}$ ) or PBS (20 mM) was administered at the right side, injected at a rate of 0.5  $\mu\text{l}/\text{min}$ . The following coordinates were used from Bregma point: AP: -0.3; ML: -1.0; DV: -2.5.

To detect stem cells, mice were injected IP with 5-Bromo-2'-Deoxyuridine (BrdU, 50 mg  $\text{kg}^{-1}$ ; Sigma-Aldrich, Saint Louis, MO, USA) dissolved in PBS, 3 times, 24 h after the surgery as described previously by Li *et al.* [191].

PRE084 (1 mg  $\text{kg}^{-1}$ , Sigma-Aldrich, Saint Louis, MO, USA) and DMT (1 mg  $\text{kg}^{-1}$ , Lipomed AG, Switzerland) were also administered IP daily between post-surgery days 7–12. Both substances were dissolved in PBS (sterile filtered, 20 mM) complemented with 1% DMSO.

Six groups of animals were developed. In the nomenclature of the groups, the first term refers to the ICV-administered solution (PBS or oA $\beta_{1-42}$ ), while the second one indicates the IP injected agent with potential disease-modifying activity (PBS again as a control, or PRE084 or DMT). Based on this nomenclature, the six groups were the following:

**1.** PBS-PBS: PBS-treated, non-diseased control; n=18; **2.** oA $\beta_{1-42}$ -PBS: AD-induced, PBS-treated control; n=18; **3.** PBS-PRE084: PRE084-treated, non-diseased control; n=11; **4.** oA $\beta_{1-42}$ -PRE084: AD-induced, PRE084-treated group; n=11; **5.** PBS-DMT: DMT-treated, non-diseased control; n=11; **6.** oA $\beta_{1-42}$ -DMT: AD-induced, DMT-treated group; n=11.

## 6.5 General description of MWM

Behavioral testing was carried out in a separated behavioral experimental room illuminated by three lamps giving diffuse light of approximately equal intensity at all points of the maze. The maze consisted of a circular pool (d=180 cm, h=60 cm) filled with water (23±1°C) and made opaque with milk. A black curtain was positioned around the pool with some high-contrasted distal paper cues. The cages were put in the behavioral testing room 1 hour before the swims for adaptation. The starting positions of the animals varied over the trials and the days. The maze was virtually divided into four quadrants (Q1-4 or NE, NW, SE, SW quadrants, Fig. 2); the part of the pool directly by the wall was the so-called peripheral zone. At the beginning of the swims, rats were placed into the water facing toward the wall of the pool in the peripheral zone. The island was placed at the center of a quadrant, always within a ring-shaped virtual part of the arena (annulus), submerged 1.5 cm below the surface to remain invisible to the animals. The animals were allowed to stay on the escape platform for 15 sec. When a rat did not find the island, it was guided by hand or placed on it. The behavior of the animals was automatically recorded with the software EthoVision 2.3 (Noldus Information Technology, The Netherlands, 2002) to calculate the time to reach the platform, swim speed, and swim path length (distance) during acquisition trials as well as percent time spent in each of the 4 virtual quadrants and time spent over the platform's position during the probe test.

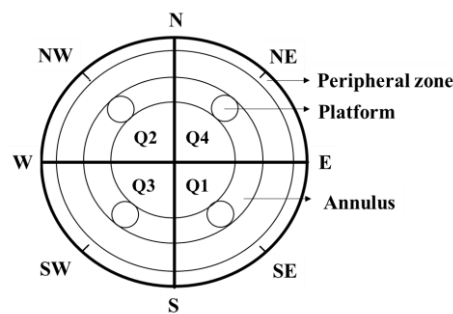


**Figure 2.** Important areas of the Morris Water Maze. The tank is divided into four virtual quadrants (Q1-4 or NE, NW, SE, and SW quadrants). The target island is located at the center of a quadrant. The annulus is the space between two concentric circles defined by lines touching the in- and outside border of the platform. The peripheral zone is close to the wall of the maze from where the animals start to swim. Behavioral data are measured in these areas by an EthoVision software, and statistically analyzed.

### 6.5.1 Fixed platform MWM

In the *IHC experiment*, spatial learning and memory were assessed on days 14 to 20 after IHC administration of fA $\beta$ <sub>1-42</sub> [204]. Memory acquisition trials (training period) were performed daily, rats swam 4 times in a row per day in blocks, for 6 days [204]. In each trial, rats were

allowed to swim freely for a maximum of 120 sec. Twenty-four hours after the last acquisition trial, retention was assessed on a 120-sec probe trial, with the platform removed.

### 6.5.2 Modified MWM (mMWM)

In the *EC experiment*, mMWM was carried out on the 15<sup>th</sup> day after the surgery. Two plastic platforms were used: a larger (d=10 cm), and a smaller (d=5 cm) hidden, escape island. On days 1 to 5 the larger, and on the 6<sup>th</sup> day the smaller platform was placed into the tank. During the experiments, two trials per day were performed from two different starting points, while the platform remained in the same position. The delay time between the two trials was 1.5 minutes. Each test lasted a maximum of 90 sec. One experiment lasted for six days.

On days 1 to 4, animals were tested with the matching-to-sample protocol [232]. In this phase, the large platform was relocated every day (from Q1 to Q4). During the first swim ('sample'), the animals had to learn the platform location. The second one served as the 'test' or 'matching' trial. On the 5<sup>th</sup> day, the large platform was again submerged in the same quadrant, as the day before (Q4/NE), while on the 6<sup>th</sup> day, the smaller platform was also located in Q4. The starting points and the target quadrants of a 6-day experiment were summarized in Table 1.

DAY	D1		D2		D3		D4		D5		D6	
TRIAL	1st	2nd	1st	2nd	1st	2nd	1st	2nd	1st	2nd	1st	2nd
STARTING POINT	NE	W	S	NE	N	SE	W	S	SE	NW	SW	SE
TARGET QUADRANT	SE		NW		SW		NE		NE		NE	

Table 1. Starting points and target quadrants in the 6-day MWM. The setting parameters correspond to Fig. 2. To assess the trial-dependent learning and memory of the rats, the matching-to-sample protocol was used on 1 to 4 days (D1-D4). In this phase, the platform was relocated every day (Q1-Q4 or SE, NW, SW, NE quadrants, respectively), and animals swam in two trials per day. Two different starting points per day were applied. On the 4<sup>th</sup>, 5<sup>th</sup>, and 6<sup>th</sup> days, the platform was submerged in the NE quadrant. On the last day, the smaller island was submerged in the tank.

## 6.6 Histological examination

In the *IHC experiment*, after the behavioral examinations, Golgi impregnation was carried out. FD Rapid GolgiStain<sup>TM</sup> Kit (FD NeuroTechnologies, Consulting & Services, Inc., USA) was used according to the manufacturers' instructions. The brains (n=6, 3 per group) were removed quickly, and tissue blocks including HC (approximately 0.7-0.8 cm) were cut from the brain. Tissue blocks were subjected to a two-phase impregnation. 100  $\mu$ m coronal sections were cut with a vibration microtome (Zeiss Microm HM 650V) and were mounted on gelatin-coated glass slides. After the staining procedure and dehydration, the slides were coverslipped with

dibutyl phthalate xylene (DPX) mountant for histology (Sigma-Aldrich, Saint Louis, MO, USA).

In the further histological experiments, rodents were anesthetized with chloral hydrate (1 mg kg<sup>-1</sup>) and were perfused transcardially with PBS, followed by 4% paraformaldehyde (PFA, Sigma-Aldrich, St. Louis, MO, USA). The brains were post-fixed in 4% PFA solution for a day and afterward, they were put in a mixture of 30% sucrose and 0.01% sodium-azide solution. All chemicals used in the immunohistochemical procedures, except the antibodies (Abs), were purchased from Sigma-Aldrich (St. Louis, MO, USA). After the immunostaining and washing steps, all sections were mounted on gelatin-coated slides, air-dried, dehydrated, and coverslipped with DPX (Fluka BioChemika, Buchs, Switzerland).

In the *EC experiment*, four animals from each group were used. After the post-fixation, specific brain regions from the dorsal HC to the posterior part of EC were slotted, and coronal, 30  $\mu$ m thick sections were cut by a freezing microtome (Leica, CM 1850, Germany).

For glial fibrillary acidic protein (GFAP) staining, the sections were quenched (0.3% H<sub>2</sub>O<sub>2</sub>) and blocked (normal goat serum, NGS, 1:10 dilution), thereafter the slides were incubated with the primary Ab (MAB360, Millipore, Billerica, MA, USA) in the presence of 20% NGS and 0.2% Triton X-100 overnight at 4°C. On the following day, the sections were washed in PBS and incubated for 1 h at RT with the biotinylated secondary goat anti-mouse Ab (1:400 dilution). The peroxidase reaction was carried out by applying the Vectastain Elite ABC Kit system (Vector Laboratories, Burlingame, CA, USA) using 3,3'-diaminobenzidine (DAB) as the substrate and NiCl<sub>2</sub> as an intensifier.

In case of the *ICV experiment*, two weeks after the administration of oA $\beta$ <sub>1-42</sub>, mice (n=8-8 from the PRE084- and DMT-treated, and n=15-15 from the control groups) were processed. Immunohistochemical analysis was carried out on 20  $\mu$ M formalin fixed cryosections. All immunohistochemical procedures were performed according to Szogi *et al.* [252, 253]. The following primary Abs were added to the samples: mouse anti-BrdU Ab (1:800; Santa Cruz Biotechnology, Dallas, Texas, USA), goat anti-doublecortin (DCX) Ab (1:4000; Santa Cruz Biotechnology, Dallas, Texas, USA), mouse anti- Neuronal Nuclei (NeuN) Ab (1:500; Merck Millipore, Darmstadt, Germany), rabbit anti- ionized calcium-binding adapter molecule 1 (Iba1) Ab (1:3600; Wako Chemicals GmbH, Neuss, Germany) and mouse anti-GFAP Ab (1:1500; Santa Cruz Biotechnology, Dallas, Texas, USA). For BrdU, DCX, and NeuN stainings, the sections were treated with a polymer-based HRP-amplifying system (Super Sensitive<sup>TM</sup> One-Step Polymer-HRP Detection System, BioGenex, Fremont, Cal., USA), according to the manufacturer's instructions. For Iba1 and GFAP labeling, the slices were



incubated with the corresponding secondary Abs: biotinylated goat anti-rabbit Ab (1:400; Jackson ImmunoResearch, West Grove, PA, USA) and biotinylated goat anti-mouse Ab (1:400; ThermoFisher Scientific, Waltham, MA USA) for 60 min. Next, the sections were rinsed 3 times in PBS, and were incubated with avidin-biotin-complex (ABC Elite Kit; Vector Laboratories, Burlingame, Ca, USA) for Iba1 in 1:1000 and for GFAP staining in 1:1500 dilutions, for 60 min at RT. The peroxidase immunolabeling was developed in 0.5 M Tris-HCl buffer (pH 7.7) with DAB (10 mM) at RT for 30 min.

### **6.7 Quantification of the data**

Golgi-impregnated sections were studied by inverse light microscopy, using oil-immersion objectives. A total of 25 pyramidal neurons from the dorsoventral hippocampal CA1 (*stratum radiatum*) were examined from each of the 6 animals (25 dendritic shafts per animal were analyzed). The spine density of the proximal apical dendrite area was analyzed (minimum 100  $\mu\text{m}$  from the soma). For each examined neuron, one 100  $\mu\text{m}$ -long segment from a second- or third-order dendrite (protruding from its parent apical dendrite) was chosen for spine density quantification as previously described [254]. The dendrites were selected under a 100 $\times$  oil immersion lens and the images of these apical dendrites were captured with a camera (AxioCam MRC V5, program: AxioVision 40 V. 4.8.1.0 Carl Zeiss Imaging Solutions GmbH) connected to a light microscope (Zeiss Observer Z1, with 10x ocular magnification) and a computer. Serial images were made from each dendrite in the whole of the analyzed segment (Z-stack). The captured multiple photomicrographs from one dendrite were then stacked into one file. To stack the images and determine the spine density, ImageJ 1.44 software (National Institute of Health, Bethesda, USA) was used.

Immunohistochemical slides were scanned by a digital slide scanner (Mirax Midi, 3DHistech Ltd., Budapest, Hungary), equipped with a Panoramic Viewer 1.15.4, a CaseViewer 2.1 program, and a QuantCenter, HistoQuant module (3DHistech Ltd., Budapest, Hungary). For quantifications, all sections derived from each animal were analyzed. In DG and HC, the regions of interest (ROI) were manually outlined. Ab-positive cell types were counted and quantified from ROIs. The number of stem cells (BrdU+) and neuroblasts (DCX+) were assessed by the observers, and to assess cell densities, we divided the total number of counted cells per animal with the DG/HC area and represented them as cells/ $\text{mm}^2$ . In case of NeuN, Iba1, and GFAP, the densities (%) of neurons (NeuN+), microglia (Iba1+), and astrocytes (GFAP+) were calculated by the quantification software.

## 6.8 Western Blot analysis

In the *EC experiment*, after removing EC of the rats (n=6/group), the samples were processed for western immunoblot (WB) analyses to detect the effects of  $\alpha\text{A}\beta_{1-42}$  on the expression of GFAP. In the *ICV experiment*, to determine the effects of  $\alpha\text{A}\beta_{1-42}$  and PRE084 or DMT on the expression of S1R, the HC and cerebral cortex samples of 3 animals per group (n=18) were identically prepared, separated, and transferred to nitrocellulose membranes as reported earlier [252]. In both experiments, the membranes were treated as described by Szogi *et al.* [252]. The levels of GFAP (mouse monoclonal Ab, MAB360, Millipore, Billerica, MA, USA, 1:1000), and S1R (mouse S1R Ab, Santa Cruz, Dallas, TX, USA, 1:1000) were analyzed in each group. For the analysis, we used glyceraldehyde 3-phosphate dehydrogenase signal (GAPDH, rabbit GAPDH Ab, Cell Signaling, Danvers, MA, USA, 1:200,000) as the loading control. The optical densities of GFAP and S1R bands from the membranes were determined and quantified with a Molecular Imager ChemiDoc XRS+ gel documentation system (Bio-Rad Hungary Ltd., Hungary, Image Lab software).

## 6.9 Statistical analysis

In the *IHC experiment*, behavioral data were analyzed by repeated measures one-way analysis of variance (rANOVA), followed by Fisher's LSD post-hoc tests for multiple comparisons. For the evaluation of the results of Golgi impregnation, a Student's t-test for independent samples was used. In the *EC experiment*, in which LPYFDa was tested, behavioral data of different groups were compared with ANOVA, followed by Fisher's LSD post-hoc tests for multiple comparisons. In the *EC and ICV experiments*, data obtained from the immunohistochemistry analyses were evaluated with ANOVA, followed by Fisher's LSD post-hoc tests. The WB data did not follow a normal distribution; thus, they were analyzed with Kruskal-Wallis nonparametric tests, followed by Mann-Whitney U tests for multiple comparisons. For the statistical analysis, SPSS software (IBM SPSS Statistics 24) was used, and the results were expressed as mean  $\pm$  (SEM). Statistical significance was generally set at  $p \leq 0.05$ .

## 7 RESULTS

### 7.1 IHC experiment

#### 7.1.1 Injection of $fA\beta_{1-42}$ induced deficits of spatial learning and memory in MWM

MWM was used to test spatial learning and memory each day on days 14 to 20 after IHC administration of  $fA\beta_{1-42}$ . Escape latency to find the platform was used as a measure for evaluating spatial memory. The results showed that the performance of both groups ( $fA\beta$ -treated and untreated) improved from day to day, reflecting the functioning of long-term memory. However, learning became slower each day in the  $fA\beta_{1-42}$ -treated group compared to the control one, as it could be seen from escape latencies analyzed by rANOVA ( $F_{1,94}=6.450$ ;  $p=0.013$ ) (Fig. 3A). A significant difference was detected between the groups also for the swimming distances ( $F_{1,94}=6.840$ ;  $p=0.010$ ) (Fig. 3B).

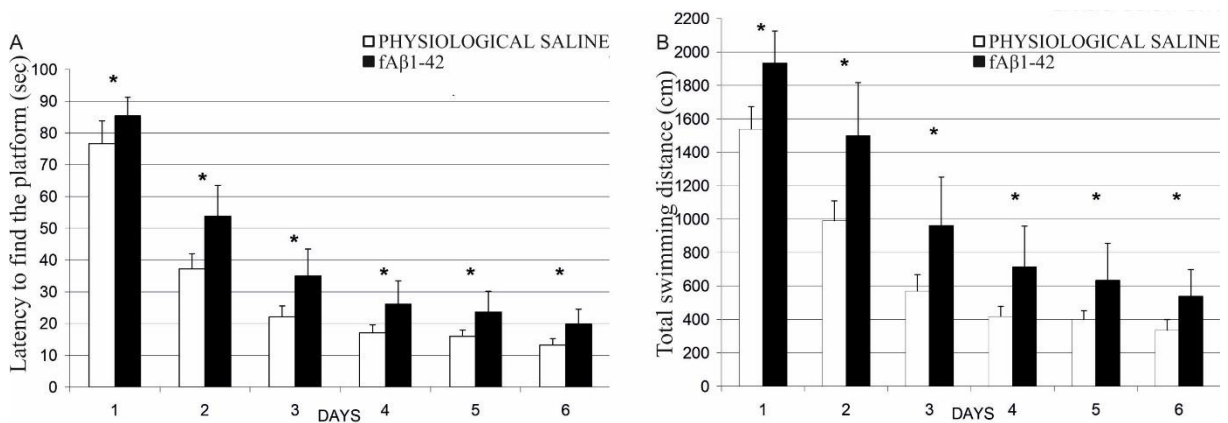


**Figure 3.**  $fA\beta_{1-42}$ -injection induced learning deficit in MWM. (A)  $fA\beta_{1-42}$ -injection resulted in an impaired learning process during the acquisition phase compared to the control group; (B)  $fA\beta_{1-42}$ -treated animals swam longer distances than the controls to find the platform.

Despite the significantly impaired learning process of the  $fA\beta_{1-42}$ -treated group, the observed performance in the probe test (conducted 24 h after the learning phase) indicated that spatial memory was not altered, as the times spent in quadrants and the number of crossing-overs in the virtual platform's position were comparable in the two groups ( $t_{22}=-1.247$ ;  $p=0.226$  and  $t_{22}=0.745$ ;  $p=0.464$ , respectively) (Fig. 4A, B).

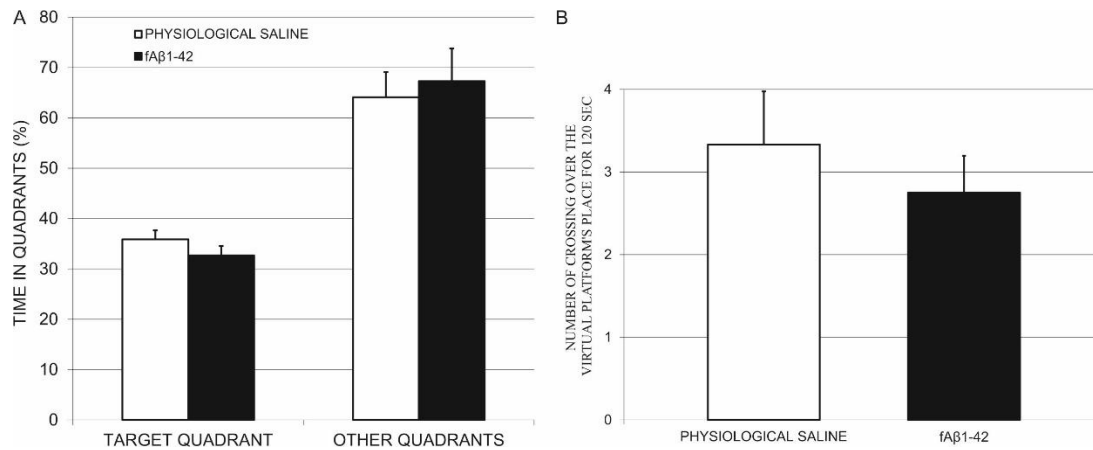


**Figure 4.** Injection of  $fA\beta_{1-42}$  did not affect the performance in MWM on the probe day. **(A)** In the target quadrant, the amyloid-treated animals spent comparable times to those of the controls. **(B)**  $fA\beta_{1-42}$ -injection did not have a significant effect on the number of crossings-over in the position of the virtual platform.

### 7.1.2 Administration of $fA\beta_{1-42}$ decreased dendritic spine density

The Golgi staining method labels the neurons randomly in the HC. Therefore, it is critical, that each analyzed sample belonging to the different groups must possess a comparable quality of staining. We counted all types of spines together and focused on determining the apical dendritic spine density. Spine density was different between the two groups ( $t_{28}=14.415$ ;  $p<0.0001$ ). In the  $fA\beta_{1-42}$ -treated group, a decrease of density was detected, compared to the controls (Fig. 5A). The photomicrographs demonstrate representative CA1 pyramidal neurons and their dendrites in a control (Fig. 5B, D) and in a  $fA\beta_{1-42}$ -injected (Fig. 5C, E) subject.

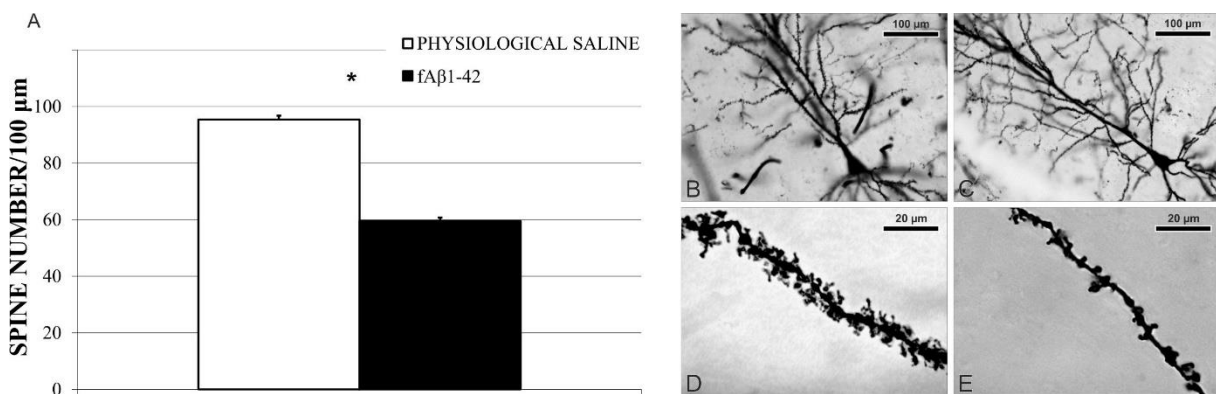


**Figure 5.** Golgi staining revealed changes in spine density after the  $fA\beta_{1-42}$ -injection. **(A)** Apical dendritic spine density analysis showed that the amyloid treatment induced a decrease in spine density. **B-C** representative photomicrographs of CA1 subfield pyramidal neurons of a control **(B)**, and an amyloid-treated **(C)** rat. **(D-E)** Photomicrographs of oblique dendritic segments from the previously presented neurons **(D)** control, **(E)** amyloid-treated). Injection of  $fA\beta_{1-42}$  reduced the local spine density in the  $fA\beta_{1-42}$ -treated group.

## 7.2 EC experiment

### 7.2.1 *oA $\beta$ <sub>1-42</sub> impaired, while LPYFDa improved the learning and memory functions when the smaller platform was used*

*oA $\beta$ <sub>1-42</sub>*-induced deficits were investigated in two different experimental paradigms, by working together with a cooperative research group in the Netherlands. For their experiments, we supplied *oA $\beta$ <sub>1-42</sub>* and LPYFDa. While they examined the impact of *oA $\beta$ <sub>1-42</sub>* injected IHC bilaterally, on the behavior of mice, with a fear conditioning test, we intended to test the effect of EC-administered *oA $\beta$ <sub>1-42</sub>* in our mMWM protocol, conducted with rats. Accordingly, both research groups examined the neuroprotective effects of LPYFDa in their own *in vivo* paradigms. LPYFDa, *oA $\beta$ <sub>1-42</sub>*, or the combination of both substances were administered directly into the EC of rats, and mMWM was conducted 15 days after the injections. To assess the working memory or trial-dependent learning of the animals, the matching-to-sample paradigm was applied.

In the experiments, two swims per day were conducted and analyzed. During the 1<sup>st</sup> swims of days 1-6, the animals learned successfully, how to find the platform, and statistical differences could not be detected in the latencies between the groups (data not shown).

In case of the 2<sup>nd</sup> swims of days 1-4, no differences were found between the groups either (Fig. 6A, days 1-4, successively:  $F_{3,37}=0.280$ ,  $p=0.840$ ;  $F_{3,37}=1.044$ ,  $p=0.385$ ;  $F_{3,37}=0.570$ ,  $p=0.638$ ;  $F_{3,37}=0.164$ ,  $p=0.920$ ). On the 5<sup>th</sup> day, the unchanged platform position did not affect the learning and memory processes of the animals (Fig. 6A, 5<sup>th</sup> day,  $F_{3,37}=1.104$ ,  $p=0.360$ ). Additionally, the pentapeptide was also ineffective in this time interval.

However, upon the evaluation of the 2<sup>nd</sup> swims of the 6<sup>th</sup> day, a significant difference was found in the latencies to find the platform (Fig. 6A,  $F_{3,37}=3.472$ ,  $p=0.026$ ). The post-hoc analysis of the results revealed that the *oA $\beta$ <sub>1-42</sub>* group had a longer escape latency compared to the other three groups (post-hoc tests: *oA $\beta$ <sub>1-42</sub>* vs. control:  $p=0.040$ , vs. LPYFDa:  $p=0.004$ ; vs. *oA $\beta$ <sub>1-42</sub>*+LPYFDa:  $p=0.027$ ), which confirms subtle learning and working memory deficits in *oA $\beta$ <sub>1-42</sub>*-treated rats, whereas LPYFDa seemed to have a positive effect on the impaired learning and memory capabilities.

On the 6<sup>th</sup> day, a new searching strategy of the *oA $\beta$ <sub>1-42</sub>*-treated animals could also be observed. During the 2<sup>nd</sup> trial, they spent a significantly longer time in the annulus zone, searching for the platform, in comparison with the other groups. Besides, an improvement of the searching strategy could also be experienced, which was exerted by the protective LPYFDa (Fig. 6B, ANOVA:  $F_{3,37}=3.723$   $p=0.049$ ; post-hoc tests: *oA $\beta$ <sub>1-42</sub>* vs. control:  $p=0.017$ ; vs. LPYFDa:  $p=0.042$ ; vs. *oA $\beta$ <sub>1-42</sub>*+LPYFDa:  $p=0.016$ ).

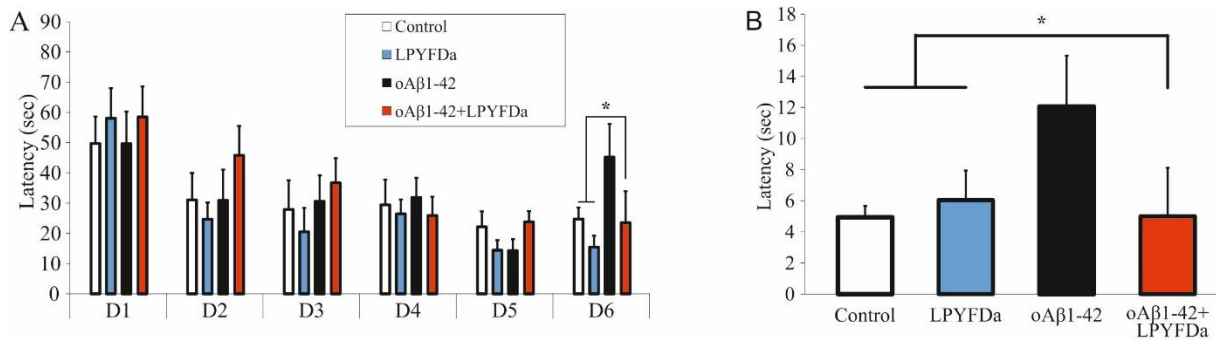


**Figure 6.** Behavioral results of LPYFDa experiments **(A)** Escape latencies of the 2<sup>nd</sup> trials of the four experimental groups during the 6-day mMWM. The entorhinal injection of oAβ<sub>1-42</sub> resulted in a significant learning and memory deficit on the 6<sup>th</sup> day when the smaller platform was used. The performance of the oAβ<sub>1-42</sub>-treated rats was significantly worse than those of the control, the LPYFDa, and the oAβ<sub>1-42</sub>+LPYFDa groups. **(B)** The total duration of searching in the annulus zone, in the 2<sup>nd</sup> trial, on the 6<sup>th</sup> day, using the smaller platform. The oAβ<sub>1-42</sub>-treated rats spent significantly longer times in the virtual annulus zone than the control ones, LPYFDa, and oAβ<sub>1-42</sub>+LPYFDa; a positive effect of LPYFDa on the searching strategy could also be detected.

### 7.2.2 LPYFDa hindered the oAβ<sub>1-42</sub>-induced neuroinflammatory processes in the rat brain

Neuroinflammation in the CNS results from the activation of the immune system, initiated by injuries, infections, and neurodegenerative processes. Hyperreactive astrocytes have a key role in the inflammatory response; their activation can be characterized by the measurement of GFAP levels. To examine the effect of oAβ<sub>1-42</sub> and LPYFDa on the activation of astrocytes, we applied immunohistochemical staining, and we found elevated numbers of hyperreactive astrocytes in the whole EC of the oAβ<sub>1-42</sub>-treated group compared to the other three groups (Fig. 7A, 7C-E, ANOVA:  $F_{3,12}=5.508$   $p=0.003$ ; post-hoc tests: oAβ<sub>1-42</sub> vs. control:  $p=0.001$ ; vs. LPYFDa:  $p=0.002$ ; vs. oAβ<sub>1-42</sub>+LPYFDa:  $p=0.046$ ).

WB analysis also revealed significant differences between the GFAP intensity levels of the different experimental groups, and it corroborated the immunohistochemical results, as the intensity of GFAP was also significantly higher in the amyloid-treated group than in the other groups (Fig. 7B, ANOVA:  $F_{3,20}=3.432$   $p<0.001$ ; post-hoc tests: oAβ<sub>1-42</sub> vs. control:  $p<0.001$ ; vs. LPYFDa:  $p<0.001$ ; vs. LPYFDa+oAβ<sub>1-42</sub>:  $p<0.001$ ).

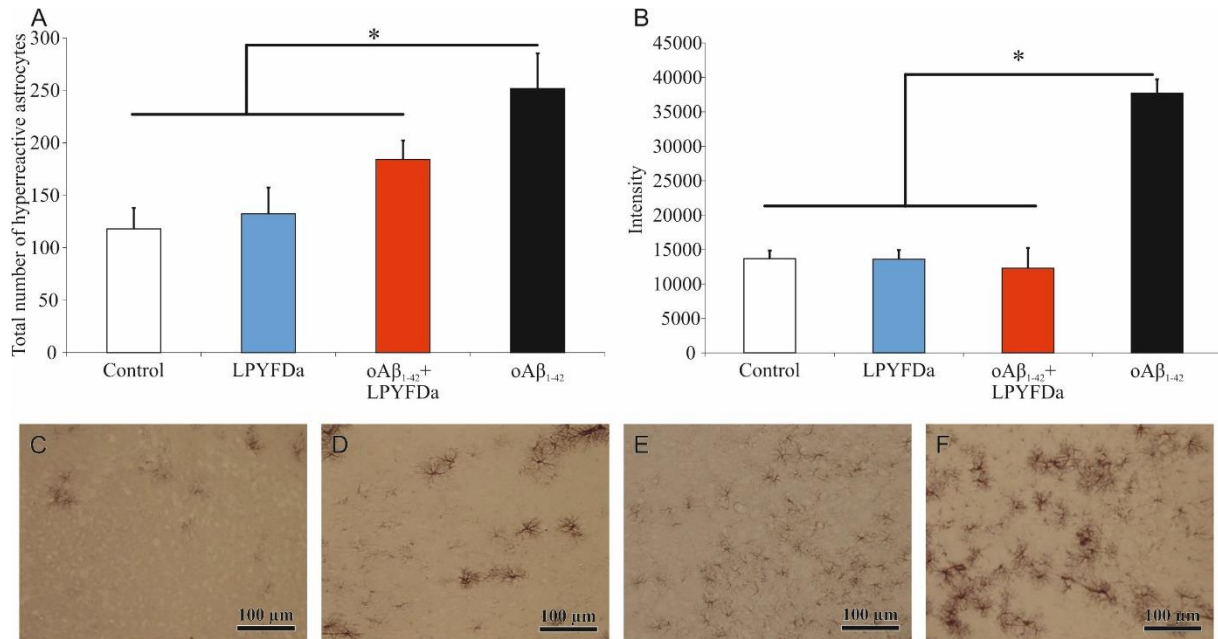


**Figure 7.** Histology results. **(A)** Quantitative immunohistochemical results of the GFAP staining. The diagram shows the numbers of hyperreactive astrocytes in EC observed in the groups. In the control, LPYFDa-treated, and oAβ<sub>1-42</sub>+LPYFDa-treated groups, low numbers of reactive astrocytes could be seen. In the oAβ<sub>1-42</sub>-treated group, numerous hyperreactive astrocytes were observed among glial elements, throughout the whole EC. **(B)** WB analysis of GFAP levels. In parallel with the results of GFAP immunocytochemistry, the oAβ<sub>1-42</sub> group had a significantly higher GFAP intensity ( $p < 0.001$ ) than the other three ones (Intensity  $\pm$  S.E.M is shown). **(C-F)** Representative photomicrographs of each group showing GFAP staining in the EC of **(B)** control, **(C)** LPYFDa, **(D)** oAβ<sub>1-42</sub>-injected, and **(E)** oAβ<sub>1-42</sub>+LPYFDa groups (scale bar: 100  $\mu$ m).

### 7.3 ICV experiment

#### 7.3.1 Effects of PRE084 and DMT on adult neurogenesis in $\text{oA}\beta_{1-42}$ and vehicle-treated mice

##### 7.3.1.1 $\text{O}\text{A}\beta_{1-42}$ and DMT impaired, while PRE084 promoted the survival of progenitor cells in DG.

Proliferating cells were labeled by three IP injections of BrdU with 6 hours intervals, which were administered 24 h after the stereotaxic surgery. BrdU is a synthetic thymidine analog, which incorporates into the DNA strand and can be detected by specific Abs. We counted BrdU+ cells 14 days after the surgery (Fig. 8). According to our results, the quantity of BrdU+ stem cells in the SGZ of the DG significantly differed among the six groups (ANOVA:  $p \leq 0.0001$ ).  $\text{O}\text{A}\beta_{1-42}$  infusion significantly reduced the number of progenitor cells compared to the respective control group (PBS-PBS vs.  $\text{oA}\beta_{1-42}$ -PBS  $p=0.001$ ).

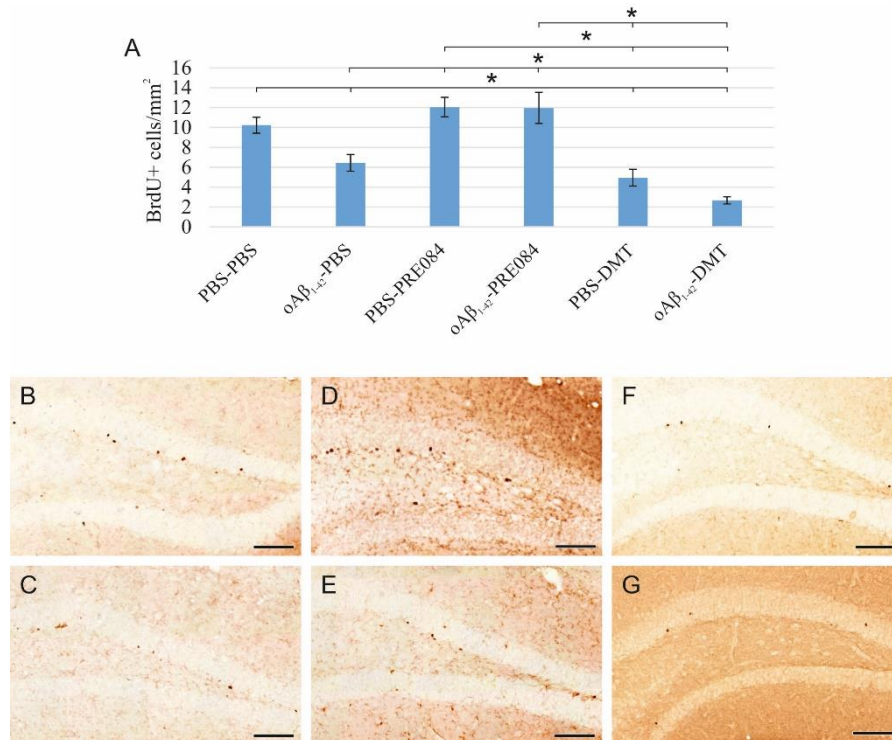


**Figure 8** (A) Results for BrdU immunolabeling. We observed significant differences in the quantity of stem cells among the six groups. (B–G) Representative images of BrdU staining: (B) PBS-PBS, (C)  $\text{oA}\beta_{1-42}$ -PBS, (D) PBS-PRE084, (E)  $\text{oA}\beta_{1-42}$ -PRE084, (F) PBS-DMT, (G)  $\text{oA}\beta_{1-42}$ -DMT. Scale bars represent 100  $\mu\text{m}$ .

Interestingly, more severe negative changes could be observed in animals treated with DMT. In those co-treated with both  $\text{oA}\beta_{1-42}$  and DMT, hardly any BrdU+ stem cells were detected in the SGZ ( $\text{oA}\beta_{1-42}$ -DMT vs. PBS-PBS  $p \leq 0.0001$ , vs.  $\text{oA}\beta_{1-42}$ -PBS  $p=0.005$ , vs.  $\text{oA}\beta_{1-42}$ -PRE084  $p \leq 0.0001$ ; PBS-DMT vs. PBS-PBS  $p=0.001$ , vs. PBS-PRE084  $p \leq 0.0001$ ). PRE084 treatment



increased the amount of BrdU+ cells; the difference between the A $\beta$ <sub>1-42</sub>-infused groups was significant (oA $\beta$ <sub>1-42</sub>-PBS *vs.* oA $\beta$ <sub>1-42</sub>-PRE084  $p \leq 0.0001$  (Fig. 8). The differences between the following groups in pairwise comparisons also reached significance: **PBS-PRE084** *vs.* oA $\beta$ <sub>1-42</sub>-PBS  $p \leq 0.0001$ , *vs.* PBS-DMT  $p \leq 0.0001$ , *vs.* oA $\beta$ <sub>1-42</sub>-DMT  $p \leq 0.0001$ ; **oA $\beta$ <sub>1-42</sub>-PRE084** *vs.* PBS-DMT  $p \leq 0.0001$ , *vs.* oA $\beta$ <sub>1-42</sub>-DMT  $p \leq 0.0001$  (Fig. 8).

### 7.3.1.2 OA $\beta$ <sub>1-42</sub> and PRE084 increased the number of premature cells, while DMT did not affect their quantity.

To understand the effects of PRE084 and DMT on the maturation of granule cells, we quantified immature neurons in the SGZ of DG. To label premature cells, we stained a microtubule-associated protein, DCX, which is expressed specifically in migrating neuronal precursors. The measured DCX densities were significantly different among the six groups (ANOVA:  $p \leq 0.0001$ , Fig. 9).

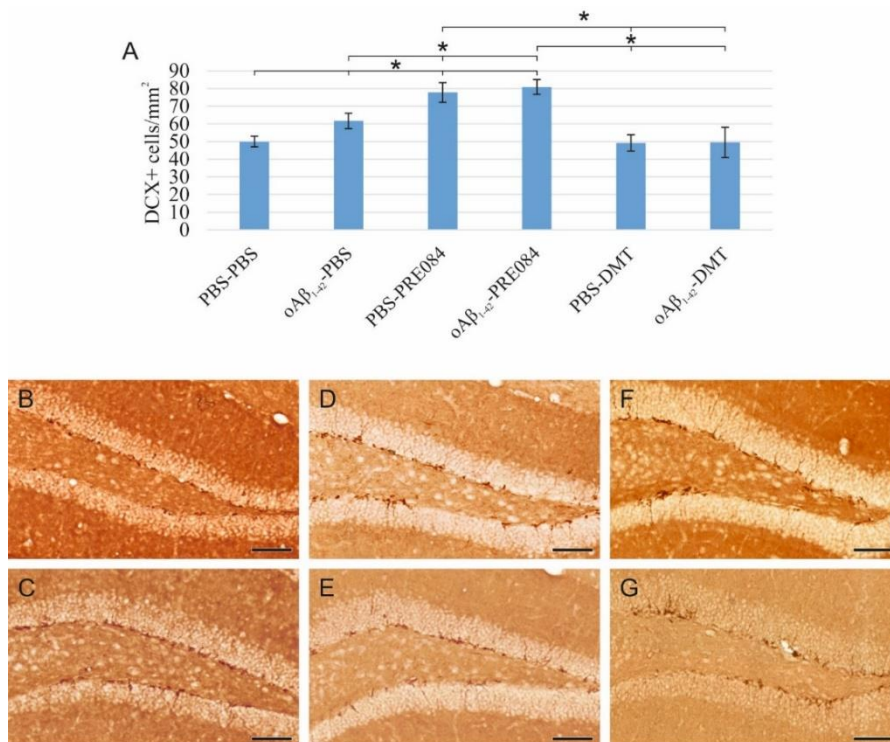


**Figure 9.** (A) Results of DCX immunostaining. Detected DCX densities significantly differed among the six groups. (B–G) Representative images of DCX immunolabeling: (B) PBS-PBS, (C) oA $\beta$ <sub>1-42</sub>-PBS, (D) PBS-PRE084, (E) oA $\beta$ <sub>1-42</sub>-PRE084, (F) PBS-DMT, (G) oA $\beta$ <sub>1-42</sub>-DMT. Scale bars represent 100  $\mu$ m.

In the oA $\beta$ <sub>1-42</sub>-PBS and PBS-PRE084 groups, the number of immature neurons was significantly higher compared to the control (**PBS-PBS** *vs.* oA $\beta$ <sub>1-42</sub>-PBS  $p = 0.037$ , *vs.* PBS-PRE084  $p \leq 0.0001$ , *vs.* oA $\beta$ <sub>1-42</sub>-PRE084  $p \leq 0.0001$ ). We also detected a significant difference

between the  $\text{oA}\beta_{1-42}$ -PBS and  $\text{oA}\beta_{1-42}$ -PRE084 groups ( $p=0.007$ ). DMT administration did not affect the number of premature neurons compared to PBS-PBS mice. Additional significances that are not relevant to the experiment were also detected:  **$\text{oA}\beta_{1-42}$ -PRE084** vs. PBS-DMT  $p\leq 0.0001$ , vs.  $\text{oA}\beta_{1-42}$ -DMT  $p\leq 0.0001$  (Fig. 9).

*7.3.1.3 The density of mature granule cells was unaffected by  $\text{oA}\beta_{1-42}$  or PRE084 administration, while DMT induced a decrease in neuronal density.*

To detect and evaluate mature granule cells in the HC, we performed NeuN immunostaining. Again, significant differences were observed among the groups (ANOVA:  $p=0.001$ ). In DMT-treated animals, significantly lower NeuN+ cell densities were evident in the HC, compared to the PBS-PBS and  $\text{oA}\beta_{1-42}$ -PBS groups (**PBS-PBS** vs. PBS-DMT  $p=0.001$ , vs.  $\text{oA}\beta_{1-42}$ -DMT  $p=0.022$ ;  **$\text{oA}\beta_{1-42}$ -PBS** vs. PBS-DMT  $p\leq 0.0001$ , vs.  $\text{oA}\beta_{1-42}$ -DMT  $p=0.003$ ; Fig. 10). Other, not relevant significances could also be identified when the groups were compared to the PBS-DMT-treated one: **PBS-DMT** vs. PBS-PRE084  $p=0.001$ , vs.  $\text{oA}\beta_{1-42}$ -PRE084  $p=0.006$ ;  $\text{oA}\beta_{1-42}$ -DMT vs. PBS-PRE084  $p=0.024$  (Fig. 10).

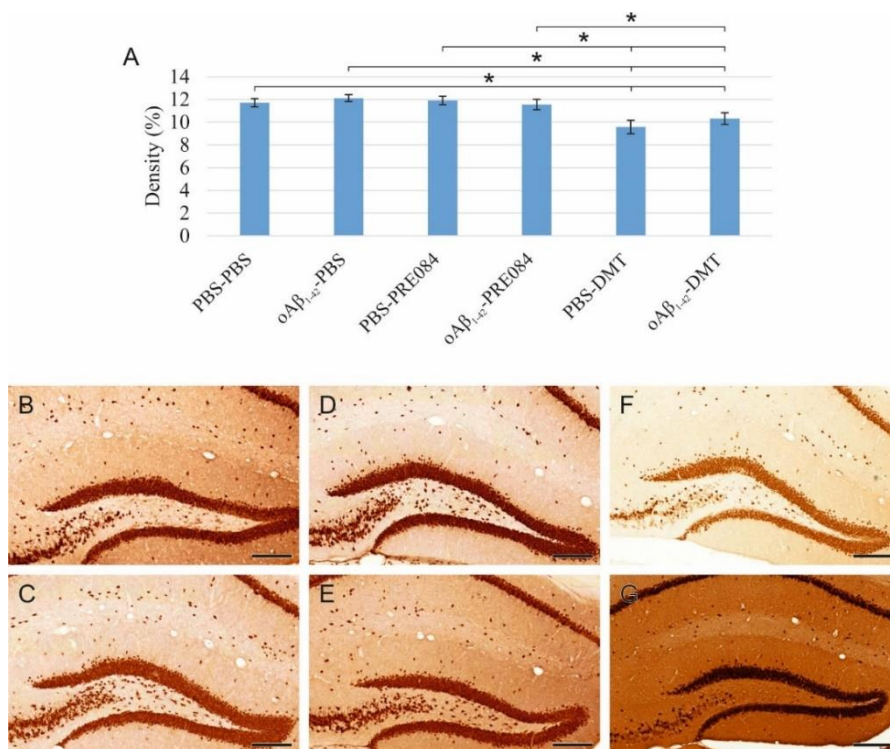


**Figure 10.** (A) Results for NeuN immunostaining. Significant differences were detected among the groups. (B–G) Representative photomicrographs of NeuN immunolabeling: (B) PBS-PBS, (C)  $\text{oA}\beta_{1-42}$ -PBS (D) PBS-PRE084, (E)  $\text{oA}\beta_{1-42}$ -PRE084, (F) PBS-DMT, (G)  $\text{oA}\beta_{1-42}$ -DMT. Scale bars represent 200  $\mu\text{m}$ .

### 7.3.2 Effects of PRE084 and DMT on neuroinflammation induced by $\text{oA}\beta_{1-42}$

#### 7.3.2.1 $\text{O}\text{A}\beta_{1-42}$ stimulated microglia activation, and neither PRE084 nor DMT alleviated this effect, while DMT alone significantly decreased microglial density.

Neuroinflammation results from the activation of an immune response in the CNS, mediated by microglia and astrocytes. This process is induced by infective agents, neurodegenerative diseases, or injuries. To identify activated microglia in the HC, we stained Iba1, expressed explicitly by monocyte-derived and resident macrophages, including microglia. Our results showed a significant difference in the density of Iba1+ microglia among the groups (ANOVA:  $p=0.002$ ).  $\text{O}\text{A}\beta_{1-42}$  administration significantly increased the density of activated microglia compared to the vehicle-treated control groups (PBS-PBS *vs.*  $\text{oA}\beta_{1-42}$ -PBS  $p=0.015$ ; PBS-PRE084 *vs.*  $\text{oA}\beta_{1-42}$ -PRE084  $p=0.035$ ; PBS-DMT *vs.*  $\text{oA}\beta_{1-42}$ -DMT  $p=0.039$ ). In the PBS-DMT group, the density of Iba1+ microglia was significantly reduced compared to PBS-PBS-treated animals (PBS-PBS *vs.* PBS-DMT  $p=0.031$ ). Still, none of the treatments was found to be able to alleviate the proinflammatory effect of  $\text{oA}\beta_{1-42}$  (Fig. 11). Additionally, significances were also detected between the following groups:  $\text{oA}\beta_{1-42}$ -PBS *vs.* PBS-PRE084  $p=0.005$ , *vs.* PBS-DMT  $p\leq 0.0001$ ;  $\text{oA}\beta_{1-42}$ -PRE084 *vs.* PBS-DMT  $p=0.002$  (Fig. 11).

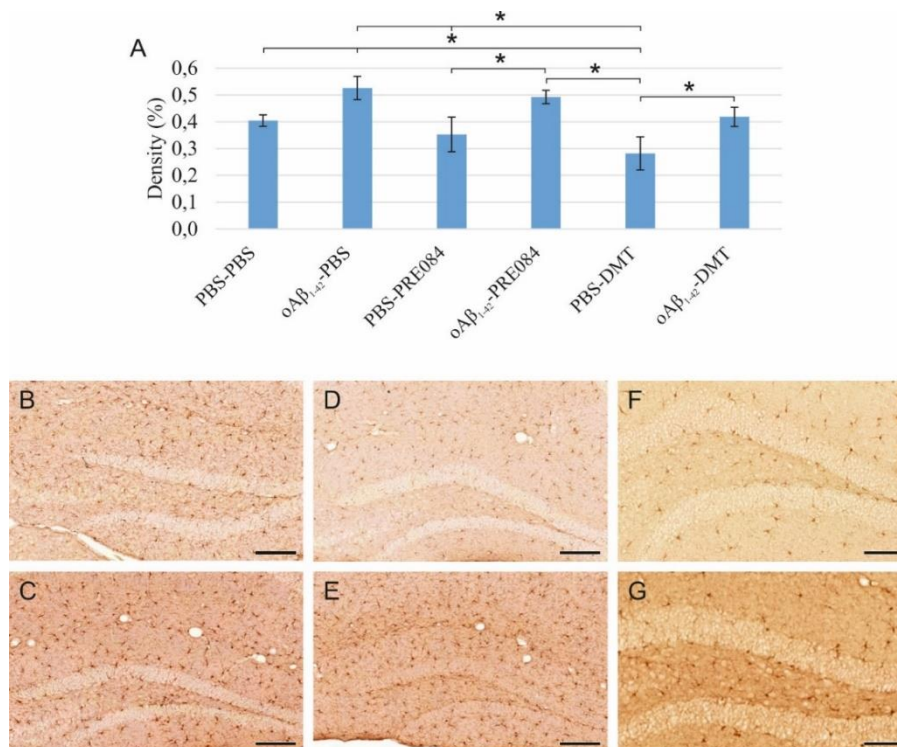


**Figure 11.** (A) Results for Iba1 immunolabeling. Significant differences were observed among the groups. (B–G) Representative images of Iba1 immunostaining: (B) PBS-PBS, (C)  $\text{oA}\beta_{1-42}$ -PBS, (D) PBS-PRE084, (E)  $\text{oA}\beta_{1-42}$ -PRE084, (F) PBS-DMT, (G)  $\text{oA}\beta_{1-42}$ -DMT. Scale bars represent 100  $\mu\text{m}$ .

7.3.2.2 *oA $\beta$ <sub>1-42</sub> stimulated astrocyte reactivation, while the administration of DMT or PRE084 reduced this effect.*

Reactive astrocytes were immunostained for GFAP, an intermediate filament protein expressed by different cell types, mainly reactive astrocytes, in the CNS. Significantly different GFAP+ cell densities were detected in the HC of the different groups (ANOVA:  $p=0.002$ ). A significant increase in the rate of reactivated astrocytes was detected in the *oA $\beta$ <sub>1-42</sub>-PBS* group compared to *PBS-PBS*-treated mice ( $p\leq 0.0001$ ). Also, GFAP+ cell densities were significantly lower in all other groups compared to *oA $\beta$ <sub>1-42</sub>-PBS*-treated mice (*oA $\beta$ <sub>1-42</sub>-PBS* vs. *PBS-PRE084*  $p=0.013$ , vs. *oA $\beta$ <sub>1-42</sub>-PRE084*  $p=0.013$ , vs. *PBS-DMT*  $p\leq 0.0001$ , vs. *oA $\beta$ <sub>1-42</sub>-DMT*,  $p=0.001$ ). The stimulatory effect of *oA $\beta$ <sub>1-42</sub>* on astrocyte reactivation was alleviated by PRE084 and DMT administration (Fig. 12).

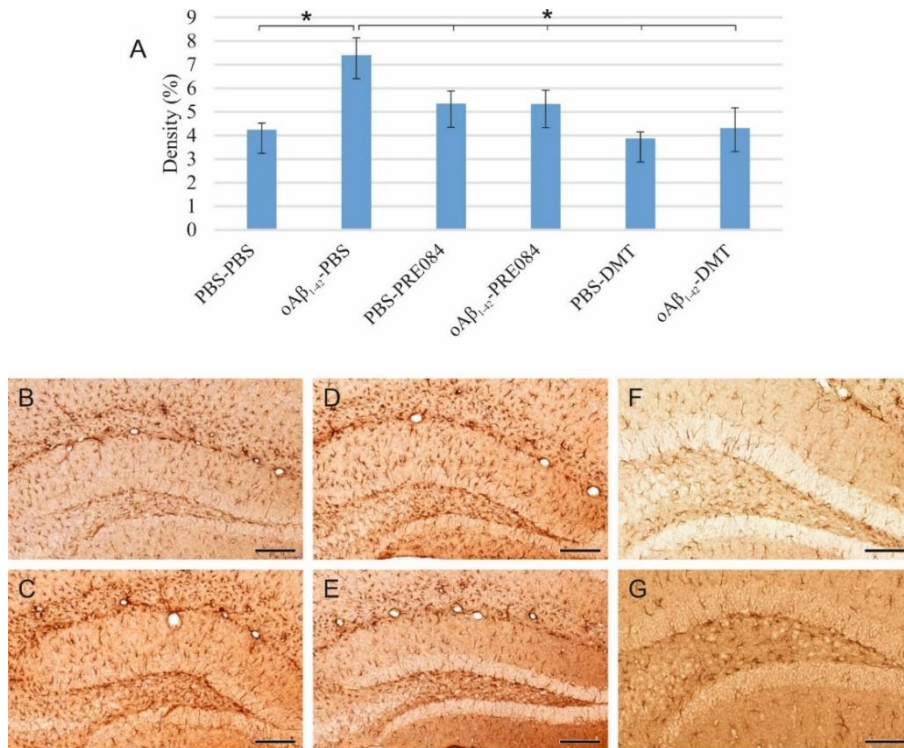


**Figure 12.** (A) Results of GFAP immunostaining. The densities of GFAP+ astrocytes differed among the groups. (B–G) Representative images of GFAP immunolabeling: (B) *PBS-PBS*, (C) *oA $\beta$ <sub>1-42</sub>-PBS*, (D) *PBS-PRE084*, (E) *oA $\beta$ <sub>1-42</sub>-PRE084*, (F) *PBS-DMT*, (G) *oA $\beta$ <sub>1-42</sub>-DMT*. Scale bars represent 100  $\mu$ m.



### 7.3.3 S1R protein level was elevated by oA $\beta$ <sub>1-42</sub> treatment, as well as by the co-administration of oA $\beta$ <sub>1-42</sub> and PRE084 or DMT

To determine the effects of oA $\beta$ <sub>1-42</sub> and PRE084 or DMT on the expression of S1R, a WB analysis using GAPDH as loading control was performed on samples of the animals. Our findings revealed a significant difference in the S1R levels among the groups (ANOVA:  $p \leq 0.0001$ ). S1R protein levels were significantly elevated in all groups, except in PBS-DMT-treated animals, as compared to control subjects (**PBS-PBS** vs. oA $\beta$ <sub>1-42</sub>-PBS  $p \leq 0.0001$ , vs. PBS-PRE084  $p = 0.018$ , vs. oA $\beta$ <sub>1-42</sub>-PRE084  $p \leq 0.0001$ , vs. PBS-DMT  $p = 0.540$ ; vs. oA $\beta$ <sub>1-42</sub>-DMT  $p \leq 0.0001$ , respectively). In comparison with oA $\beta$ <sub>1-42</sub>-PBS-treated mice, the oA $\beta$ <sub>1-42</sub>-PRE084 ( $p = 0.004$ ) and oA $\beta$ <sub>1-42</sub>-DMT ( $p = 0.673$ ) groups showed higher protein levels, while significantly lower levels of S1R were detected in PBS-PRE084 ( $p = 0.032$ ) and PBS-DMT ( $p = 0.001$ ) treated mice. As expected, the co-administration of oA $\beta$ <sub>1-42</sub> and either of the S1R agonists increased the S1R protein level compared to the respective control group (oA $\beta$ <sub>1-42</sub>-PRE084 vs. PBS-PRE084  $p \leq 0.0001$ ; oA $\beta$ <sub>1-42</sub>-DMT vs. PBS-DMT  $p = 0.015$ ). Notably, the expression of S1R was significantly increased in oA $\beta$ <sub>1-42</sub>-PRE084-treated animals compared to the oA $\beta$ <sub>1-42</sub>-DMT group ( $p \leq 0.0001$ ). (Fig. 13). Also, significant differences were detected in the S1R expression upon the pairwise comparisons of the following groups: **oA $\beta$ <sub>1-42</sub>-PBS** vs. PBS-PRE084  $p = 0.032$ , vs. PBS-DMT  $p = 0.001$ ; **oA $\beta$ <sub>1-42</sub>-PRE084** vs. PBS-DMT  $p \leq 0.0001$ , respectively (Fig. 13).

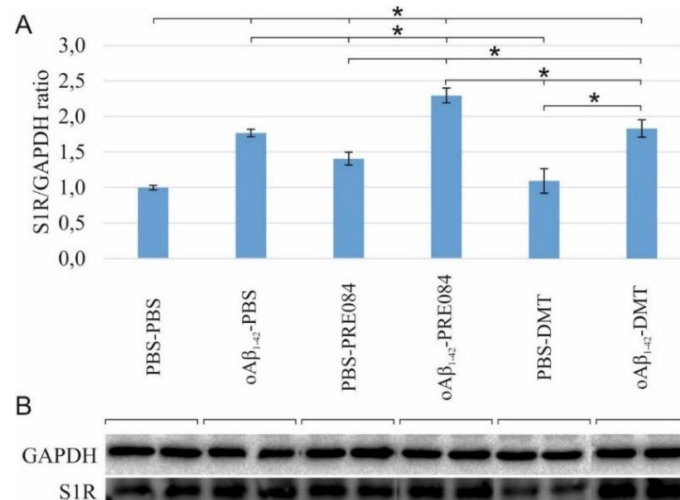


**Figure 13.** (A) Results for the WB analysis. Significant differences were observed in the S1R levels among the groups. (B) WB gel electrophoresis images of S1R and GAPDH lines of the experimental groups.

## 8 DISCUSSION

Alzheimer's disease is the most common form of dementia characterized by cognitive dysfunctions [23]. The main pathological hallmarks of AD are extracellular amyloid plaques and intracellular NFTs [10] accumulated in the cerebral tissue. They appear initially in the hippocampal and entorhinal regions of the brain [3, 7], accounting for the impairment of cognitive functions. Pharmacological interventions to slow the progression of AD are intensively studied. Recognizing potential targets or ligands (e.g., S1R) as promising therapeutic agents that may alleviate the severity of AD, is one of the main aims of the research. Another goal is to create and use valid animal models that mimic specific features of AD, whereby novel strategies for its curation could be found. Results in the field have pointed out that an early diagnosis and a possible treatment before the onset of dementia would be equally necessary. Furthermore, AD patients have an impaired ability to learn and retrieve information in a changing context, and interfering effects (e.g., simultaneous solving of concurrent tasks) worsen their learning and memory retention [255-257]. Therefore, in an optimal case, behavioral protocols, applied in non-human experiments, should also simulate this complex context. With our models, we attempted to achieve all goals mentioned above: to rapidly establish the symptoms of AD in the murine brain by the injection of different A $\beta$  forms, and to test the neurobiological and behavioral impacts of both A $\beta$  and different compounds in these models.

### 8.1 Non-transgenic AD rodent models induced by the administration of exogenous A $\beta$ <sub>1-42</sub>

Firstly, AD-like symptoms were induced by extracellular administration of oA $\beta$ <sub>1-42</sub> or fA $\beta$ <sub>1-42</sub> in two widely used rodent models [191, 203, 204, 206, 210]. One might ask, why the application of injected models can be advantageous instead of transgenic lines. One possible answer is that gene-modified strains do not provide opportunities to test the immediate impact of different A $\beta$  aggregates on the progression of symptoms. Considering our incomplete knowledge regarding this issue, it would be important to set up animal models where AD-like changes develop after the injection of a well-defined aggregated A $\beta$  form into the brain [203]. At the beginning of our experiments, the fibrillar form of A $\beta$ <sub>1-42</sub> - contributing to the senile plaques and associated with local synapse and dendritic spine loss - was applied, because it was well characterized and thought to be the most toxic form of A $\beta$  peptides [1, 97, 258, 259]. Our results proved that synthetic fA $\beta$ <sub>1-42</sub> decreased spatial learning ability and dendritic spine density in the rat HC

CA1 region. However, at the time of those experiments, conflicting results arose regarding the neurotoxicity of  $\beta$ -amyloid plaque depositions, although the toxic effect of the fA $\beta$  forms on synapses had previously been widely acknowledged [62, 260]. In that era, several studies demonstrated that the accumulation of pathogenic A $\beta$  assemblies, mainly soluble oligomeric iA $\beta$  in the HC, and the EC, is linked to the progression of AD [15, 56, 261-263]. It is also proved that together with fA $\beta$  assemblies there are also A $\beta$  oligomers present [264], keeping up a dynamic aggregation equilibrium between the two forms. Encouraged by the paradigm shift in the amyloid cascade hypothesis, we decided to establish models applying pure oA $\beta$ <sub>1-42</sub>, in order to induce AD-like changes (e.g., cognitive dysfunctions, neuroinflammation, and impaired neurogenesis) in our further experiments.

In the experiments conducted with synthetic A $\beta$ , not only its aggregation grade can be varied, but the length of the peptide sequence as well. Several research groups administer shorter A $\beta$  fragments, e.g., A $\beta$ <sub>25-35</sub> [147, 159, 191, 265], but A $\beta$ <sub>25-35</sub> is a non-natural, truncated sequence, and although it is prone to aggregation, its aggregation kinetics differ from that of the native A $\beta$ <sub>1-42</sub> peptide. Therefore, using this latter peptide should yield biologically more relevant findings [266]. Nowadays, it is accepted that an imbalance between the production and clearance of A $\beta$  results in its accumulation and aggregation [40, 267]. It is also recognized that soluble oA $\beta$ , iA $\beta$ , and plaques containing fA $\beta$  are together responsible for the observed neurotoxicity; they can damage the neurons, dendritic spines, and synapses, which leads to neurodegeneration and dementia [40, 268, 269].

In our experiments, three different brain areas were selected for A $\beta$ <sub>1-42</sub> administration. Among these, the temporal neocortical targets (HC and EC) play major parts in cognitive dysfunction observed at the early stage of AD. Both regions, with their extensive cortical and subcortical connections, are involved in spatial (working) learning and memory processing [98, 270, 271]. Lesions in EC or HC impair memory functions, including spatial and recognition memory [204, 205, 211, 272-274]. Numerous articles reported that ICV administration of A $\beta$ <sub>1-42</sub> induces early AD-like changes [221, 223, 275-279]. In our *IHC and EC experiments*, besides impairments of spatial learning and memory, pathological changes were also detected, such as impaired numbers of dendritic spines, and elevated levels of hyperreactive astrocytes. Furthermore, in our *ICV experiment*, AD-like cerebral neurogenic and neuroinflammatory changes could be observed as early as two weeks after the ICV administration of oA $\beta$ <sub>1-42</sub>.

Regarding the injection modes, there is no consensus in the literature, on which one is more suitable for the experiments with exogenous A $\beta$ . Some groups criticize ICV injection and prefer IHC instead, stating that the latter would be more effective in contributing to memory

dysfunction [280]. This statement can be explained by major anatomical differences between the two areas. In the walls of ventricles, special ependymal cells (tanocytes) can be found, which transfer chemical signals from the cerebrospinal fluid to the CNS and probably inhibit the penetration of the molecules with large molecular mass to the brain tissue. Still, intraparenchymal (IHC or EC) injection might directly injure relevant brain circuits and connections which are responsible for the cognitive processes. Moreover, an intensive clearance might strongly influence the effective concentration of the intraparenchymally injected A $\beta$  [267]. Considering our results, we could observe biological effects in all experimental setups. Nevertheless, based on our experience, we prefer the ICV injection because the administration of substances is easy, it is a less invasive technique thus causing fewer mechanical lesions in the relevant brain areas. Furthermore, we experienced the most robust behavioral and histological impact of A $\beta$  by this injection mode.

## **8.2 Application of the traditional and modified MWM protocols to model early symptoms of AD; behavioral and molecular outcomes**

Behavioral assays such as MWM [99, 230, 232, 255], novel object recognition [281], and Y-maze tests are applied in both fundamental and targeted pharmaceutical studies of AD. Besides the abovementioned cognitive tests, the MWM is extensively used to measure learning and memory processes in non-human experiments. Although spatial memory and learning deficits were detected in our experiments, in case of a traditional MWM protocol, we came to the conclusion that MWM with a fixed platform location may not be suitable enough to mimic contextual variations. The modified versions of MWM (e.g., matching-to-sample, or smaller platform) increase the task difficulty so they may imitate the contextual changes more effectively, thereby becoming useful models to detect the earliest AD symptoms (i.e., deficits in spatial working memory and learning). In our *EC experiment*, differences could not be detected between the oA $\beta_{1-42}$ -treated and the control groups on 1-5 days, in any of the related cognitive processes, like accuracy of learning, spatial working memory, switching ability, and flexibility. A subtle but significant spatial deficit could only be observed when the target was reduced. During the 2<sup>nd</sup> trial of the 6<sup>th</sup> day, the oA $\beta_{1-42}$ -treated rats found the smaller platform significantly slower, and they possessed lower switching ability and flexibility in learning under changed context than the control subjects. It seems that spatial impairment of the oA $\beta_{1-42}$ -treated animals could be detected only when the task difficulty was increased. As a consequence, we hypothesize, that our rat model mimics the prodromal phase of AD ('mild cognitive impairment'), that is when only minor, hardly detectable memory malfunctions can be detected.



At the beginning of our work, we focused on the detection of cognitive dysfunction; but even then, molecular examinations were also conducted to support the *in vivo* behavioral tests. In the *IHC experiment*, fA $\beta$  injection resulted in the loss of dendritic spine density in the HC of rats. Although the injected sample contained mainly fibrillar aggregates, we cannot exclude the presence of diffusible A $\beta$  oligomers, which would also be responsible for the direct neurotoxic effects. The measured spine loss in the CA1 region can explain the decreased learning ability since the formation and maturation of dendritic spines of the pyramidal cells are necessary for the development of the spatial memory unit. In the *EC experiment*, the injected oA $\beta_{1-42}$  elevated the number of reactive astrocytes in the EC of the rats, proving that already a single injection of neurotoxic species can initiate immunological processes, which can lead to inflammation. In our later work (*ICV experiment*), neurogenesis and neuroinflammation were examined in parallel. Lately, it has been recognized that adult neurogenesis declines with age, being partially responsible for cognitive impairments [282]. In AD, the cognitive symptoms become much more pronounced due to a decreased rate of neurogenesis, increased destruction of mature neurons, and enhanced neuroinflammatory responses. The early alternation in adult neurogenesis and the neuroinflammation may appear several years before the diagnosis of AD, and probably they both contribute to the onset of neurological symptoms. We demonstrated that a single administration of oA $\beta_{1-42}$  directly into the lateral ventricles significantly impaired the proliferation and increased the number of immature cells in mice. The effects of A $\beta$  on neurogenesis are highly controversial in the literature. Numerous reports indicate that A $\beta$  significantly decreases the formation of new neurons, possibly by impairing their ability to divide, as well as by diminishing the survival of NSCs in DG [191, 265, 283-287]. However, some research groups have published that A $\beta$  can induce the initial proliferation step of neuron formation in transgenic mouse strains [191, 285, 288-290] or in cellular models of AD [291-296]. In our experiments, an increase in the number of differentiating immature neurons was observed in oA $\beta_{1-42}$ -treated animals, which may be explained by a compensatory cerebral mechanism [297, 298]. Specifically, this enhancement of neuronal cell differentiation may be a response to the disturbed homeostasis resulting from the decrease of the stem cell population, aiming to restore the balance within the CNS. As we expected, in our experimental model no significant reduction was detected in the density of mature, functional neurons in HC two weeks after the administration of oA $\beta_{1-42}$ , indicating that the existing neuronal system may remain unaffected. Regarding neuroinflammation, we found that a single administration of oA $\beta_{1-42}$  stimulated neuroinflammatory processes, causing a significant increase in the densities of activated microglia and hyperreactive astrocytes. In line with our observations, several *in vivo*

experiments have demonstrated the neuroinflammation-inducing effects of A $\beta$  fibrils and oligomers injected into the brain tissue in different experimental models [299-301]. This neuroinflammatory environment may affect adult neurogenesis either positively or negatively [115, 302-308]. It is known that cytokines and chemokines produced by activated microglia and astrocytes play an important role in neuroinflammatory processes. Certain anti- (IL-4, IL-10) and proinflammatory (IL-6, TNF- $\alpha$ ) factors substantially influence neurogenesis, e.g., they can diminish proliferation and cell survival, while they may also stimulate cell differentiation [131]. Thus, beyond its direct effects on immature neurons, A $\beta_{1-42}$  may also affect neurogenesis by generating a relatively mild, but chronic neuroinflammatory environment. Further research is needed to clarify the relative contribution of these two processes (direct and indirect) to the resulting decline of adult neurogenesis in AD.

### **8.3 Neuroprotection with small molecular substances acting on different pathways**

The uniquely structured S1R protein, functioning as a ligand-operated chaperone, is known to play a major role in both neurogenesis and neuroinflammation. Thus, it is assumed that the activation of S1Rs may be a promising therapeutic strategy to stimulate adult neurogenesis and alleviate neuroinflammatory processes. As changes in S1R expression levels have not been studied in exogenous A $\beta$ -induced AD models, in the *ICV experiment*, we examined the expression of this protein and experienced an increase after a single administration of A $\beta_{1-42}$ . This finding may contradict some literature data, which report on the down-regulation of S1R in the early stage of human AD [144]. In the reported cases, both the amount and the binding potential of S1R were found to be decreased, presumably as a consequence of hippocampal neuronal death [144, 156, 157, 309, 310]. In contrast, other studies indicate that AD-related ER stress can lead to an up-regulation of S1R [76, 142, 311, 312], which, serving as a chaperon, modulates the canonical UPR pathways (PERK, IRE1a, ATF6) [76, 313]. In our study, the observed elevation of the level of S1R may be a consequence of the cytotoxic effect of A $\beta_{1-42}$ , which induces ER stress, and thus activates the UPR pathways and upregulates S1R expression. It is hypothesized that certain molecules, which act either as intensive protectors of neurons and glial cells (LPYFDa) or effectors against neuroinflammation (DMT, PRE084) could slow down the rate of decline of cognitive skills in AD.

In our previous studies, LPYFDa had exerted a neuroprotective effect on differentiated neuroblastoma cells, and on primary cortical neurons [249, 314], and it also protected neurons and synapses of HC against the toxic effect of A $\beta_{1-42}$  *in vivo* [249, 250, 314]. LPYFDa was able to prevent A $\beta_{1-42}$ -induced memory impairments when oA $\beta_{1-42}$  was injected in mice 1 hour

before the behavior test [314]. In our experiments, LPYFDa *per se* did not prove to be harmful and also did not influence the exploratory behavior of the rats. In the *EC experiment*, on days 1 to 5, no differences in learning and memory performance could be detected between the groups. On the 6<sup>th</sup> day of mMWM, LPYFDa could block the toxic effect of  $\text{oA}\beta_{1-42}$  and thus maintain the ability of learning and memory in a changed context.

To date, the biological effects of DMT and PRE084 have not been studied in an  $\text{A}\beta$ -induced model of early AD with demonstrated changes in neurogenesis and S1R expression levels, as well as neuroinflammation. Therefore, we aimed to assess whether the modulation of S1Rs with these ligands could restore  $\text{A}\beta_{1-42}$ -induced alternations in adult neurogenesis and reduce neuroinflammation. In our study, DMT significantly diminished the number of NSCs and densities of neurons. Similar to our finding, another tryptamine, psilocybin (4-phosphoryloxy-N, N-dimethyltryptamine) with a chemical structure close to that of DMT and a high binding affinity to 5-HT<sub>2A</sub> receptors (K<sub>d</sub>=6 nM), was also found to impair synaptic growth and neurogenesis (proliferation and neuronal survival) [315]. However, the neuroprotective and neurogenesis-stimulating effects of DMT and its analog, 5-methoxy-DMT, exerted via S1Rs, were also described in *in vitro* cell cultures and in a wild-type rodent model [170, 172, 175, 180]. In our study, DMT was administered at a concentration of 1 mg kg<sup>-1</sup>, thus it is supposed to have occupied both S1R and 5-HT<sub>2A</sub>, so their mixed effects could have been observed. Comparison of the K<sub>d</sub> values (DMT-S1R K<sub>d</sub>=14.75  $\mu\text{M}$ , DMT-5-HT<sub>2A</sub> receptor K<sub>d</sub>=130 nM) indicates that DMT binds to the 5-HT<sub>2A</sub> receptor with higher affinity than to S1R, thus, it is more likely to act on the 5-HT<sub>2A</sub> receptors than on S1R [165, 179]. Therefore, we suppose that DMT exerted its negative effect on neurogenesis via the 5-HT<sub>2A</sub> receptors. The results of our WB analysis support this hypothesis since the expression of the S1R protein was only slightly elevated after DMT treatment.

Regarding the relationship between DMT and neuroinflammation, conflicting findings are published in the literature. Some of them support the theory that DMT can alleviate neuroinflammatory processes, thus it may reduce the density of reactive astrocytes [153, 167-169, 178]. This effect may be related to the ability of DMT to bind to S1R [167-169, 178], but the serotonergic receptors may also have roles in this process [316]. Morales-Garcia *et al.* reported that DMT induces a significant increase in the density of GFAP<sup>+</sup> astrocytes via the activation of S1R, but these researchers conclude that this elevated GFAP level promotes neurogenesis [175]. In our experiments, DMT treatment was found to exert a positive effect on activated microglia and hyperreactive astrocytes against the  $\text{A}\beta_{1-42}$ -induced neurotoxicity, but it was not detected to promote neurogenesis. These contradictory results may be explained by

the application of different protocols (injection and doses of BrdU and DMT, different survival times). It is also known that although DMT can penetrate the blood-brain barrier, upon exogenous administration its concentration in the CNS is elevated for a relatively short time only (elimination half-life ~15 min [170]). Therefore, it is also possible that in our model, the concentration of DMT in the CNS after IP administration was not sufficient to exert its effects on S1R as Morales-Garcia reported [175]. Further experiments are required to elucidate the exact mode of action of DMT regarding neurogenesis and neuroinflammation.

To study the effect of an exogenous S1R agonist on neurogenesis and neuroinflammation, we applied PRE084 ( $K_d=2.2$  nM, [317]). Similarly, as Li *et al.* reported in an  $A\beta_{25-35}$ -induced mouse model of AD, we have demonstrated that PRE084 promotes neurogenesis upon treatment with  $A\beta_{1-42}$ , as it is indicated by the quantitative increase of stem cells and immature neurons after PRE084 administration. Regarding neuroinflammation, the density of hyperreactive astrocytes and the degree of  $A\beta_{1-42}$ -induced astrogliosis were reduced by the administration of PRE084. However, the substance neither *per se* nor in combination with  $A\beta_{1-42}$  could impair microglial activation. It is known that in case of CNS tissue damage, activated microglia may behave either neurotoxic or neuroprotective, depending on their morphological and functional states. According to the literature, PRE084 can stimulate the proliferation of the anti-inflammatory type of microglia (M2), while it suppresses pro-inflammatory M1 microglia, thus it maintains the delicate balance between functional restorative and inflammatory glial phenotypes [154, 318]. As we did not analyze the distribution and morphology of the microglia, we assume that the apparent ineffectiveness of PRE084 treatment on microglial activation may result from the abovementioned two mutual processes. PRE084 binds to S1R with high affinity, either alone (compared to PBS and DMT controls) and when co-administered with  $A\beta_{1-42}$  (compared to  $A\beta_{1-42}$ -PBS or  $A\beta_{1-42}$ -DMT animals), and significantly induces the expression of this receptor protein. These results may confirm that PRE084 activates the S1R receptors effectively, so its neurogenic impact is more pronounced than that of DMT.

## 9 SUMMARY

In our research, we proved that murine models developed by the intraparenchymal and the ICV administration of oligomeric or fibrillary  $A\beta_{1-42}$  are valid and reproducible, thus useful paradigms for the detection of early behavioral and molecular symptoms of AD.

In case of the behavioral experiments, we suggested an mMWM protocol, which can be properly used for the sensitive measurement of mild cognitive deficits caused by  $oA\beta_{1-42}$  in a rat model. This method for rodents might successfully mimic the changing context in which AD patients have spatial learning and memory difficulties. The  $oA\beta_{1-42}$ -treated rats showed mild spatial learning and memory impairments when the ratio of searching, and target areas were changed. The protective effect of the pentapeptide LPYFDa was also proven by behavioral and histological experiments.

In the ICV study, we established a model of early AD induced by  $oA\beta_{1-42}$ , in which acute neuroinflammation, impaired neurogenesis, and elevated S1R levels were detected.

Adult neurogenesis is essential for CNS plasticity. During the treatment of AD, neurogenesis should be promoted, while neuroinflammation should be suppressed. S1R plays an important role in both processes. In our model, two S1R agonists were tested. DMT, binding moderately to S1R but presumably with a high affinity to 5-HT receptors, negatively influenced the early phase of neurogenesis. In contrast, the highly selective S1R agonist, PRE084 improved the proliferation and differentiation of hippocampal stem cells, manifesting in a quantitative increase of progenitor cells and immature neurons. Further experiments are required to investigate the main molecular pathways targeted by DMT, through which it affects neurogenesis and the survival of mature neurons. Moreover, DMT and PRE084 were found to significantly reduce  $A\beta_{1-42}$ -induced hyperreactive astrogliosis, however, none of these ligands had a remarkable effect on microglial activation. Therefore, further studies are needed to clarify the role of DMT and PRE084 in neuroinflammatory processes induced by  $A\beta_{1-42}$  and to assess the translatability of the results to human AD cases.

## 10 ACKNOWLEDGEMENTS

I would like to thank the following persons without whom I would not have been able to complete and make it through my Ph.D. degree.

I am thankful to my first supervisors and mentors, Prof. Dr. József Toldi and Dr. Katalin Kóródi, for initiating my scientific career.

I am especially grateful to Prof. Dr. Botond Penke and Dr. Zsuzsa Penke-Verdier for their professional mentorship, scientific guidance, encouragement, and support throughout my Ph.D. studies.

I would like to express my special thanks to my last supervisor and mentor, Dr. Lívía Fülöp who made this work possible. I am grateful for her significant support.

I wish to thank all the members of the laboratory, especially Titanilla Szilágyi-Szögi for her excellent help and friendship.

I thank the members of the Department of Medical Chemistry for their help.

Finally, I am extremely grateful to my entire family for their untiring support.

This research was supported by the following grants:

European Union Seventh Framework Programme Food Grant 211 696 (LipiDiDiet) as well as by the Hungarian research grant TÁMOP 4.2.2/A-11/1/KONV-2012-0052.

National Research, Development, and Innovation Office (GINOP-2.3.2-15-2016-00060) and by the Hungarian Brain Research Programs I and II - Grant No. KTIA\_13\_NAP-A-III/7, and 2017-1.2.1-NKP-2017-00002.

## 11 REFERENCES

1. Terry, R.D., et al., *Physical basis of cognitive alterations in Alzheimer's disease: synapse loss is the major correlate of cognitive impairment*. Ann Neurol, 1991. **30**(4): p. 572-80.
2. Alzheimer's, A., *2012 Alzheimer's disease facts and figures*. Alzheimers Dement, 2012. **8**(2): p. 131-68.
3. Lam, B., et al., *Clinical, imaging, and pathological heterogeneity of the Alzheimer's disease syndrome*. Alzheimers Res Ther, 2013. **5**(1): p. 1.
4. Pause, B.M., et al., *Perspectives on episodic-like and episodic memory*. Front Behav Neurosci, 2013. **7**: p. 33.
5. Querfurth, H.W. and F.M. LaFerla, *Alzheimer's disease*. N Engl J Med, 2010. **362**(4): p. 329-44.
6. Calabro, M., et al., *The biological pathways of Alzheimer disease: a review*. AIMS Neurosci, 2021. **8**(1): p. 86-132.
7. Mattson, M.P., *Pathways towards and away from Alzheimer's disease*. Nature, 2004. **430**(7000): p. 631-9.
8. Selkoe, D.J., *Alzheimer's disease results from the cerebral accumulation and cytotoxicity of amyloid beta-protein*. J Alzheimers Dis, 2001. **3**(1): p. 75-80.
9. Castellani, R.J., R.K. Rolston, and M.A. Smith, *Alzheimer disease*. Dis Mon, 2010. **56**(9): p. 484-546.
10. Alzheimer, A., et al., *An English translation of Alzheimer's 1907 paper, "Uber eine eigenartige Erkrankung der Hirnrinde"*. Clin Anat, 1995. **8**(6): p. 429-31.
11. Braak, H. and E. Braak, *Staging of Alzheimer's disease-related neurofibrillary changes*. Neurobiol Aging, 1995. **16**(3): p. 271-8; discussion 278-84.
12. Mucke, L., *Neuroscience: Alzheimer's disease*. Nature, 2009. **461**(7266): p. 895-7.
13. Baloyannis, S.J., V. Costa, and I.S. Baloyannis, *Morphological alterations of the synapses in the locus coeruleus in Parkinson's disease*. J Neurol Sci, 2006. **248**(1-2): p. 35-41.
14. Butterfield, D.A., M. Perluigi, and R. Sultana, *Oxidative stress in Alzheimer's disease brain: new insights from redox proteomics*. Eur J Pharmacol, 2006. **545**(1): p. 39-50.
15. LaFerla, F.M., K.N. Green, and S. Oddo, *Intracellular amyloid-beta in Alzheimer's disease*. Nat Rev Neurosci, 2007. **8**(7): p. 499-509.
16. Braak, H. and E. Braak, *Neuropathological stageing of Alzheimer-related changes*. Acta Neuropathol, 1991. **82**(4): p. 239-59.
17. Duyckaerts, C., B. Delatour, and M.C. Potier, *Classification and basic pathology of Alzheimer disease*. Acta Neuropathol, 2009. **118**(1): p. 5-36.
18. Selkoe, D.J. and D. Schenk, *Alzheimer's disease: molecular understanding predicts amyloid-based therapeutics*. Annu Rev Pharmacol Toxicol, 2003. **43**: p. 545-84.
19. Lambert, J.C., et al., *Evidence of the association of BIN1 and PICALM with the AD risk in contrasting European populations*. Neurobiol Aging, 2011. **32**(4): p. 756 e11-5.
20. Prince, M., et al., *Recent global trends in the prevalence and incidence of dementia, and survival with dementia*. Alzheimers Res Ther, 2016. **8**(1): p. 23.
21. Proctor, C.J. and D.A. Gray, *A unifying hypothesis for familial and sporadic Alzheimer's disease*. Int J Alzheimers Dis, 2012. **2012**: p. 978742.
22. Selkoe, D.J. and J. Hardy, *The amyloid hypothesis of Alzheimer's disease at 25 years*. EMBO Mol Med, 2016. **8**(6): p. 595-608.
23. Karlawish, J., *2017 Alzheimer's disease facts and figures*. 2017, Alzheimer's Association. p. 88.

24. Kishimoto, Y., et al., *Early Contextual Fear Memory Deficits in a Double-Transgenic Amyloid-beta Precursor Protein/Presenilin 2 Mouse Model of Alzheimer's Disease*. Int J Alzheimers Dis, 2017. **2017**: p. 8584205.
25. Rhein, V., et al., *Amyloid-beta and tau synergistically impair the oxidative phosphorylation system in triple transgenic Alzheimer's disease mice*. Proc Natl Acad Sci U S A, 2009. **106**(47): p. 20057-62.
26. Ciechanover, A. and Y.T. Kwon, *Degradation of misfolded proteins in neurodegenerative diseases: therapeutic targets and strategies*. Exp Mol Med, 2015. **47**: p. e147.
27. Onos, K.D., et al., *Toward more predictive genetic mouse models of Alzheimer's disease*. Brain Res Bull, 2016. **122**: p. 1-11.
28. Bowen, D.M., et al., *Neurotransmitter-related enzymes and indices of hypoxia in senile dementia and other abiotrophies*. Brain, 1976. **99**(3): p. 459-96.
29. Whitehouse, P.J., et al., *Alzheimer disease: evidence for selective loss of cholinergic neurons in the nucleus basalis*. Ann Neurol, 1981. **10**(2): p. 122-6.
30. Doody, R.S., *Current treatments for Alzheimer's disease: cholinesterase inhibitors*. J Clin Psychiatry, 2003. **64 Suppl 9**: p. 11-7.
31. Francis, P.T., et al., *The cholinergic hypothesis of Alzheimer's disease: a review of progress*. J Neurol Neurosurg Psychiatry, 1999. **66**(2): p. 137-47.
32. Hardy, J. and D. Allsop, *Amyloid deposition as the central event in the aetiology of Alzheimer's disease*. Trends Pharmacol Sci, 1991. **12**(10): p. 383-8.
33. Hiltunen, M., T. van Groen, and J. Jolkkonen, *Functional roles of amyloid-beta protein precursor and amyloid-beta peptides: evidence from experimental studies*. J Alzheimers Dis, 2009. **18**(2): p. 401-12.
34. Oltersdorf, T., et al., *The secreted form of the Alzheimer's amyloid precursor protein with the Kunitz domain is protease nexin-II*. Nature, 1989. **341**(6238): p. 144-7.
35. Mattson, M.P., et al., *Evidence for excitoprotective and intraneuronal calcium-regulating roles for secreted forms of the beta-amyloid precursor protein*. Neuron, 1993. **10**(2): p. 243-54.
36. Mucke, L., et al., *Synaptotrophic effects of human amyloid beta protein precursors in the cortex of transgenic mice*. Brain Res, 1994. **666**(2): p. 151-67.
37. Esteban, J.A., *Living with the enemy: a physiological role for the beta-amyloid peptide*. Trends Neurosci, 2004. **27**(1): p. 1-3.
38. Wang, H., et al., *Consequences of inhibiting amyloid precursor protein processing enzymes on synaptic function and plasticity*. Neural Plast, 2012. **2012**: p. 272374.
39. Rahman, M.A., et al., *Emerging risk of environmental factors: insight mechanisms of Alzheimer's diseases*. Environ Sci Pollut Res Int, 2020. **27**(36): p. 44659-44672.
40. Hardy, J. and D.J. Selkoe, *The amyloid hypothesis of Alzheimer's disease: progress and problems on the road to therapeutics*. Science, 2002. **297**(5580): p. 353-6.
41. Walsh, D.M., et al., *Naturally secreted oligomers of amyloid beta protein potently inhibit hippocampal long-term potentiation in vivo*. Nature, 2002. **416**(6880): p. 535-9.
42. Hartley, D.M., et al., *Protofibrillar intermediates of amyloid beta-protein induce acute electrophysiological changes and progressive neurotoxicity in cortical neurons*. J Neurosci, 1999. **19**(20): p. 8876-84.
43. Krafft, G.A. and W.L. Klein, *ADDLs and the signaling web that leads to Alzheimer's disease*. Neuropharmacology, 2010. **59**(4-5): p. 230-42.
44. Schliebs, R. and T. Arendt, *The cholinergic system in aging and neuronal degeneration*. Behav Brain Res, 2011. **221**(2): p. 555-63.
45. Patel, A.N. and J.H. Jhamandas, *Neuronal receptors as targets for the action of amyloid-beta protein (Abeta) in the brain*. Expert Rev Mol Med, 2012. **14**: p. e2.



46. Volgyi, K., et al., *Dysfunction of Endoplasmic Reticulum (ER) and Mitochondria (MT) in Alzheimer's Disease: The Role of the ER-MT Cross-Talk*. Curr Alzheimer Res, 2015. **12**(7): p. 655-72.
47. Mossmann, D., et al., *Amyloid-beta peptide induces mitochondrial dysfunction by inhibition of preprotein maturation*. Cell Metab, 2014. **20**(4): p. 662-9.
48. Penke, B., F. Bogar, and L. Fulop, *beta-Amyloid and the Pathomechanisms of Alzheimer's Disease: A Comprehensive View*. Molecules, 2017. **22**(10).
49. Hetz, C., *The unfolded protein response: controlling cell fate decisions under ER stress and beyond*. Nat Rev Mol Cell Biol, 2012. **13**(2): p. 89-102.
50. Selkoe, D.J., *Alzheimer's disease is a synaptic failure*. Science, 2002. **298**(5594): p. 789-91.
51. Hardy, J., *The amyloid hypothesis for Alzheimer's disease: a critical reappraisal*. J Neurochem, 2009. **110**(4): p. 1129-34.
52. Claeyssen, S., et al., *Alzheimer culprits: cellular crossroads and interplay*. Cell Signal, 2012. **24**(9): p. 1831-40.
53. Penke, B., F. Bogár, and L. Fülöp,  *$\beta$ -Amyloid and the Pathomechanisms of Alzheimer's Disease: A Comprehensive View*. Molecules, 2017. **22**(10).
54. Weintraub, S., A.H. Wicklund, and D.P. Salmon, *The neuropsychological profile of Alzheimer disease*. Cold Spring Harb Perspect Med, 2012. **2**(4): p. a006171.
55. Cleary, J.P., et al., *Natural oligomers of the amyloid-beta protein specifically disrupt cognitive function*. Nat Neurosci, 2005. **8**(1): p. 79-84.
56. Tampellini, D., et al., *Effects of synaptic modulation on beta-amyloid, synaptophysin, and memory performance in Alzheimer's disease transgenic mice*. J Neurosci, 2010. **30**(43): p. 14299-304.
57. Tampellini, D., et al., *Impaired beta-amyloid secretion in Alzheimer's disease pathogenesis*. J Neurosci, 2011. **31**(43): p. 15384-90.
58. Shankar, G.M., et al., *Amyloid-beta protein dimers isolated directly from Alzheimer's brains impair synaptic plasticity and memory*. Nat Med, 2008. **14**(8): p. 837-42.
59. Trojanowski, J.Q. and V.M. Lee, *Phosphorylation of paired helical filament tau in Alzheimer's disease neurofibrillary lesions: focusing on phosphatases*. FASEB J, 1995. **9**(15): p. 1570-6.
60. Iqbal, K., et al., *Tau pathology in Alzheimer disease and other tauopathies*. Biochim Biophys Acta, 2005. **1739**(2-3): p. 198-210.
61. Iqbal, K., et al., *Mechanisms of tau-induced neurodegeneration*. Acta Neuropathol, 2009. **118**(1): p. 53-69.
62. Snowdon, D.A. and S. Nun, *Healthy aging and dementia: findings from the Nun Study*. Ann Intern Med, 2003. **139**(5 Pt 2): p. 450-4.
63. Gong, C.X., I. Grundke-Iqbal, and K. Iqbal, *Targeting tau protein in Alzheimer's disease*. Drugs Aging, 2010. **27**(5): p. 351-65.
64. Liao, D., E.C. Miller, and P.J. Teravskis, *Tau acts as a mediator for Alzheimer's disease-related synaptic deficits*. Eur J Neurosci, 2014. **39**(7): p. 1202-13.
65. de la Torre, J.C. and G.B. Stefano, *Evidence that Alzheimer's disease is a microvascular disorder: the role of constitutive nitric oxide*. Brain Res Brain Res Rev, 2000. **34**(3): p. 119-36.
66. van Norden, A.G., et al., *Dementia: Alzheimer pathology and vascular factors: from mutually exclusive to interaction*. Biochim Biophys Acta, 2012. **1822**(3): p. 340-9.
67. van Groen, T., et al., *Transformation of diffuse beta-amyloid precursor protein and beta-amyloid deposits to plaques in the thalamus after transient occlusion of the middle cerebral artery in rats*. Stroke, 2005. **36**(7): p. 1551-6.

68. de la Torre, J., *The Vascular Hypothesis of Alzheimer's Disease: A Key to Preclinical Prediction of Dementia Using Neuroimaging*. J Alzheimers Dis, 2018. **63**(1): p. 35-52.
69. Du, X., X. Wang, and M. Geng, *Alzheimer's disease hypothesis and related therapies*. Transl Neurodegener, 2018. **7**: p. 2.
70. Rivers-Auty, J., et al., *Anti-inflammatories in Alzheimer's disease-potential therapy or spurious correlate?* Brain Commun, 2020. **2**(2): p. fcaa109.
71. Labbadia, J. and R.I. Morimoto, *The biology of proteostasis in aging and disease*. Annu Rev Biochem, 2015. **84**: p. 435-64.
72. Zhao, L. and S.L. Ackerman, *Endoplasmic reticulum stress in health and disease*. Curr Opin Cell Biol, 2006. **18**(4): p. 444-52.
73. Walter, P. and D. Ron, *The unfolded protein response: from stress pathway to homeostatic regulation*. Science, 2011. **334**(6059): p. 1081-6.
74. Ajuolabady, A., et al., *ER stress and UPR in Alzheimer's disease: mechanisms, pathogenesis, treatments*. Cell Death Dis, 2022. **13**(8): p. 706.
75. Marchi, S., S. Patergnani, and P. Pinton, *The endoplasmic reticulum-mitochondria connection: one touch, multiple functions*. Biochim Biophys Acta, 2014. **1837**(4): p. 461-9.
76. Penke, B., et al., *The Role of Sigma-1 Receptor, an Intracellular Chaperone in Neurodegenerative Diseases*. Curr Neuropharmacol, 2018. **16**(1): p. 97-116.
77. Loncke, J., et al., *Balancing ER-Mitochondrial Ca(2+) Fluxes in Health and Disease*. Trends Cell Biol, 2021. **31**(7): p. 598-612.
78. Area-Gomez, E. and E.A. Schon, *On the Pathogenesis of Alzheimer's Disease: The MAM Hypothesis*. FASEB J, 2017. **31**(3): p. 864-867.
79. Yu, W., H. Jin, and Y. Huang, *Mitochondria-associated membranes (MAMs): a potential therapeutic target for treating Alzheimer's disease*. Clin Sci (Lond), 2021. **135**(1): p. 109-126.
80. Small, S.A. and K. Duff, *Linking Abeta and tau in late-onset Alzheimer's disease: a dual pathway hypothesis*. Neuron, 2008. **60**(4): p. 534-42.
81. Liu, P.P., et al., *Erratum: Author Correction: History and progress of hypotheses and clinical trials for Alzheimer's disease*. Signal Transduct Target Ther, 2019. **4**: p. 37.
82. Moser, E.I., et al., *Impaired spatial learning after saturation of long-term potentiation*. Science, 1998. **281**(5385): p. 2038-42.
83. Amaral, D.G. and M.P. Witter, *The three-dimensional organization of the hippocampal formation: a review of anatomical data*. Neuroscience, 1989. **31**(3): p. 571-91.
84. Squire, L.R., C.E. Stark, and R.E. Clark, *The medial temporal lobe*. Annu Rev Neurosci, 2004. **27**: p. 279-306.
85. Moser, M.B. and E.I. Moser, *Functional differentiation in the hippocampus*. Hippocampus, 1998. **8**(6): p. 608-19.
86. Gidyk, D.C., et al., *Barriers to developing a valid rodent model of Alzheimer's disease: from behavioral analysis to etiological mechanisms*. Front Neurosci, 2015. **9**: p. 245.
87. Freund, T.F. and G. Buzsaki, *Interneurons of the hippocampus*. Hippocampus, 1996. **6**(4): p. 347-470.
88. Canto, C.B., F.G. Wouterlood, and M.P. Witter, *What does the anatomical organization of the entorhinal cortex tell us?* Neural Plast, 2008. **2008**: p. 381243.
89. Nimchinsky, E.A., B.L. Sabatini, and K. Svoboda, *Structure and function of dendritic spines*. Annu Rev Physiol, 2002. **64**: p. 313-53.
90. Alvarez, V.A. and B.L. Sabatini, *Anatomical and physiological plasticity of dendritic spines*. Annu Rev Neurosci, 2007. **30**: p. 79-97.

91. Luebke, J.I., et al., *Dendritic vulnerability in neurodegenerative disease: insights from analyses of cortical pyramidal neurons in transgenic mouse models*. Brain Struct Funct, 2010. **214**(2-3): p. 181-99.
92. Bhatt, D.H., S. Zhang, and W.B. Gan, *Dendritic spine dynamics*. Annu Rev Physiol, 2009. **71**: p. 261-82.
93. Butterfield, D.A., et al., *Evidence that amyloid beta-peptide-induced lipid peroxidation and its sequelae in Alzheimer's disease brain contribute to neuronal death*. Neurobiol Aging, 2002. **23**(5): p. 655-64.
94. Baloyannis, S.J., *Dendritic pathology in Alzheimer's disease*. J Neurol Sci, 2009. **283**(1-2): p. 153-7.
95. Smith, D.L., et al., *Reversal of long-term dendritic spine alterations in Alzheimer disease models*. Proc Natl Acad Sci U S A, 2009. **106**(39): p. 16877-82.
96. Jain, S., et al., *Cellular source-specific effects of apolipoprotein (apo) E4 on dendrite arborization and dendritic spine development*. PLoS One, 2013. **8**(3): p. e59478.
97. Chabrier, M.A., et al., *Synergistic effects of amyloid-beta and wild-type human tau on dendritic spine loss in a floxed double transgenic model of Alzheimer's disease*. Neurobiol Dis, 2014. **64**: p. 107-17.
98. Buzsaki, G. and E.I. Moser, *Memory, navigation and theta rhythm in the hippocampal-entorhinal system*. Nat Neurosci, 2013. **16**(2): p. 130-8.
99. Vorhees, C.V. and M.T. Williams, *Reprint of "Value of water mazes for assessing spatial and egocentric learning and memory in rodent basic research and regulatory studies"*. Neurotoxicol Teratol, 2015. **52**(Pt A): p. 93-108.
100. Silva, A. and M.C. Martinez, *Spatial memory deficits in Alzheimer's disease and their connection to cognitive maps' formation by place cells and grid cells*. Front Behav Neurosci, 2022. **16**: p. 1082158.
101. Li, Y., et al., *Xanthoceras sorbifolia extracts ameliorate dendritic spine deficiency and cognitive decline via upregulation of BDNF expression in a rat model of Alzheimer's disease*. Neurosci Lett, 2016. **629**: p. 208-214.
102. Altman, J., *Autoradiographic and histological studies of postnatal neurogenesis. IV. Cell proliferation and migration in the anterior forebrain, with special reference to persisting neurogenesis in the olfactory bulb*. J Comp Neurol, 1969. **137**(4): p. 433-57.
103. Altman, J. and G.D. Das, *Autoradiographic and histological evidence of postnatal hippocampal neurogenesis in rats*. J Comp Neurol, 1965. **124**(3): p. 319-35.
104. Chen, Q., et al., *Adult neurogenesis is functionally associated with AD-like neurodegeneration*. Neurobiol Dis, 2008. **29**(2): p. 316-26.
105. Lazarov, O. and R.A. Marr, *Of mice and men: neurogenesis, cognition and Alzheimer's disease*. Front Aging Neurosci, 2013. **5**: p. 43.
106. Kempermann, G., *Adult Neurogenesis: An Evolutionary Perspective*. Cold Spring Harb Perspect Biol, 2015. **8**(2): p. a018986.
107. Gage, F.H., *Adult neurogenesis in mammals*. Science, 2019. **364**(6443): p. 827-828.
108. Ming, G.L. and H. Song, *Adult neurogenesis in the mammalian central nervous system*. Annu Rev Neurosci, 2005. **28**: p. 223-50.
109. Bruel-Jungerman, E., S. Davis, and S. Laroche, *Brain plasticity mechanisms and memory: a party of four*. Neuroscientist, 2007. **13**(5): p. 492-505.
110. Chuang, T.T., *Neurogenesis in mouse models of Alzheimer's disease*. Biochim Biophys Acta, 2010. **1802**(10): p. 872-80.
111. Lazarov, O., et al., *When neurogenesis encounters aging and disease*. Trends Neurosci, 2010. **33**(12): p. 569-79.
112. Kempermann, G., et al., *Milestones of neuronal development in the adult hippocampus*. Trends Neurosci, 2004. **27**(8): p. 447-52.

113. Dard, R.F., L. Dahan, and C. Rampon, *Targeting hippocampal adult neurogenesis using transcription factors to reduce Alzheimer's disease-associated memory impairments*. *Hippocampus*, 2019. **29**(7): p. 579-586.
114. Shruster, A., E. Melamed, and D. Offen, *Neurogenesis in the aged and neurodegenerative brain*. *Apoptosis*, 2010. **15**(11): p. 1415-21.
115. Sung, P.S., et al., *Neuroinflammation and Neurogenesis in Alzheimer's Disease and Potential Therapeutic Approaches*. *Int J Mol Sci*, 2020. **21**(3).
116. Winner, B. and J. Winkler, *Adult neurogenesis in neurodegenerative diseases*. *Cold Spring Harb Perspect Biol*, 2015. **7**(4): p. a021287.
117. Mu, Y. and F.H. Gage, *Adult hippocampal neurogenesis and its role in Alzheimer's disease*. *Mol Neurodegener*, 2011. **6**: p. 85.
118. Sorrells, S.F., et al., *Human hippocampal neurogenesis drops sharply in children to undetectable levels in adults*. *Nature*, 2018. **555**(7696): p. 377-381.
119. Boldrini, M., et al., *Human Hippocampal Neurogenesis Persists throughout Aging*. *Cell Stem Cell*, 2018. **22**(4): p. 589-599 e5.
120. Choi, S.H. and R.E. Tanzi, *Is Alzheimer's Disease a Neurogenesis Disorder?* *Cell Stem Cell*, 2019. **25**(1): p. 7-8.
121. Moreno-Jiménez, E.P., et al., *Adult hippocampal neurogenesis is abundant in neurologically healthy subjects and drops sharply in patients with Alzheimer's disease*. *Nat Med*, 2019. **25**(4): p. 554-560.
122. Tobin, M.K., et al., *Human Hippocampal Neurogenesis Persists in Aged Adults and Alzheimer's Disease Patients*. *Cell Stem Cell*, 2019. **24**(6): p. 974-982.e3.
123. Kinney, J.W., et al., *Inflammation as a central mechanism in Alzheimer's disease*. *Alzheimers Dement (N Y)*, 2018. **4**: p. 575-590.
124. Hoozemans, J.J., et al., *Neuroinflammation and regeneration in the early stages of Alzheimer's disease pathology*. *Int J Dev Neurosci*, 2006. **24**(2-3): p. 157-65.
125. Nazem, A., et al., *Rodent models of neuroinflammation for Alzheimer's disease*. *J Neuroinflammation*, 2015. **12**: p. 74.
126. Gomez-Nicola, D. and D. Boche, *Post-mortem analysis of neuroinflammatory changes in human Alzheimer's disease*. *Alzheimers Res Ther*, 2015. **7**(1): p. 42.
127. Chandra, A., et al., *Applications of amyloid, tau, and neuroinflammation PET imaging to Alzheimer's disease and mild cognitive impairment*. *Hum Brain Mapp*, 2019. **40**(18): p. 5424-5442.
128. Ekdahl, C.T., et al., *Inflammation is detrimental for neurogenesis in adult brain*. *Proc Natl Acad Sci U S A*, 2003. **100**(23): p. 13632-7.
129. Liu, Y.P., H.I. Lin, and S.F. Tzeng, *Tumor necrosis factor-alpha and interleukin-18 modulate neuronal cell fate in embryonic neural progenitor culture*. *Brain Res*, 2005. **1054**(2): p. 152-8.
130. Villeda, S.A., et al., *The ageing systemic milieu negatively regulates neurogenesis and cognitive function*. *Nature*, 2011. **477**(7362): p. 90-4.
131. Fuster-Matanzo, A., et al., *Role of neuroinflammation in adult neurogenesis and Alzheimer disease: therapeutic approaches*. *Mediators Inflamm*, 2013. **2013**: p. 260925.
132. Bowen, W.D., S.B. Hellewell, and K.A. McGarry, *Evidence for a multi-site model of the rat brain sigma receptor*. *Eur J Pharmacol*, 1989. **163**(2-3): p. 309-18.
133. Hellewell, S.B. and W.D. Bowen, *A sigma-like binding site in rat pheochromocytoma (PC12) cells: decreased affinity for (+)-benzomorphans and lower molecular weight suggest a different sigma receptor form from that of guinea pig brain*. *Brain Res*, 1990. **527**(2): p. 244-53.

134. Hellewell, S.B., et al., *Rat liver and kidney contain high densities of sigma 1 and sigma 2 receptors: characterization by ligand binding and photoaffinity labeling*. Eur J Pharmacol, 1994. **268**(1): p. 9-18.
135. Schmidt, H.R., et al., *Crystal structure of the human  $\sigma 1$  receptor*. Nature, 2016. **532**(7600): p. 527-30.
136. Yang, K., C. Wang, and T. Sun, *The Roles of Intracellular Chaperone Proteins, Sigma Receptors, in Parkinson's Disease (PD) and Major Depressive Disorder (MDD)*. Front Pharmacol, 2019. **10**: p. 528.
137. Hayashi, T. and T.P. Su, *An update on the development of drugs for neuropsychiatric disorders: focusing on the sigma 1 receptor ligand*. Expert Opin Ther Targets, 2008. **12**(1): p. 45-58.
138. Tesei, A., et al., *Sigma Receptors as Endoplasmic Reticulum Stress "Gatekeepers" and their Modulators as Emerging New Weapons in the Fight Against Cancer*. Front Pharmacol, 2018. **9**: p. 711.
139. Alon, A., et al., *Structural Perspectives on Sigma-1 Receptor Function*. Adv Exp Med Biol, 2017. **964**: p. 5-13.
140. Salaciak, K. and K. Pytko, *Revisiting the sigma-1 receptor as a biological target to treat affective and cognitive disorders*. Neurosci Biobehav Rev, 2022. **132**: p. 1114-1136.
141. Su, T.P., et al., *The Sigma-1 Receptor as a Pluripotent Modulator in Living Systems*. Trends Pharmacol Sci, 2016. **37**(4): p. 262-278.
142. Hayashi, T. and T.P. Su, *Sigma-1 receptor chaperones at the ER-mitochondrion interface regulate Ca(2+) signaling and cell survival*. Cell, 2007. **131**(3): p. 596-610.
143. Maurice, T. and N. Gogvadze, *Role of  $\sigma$* . Adv Exp Med Biol, 2017. **964**: p. 213-233.
144. Jin, J.L., et al., *Roles of sigma-1 receptors in Alzheimer's disease*. Int J Clin Exp Med, 2015. **8**(4): p. 4808-20.
145. Maurice, T., et al., *Interaction with sigma(1) protein, but not N-methyl-D-aspartate receptor, is involved in the pharmacological activity of donepezil*. J Pharmacol Exp Ther, 2006. **317**(2): p. 606-14.
146. Maurice, T. and A. Privat, *SA4503, a novel cognitive enhancer with sigma1 receptor agonist properties, facilitates NMDA receptor-dependent learning in mice*. Eur J Pharmacol, 1997. **328**(1): p. 9-18.
147. Meunier, J., J. Ieni, and T. Maurice, *The anti-amnesic and neuroprotective effects of donepezil against amyloid beta25-35 peptide-induced toxicity in mice involve an interaction with the sigma1 receptor*. Br J Pharmacol, 2006. **149**(8): p. 998-1012.
148. Maurice, T. and N. Gogvadze, *Sigma-1 ( $\sigma$ )*. Handb Exp Pharmacol, 2017. **244**: p. 81-108.
149. Sha, S., et al., *Sigma-1 receptor knockout impairs neurogenesis in dentate gyrus of adult hippocampus via down-regulation of NMDA receptors*. CNS Neurosci Ther, 2013. **19**(9): p. 705-13.
150. Tsai, S.A. and T.P. Su, *Sigma-1 Receptors Fine-Tune the Neuronal Networks*. Adv Exp Med Biol, 2017. **964**: p. 79-83.
151. Ajmo, C.T., Jr., et al., *Sigma receptor activation reduces infarct size at 24 hours after permanent middle cerebral artery occlusion in rats*. Curr Neurovasc Res, 2006. **3**(2): p. 89-98.
152. Zhao, Q., et al., *The Protective Effects of Dexmedetomidine against Hypoxia/Reoxygenation-Induced Inflammatory Injury and Permeability in Brain Endothelial Cells Mediated by Sigma-1 Receptor*. ACS Chem Neurosci, 2021. **12**(11): p. 1940-1947.

153. Szabó, Í., et al., *N,N-Dimethyltryptamine attenuates spreading depolarization and restrains neurodegeneration by sigma-1 receptor activation in the ischemic rat brain*. *Neuropharmacology*, 2021. **192**: p. 108612.
154. Peviani, M., et al., *Neuroprotective effects of the Sigma-1 receptor (S1R) agonist PRE-084, in a mouse model of motor neuron disease not linked to SOD1 mutation*. *Neurobiol Dis*, 2014. **62**: p. 218-32.
155. Hall, H., et al., *AF710B, an M1/sigma-1 receptor agonist with long-lasting disease-modifying properties in a transgenic rat model of Alzheimer's disease*. *Alzheimers Dement*, 2018. **14**(6): p. 811-823.
156. Mishina, M., et al., *Low density of sigma1 receptors in early Alzheimer's disease*. *Ann Nucl Med*, 2008. **22**(3): p. 151-6.
157. Jansen, K.L., et al., *Loss of sigma binding sites in the CA1 area of the anterior hippocampus in Alzheimer's disease correlates with CA1 pyramidal cell loss*. *Brain Res*, 1993. **623**(2): p. 299-302.
158. Krogmann, A., et al., *Keeping up with the therapeutic advances in schizophrenia: a review of novel and emerging pharmacological entities*. *CNS Spectr*, 2019. **24**(S1): p. 38-69.
159. Maurice, T., T.P. Su, and A. Privat, *Sigma1 (sigma 1) receptor agonists and neurosteroids attenuate B25-35-amyloid peptide-induced amnesia in mice through a common mechanism*. *Neuroscience*, 1998. **83**(2): p. 413-28.
160. Urani, A., et al., *The antidepressant-like effect induced by the sigma(1) (sigma(1)) receptor agonist igmesine involves modulation of intracellular calcium mobilization*. *Psychopharmacology (Berl)*, 2002. **163**(1): p. 26-35.
161. van Waarde, A., et al., *The cholinergic system, sigma-1 receptors and cognition*. *Behav Brain Res*, 2011. **221**(2): p. 543-54.
162. Dvoracsko, S., et al., *Novel High Affinity Sigma-1 Receptor Ligands from Minimal Ensemble Docking-Based Virtual Screening*. *Int J Mol Sci*, 2021. **22**(15).
163. Christ, M.G., et al., *Sigma-1 Receptor Activation Induces Autophagy and Increases Proteostasis Capacity In Vitro and In Vivo*. *Cells*, 2019. **8**(3).
164. Nichols, D.E., *N,N-dimethyltryptamine and the pineal gland: Separating fact from myth*. *J Psychopharmacol*, 2018. **32**(1): p. 30-36.
165. Fontanilla, D., et al., *The hallucinogen N,N-dimethyltryptamine (DMT) is an endogenous sigma-1 receptor regulator*. *Science*, 2009. **323**(5916): p. 934-7.
166. Barker, S.A., *N, N-Dimethyltryptamine (DMT), an Endogenous Hallucinogen: Past, Present, and Future Research to Determine Its Role and Function*. *Front Neurosci*, 2018. **12**: p. 536.
167. Szabo, A., et al., *The Endogenous Hallucinogen and Trace Amine N,N-Dimethyltryptamine (DMT) Displays Potent Protective Effects against Hypoxia via Sigma-1 Receptor Activation in Human Primary iPSC-Derived Cortical Neurons and Microglia-Like Immune Cells*. *Front Neurosci*, 2016. **10**: p. 423.
168. Szabo, A., et al., *Psychedelic N,N-dimethyltryptamine and 5-methoxy-N,N-dimethyltryptamine modulate innate and adaptive inflammatory responses through the sigma-1 receptor of human monocyte-derived dendritic cells*. *PLoS One*, 2014. **9**(8): p. e106533.
169. Szabo, A. and E. Frecska, *Dimethyltryptamine (DMT): a biochemical Swiss Army knife in neuroinflammation and neuroprotection?* *Neural Regen Res*, 2016. **11**(3): p. 396-7.
170. Ly, C., et al., *Psychedelics Promote Structural and Functional Neural Plasticity*. *Cell Rep*, 2018. **23**(11): p. 3170-3182.

171. Lima da Cruz, R.V., et al., *Corrigendum: A Single Dose of 5-MeO-DMT Stimulates Cell Proliferation, Neuronal Survivability, Morphological and Functional Changes in Adult Mice Ventral Dentate Gyrus*. Front Mol Neurosci, 2019. **12**: p. 79.
172. Lima da Cruz, R.V., et al., *A Single Dose of 5-MeO-DMT Stimulates Cell Proliferation, Neuronal Survivability, Morphological and Functional Changes in Adult Mice Ventral Dentate Gyrus*. Front Mol Neurosci, 2018. **11**: p. 312.
173. Cameron, L.P., et al., *Chronic, Intermittent Microdoses of the Psychedelic*. ACS Chem Neurosci, 2019. **10**(7): p. 3261-3270.
174. Dakic, V., et al., *Short term changes in the proteome of human cerebral organoids induced by 5-MeO-DMT*. Sci Rep, 2017. **7**(1): p. 12863.
175. Morales-Garcia, J.A., et al., *N,N-dimethyltryptamine compound found in the hallucinogenic tea ayahuasca, regulates adult neurogenesis in vitro and in vivo*. Transl Psychiatry, 2020. **10**(1): p. 331.
176. Carbonaro, T.M. and M.B. Gatch, *Neuropharmacology of N,N-dimethyltryptamine*. Brain Res Bull, 2016. **126**(Pt 1): p. 74-88.
177. Simão, A.Y., et al., *Evaluation of the Cytotoxicity of Ayahuasca Beverages*. Molecules, 2020. **25**(23).
178. Frecska, E., et al., *A possibly sigma-1 receptor mediated role of dimethyltryptamine in tissue protection, regeneration, and immunity*. J Neural Transm (Vienna), 2013. **120**(9): p. 1295-303.
179. Keiser, M.J., et al., *Predicting new molecular targets for known drugs*. Nature, 2009. **462**(7270): p. 175-81.
180. Inserra, A., *Hypothesis: The Psychedelic Ayahuasca Heals Traumatic Memories via a Sigma 1 Receptor-Mediated Epigenetic-Mnemonic Process*. Front Pharmacol, 2018. **9**: p. 330.
181. Rickli, A., et al., *Receptor interaction profiles of novel psychoactive tryptamines compared with classic hallucinogens*. Eur Neuropsychopharmacol, 2016. **26**(8): p. 1327-37.
182. Cameron, L.P. and D.E. Olson, *Dark Classics in Chemical Neuroscience: N, N-Dimethyltryptamine (DMT)*. ACS Chem Neurosci, 2018. **9**(10): p. 2344-2357.
183. Entrena, J.M., et al., *Sigma-1 Receptor Agonism Promotes Mechanical Allodynia After Priming the Nociceptive System with Capsaicin*. Sci Rep, 2016. **6**: p. 37835.
184. Francardo, V., et al., *Pharmacological stimulation of sigma-1 receptors has neurorestorative effects in experimental parkinsonism*. Brain, 2014. **137**(Pt 7): p. 1998-2014.
185. Penas, C., et al., *Sigma receptor agonist 2-(4-morpholinethyl)1 phenylcyclohexanecarboxylate (Pre084) increases GDNF and BiP expression and promotes neuroprotection after root avulsion injury*. J Neurotrauma, 2011. **28**(5): p. 831-40.
186. Xu, Q., et al., *Sigma 1 receptor activation regulates brain-derived neurotrophic factor through NR2A-CaMKIV-TORC1 pathway to rescue the impairment of learning and memory induced by brain ischaemia/reperfusion*. Psychopharmacology (Berl), 2015. **232**(10): p. 1779-91.
187. Koshibu, K., *Nootropics with potential to (re)build neuroarchitecture*. Neural Regen Res, 2016. **11**(1): p. 79-80.
188. Brimson, J.M., et al., *Dipentylammonium Binds to the Sigma-1 Receptor and Protects Against Glutamate Toxicity, Attenuates Dopamine Toxicity and Potentiates Neurite Outgrowth in Various Cultured Cell Lines*. Neurotox Res, 2018. **34**(2): p. 263-272.
189. Maurice, T., *Beneficial effect of the sigma(1) receptor agonist PRE-084 against the spatial learning deficits in aged rats*. Eur J Pharmacol, 2001. **431**(2): p. 223-7.

190. Marrazzo, A., et al., *Neuroprotective effects of sigma-1 receptor agonists against beta-amyloid-induced toxicity*. Neuroreport, 2005. **16**(11): p. 1223-6.
191. Li, L., et al., *DHEA prevents A $\beta$ 25-35-impaired survival of newborn neurons in the dentate gyrus through a modulation of PI3K-Akt-mTOR signaling*. Neuropharmacology, 2010. **59**(4-5): p. 323-33.
192. Griesmaier, E., et al., *Neuroprotective effects of the sigma-1 receptor ligand PRE-084 against excitotoxic perinatal brain injury in newborn mice*. Exp Neurol, 2012. **237**(2): p. 388-95.
193. Sánchez-Blázquez, P., et al., *The Sigma-1 Receptor Antagonist, SIRA, Reduces Stroke Damage, Ameliorates Post-Stroke Neurological Deficits and Suppresses the Overexpression of MMP-9*. Mol Neurobiol, 2018. **55**(6): p. 4940-4951.
194. Fish, P.V., et al., *New approaches for the treatment of Alzheimer's disease*. Bioorg Med Chem Lett, 2019. **29**(2): p. 125-133.
195. Ma, W.H., et al., *Sigma ligands as potent inhibitors of A $\beta$  and A $\beta$ Os in neurons and promising therapeutic agents of Alzheimer's disease*. Neuropharmacology, 2020: p. 108342.
196. Ruscher, K. and T. Wieloch, *The involvement of the sigma-1 receptor in neurodegeneration and neurorestoration*. J Pharmacol Sci, 2015. **127**(1): p. 30-5.
197. Dodart, J.C. and P. May, *Overview on rodent models of Alzheimer's disease*. Curr Protoc Neurosci, 2005. **Chapter 9**: p. Unit 9 22.
198. Mhatre, S.D., et al., *Invertebrate models of Alzheimer's disease*. J Alzheimers Dis, 2013. **33**(1): p. 3-16.
199. Chen, Z.Y. and Y. Zhang, *Animal models of Alzheimer's disease: Applications, evaluation, and perspectives*. Zool Res, 2022. **43**(6): p. 1026-1040.
200. Zussy, C., et al., *Alzheimer's disease related markers, cellular toxicity and behavioral deficits induced six weeks after oligomeric amyloid-beta peptide injection in rats*. PLoS One, 2013. **8**(1): p. e53117.
201. Cohen, R.M., et al., *A transgenic Alzheimer rat with plaques, tau pathology, behavioral impairment, oligomeric abeta, and frank neuronal loss*. J Neurosci, 2013. **33**(15): p. 6245-56.
202. Foidl, B.M. and C. Humpel, *Can mouse models mimic sporadic Alzheimer's disease?* Neural Regen Res, 2020. **15**(3): p. 401-406.
203. Sipos, E., et al., *Beta-amyloid pathology in the entorhinal cortex of rats induces memory deficits: implications for Alzheimer's disease*. Neuroscience, 2007. **147**(1): p. 28-36.
204. He, F.Q., et al., *Tetrandrine attenuates spatial memory impairment and hippocampal neuroinflammation via inhibiting NF-kappaB activation in a rat model of Alzheimer's disease induced by amyloid-beta(1-42)*. Brain Res, 2011. **1384**: p. 89-96.
205. Wan, B., et al., *Effects of triptolide on degeneration of dendritic spines induced by Abeta1-40 injection in rat hippocampus*. Neurol Sci, 2014. **35**(1): p. 35-40.
206. Chacon, M.A., et al., *Beta-sheet breaker peptide prevents Abeta-induced spatial memory impairments with partial reduction of amyloid deposits*. Mol Psychiatry, 2004. **9**(10): p. 953-61.
207. Zhong, S.Z., et al., *Peoniflorin attenuates Abeta((1-42))-mediated neurotoxicity by regulating calcium homeostasis and ameliorating oxidative stress in hippocampus of rats*. J Neurol Sci, 2009. **280**(1-2): p. 71-8.
208. Quan, Q., et al., *Ginsenoside Rg1 decreases Abeta(1-42) level by upregulating PPARgamma and IDE expression in the hippocampus of a rat model of Alzheimer's disease*. PLoS One, 2013. **8**(3): p. e59155.



209. He, P., et al., *A novel melatonin agonist Neu-P11 facilitates memory performance and improves cognitive impairment in a rat model of Alzheimer' disease*. *Horm Behav*, 2013. **64**(1): p. 1-7.
210. Zheng, M., et al., *Intrahippocampal injection of Abeta1-42 inhibits neurogenesis and down-regulates IFN-gamma and NF-kappaB expression in hippocampus of adult mouse brain*. *Amyloid*, 2013. **20**(1): p. 13-20.
211. Jia, J., et al., *Amelioratory effects of testosterone treatment on cognitive performance deficits induced by soluble Abeta1-42 oligomers injected into the hippocampus*. *Horm Behav*, 2013. **64**(3): p. 477-86.
212. Yin, Y., et al., *Protective effects of bilobalide on Abeta(25-35) induced learning and memory impairments in male rats*. *Pharmacol Biochem Behav*, 2013. **106**: p. 77-84.
213. Zhang, J., et al., *Salidroside attenuates beta amyloid-induced cognitive deficits via modulating oxidative stress and inflammatory mediators in rat hippocampus*. *Behav Brain Res*, 2013. **244**: p. 70-81.
214. Gordon, R.Y., et al., *Analysis of the Effect of Neuroprotectors That Reduce the Level of Degeneration of Neurons in the Rat Hippocampus Caused by Administration of Beta-Amyloid Peptide Abeta25-35*. *Bull Exp Biol Med*, 2022. **172**(4): p. 441-446.
215. Facchinetti, R., M.R. Bronzuoli, and C. Scuderi, *An Animal Model of Alzheimer Disease Based on the Intrahippocampal Injection of Amyloid beta-Peptide (1-42)*. *Methods Mol Biol*, 2018. **1727**: p. 343-352.
216. Hu, X., et al., *Tau pathogenesis is promoted by Abeta1-42 but not Abeta1-40*. *Mol Neurodegener*, 2014. **9**: p. 52.
217. Pourbadie, H.G., et al., *Decrease of high voltage Ca(2+) currents in the dentate gyrus granule cells by entorhinal amyloidopathy is reversed by calcium channel blockade*. *Eur J Pharmacol*, 2017. **794**: p. 154-161.
218. Kim, H.Y., et al., *Intracerebroventricular Injection of Amyloid-beta Peptides in Normal Mice to Acutely Induce Alzheimer-like Cognitive Deficits*. *J Vis Exp*, 2016(109).
219. Schmid, S., et al., *Intracerebroventricular injection of beta-amyloid in mice is associated with long-term cognitive impairment in the modified hole-board test*. *Behav Brain Res*, 2017. **324**: p. 15-20.
220. Borbely, E., et al., *Impact of Two Neuronal Sigma-1 Receptor Modulators, PRE084 and DMT, on Neurogenesis and Neuroinflammation in an Abeta1-42-Injected, Wild-Type Mouse Model of AD*. *Int J Mol Sci*, 2022. **23**(5).
221. Kasza, A., et al., *Studies for Improving a Rat Model of Alzheimer's Disease: Icv Administration of Well-Characterized beta-Amyloid 1-42 Oligomers Induce Dysfunction in Spatial Memory*. *Molecules*, 2017. **22**(11).
222. Borlikova, G.G., et al., *Alzheimer brain-derived amyloid beta-protein impairs synaptic remodeling and memory consolidation*. *Neurobiol Aging*, 2013. **34**(5): p. 1315-27.
223. Balducci, C. and G. Forloni, *In vivo application of beta amyloid oligomers: a simple tool to evaluate mechanisms of action and new therapeutic approaches*. *Curr Pharm Des*, 2014. **20**(15): p. 2491-505.
224. de Oliveira, J., et al., *Increased susceptibility to amyloid-beta-induced neurotoxicity in mice lacking the low-density lipoprotein receptor*. *J Alzheimers Dis*, 2014. **41**(1): p. 43-60.
225. Souza, L.C., et al., *Indoleamine-2,3-dioxygenase mediates neurobehavioral alterations induced by an intracerebroventricular injection of amyloid-beta1-42 peptide in mice*. *Brain Behav Immun*, 2016. **56**: p. 363-77.
226. Navigatore Fonzo, L., et al., *An intracerebroventricular injection of amyloid-beta peptide (1-42) aggregates modifies daily temporal organization of clock factors*

- expression, protein carbonyls and antioxidant enzymes in the rat hippocampus.* Brain Res, 2021. **1767**: p. 147449.
227. Hugon, G., et al., *Impact of Donepezil on Brain Glucose Metabolism Assessed Using [(18)F]2-Fluoro-2-deoxy-D-Glucose Positron Emission Tomography Imaging in a Mouse Model of Alzheimer's Disease Induced by Intracerebroventricular Injection of Amyloid-Beta Peptide.* Front Neurosci, 2022. **16**: p. 835577.
228. Eisele, Y.S., et al., *Induction of cerebral beta-amyloidosis: intracerebral versus systemic Abeta inoculation.* Proc Natl Acad Sci U S A, 2009. **106**(31): p. 12926-31.
229. Moser, E., M.B. Moser, and P. Andersen, *Spatial learning impairment parallels the magnitude of dorsal hippocampal lesions, but is hardly present following ventral lesions.* J Neurosci, 1993. **13**(9): p. 3916-25.
230. Morris, R.G., et al., *Place navigation impaired in rats with hippocampal lesions.* Nature, 1982. **297**(5868): p. 681-3.
231. Morris, R., *Developments of a water-maze procedure for studying spatial learning in the rat.* J Neurosci Methods, 1984. **11**(1): p. 47-60.
232. Vorhees, C.V. and M.T. Williams, *Morris water maze: procedures for assessing spatial and related forms of learning and memory.* Nat Protoc, 2006. **1**(2): p. 848-58.
233. D'Hooge, R. and P.P. De Deyn, *Applications of the Morris water maze in the study of learning and memory.* Brain Res Brain Res Rev, 2001. **36**(1): p. 60-90.
234. Harrison, F.E., A.H. Hosseini, and M.P. McDonald, *Endogenous anxiety and stress responses in water maze and Barnes maze spatial memory tasks.* Behav Brain Res, 2009. **198**(1): p. 247-51.
235. Qin, T., et al., *Utility of Animal Models to Understand Human Alzheimer's Disease, Using the Mastermind Research Approach to Avoid Unnecessary Further Sacrifices of Animals.* Int J Mol Sci, 2020. **21**(9).
236. Higa, K.K., J.W. Young, and M.A. Geyer, *Wet or dry: translatable "water mazes" for mice and humans.* J Clin Invest, 2016. **126**(2): p. 477-9.
237. Ricciarelli, R. and E. Fedele, *The Amyloid Cascade Hypothesis in Alzheimer's Disease: It's Time to Change Our Mind.* Curr Neuropharmacol, 2017. **15**(6): p. 926-935.
238. Gilman, S., et al., *Clinical effects of Abeta immunization (AN1792) in patients with AD in an interrupted trial.* Neurology, 2005. **64**(9): p. 1553-62.
239. Plotkin, S.S. and N.R. Cashman, *Passive immunotherapies targeting Abeta and tau in Alzheimer's disease.* Neurobiol Dis, 2020. **144**: p. 105010.
240. Abushouk, A.I., et al., *Bapineuzumab for mild to moderate Alzheimer's disease: a meta-analysis of randomized controlled trials.* BMC Neurol, 2017. **17**(1): p. 66.
241. Doody, R.S., et al., *Phase 3 trials of solanezumab for mild-to-moderate Alzheimer's disease.* N Engl J Med, 2014. **370**(4): p. 311-21.
242. Barao, S., et al., *BACE1 Physiological Functions May Limit Its Use as Therapeutic Target for Alzheimer's Disease.* Trends Neurosci, 2016. **39**(3): p. 158-169.
243. Hardy, J. and B. De Strooper, *Alzheimer's disease: where next for anti-amyloid therapies?* Brain, 2017. **140**(4): p. 853-855.
244. Imbimbo, B.P., *An update on the efficacy of non-steroidal anti-inflammatory drugs in Alzheimer's disease.* Expert Opin Investig Drugs, 2009. **18**(8): p. 1147-68.
245. Bogar, F., L. Fulop, and B. Penke, *Novel Therapeutic Target for Prevention of Neurodegenerative Diseases: Modulation of Neuroinflammation with Sig-1R Ligands.* Biomolecules, 2022. **12**(3).
246. Villard, V., et al., *Antiamnesic and neuroprotective effects of the aminotetrahydrofuran derivative ANAVEX1-41 against amyloid beta(25-35)-induced toxicity in mice.* Neuropsychopharmacology, 2009. **34**(6): p. 1552-66.

247. Bozso, Z., et al., *Controlled in situ preparation of A beta(1-42) oligomers from the isopeptide "iso-A beta(1-42)", physicochemical and biological characterization.* Peptides, 2010. **31**(2): p. 248-56.
248. Stine, W.B., Jr., et al., *In vitro characterization of conditions for amyloid-beta peptide oligomerization and fibrillogenesis.* J Biol Chem, 2003. **278**(13): p. 11612-22.
249. Datki, Z., et al., *In vitro model of neurotoxicity of Abeta 1-42 and neuroprotection by a pentapeptide: irreversible events during the first hour.* Neurobiol Dis, 2004. **17**(3): p. 507-15.
250. Szegedi, V., et al., *Pentapeptides derived from Abeta 1-42 protect neurons from the modulatory effect of Abeta fibrils--an in vitro and in vivo electrophysiological study.* Neurobiol Dis, 2005. **18**(3): p. 499-508.
251. Paxinos, G., C.R. Watson, and P.C. Emson, *AChE-stained horizontal sections of the rat brain in stereotaxic coordinates.* J Neurosci Methods, 1980. **3**(2): p. 129-49.
252. Szögi, T., et al., *Effects of the Pentapeptide P33 on Memory and Synaptic Plasticity in APP/PS1 Transgenic Mice: A Novel Mechanism Presenting the Protein Fe65 as a Target.* Int J Mol Sci, 2019. **20**(12).
253. Szogi, T., et al., *Examination of Longitudinal Alterations in Alzheimer's Disease-Related Neurogenesis in an APP/PS1 Transgenic Mouse Model, and the Effects of P33, a Putative Neuroprotective Agent Thereon.* Int J Mol Sci, 2022. **23**(18).
254. Nagy, D., et al., *Kainate postconditioning restores LTP in ischemic hippocampal CA1: onset-dependent second pathophysiological stress.* Neuropharmacology, 2011. **61**(5-6): p. 1026-32.
255. Possin, K.L., et al., *Cross-species translation of the Morris maze for Alzheimer's disease.* J Clin Invest, 2016. **126**(2): p. 779-83.
256. Albert, M.S., *Changes in cognition.* Neurobiol Aging, 2011. **32 Suppl 1**: p. S58-63.
257. Duff, M.C., et al., *Learning in Alzheimer's disease is facilitated by social interaction.* J Comp Neurol, 2013. **521**(18): p. 4356-69.
258. Knafo, S., et al., *Widespread changes in dendritic spines in a model of Alzheimer's disease.* Cereb Cortex, 2009. **19**(3): p. 586-92.
259. Tsai, J., et al., *Fibrillar amyloid deposition leads to local synaptic abnormalities and breakage of neuronal branches.* Nat Neurosci, 2004. **7**(11): p. 1181-3.
260. Bishop, G.M. and S.R. Robinson, *The amyloid hypothesis: let sleeping dogmas lie?* Neurobiol Aging, 2002. **23**(6): p. 1101-5.
261. Rosenblum, W.I., *Why Alzheimer trials fail: removing soluble oligomeric beta amyloid is essential, inconsistent, and difficult.* Neurobiol Aging, 2014. **35**(5): p. 969-74.
262. Cavallucci, V., M. D'Amelio, and F. Cecconi, *Abeta toxicity in Alzheimer's disease.* Mol Neurobiol, 2012. **45**(2): p. 366-78.
263. Walsh, D.M. and D.J. Selkoe, *A beta oligomers - a decade of discovery.* J Neurochem, 2007. **101**(5): p. 1172-84.
264. Sandberg, A., et al., *Stabilization of neurotoxic Alzheimer amyloid-beta oligomers by protein engineering.* Proc Natl Acad Sci U S A, 2010. **107**(35): p. 15595-600.
265. Ramírez, E., et al., *Neurogenesis and morphological-neural alterations closely related to amyloid  $\beta$ -peptide (25-35)-induced memory impairment in male rats.* Neuropeptides, 2018. **67**: p. 9-19.
266. Chen, G.F., et al., *Amyloid beta: structure, biology and structure-based therapeutic development.* Acta Pharmacol Sin, 2017. **38**(9): p. 1205-1235.
267. Iliff, J.J., et al., *A paravascular pathway facilitates CSF flow through the brain parenchyma and the clearance of interstitial solutes, including amyloid beta.* Sci Transl Med, 2012. **4**(147): p. 147ra111.

268. Ciccone, L., et al., *The Positive Side of the Alzheimer's Disease Amyloid Cross-Interactions: The Case of the Abeta 1-42 Peptide with Tau, TTR, CysC, and ApoA1*. *Molecules*, 2020. **25**(10).
269. Scheltens, P., et al., *Alzheimer's disease*. *Lancet*, 2016. **388**(10043): p. 505-17.
270. Van Cauter, T., B. Poucet, and E. Save, *Delay-dependent involvement of the rat entorhinal cortex in habituation to a novel environment*. *Neurobiol Learn Mem*, 2008. **90**(1): p. 192-9.
271. Poucet, B., et al., *Place cells, neocortex and spatial navigation: a short review*. *J Physiol Paris*, 2003. **97**(4-6): p. 537-46.
272. Parron, C., B. Poucet, and E. Save, *Entorhinal cortex lesions impair the use of distal but not proximal landmarks during place navigation in the rat*. *Behav Brain Res*, 2004. **154**(2): p. 345-52.
273. Parron, C. and E. Save, *Evidence for entorhinal and parietal cortices involvement in path integration in the rat*. *Exp Brain Res*, 2004. **159**(3): p. 349-59.
274. Parron, C. and E. Save, *Comparison of the effects of entorhinal and retrosplenial cortical lesions on habituation, reaction to spatial and non-spatial changes during object exploration in the rat*. *Neurobiol Learn Mem*, 2004. **82**(1): p. 1-11.
275. Guzman-Ruiz, M.A., et al., *Protective effects of intracerebroventricular adiponectin against olfactory impairments in an amyloid beta1-42 rat model*. *BMC Neurosci*, 2021. **22**(1): p. 14.
276. Shin, E.J., et al., *An adenoviral vector encoded with the GPx-1 gene attenuates memory impairments induced by beta-amyloid (1-42) in GPx-1 KO mice via activation of M1 mAChR-mediated signalling*. *Free Radic Res*, 2021. **55**(1): p. 11-25.
277. Babri, S., et al., *Effect of Aggregated beta-Amyloid (1-42) on Synaptic Plasticity of Hippocampal Dentate Gyrus Granule Cells in Vivo*. *Bioimpacts*, 2012. **2**(4): p. 189-94.
278. Souza, L.C., et al., *Swimming exercise prevents behavioural disturbances induced by an intracerebroventricular injection of amyloid-beta1-42 peptide through modulation of cytokine/NF-kappaB pathway and indoleamine-2,3-dioxygenase in mouse brain*. *Behav Brain Res*, 2017. **331**: p. 1-13.
279. Kashani, M.S., et al., *Aqueous extract of lavender (*Lavandula angustifolia*) improves the spatial performance of a rat model of Alzheimer's disease*. *Neurosci Bull*, 2011. **27**(2): p. 99-106.
280. Kaushal, A., et al., *Spontaneous and induced nontransgenic animal models of AD: modeling AD using combinatorial approach*. *Am J Alzheimers Dis Other Dement*, 2013. **28**(4): p. 318-26.
281. Antunes, M. and G. Biala, *The novel object recognition memory: neurobiology, test procedure, and its modifications*. *Cogn Process*, 2012. **13**(2): p. 93-110.
282. Eriksson, P.S., et al., *Neurogenesis in the adult human hippocampus*. *Nat Med*, 1998. **4**(11): p. 1313-7.
283. Zheng, M., et al., *Intrahippocampal injection of Aβ1-42 inhibits neurogenesis and down-regulates IFN-γ and NF-κB expression in hippocampus of adult mouse brain*. *Amyloid*, 2013. **20**(1): p. 13-20.
284. Verret, L., et al., *Alzheimer's-type amyloidosis in transgenic mice impairs survival of newborn neurons derived from adult hippocampal neurogenesis*. *J Neurosci*, 2007. **27**(25): p. 6771-80.
285. Unger, M.S., et al., *Early Changes in Hippocampal Neurogenesis in Transgenic Mouse Models for Alzheimer's Disease*. *Mol Neurobiol*, 2016. **53**(8): p. 5796-806.
286. Hu, Y.S., et al., *Complex environment experience rescues impaired neurogenesis, enhances synaptic plasticity, and attenuates neuropathology in familial Alzheimer's disease-linked APP<sup>swe</sup>/PS1<sup>DeltaE9</sup> mice*. *FASEB J*, 2010. **24**(6): p. 1667-81.

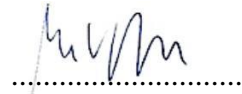
287. Demars, M., et al., *Impaired neurogenesis is an early event in the etiology of familial Alzheimer's disease in transgenic mice*. J Neurosci Res, 2010. **88**(10): p. 2103-17.
288. López-Toledano, M.A. and M.L. Shelanski, *Increased neurogenesis in young transgenic mice overexpressing human APP(Sw, Ind)*. J Alzheimers Dis, 2007. **12**(3): p. 229-40.
289. Jin, K., et al., *Enhanced neurogenesis in Alzheimer's disease transgenic (PDGF-APP<sup>Sw,Ind</sup>) mice*. Proc Natl Acad Sci U S A, 2004. **101**(36): p. 13363-7.
290. Jin, K., et al., *Increased hippocampal neurogenesis in Alzheimer's disease*. Proc Natl Acad Sci U S A, 2004. **101**(1): p. 343-7.
291. López-Toledano, M.A. and M.L. Shelanski, *Neurogenic effect of beta-amyloid peptide in the development of neural stem cells*. J Neurosci, 2004. **24**(23): p. 5439-44.
292. Heo, C., et al., *Effects of the monomeric, oligomeric, and fibrillar Abeta42 peptides on the proliferation and differentiation of adult neural stem cells from subventricular zone*. J Neurochem, 2007. **102**(2): p. 493-500.
293. Itokazu, Y. and R.K. Yu, *Amyloid  $\beta$ -peptide 1-42 modulates the proliferation of mouse neural stem cells: upregulation of fucosyltransferase IX and notch signaling*. Mol Neurobiol, 2014. **50**(1): p. 186-96.
294. Fonseca, M.B., et al., *Amyloid  $\beta$  peptides promote autophagy-dependent differentiation of mouse neural stem cells: A $\beta$ -mediated neural differentiation*. Mol Neurobiol, 2013. **48**(3): p. 829-40.
295. Chen, Y. and C. Dong, *Abeta40 promotes neuronal cell fate in neural progenitor cells*. Cell Death Differ, 2009. **16**(3): p. 386-94.
296. Bernabeu-Zornoza, A., et al., *Physiological and pathological effects of amyloid- $\beta$  species in neural stem cell biology*. Neural Regen Res, 2019. **14**(12): p. 2035-2042.
297. Hamilton, A. and C. Holscher, *The effect of ageing on neurogenesis and oxidative stress in the APP(swe)/PS1(deltaE9) mouse model of Alzheimer's disease*. Brain Res, 2012. **1449**: p. 83-93.
298. Perry, E.K., et al., *Neurogenic abnormalities in Alzheimer's disease differ between stages of neurogenesis and are partly related to cholinergic pathology*. Neurobiol Dis, 2012. **47**(2): p. 155-62.
299. Calvo-Flores Guzmán, B., et al., *The Interplay Between Beta-Amyloid 1-42 (A $\beta$ )*. Front Mol Neurosci, 2020. **13**: p. 522073.
300. Dhawan, G., A.M. Floden, and C.K. Combs, *Amyloid- $\beta$  oligomers stimulate microglia through a tyrosine kinase dependent mechanism*. Neurobiol Aging, 2012. **33**(10): p. 2247-61.
301. Mudò, G., et al., *Anti-inflammatory and cognitive effects of interferon- $\beta$ 1a (IFN $\beta$ 1a) in a rat model of Alzheimer's disease*. J Neuroinflammation, 2019. **16**(1): p. 44.
302. Minter, M.R., J.M. Taylor, and P.J. Crack, *The contribution of neuroinflammation to amyloid toxicity in Alzheimer's disease*. J Neurochem, 2016. **136**(3): p. 457-74.
303. Edler, M.K., I. Mhatre-Winters, and J.R. Richardson, *Microglia in Aging and Alzheimer's Disease: A Comparative Species Review*. Cells, 2021. **10**(5).
304. Frost, G.R. and Y.M. Li, *The role of astrocytes in amyloid production and Alzheimer's disease*. Open Biol, 2017. **7**(12).
305. González-Reyes, R.E., et al., *Involvement of Astrocytes in Alzheimer's Disease from a Neuroinflammatory and Oxidative Stress Perspective*. Front Mol Neurosci, 2017. **10**: p. 427.
306. Hansen, D.V., J.E. Hanson, and M. Sheng, *Microglia in Alzheimer's disease*. J Cell Biol, 2018. **217**(2): p. 459-472.
307. Heneka, M.T., M.P. Kummer, and E. Latz, *Innate immune activation in neurodegenerative disease*. Nat Rev Immunol, 2014. **14**(7): p. 463-77.

308. Leng, F. and P. Edison, *Neuroinflammation and microglial activation in Alzheimer disease: where do we go from here?* Nat Rev Neurol, 2021. **17**(3): p. 157-172.
309. Ryskamp, D.A., et al., *Neuronal Sigma-1 Receptors: Signaling Functions and Protective Roles in Neurodegenerative Diseases*. Front Neurosci, 2019. **13**: p. 862.
310. Yin, J., et al., *Sigma-1 ( $\sigma_1$ ) receptor deficiency reduces  $\beta$ -amyloid(25-35)-induced hippocampal neuronal cell death and cognitive deficits through suppressing phosphorylation of the NMDA receptor NR2B*. Neuropharmacology, 2015. **89**: p. 215-24.
311. Maurice, T., *Bi-phasic dose response in the preclinical and clinical developments of sigma-1 receptor ligands for the treatment of neurodegenerative disorders*. Expert Opin Drug Discov, 2021. **16**(4): p. 373-389.
312. Meunier, J. and T. Hayashi, *Sigma-1 receptors regulate Bcl-2 expression by reactive oxygen species-dependent transcriptional regulation of nuclear factor kappaB*. J Pharmacol Exp Ther, 2010. **332**(2): p. 388-97.
313. Mori, T., et al., *Sigma-1 receptor chaperone at the ER-mitochondrion interface mediates the mitochondrion-ER-nucleus signaling for cellular survival*. PLoS One, 2013. **8**(10): p. e76941.
314. Granic, I., et al., *LPYFDa neutralizes amyloid-beta-induced memory impairment and toxicity*. J Alzheimers Dis, 2010. **19**(3): p. 991-1005.
315. Catlow, B.J., et al., *Effects of psilocybin on hippocampal neurogenesis and extinction of trace fear conditioning*. Exp Brain Res, 2013. **228**(4): p. 481-91.
316. Szabo, A., *Psychedelics and Immunomodulation: Novel Approaches and Therapeutic Opportunities*. Front Immunol, 2015. **6**: p. 358.
317. Wang, J., et al., *Comparison of Sigma 1 Receptor Ligands SA4503 and PRE084 to (+)-Pentazocine in the rd10 Mouse Model of RP*. Invest Ophthalmol Vis Sci, 2020. **61**(13): p. 3.
318. Jia, J., et al., *Sigma-1 Receptor-Modulated Neuroinflammation in Neurological Diseases*. Front Cell Neurosci, 2018. **12**: p. 314.

**12 APPENDIX****Co-author certification**

I, myself as a corresponding author of the following publication(s) declare that the authors have no conflict of interest, and Emőke Borbély Ph.D. candidate had significant contribution to the jointly published research(es). The results discussed in her thesis were not used and not intended to be used in any other qualification process for obtaining a PhD degree.

Prof. Dr. Ulrich L.M. Eisel



08.30.2023.

author

The publication(s) relevant to the applicant's thesis:

**LPYFDa neutralizes amyloid-beta-induced memory impairment and toxicity.** Journal of Alzheimer's Disease 2010 Jan;19(3):991-1005.

Ivica Granic, Marcelo F. Masman, Cornelius Mulder, Ingrid M. Nijholt, Pieter J.W. Naude, Ammerins de Haan, Emőke Borbély, Botond Penke, Paul G.M Luiten, Ulrich L.M. Eisel. (IF: 4,261)

## Research Article

# Simultaneous Changes of Spatial Memory and Spine Density after Intrahippocampal Administration of Fibrillar $A\beta_{1-42}$ to the Rat Brain

**Emőke Borbély, János Horváth, Szabina Furdan, Zsolt Bozsó, Botond Penke, and Livia Fülöp**

*Department of Medical Chemistry, University of Szeged, Dóm tér 8, Szeged 6720, Hungary*

Correspondence should be addressed to Livia Fülöp; [fulop.livia@med.u-szeged.hu](mailto:fulop.livia@med.u-szeged.hu)

Received 16 March 2014; Revised 25 May 2014; Accepted 2 June 2014; Published 23 June 2014

Academic Editor: Raymond Chuen-Chung Chang

Copyright © 2014 Emőke Borbély et al. This is an open access article distributed under the Creative Commons Attribution License, which permits unrestricted use, distribution, and reproduction in any medium, provided the original work is properly cited.

Several animal models of Alzheimer's disease have been used in laboratory experiments. Intrahippocampal injection of fibrillar amyloid-beta ( $fA\beta$ ) peptide represents one of the most frequently used models, mimicking  $A\beta$  deposits in the brain. In our experiment synthetic  $fA\beta_{1-42}$  peptide was administered to rat hippocampus. The effect of the  $A\beta$  peptide on spatial memory and dendritic spine density was studied. The  $fA\beta_{1-42}$ -treated rats showed decreased spatial learning ability measured in Morris water maze (MWM). Simultaneously,  $fA\beta_{1-42}$  caused a significant reduction of the dendritic spine density in the rat hippocampus CA1 region. The decrease of learning ability and the loss of spine density were in good correlation. Our results prove that both methods (MWM and dendritic spine density measurement) are suitable for studying  $A\beta$ -triggered neurodegeneration processes.

## 1. Introduction

Alzheimer's disease (AD) is a progressive neurodegenerative disorder characterized by deficit of learning process, severe memory loss, and complex behavioural changes [1–5]. Neuropathological hallmarks of AD include the cerebral accumulation of extracellular senile plaques containing various forms of amyloid-beta ( $A\beta$ ) peptide assemblies and the presence of intracellular neurofibrillary tangles containing tau protein [6–8]. Other features of AD are neuroinflammation, cerebrovascular alterations, activated astrocytes, and microglia as well as synaptic and neuronal loss in specific brain regions [9–11]. The affected brain regions are forebrain and medial temporal lobe structures like the hippocampus (HC), the entorhinal cortex, and the amygdala [11]. Synapse loss is strongly correlated with cognitive impairment; thus synapse number is the best indicator of cognitive decline in AD [1, 12]. The senile plaques are associated with local synapse and dendritic spine loss [13, 14]. Moreover, the fibrillar deposits are surrounded by a halo of oligomeric  $A\beta$  assemblies [15]. Extracellular oligomeric  $A\beta$  associates

with dendritic spines covering their surface [15]. In addition, intracellular  $A\beta$  may also contribute to AD pathology by tau hyperphosphorylation and synaptic dysfunction [16]. The toxic effects of different aggregation forms of  $A\beta$  (oligomers, protofibrils, and fibrils) have not been revealed completely yet.

Dendritic spines are cellular compartments containing the molecular machinery important for synaptic transmission and plasticity [17]. In pyramidal neurons of the hippocampus, there is an almost one-to-one relationship between the number of dendritic spines and excitatory synapses [17, 18]. The loss of dendritic spines and the presence of dystrophic neurites have been reported both in the amyloid precursor protein (APP) overexpressing transgenic mouse model of AD and in the AD-affected human brain [2, 8, 19, 20]. The spine density of prefrontal cortex neurons is greatly reduced in aged monkeys as a hallmark of cognitive decline [21]. Neurocortical pyramidal neurons have extensive apical and basilar dendritic trees to integrate information from excitatory and inhibitory synaptic inputs. In the neuronal network, dendritic spines represent the principal receptive



sites for the excitatory inputs to the neurons. The strength, stability, and function of the excitatory synaptic connections constitute the basis of cognitive function [22]. In the cerebral cortex of mammals, the rapid synaptogenesis during early postnatal life is followed by a substantial loss of synapses/spines that extends through adolescence. In adulthood, the number of spines remains relatively stable and then decreases progressively with aging [22, 23]. Spines appear and disappear through life, but their turnover rate declines with the age and is regulated by the neuronal activity [18]. Dendritic spines undergo structural modifications when the synaptic strength is experimentally modified (e.g., by evoking long-term potentiation or long-term depression) [18, 22, 24].

Extracellular delivery of  $A\beta$  peptides can initiate synaptic loss in rodent brains [25]. Intrahippocampal (IHC) administration of  $A\beta$  is a widely used animal model to study AD [4, 25–38]. The injection of  $A\beta$  into murine brain rapidly establishes the symptoms of AD. This method is suitable for studying the effects of the different aggregates of  $A\beta$ . There are conflicting results about the neurotoxicity of  $\beta$ -amyloid plaque depositions [39]; however, the toxic effect of  $A\beta$  peptides on synapses has been widely acknowledged.

Reduction of dendritic spine density has been shown in cell cultures after  $A\beta$  treatment [40–43]. Furthermore, IHC administration of fibrillar  $A\beta_{1-40}$  has been shown to decrease spine density [25, 28]. Interestingly, no experiments have been performed using well characterized  $A\beta_{1-42}$ , the most toxic form of  $A\beta$  peptides. Thus the aim of this study was to assess the impact of fibrillar  $A\beta_{1-42}$  ( $fA\beta_{1-42}$ ) administration on spatial memory of rats and dendritic spine density in the hippocampus. Our hypothesis was that IHC injected synthetic, fibrillar form of  $A\beta_{1-42}$  could simultaneously influence and reduce the learning process and dendritic spine density. Since hippocampal dendritic spines are the key elements in acquisition and retention and have been implicated in learning and memory processes [44, 45], we also compared the correlation between the changes of dendritic spine density (induced by  $fA\beta_{1-42}$  administration) and the spatial memory of rats.

## 2. Materials and Methods

**2.1. Animals.** Male Charles-River Wistar rats ( $n = 24$ ), weighing about 210–230 g at the beginning of the experiment, were used as subjects. Two groups, control ( $n = 12$ ) and  $fA\beta_{1-42}$ -treated ( $n = 12$ ), were formed. They were housed in groups of three under constant temperature, humidity, and lighting conditions (23°C, 12:12 h light/dark cycle, lights on at 7 a.m.). Standard rat chow and tap water were supplied *ad libitum*. All behavioural procedures were conducted during the light phase. Handling was done daily at the same time. Experiments were performed in accordance with the European Communities Council Directive of 22 September 2010 (2010/63/EU on the protection of animals used for scientific purposes). Formal approval to conduct the experiments was obtained from the Animal Experimentation Committee of the University of Szeged.

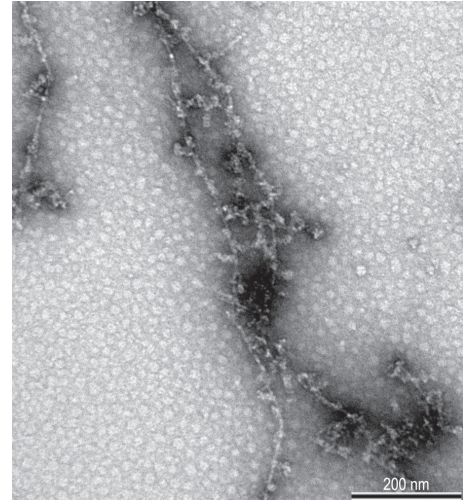


FIGURE 1: Representative electron microscope photomicrograph of the injected amyloid-beta fibrils.

**2.2. Synthesis of  $A\beta_{1-42}$  and Preparation of the Fibrillar Peptide Aggregates.** The synthesis was performed as reported earlier in Bozso et al. [46]. The  $fA\beta_{1-42}$  was prepared as described by He et al. [4]. Briefly,  $A\beta_{1-42}$  was dissolved in hexafluoroisopropanol (HFIP, Sigma Aldrich) to 1 mM; HFIP was removed *in vacuo*. The peptide was suspended to make a 5 mM solution in dimethyl sulfoxide (DMSO, Sigma Aldrich). The fibrillar form was prepared diluting the DMSO stock solution of the peptide with a 100 mM HEPES buffer to a final concentration of 222  $\mu$ M. The solution was incubated at 37°C for 7 days. After the aggregation period the sample was centrifuged for 10 min at 15000 g at room temperature. The pellet containing the freshly prepared fibrillar  $A\beta_{1-42}$  was resuspended in 100 mM HEPES buffer (pH 7.5) and used in the experiment. The samples containing  $A\beta$  fibrils were characterized by transmission electron microscope (Philips CM10, FEI, Eindhoven, Figure 1).

**2.3. Surgery.** Rats were anaesthetized with an intraperitoneal injection of a mixture of ketamine (10.0 mg/0.1 kg) and xylazine (0.8 mg/0.1 kg). The animals were then placed in a stereotaxic apparatus, a midline incision of the scalp was made, the skin and muscles were carefully retracted to expose the skull, and a hole was drilled above the target area. The solution was injected with a Hamilton syringe into the right HC unilaterally at a rate of 1.0  $\mu$ L/min, beginning 2 min after the needle was lowered. The needle was removed very slowly 2 min after the end of injection. The following coordinates were used (from Bregma point): AP: -3.6; ML: -2.4; DV: -2.8 [47]. Rats were randomly injected either with the fibrillar form of  $A\beta_{1-42}$  (222  $\mu$ M  $A\beta_{1-42}$ ) or with vehiculum (physiological saline). The  $A\beta_{1-42}$ -injected and the control animals were treated with antibiotics and analgesics after the surgery.

**2.4. Spatial Navigation in the Morris Water Maze.** Spatial learning and memory were assessed in a Morris water maze

(MWM) on days 14 to 20 after IHC  $fA\beta_{1-42}$  administration. Behavioural testing was carried out in a room illuminated by three lamps giving diffuse light of approximately equal intensity at all points of the maze. The maze consisted of a circular pool ( $d = 180$  cm,  $h = 60$  cm) filled with water ( $23 \pm 1^\circ\text{C}$ ) and made opaque with milk. A black curtain was positioned around the pool with distal cues. A video camera was mounted on the ceiling directly above the test apparatus and relied to a video tracking system. The behaviour of the animals was automatically recorded with the software EthoVision 2.3 (Noldus Information Technology, The Netherlands, 2002).

Memory acquisition trials (training period) were performed daily during the light phase, in blocks of 4, for 6 days [4]. The pool was divided into four virtual quadrants, and an invisible escape platform (diameter: 10 cm) was submerged in the middle of one of the four quadrants 1.5 cm below the water surface. At each trial, the rats were allowed to swim freely for a maximum of 120 sec until they found the platform and were then allowed to stay on it for 10 sec. If the rat failed to find the platform within 120 sec, it was guided to or was placed on the island manually for 10 sec. During the acquisition period, four different starting points were used and the starting positions were varied pseudorandomly over the trials. Twenty-four hours after the last acquisition trial, retention was assessed in a 120 sec probe trial, with the platform removed.

The data recorded by video tracking were used to calculate the time to reach the platform, swim speed, and swim path length (distance) during acquisition trials as well as percent time spent in each of the 4 virtual quadrants and time spent and number of crossings over the platform's position during the probe test.

**2.5. Quantification of Dendritic Spine Density Using Golgi Impregnation.** FD Rapid GolgiStain Kit (FD NeuroTechnologies, Consulting & Services, Inc., USA) was used according to the manufacturers' instructions. Rats ( $n = 6$ , 3 per group) were deeply anesthetized before the brain was removed from the skull. The sacrificing was made after 29 days of the IHC injection. The brains were removed quickly and handled carefully to avoid damage of the tissue, and then tissue blocks including hippocampus (approximately 0.7-0.8 cm) were cut from the brain. The tissue blocks were immersed in the impregnation solution (A + B solution) and stored at room temperature for 2 weeks in the dark. After the first impregnation period the brains were transferred into the second solution (C) and stored at  $4^\circ\text{C}$  in the dark for at least 48 hours.

100  $\mu\text{m}$  coronal sections were cut with a vibration microtome (Zeiss Microm HM 650 V) and were mounted on gelatin coated glass slides. After the staining procedure (D, E solution) and dehydration, the slides were coverslipped with DPX mountant for histology (VWR International).

**2.6. Quantitative Analysis.** The Golgi sections were studied by inverse light microscopy, using oil immersion objectives. A total of 25 pyramidal neurons from the dorsoventral hippocampal CA1 (stratum radiatum) were studied from each

of the 6 animals (75 dendritic shafts per group were analyzed). The spine density of the proximal apical dendrite area was analyzed (minimum 100  $\mu\text{m}$  from soma). For each examined neuron, one 100  $\mu\text{m}$  long segment from a second- or third-order dendrite (protruding from its parent apical dendrite) was chosen for spine density quantification as previously described [48]. The dendrites were selected under a 100x oil immersion lens and the images of these apical dendrites were captured through a camera (AxioCam MRC V5, program: AxioVision 40 V. 4.8.1.0 Carl Zeiss Imaging Solutions GmbH) connected to a light microscope (Zeiss Observer Z1, with 10x ocular magnification) and a computer. Serial images were made from each dendrite in the whole of the analyzed segment (Z-stack). The captured multiple photomicrographs from one dendrite were then stacked into one file. To stack the images and determine the spine density, ImageJ 1.44 software (National Institute of Health, Bethesda, USA) was used.

**2.7. Statistical Analysis.** Behavioural data were analyzed by repeated measures ANOVA, followed by Fisher's LSD post hoc tests for multiple comparisons. For the evaluation of the results of Golgi impregnation, Student's  $t$ -test for independent samples was used. Statistical significance was set at  $P < 0.05$ . The data were expressed as the means  $\pm$  (S.E.M.).

### 3. Results

**3.1. Spatial Learning and Memory in the Morris Water Maze.** MWM was used to test spatial learning and memory each day on days 14 to 20 after IHC administration of  $fA\beta_{1-42}$ . Escape latency to find the platform was used as a measure for evaluating spatial memory. The results showed that the performance of both groups ( $fA\beta$ -treated and untreated) improved from day to day, reflecting long-term memory. However, learning was slower each day in the  $fA\beta_{1-42}$ -treated compared to the control group: escape latencies were significantly longer in rats with  $fA\beta_{1-42}$  treatment than in the control animals analysed by repeated measures ANOVA ( $F_{1,94} = 6.450$ ;  $P = 0.013$ ) (Figure 2(a)). A significant difference was observed between the groups also for swimming distance (repeated measures ANOVA:  $F_{1,94} = 6.840$ ;  $P = 0.010$ ) (Figure 2(b)).

Despite the significantly slower learning in the  $fA\beta_{1-42}$ -treated group, performance at the probe test (given 24 h after the learning phase) indicated that spatial memory was not impaired, as the time spent in quadrants and the number of crossings over the virtual platform's position were comparable in the two groups ( $t_{22} = -1.247$ ;  $P = 0.226$  and  $t_{22} = 0.745$ ;  $P = 0.464$ , resp.) (Figures 3(a) and 3(b)).

**3.2. Dendritic Spine Density.** The Golgi staining method labelled a subset of neurons in the hippocampus. In general, 20-30 fully impregnated CA1 pyramidal cells could be detected per slice. There was no difference between the groups in staining.

We investigated all types of spines but solely focused on determining dendritic spine density. Spine numerical density was different between the two groups ( $t_{28} = 14.415$ ;  $P < 0.0001$ ). In the  $fA\beta_{1-42}$ -treated group decreasing

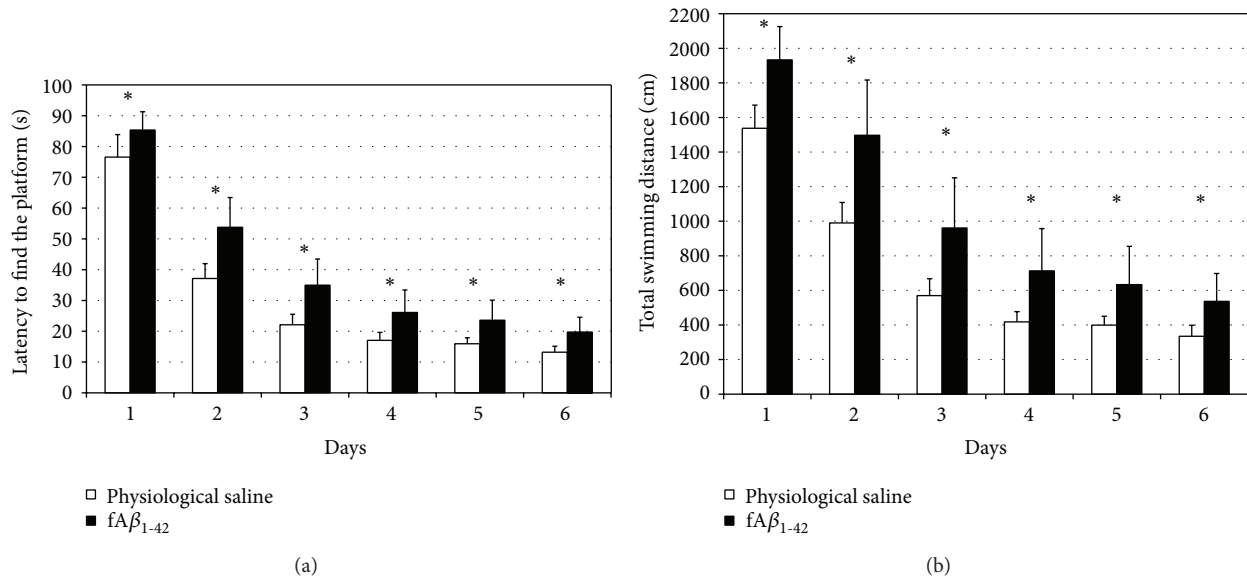


FIGURE 2:  $fA\beta_{1-42}$ -injection induced learning deficit in the Morris water maze test. (a)  $fA\beta_{1-42}$ -injection resulted in slower learning during the acquisition phase compared to control group ( $P = 0.013$ ); (b)  $fA\beta_{1-42}$ -treated animals swam longer distance than the controls to find the platform ( $P = 0.010$ ). Each value represents the mean ( $\pm$ S.E.M.) ( $n = 12$  rats per group).

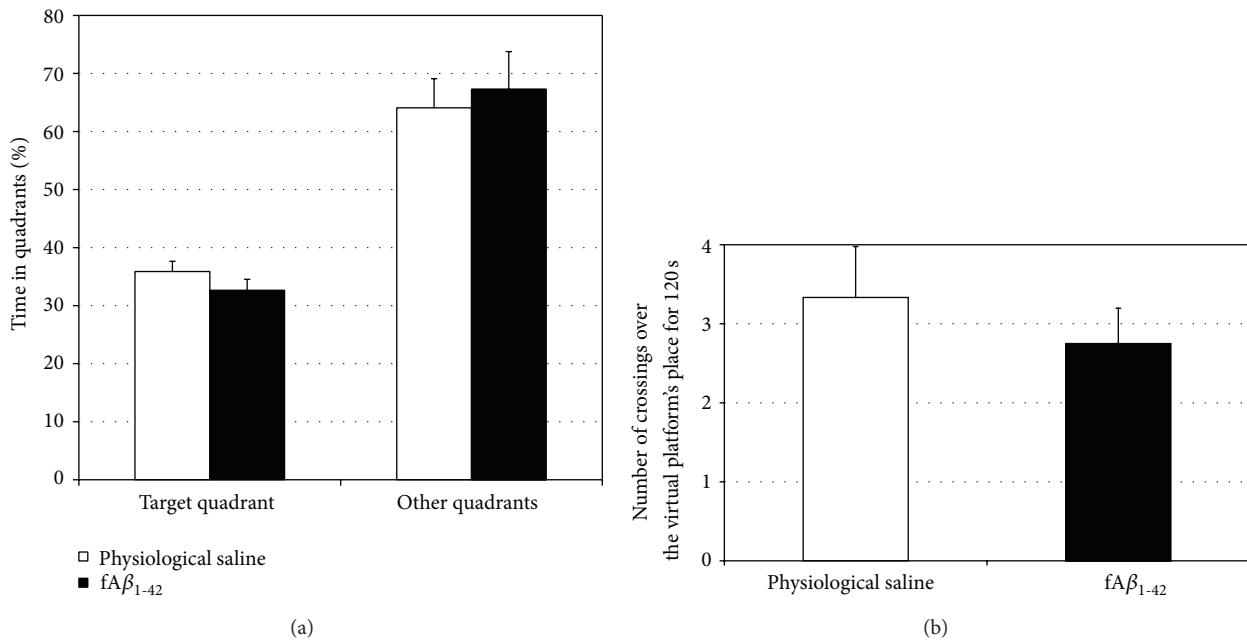


FIGURE 3: Injection of  $fA\beta_{1-42}$  did not affect performance in the Morris water maze probe test. (a) In the target quadrant, the amyloid-treated animals spent time comparable to controls. (b)  $fA\beta_{1-42}$ -injection did not have a significant effect on the number of crossings over where the virtual platform had been in the maze. Each value represents the mean ( $\pm$ S.E.M.) ( $n = 12$  rats per group).

spine density (spine number) was detected compared to the controls (Figure 4). Each column represents the mean value of the dendritic spine number of 75-75 pyramidal neurons.

Photomicrographs of the pyramidal neurons from control, nontreated rats (Figures 5(a) and 6), and  $fA\beta_{1-42}$ -treated rats (Figures 5(b) and 7) clearly demonstrate the difference in dendritic spine density in the two experimental groups.

#### 4. Discussion

The present study explored the effects of  $fA\beta_{1-42}$  on spatial behaviour and on hippocampal dendritic spines in nontransgenic rats.  $A\beta$  accumulation in the specific brain regions is a hallmark of AD pathology; however, the role of amyloid plaques has been debated. Depositions of  $fA\beta$  in plaques

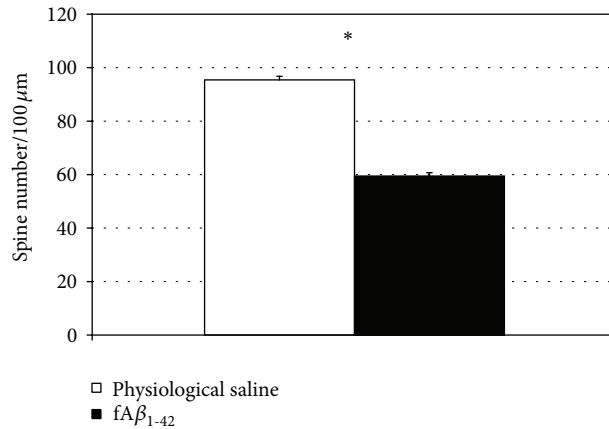


FIGURE 4: Golgi staining revealed changes in spine density after the fA $\beta_{1-42}$ -injection (A). Apical dendritic spine density analysis showed that the amyloid treatment induced a decrease in spine density ( $P < 0.0001$ ). In each experimental group 75 dendritic shafts of 3 animals were studied. The values represent the mean ( $\pm$ S.E.M.) ( $n = 3$  rats per group).

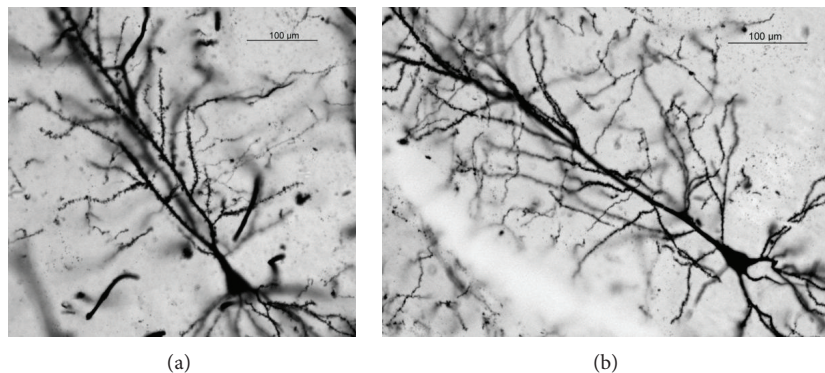


FIGURE 5: Representative photomicrograph of a CA1 subfield pyramidal neuron from a control (a) and an amyloid-treated (b) rat.

and the surrounding oligomeric A $\beta$  are considered as trigger signals to induce dendritic spine loss and synapse dysfunction in AD. A $\beta$  assemblies are synaptotoxic: they can be bound to axons and membrane proteins, resulting in Ca<sup>2+</sup> influx into the neurons [49]. The synapse and dendritic spine loss are strongly correlated with cognitive impairment in AD, and A $\beta$  has been shown to target synapses [40, 50].

Numerous studies have reported significant changes after IHC administration of various types and aggregation forms of A $\beta$  [4, 25–38]. Some studies reported that synapse dysfunction was triggered by A $\beta$  oligomers [49, 51]. Other studies proposed fA $\beta$  deposits as causative factor for the local synaptic abnormalities since decrease of dendritic spine density was detected nearby the A $\beta$  plaques [13, 52–54]. However, it has not been clear how the nondiffusible, immobile A $\beta$  fibrils interact with neuronal structure. As of today, senile plaques are considered mostly as nontoxic “outburns” sequestering toxic A $\beta$  species to nontoxic fibrils. However, bilateral IHC injection of fA $\beta_{1-42}$  results in reduction of neuronal density and increases of glial fibrillary acidic protein intensity, with simultaneous appearance of numerous A $\beta$  deposits and behavioural performance deficits [4, 26]. IHC administration

of shorter form of A $\beta$  (A $\beta_{1-40}$ ) results in decreased density of dendritic spines in hippocampus [25, 28].

Our current findings demonstrated that synthetic fA $\beta_{1-42}$  simultaneously decreased spatial learning ability measured in MWM (Figure 2(a)) and reduced dendritic spine density in the rat hippocampus CA1 region (Figures 4–6). According to the literature data, the synthetic fA $\beta$  assemblies have also a surrounding of A $\beta$  oligomers [55], in accordance with the law of chemical equilibriums. After fA $\beta$  injection, diffusible A $\beta$  oligomers could be formed in the rat hippocampus and initiate dendritic spine density loss. The measured spine loss in HC CA1 region may explain the decreased learning ability since the presence and maturation of dendritic spines on the CA1 pyramidal cells are necessary to evolve the spatial memory unit [56]. It is generally accepted that misfolded proteins initiate dendritic spine reduction and memory decline. A $\beta$  and  $\alpha$ -synuclein oligomers decrease the amount of synaptic proteins and vesicles and via tau hyperphosphorylation initiate the loss of dendritic spines [57, 58]. The instability of dendritic spines leads to progressive neocortical spine loss in a mouse model of Huntington’s disease [59]. Our results support the theory that decreasing spine density in AD can



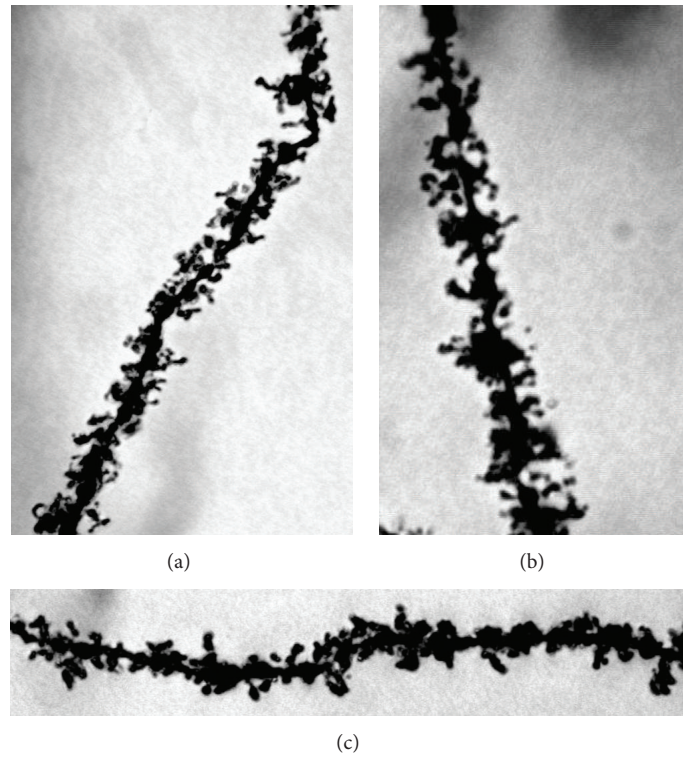


FIGURE 6: Representative photomicrographs of oblique dendritic segments from hippocampal CA1 pyramidal neurons of three control rats ((a), (b), and (c)). The dendritic spine density of vehiculum treated animals was significantly higher compared to the  $fA\beta_{1-42}$ -treated rats. (1000x).

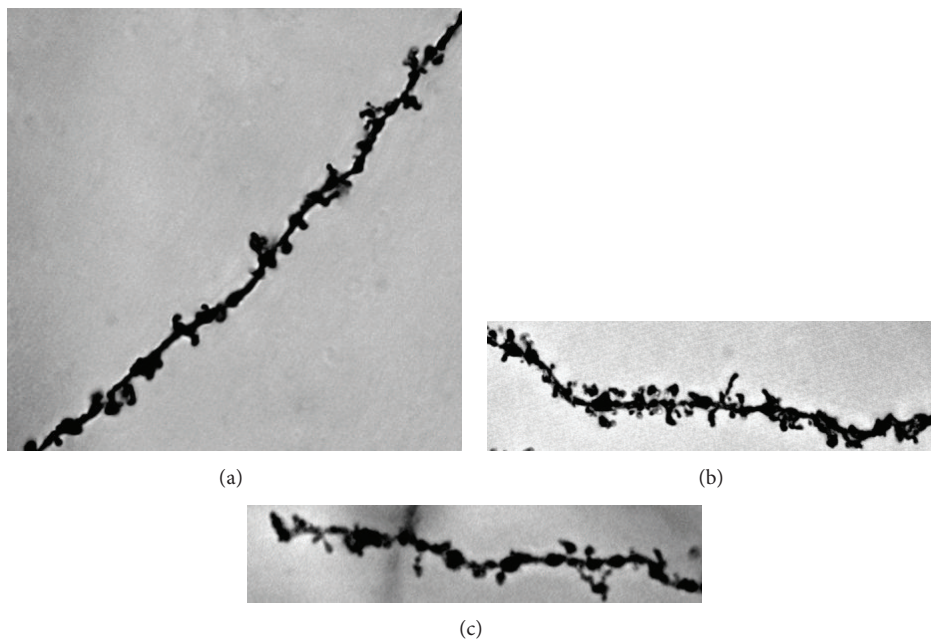


FIGURE 7: Representative photomicrographs of oblique dendritic segments from hippocampal CA1 pyramidal neurons of every amyloid-treated Golgi impregnated rat ((a), (b), and (c)). The  $fA\beta_{1-42}$  locally reduced the spine density in the  $fA\beta_{1-42}$ -injected group (1000x).

cause or contribute to the memory decline: dendritic spines are the site of most excitatory synapses and their loss is in good correlation with the cognitive dysfunction.

## Abbreviations

AD: Alzheimer's disease  
 APP: Amyloid precursor protein  
 A $\beta$ : Amyloid-beta  
 DMSO: Dimethyl sulfoxide  
 fA $\beta_{1-42}$ : Fibrillar A $\beta_{1-42}$   
 HC: Hippocampus  
 HFIP: Hexafluoroisopropanol  
 IHC: Intrahippocampal  
 MWM: Morris water maze.

## Conflict of Interests

The authors declare that there is no conflict of interests regarding the publication of this paper.

## Authors' Contribution

Emőke Borbély and János Horváth contributed equally to this work.

## Acknowledgments

The authors thank Zsuzsa Penke, Ph.D., for the helpful discussion and writing assistance and Titanilla Szögi for her technical assistance. This work was supported by the European Union Seventh Framework Programme Food Grant 211 696 (LipiDiDiet) as well as by the Hungarian research Grant TÁMOP 4.2.2/A-11/1/KONV-2012-0052.

## References

- [1] R. D. Terry, E. Masliah, D. P. Salmon et al., "Physical basis of cognitive alterations in Alzheimer's disease: synapse loss is the major correlate of cognitive impairment," *Annals of Neurology*, vol. 30, no. 4, pp. 572–580, 1991.
- [2] D. Allan Butterfield, A. Castegna, C. M. Lauderback, and J. Drake, "Evidence that amyloid beta-peptide-induced lipid peroxidation and its sequelae in Alzheimer's disease brain contribute to neuronal death," *Neurobiology of Aging*, vol. 23, no. 5, pp. 655–664, 2002.
- [3] S. Kar, S. P. M. Slowikowski, D. Westaway, and H. T. J. Mount, "Interactions between  $\beta$ -amyloid and central cholinergic neurons: implications for Alzheimer's disease," *Journal of Psychiatry and Neuroscience*, vol. 29, no. 6, pp. 427–441, 2004.
- [4] F.-Q. He, B.-Y. Qiu, X.-H. Zhang et al., "Tetrandrine attenuates spatial memory impairment and hippocampal neuroinflammation via inhibiting NF- $\kappa$ B activation in a rat model of Alzheimer's disease induced by amyloid- $\beta_{1-42}$ ," *Brain Research*, vol. 1384, pp. 89–96, 2011.
- [5] B. M. Pause, A. Zlomuzica, K. Kinugawa, J. Mariani, R. Pietrowsky, and E. Dere, "Perspectives on episodic-like and episodic memory," *Frontiers in Behavioral Neuroscience*, 2013.
- [6] H. Braak and E. Braak, "Neuropathological staging of Alzheimer-related changes," *Acta Neuropathologica*, vol. 82, no. 4, pp. 239–259, 1991.
- [7] D. A. Butterfield, M. Perluigi, and R. Sultana, "Oxidative stress in Alzheimer's disease brain: new insights from redox proteomics," *European Journal of Pharmacology*, vol. 545, no. 1, pp. 39–50, 2006.
- [8] S. J. Baloyannis, "Dendritic pathology in Alzheimer's disease," *Journal of the Neurological Sciences*, vol. 283, no. 1-2, pp. 153–157, 2009.
- [9] D. J. Selkoe, "Translating cell biology into therapeutic advances in Alzheimer's disease," *Nature*, vol. 399, no. 6738, supplement, pp. A23–A31, 1999.
- [10] D. J. Selkoe, "Alzheimer's disease results from the cerebral accumulation and cytotoxicity of amyloid  $\beta$ -protein," *Journal of Alzheimer's Disease*, vol. 3, no. 1, pp. 75–81, 2001.
- [11] M. P. Mattson, "Pathways towards and away from Alzheimer's disease," *Nature*, vol. 430, no. 7000, pp. 631–639, 2004.
- [12] M. A. Chabrier, D. Cheng, N. A. Castello, K. N. Green, and F. M. Laferla, "Synergistic effects of amyloid-beta and wild-type human tau on dendritic spine loss in a floxed double transgenic model of Alzheimer's disease," *Neurobiology of Disease*, vol. 64, pp. 107–117, 2014.
- [13] J. Tsai, J. Grutzendler, K. Duff, and W.-B. Gan, "Fibrillar amyloid deposition leads to local synaptic abnormalities and breakage of neuronal branches," *Nature Neuroscience*, vol. 7, no. 11, pp. 1181–1183, 2004.
- [14] S. Knafo, L. Alonso-Nanclares, J. Gonzalez-Soriano et al., "Widespread changes in dendritic spines in a model of Alzheimer's Disease," *Cerebral Cortex*, vol. 19, no. 3, pp. 586–592, 2009.
- [15] R. M. Koffie, M. Meyer-Luehmann, T. Hashimoto et al., "Oligomeric amyloid  $\beta$  associates with postsynaptic densities and correlates with excitatory synapse loss near senile plaques," *Proceedings of the National Academy of Sciences of the United States of America*, vol. 106, no. 10, pp. 4012–4017, 2009.
- [16] F. M. LaFerla, K. N. Green, and S. Oddo, "Intracellular amyloid- $\beta$  in Alzheimer's disease," *Nature Reviews Neuroscience*, vol. 8, no. 7, pp. 499–509, 2007.
- [17] E. A. Nimchinsky, B. L. Sabatini, and K. Svoboda, "Structure and function of dendritic spines," *Annual Review of Physiology*, vol. 64, pp. 313–353, 2002.
- [18] V. A. Alvarez and B. L. Sabatini, "Anatomical and physiological plasticity of dendritic spines," *Annual Review of Neuroscience*, vol. 30, pp. 79–97, 2007.
- [19] D. L. Smith, J. Pozueta, B. Gong, O. Arancio, and M. Shelanski, "Reversal of long-term dendritic spine alterations in Alzheimer disease models," *Proceedings of the National Academy of Sciences of the United States of America*, vol. 106, no. 39, pp. 16877–16882, 2009.
- [20] S. Jain, S. Y. Yoon, L. Leung, J. Knoferle, and Y. Huang, "Cellular source-specific effects of apolipoprotein (apo) E4 on dendrite arborization and dendritic spine development," *PLoS ONE*, vol. 8, no. 3, Article ID e59478, 2013.
- [21] J. H. Morrison and M. G. Baxter, "The ageing cortical synapse: Hallmarks and implications for cognitive decline," *Nature Reviews Neuroscience*, vol. 13, no. 4, pp. 240–250, 2012.
- [22] J. I. Luebke, C. M. Weaver, A. B. Rocher et al., "Dendritic vulnerability in neurodegenerative disease: insights from analyses of cortical pyramidal neurons in transgenic mouse models," *Brain Structure and Function*, vol. 214, no. 2-3, pp. 181–199, 2010.

- [23] D. H. Bhatt, S. Zhang, and W.-B. Gan, "Dendritic spine dynamics," *Annual Review of Physiology*, vol. 71, pp. 261–282, 2009.
- [24] M. Matsuzaki, N. Honkura, G. C. R. Ellis-Davies, and H. Kasai, "Structural basis of long-term potentiation in single dendritic spines," *Nature*, vol. 429, no. 6993, pp. 761–766, 2004.
- [25] B. Wan, X. Hu, J. Nie et al., "Effects of triptolide on degeneration of dendritic spines induced by  $A\beta_{1-40}$  injection in rat hippocampus," *Neurological Sciences*, 2013.
- [26] M. A. Chacón, M. I. Barriá, C. Soto, and N. C. Inestrosa, " $\beta$ -sheet breaker prevents  $A\beta$ -induced spatial memory impairments with partial reduction of amyloid deposits," *Molecular Psychiatry*, vol. 9, no. 10, pp. 953–961, 2004.
- [27] S.-Z. Zhong, Q.-H. Ge, Q. Li, R. Qu, and S.-P. Ma, "Peoniflorin attenuates  $A\beta_{1-42}$ -mediated neurotoxicity by regulating calcium homeostasis and ameliorating oxidative stress in hippocampus of rats," *Journal of the Neurological Sciences*, vol. 280, no. 1–2, pp. 71–78, 2009.
- [28] X. Gong, X. Lu, L. Zhan et al., "Role of the SNK-SPAR pathway in the development of Alzheimer's disease," *IUBMB Life*, vol. 62, no. 3, pp. 214–221, 2010.
- [29] J. Li, G. Wang, J. Liu et al., "Puerarin attenuates amyloid-beta-induced cognitive impairment through suppression of apoptosis in rat hippocampus in vivo," *European Journal of Pharmacology*, vol. 649, no. 1–3, pp. 195–201, 2010.
- [30] J. G. Choi, M. Moon, H. G. Kim et al., "Gami-Chunghyuldan ameliorates memory impairment and neurodegeneration induced by intrahippocampal  $A\beta_{1-42}$  oligomer injection," *Neurobiology of Learning and Memory*, vol. 96, no. 2, pp. 306–314, 2011.
- [31] N. Jantarotnotai, J. K. Ryu, C. Schwab, P. L. McGeer, and J. G. McLarnon, "Comparison of vascular perturbations in an  $A\beta$ -injected animal model and in AD brain," *International Journal of Alzheimer's Disease*, vol. 2011, Article ID 918280, 8 pages, 2011.
- [32] Q. Quan, J. Wang, X. Li, and Y. Wang, "Ginsenoside Rg1 decreases  $A\beta_{1-42}$  level by upregulating PPAR $\gamma$  and IDE expression in the hippocampus of a rat model of Alzheimer's disease," *PLoS ONE*, vol. 8, no. 3, Article ID e59155, 2013.
- [33] P. He, X. Ouyang, S. Zhou et al., "A novel melatonin agonist NeuP11 facilitates memory performance and improves cognitive impairment in a rat model of Alzheimer's disease," *Hormones and Behavior*, vol. 64, no. 1, pp. 1–7, 2013.
- [34] X.-J. Liu, L. Yuan, D. Yang et al., "Melatonin protects against amyloid- $\beta$ -induced impairments of hippocampal LTP and spatial learning in rats," *Synapse*, vol. 67, no. 9, pp. 626–636, 2013.
- [35] M. Zheng, J. Liu, Z. Ruan et al., "Intrahippocampal injection of  $A\beta_{1-42}$  inhibits neurogenesis and down-regulates IFN- $\gamma$  and NF- $\kappa$ B expression in hippocampus of adult mouse brain," *Amyloid*, vol. 20, no. 1, pp. 13–20, 2013.
- [36] J. Jia, L. Kang, S. Li et al., "Amelioratory effects of testosterone treatment on cognitive performance deficits induced by soluble  $A\beta_{1-42}$  oligomers injected into the hippocampus," *Hormones and Behavior*, vol. 64, no. 3, pp. 477–486, 2013.
- [37] Y. Yin, Y. Ren, W. Wu et al., "Protective effects of bilobalide on  $A\beta_{25-35}$  induced learning and memory impairments in male rats," *Pharmacology Biochemistry and Behavior*, vol. 106, pp. 77–84, 2013.
- [38] J. Zhang, Y.-F. Zhena, L.-G. Song et al., "Salidroside attenuates beta amyloid-induced cognitive deficits via modulating oxidative stress and inflammatory mediators in rat hippocampus," *Behavioural Brain Research*, vol. 244, pp. 70–81, 2013.
- [39] G. M. Bishop and S. R. Robinson, "The amyloid hypothesis: let sleeping dogmas lie?" *Neurobiology of Aging*, vol. 23, no. 6, pp. 1101–1105, 2002.
- [40] W. Wei, L. N. Nguyen, H. W. Kessels, H. Hagiwara, S. Sisodia, and R. Malinow, "Amyloid beta from axons and dendrites reduces local spine number and plasticity," *Nature Neuroscience*, vol. 13, no. 2, pp. 190–196, 2010.
- [41] P. K.-Y. Chang, S. Boridy, R. A. McKinney, and D. Maysinger, "Letrozole potentiates mitochondrial and dendritic spine impairments induced by  $\beta$  amyloid," *Journal of Aging Research*, vol. 2013, Article ID 538979, 11 pages, 2013.
- [42] C. Meng, Z. He, and D. Xing, "Low-level laser therapy rescues dendrite atrophy via upregulating BDNF expression: implications for Alzheimer's disease," *Journal of Neuroscience*, vol. 33, no. 33, pp. 13505–13517, 2013.
- [43] S. Nath, L. Agholme, F. R. Kurudenkandy, B. Granseth, J. Marcusson, and M. Hallbeck, "Spreading of neurodegenerative pathology via neuron-to-neuron transmission of  $\beta$ -amyloid," *Journal of Neuroscience*, vol. 32, no. 26, pp. 8767–8777, 2012.
- [44] B. Leuner, S. Mendolia-Loffredo, Y. Kozorovitskiy, D. Samburg, E. Gould, and T. J. Shors, "Learning enhances the survival of new neurons beyond the time when the hippocampus is required for memory," *Journal of Neuroscience*, vol. 24, no. 34, pp. 7477–7481, 2004.
- [45] B. Leuner and T. J. Shors, "New spines, new memories," *Molecular Neurobiology*, vol. 29, no. 2, pp. 117–130, 2004.
- [46] Z. Bozso, B. Penke, D. Simon et al., "Controlled in situ preparation of  $A\beta_{1-42}$  oligomers from the isopeptide "iso- $A\beta_{1-42}$ ", physicochemical and biological characterization," *Peptides*, vol. 31, no. 2, pp. 248–256, 2010.
- [47] G. Paxinos and C. Watson, *The Rat Brain in Stereotaxic Coordinates*, Academic Press, London, UK, 1982.
- [48] D. Nagy, K. Kocsis, J. Fuzik et al., "Kainate postconditioning restores LTP in ischemic hippocampal CA1: onset-dependent second pathophysiological stress," *Neuropharmacology*, vol. 61, no. 5–6, pp. 1026–1032, 2011.
- [49] D. J. Selkoe, "Alzheimer's disease is a synaptic failure," *Science*, vol. 298, no. 5594, pp. 789–791, 2002.
- [50] P. N. Lacor, M. C. Buniel, L. Chang et al., "Synaptic targeting by Alzheimer's-related amyloid  $\beta$  oligomers," *Journal of Neuroscience*, vol. 24, no. 45, pp. 10191–10200, 2004.
- [51] P. N. Lacor, M. C. Buniel, P. W. Furlow et al., " $A\beta$  oligomer-induced aberrations in synapse composition, shape, and density provide a molecular basis for loss of connectivity in Alzheimer's disease," *Journal of Neuroscience*, vol. 27, no. 4, pp. 796–807, 2007.
- [52] J. Grutzendler, K. Helmin, J. Tsai, and W.-B. Gan, "Various dendritic abnormalities are associated with fibrillar amyloid deposits in Alzheimer's disease," *Annals of the New York Academy of Sciences*, vol. 1097, pp. 30–39, 2007.
- [53] C. M. Kirkwood, J. Ciuchta, M. D. Ikonovic et al., "Dendritic spine density, morphology, and fibrillar actin content surrounding amyloid- $\beta$  plaques in a mouse model of amyloid- $\beta$  deposition," *Journal of Neuropathology and Experimental Neurology*, vol. 72, no. 8, pp. 791–800, 2013.
- [54] R. Le, L. Cruz, B. Urbanc et al., "Plaque-induced abnormalities in neurite geometry in transgenic models of Alzheimer disease: implications for neural system disruption," *Journal of Neuropathology and Experimental Neurology*, vol. 60, no. 8, pp. 753–758, 2001.

- [55] A. Sandberg, L. M. Luheshi, S. Sollvander et al., "Stabilization of neurotoxic Alzheimer amyloid-beta oligomers by protein engineering," *Proceedings of the National Academy of Sciences of the United States of America*, vol. 107, no. 35, pp. 15595–15600, 2010.
- [56] A. Feria-Velasco, A. R. del Angel, and I. Gonzalez-Burgos, "Modification of dendritic development," *Progress in Brain Research*, vol. 136, pp. 135–143, 2002.
- [57] M. L. Kramer and W. J. Schulz-Schaeffer, "Presynaptic  $\alpha$ -synuclein aggregates, not Lewy bodies, cause neurodegeneration in dementia with lewy bodies," *Journal of Neuroscience*, vol. 27, no. 6, pp. 1405–1410, 2007.
- [58] C. R. Overk and E. Masliah, "Pathogenesis of synaptic degeneration in Alzheimer's disease and Lewy body disease," *Biochemical Pharmacology*, vol. 88, no. 4, pp. 508–516, 2014.
- [59] R. P. Murmu, W. Li, A. Holtmaat, and J.-Y. Li, "Dendritic spine instability leads to progressive neocortical spine loss in a mouse model of huntington's disease," *Journal of Neuroscience*, vol. 33, no. 32, pp. 12997–13009, 2013.



# LPYFDa Neutralizes Amyloid- $\beta$ -Induced Memory Impairment and Toxicity

Ivica Granic<sup>a</sup>, Marcelo F. Masman<sup>a</sup>, Cornelis (Kees) Mulder<sup>a</sup>, Ingrid M. Nijholt<sup>a,b</sup>, Pieter J.W. Naude<sup>a,c</sup>, Ammerins de Haan<sup>a</sup>, Emöke Borbély<sup>d</sup>, Botond Penke<sup>d</sup>, Paul G.M. Luiten<sup>a,c</sup> and Ulrich L.M. Eisel<sup>a,\*</sup>

<sup>a</sup>Department of Molecular Neurobiology, University of Groningen, Haren, The Netherlands

<sup>b</sup>Department of Neuroscience, Section Anatomy, University Medical Center Groningen, The Netherlands

<sup>c</sup>Department of Biological Psychiatry, University Medical Center Groningen, The Netherlands

<sup>d</sup>Department of Medical Chemistry, University of Szeged, Szeged, Hungary

Accepted 29 September 2009

**Abstract.** Misfolding, oligomerization, and aggregation of the amyloid- $\beta$  ( $A\beta$ ) peptide is widely recognized as a central event in the pathogenesis of Alzheimer's disease (AD). Recent studies have identified soluble  $A\beta$  oligomers as the main pathogenic agents and provided evidence that such oligomeric  $A\beta$  aggregates are neurotoxic, disrupt synaptic plasticity, and inhibit long-term potentiation. A promising therapeutic strategy in the battle against AD is the application of short synthetic peptides which are designed to bind to specific  $A\beta$ -regions thereby neutralizing or interfering with the devastating properties of oligomeric  $A\beta$  species. In the present study, we investigated the neuroprotective properties of the amyloid sequence derived pentapeptide LPYFDa *in vitro* as well as its memory preserving capacity against  $A\beta_{42}$ -induced learning deficits *in vivo*. *In vitro* we showed that neurons in culture treated with LPYFDa are protected against  $A\beta_{42}$ -induced cell death. Moreover, *in vivo* LPYFDa prevented memory impairment tested in a contextual fear conditioning paradigm in mice after bilateral intrahippocampal  $A\beta_{42}$  injections. We thus showed for the first time that an anti-amyloid peptide like LPYFDa can preserve memory by reverting  $A\beta_{42}$  oligomer-induced learning deficits.

**Keywords:** Alzheimer's disease, amyloid- $\beta$  oligomers,  $\beta$ -sheet breaker peptides, behavioral tests, circular dichroism spectrometry, fear conditioning, hippocampus, molecular modeling, neuroprotection, primary cortical neurons

## INTRODUCTION

Progressive neurodegeneration and cognitive decline are typical features of Alzheimer's disease (AD), the most common form of dementia [1]. Besides the formation of neurofibrillary tangles, it is widely acknowledged that the aggregation of amyloid- $\beta$  ( $A\beta$ ) initiates a complex series of events that ultimately results in neuronal cell death particularly in forebrain regions, which is paralleled by the cognitive and behavioral de-

cline that is characteristic for pathogenesis of AD.  $A\beta$  is generated by sequential proteolytic cleavage from the amyloid- $\beta$  protein precursor ( $A\beta$ PP) by  $\beta$ - and  $\gamma$ -secretases (amyloidogenic processing). Alternatively  $A\beta$ PP can be cleaved by  $\alpha$ -secretase within the  $A\beta$  sequence which prevents the generation of  $A\beta$  peptide. Once released,  $A\beta$  due to its physico-chemical properties has the strong tendency to misfold, oligomerize and to aggregate into fibrils and plaques [2].

Although amyloid plaques represent a major hallmark of AD, they correlate poorly with the progression of the disease [3]. Interestingly, more recent studies have identified soluble  $A\beta$ -oligomer assemblies as the main pathogenic agents which, in contrast to plaques, do correlate well with the mental decline ob-

\*Correspondence to: Prof. Dr. Ulrich L. M. Eisel, Department of Molecular Neurobiology, University of Groningen, Kerklaan 30, 9751 NN Haren, The Netherlands. Tel.: +31 50 363 2366; Fax: +31 50 363 2331; E-mail: U.L.M.Eisel@rug.nl.

served in AD patients [1,4–7]. Furthermore, soluble A $\beta$  oligomers have been shown to be neuro- and synaptotoxic and to inhibit long-term potentiation (LTP) [8–12]. Acute application of oligomeric A $\beta$  leads to internalization of glutamatergic AMPA and NMDA receptors and finally to synaptic downscaling [13,14]. However, it should be appreciated that next to its pathological properties, A $\beta$ , notably in very low physiological concentrations, may have an important role in synaptic plasticity and normal brain functioning [10,15,16]. The endogenous level of A $\beta$  in the brain is regulated by synaptic activity *in vivo*, suggesting a dynamic feedback loop involving A $\beta$ PP metabolism and A $\beta$  that may modulate synaptic activity [1]. Recently, Garcia-Osta and coworkers showed that depletion of endogenous A $\beta$  by a single intrahippocampal (i.h.) administration of anti-A $\beta$ -antibody leads to disrupted memory retention in rats [17]. During the pathogenesis of AD, the equilibrium of A $\beta$  generation and A $\beta$  clearance is disturbed, which eventually leads to elevated A $\beta$  levels, increased A $\beta$  aggregation, and impaired memory function [10].

Multiple therapeutic strategies have been developed since the second half of the previous century [18]. Unfortunately, most of the currently available therapies target only the symptoms, acting on presumed downstream neurotoxic pathogenic mechanisms without tackling the cause and thus hardly able to affect the progression of the disease. Experimental data from animal studies using immunotherapy in order to remove A $\beta$  from the brain were highly promising [19]. However, clinical trials with active immunization against A $\beta$  were halted due to severe brain inflammation and premature death of several patients [20,21].

Consequently, as a therapeutic strategy, compounds were developed that could inhibit or delay the development of A $\beta$  aggregation, fibrillization, and/or plaque formation and were thus potentially capable of protecting neurons from A $\beta$  toxicity. As part of this approach, small peptides derived from the A $\beta$  sequence were designed, such as the pentapeptide LPYFDa, which seemed to offer a promising starting point to develop potential drugs that can somehow revert the devastating impact of A $\beta$  aggregates. The advantage of such compounds, in comparison to other putative therapeutic approaches for AD such as vaccination, is that they specifically target the abnormal conformation of A $\beta$  without interfering with any possible physiological function of the soluble, monomeric A $\beta$  peptide.

There have been numerous attempts to develop treatments developed to interfere with various key steps in

the amyloidogenic process. Promising putative treatments may be those designed to inhibit steps that precede A $\beta$  peptide aggregation, by blocking production of the toxic soluble A $\beta$  oligomers in the first place, or by reversing, somehow, the toxic effect of these oligomers.

In the present study we established an *in vivo* model in the mouse for A $\beta$ -induced memory impairment through a single bilateral injection of oligomeric A $\beta_{42}$  into the hippocampus and explored in this model whether LPYFDa can be beneficial against the A $\beta$ -induced cognitive deficits. Furthermore, we investigated the neuroprotective properties of A $\beta$ -derived synthetic  $\beta$ -sheet breaker peptide Leu-Pro-Tyr-Phe-Asp-amide (LPYFDa) [22,24] against the neurotoxic effects of soluble A $\beta_{42}$  oligomers in cultured mouse primary cortical neurons (PCN). Finally, we employed molecular modeling and docking experiments to reveal part of the putative mechanism of action of these peptides.

## MATERIAL AND METHODS

### Compounds

The  $\beta$ -sheet breaker LPYFDa was synthesized in our laboratories by a solid-phase procedure involving the use of Merrifield resin and Boc chemistry. Purity control and structure verification were carried out by amino acid analysis and mass spectrometry as previously described [25]. The control peptide (scrP), which is a scrambled version of the LPYFD peptide (Pro-Asp-Tyr-Leu-Phe-amide), and A $\beta_{1-42}$  (A $\beta_{42}$ ) were purchased from EZBiolab Inc. (Carmel, USA). Anti-A $\beta$  antibody (6E10) was obtained from Covance (Emeryville, USA). Other compounds used in this study were purchased from Invitrogen (Carlsbad, USA) or Sigma-Aldrich Corporation (St. Louis, USA).

### Preparation of A $\beta$ -oligomers

Oligomeric A $\beta_{42}$  was prepared as described by Dahlgren and colleagues [26]. In short, the synthetic A $\beta_{42}$  peptide was initially dissolved in 1,1,1,3,3,3-hexafluoro-2-propanol (HFIP) to a concentration of 1 mM. The peptide solution was divided into aliquots and the HFIP removed by evaporation under vacuum (SpeedVac; Savant Instruments, Hyderabad, India). The dry peptide films were stored at  $-20^{\circ}\text{C}$  until further processing. Before use, the dry film A $\beta_{42}$  was dissolved in anhydrous DMSO to 5 mM followed by bath sonication (Decon, Hove Sussex, UK) for 10 min,

subsequently diluted in neurobasal medium to a final concentration of 100  $\mu$ M (stock solution) and incubated at 4°C for 24 h to enable A $\beta$ <sub>42</sub> oligomerization. The aggregation state and the secondary structure of the oligomeric A $\beta$ <sub>42</sub> preparation was examined by sodium dodecyl sulfate (SDS)-PAGE Western blotting and Circular Dichroism (CD) spectrometry (Fig. 1).

#### Gel electrophoresis and Western blot analysis

Gel electrophoresis and Western blot analysis were adopted from Stine et al. [27]. Briefly, unheated samples in SDS sample buffer were applied to 10–20% tris-tricine gradient gels (BioRad, Munich, Germany), electrophoresed using tricine running buffer, and subsequently transferred to 0.45- $\mu$ m polyvinylidene difluoride membranes (Millipore, Bilerca, USA). Membranes were blocked with 1% I-Block (Tropix, Bedford, USA) in Trisbuffered saline containing 0.0625% Tween-20. Blots were incubated with primary antibody 6E10 overnight (1:2000; mouse monoclonal against A $\beta$  residues 1–16; Covance Emeryville, USA). Immunoreactivity was detected using enhanced chemiluminescence (Pierce Biotechnology, Rockford, USA) and imaged on an Kodak X-Ray film (Eastman Kodak Company, Rochester, USA) (Fig. 1A). Molecular weight values were estimated using the PageRuler (Fermentas International, Ontario, Canada) pre-stained molecular weight marker.

#### CD spectrometry

CD measurements were performed at 25°C on a CD Spectrometer Model 62DS (AVIV Associates Inc., Lakewood, USA) using a quartz cell of 0.1 cm path-length. All spectra were averages of four scans; the resolution was 1 nm. The oligomerized A $\beta$  was diluted in PBS to a concentration of 25  $\mu$ M. The samples were sonicated for 10 min immediately after dissolution. CD spectra were expressed as mean residue ellipticity  $[\Theta]_{MR}$  in units of deg cm<sup>2</sup> dmol<sup>-1</sup> (Fig. 1B). The percentages of secondary structures were analyzed using the K2D2 program [28].

#### Molecular modeling

##### Stochastic conformational search. EDMC calculations

The conformational space was explored using the method previously employed by Liwo et al. [29], which includes the electrostatically driven Monte Carlo

(EDMC) method [30,31] implemented in the ECEPPAK [32] package. Conformational energy was evaluated using the ECEPP/3 force field [33]. Hydration energy was evaluated using a hydration-shell model with a solvent sphere radius of 1.4 Å and atomic hydration parameters that have been optimized using nonpeptide data (SRFOPT) [34,35]. In order to explore the conformational space extensively, we carried out 10 different runs, each of them with a different random number. Therefore, we collected a total of 5000 accepted conformations. Each EDMC run was terminated after 500 energy-minimized conformations had been accepted. The parameters controlling the runs were the following: a temperature of 298.15 K was used for the simulations. A temperature jump of 1,000 K was used; the maximum number of allowed repetitions of the same minimum was 50. The maximum number of electrostatically predicted conformations per iteration was 400; the maximum number of random-generated conformations per iteration was 100; the fraction of random/electrostatically predicted conformations was 0.30. The maximum number of steps at one increased temperature was 20; and the maximum number of rejected conformations until a temperature jump is executed was 100. Only *trans* peptide bonds ( $\omega \cong 180^\circ$ ) were considered. All accepted conformations were then clustered into families using the program ANALYZE [36,37] by applying the minimal-tree clustering algorithm for separation, using all heavy atoms, energy threshold of 30 kcal.mol<sup>-1</sup>, and RMSD of 0.75 Å as separation criteria. This clustering step allows a substantial reduction of the number of conformations and the elimination of repetitions. A more detailed description of the procedure used here is given in section 4.4 *Computational Methods* of reference [38].

#### Docking studies

Two models for A $\beta$  were used as target systems; the monomeric A $\beta$ <sub>42</sub> elucidated by Crescenzi et al. (monomeric model) [39], PDB code 1IYT, and the pentameric aggregate A $\beta$ <sub>42</sub> developed by Masman et al. (pentameric model) [40]. The structures were prepared for docking study as follows: for the A $\beta$ <sub>42</sub> molecules, water molecules were removed from the PDB file and hydrogen atoms were added; Gasteiger charges, atomic solvation parameters and fragmental volumes were merged to the target system. For both LPYFDa and scrP, the structure of the most populated family (results from the EDMC calculations) was taken as initial conformation. Gasteiger charges were assigned and

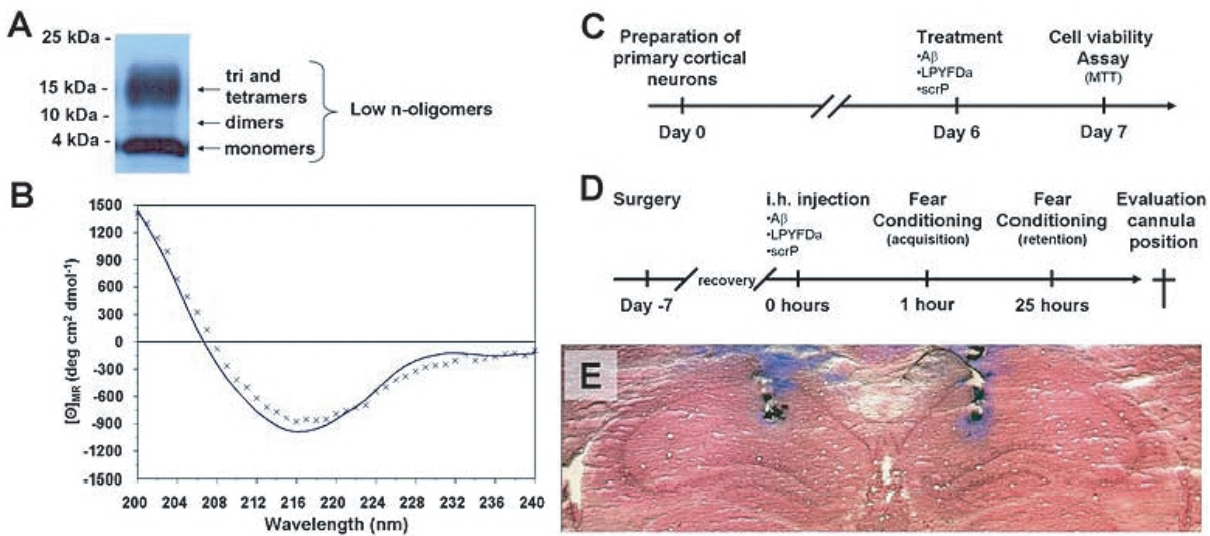


Fig. 1. **A**) Oligomeric preparation of A $\beta$ <sub>42</sub> was examined by Western blot using the anti-A $\beta$  antibody 6E10 (1:2000). Bands correspond to monomeric up to tetrameric forms of A $\beta$ <sub>42</sub>. **B**) CD spectrum of (×) A $\beta$ <sub>42</sub> in PBS after 24 hours incubation at 4°C. (–) fitted line data using K2D2 program. **C**) Schematic outline of the experimental procedure *in vitro*. PCN from C57BL6 mouse embryos (E14) were cultured for 6 days and then treated for 24 h with different concentrations of oligomerized A $\beta$ <sub>42</sub>,  $\beta$ -sheet breaker peptides or combinations of both. On day 7 medium was completely exchanged and 24 h later the cell viability was assessed by an MTT reduction assay. **D**) Schematic outline of the experimental setup *in vivo*. C57BL/6J mice were cannulated 7 days prior i.h. injection with oligomerized A $\beta$ <sub>42</sub> and/or  $\beta$ -sheet breaker peptides. One hour after the injection the animals were trained in a contextual fear conditioning paradigm. 24 hours after the training session memory performance was assessed. Cannula position was evaluated by methylene blue injection after the behavioural test. **E**) Representative coronal brain sections of a bilateral dorsal hippocampal (i.h.) injection with methylene blue counterstained with nuclear fast red.

non-polar hydrogen atoms were merged. All torsions were allowed to rotate during docking. The docking energy grid was produced with the auxiliary program AutoGrid. The grid dimensions were 60 × 60 × 60 for the monomeric model, and 90 × 60 × 60 for the pentameric model, points along the x-, y- and z-axes, with points separated by 0.375 Å. The grids were chosen to be sufficiently large to cover significant portions of the putative binding sites. The center of the pentapeptide was positioned at the grid center. All graphic manipulations and visualizations were performed by means of the AutoDock Tools [41] and the Chimera [42] programs, and ligand docking with AUTODOCK 4 [43]. The Lamarckian genetic algorithm was utilized and the energy evaluations were set at  $2.5 \times 10^6$ . A total of 250 accepted conformations were collected. Other parameters were set to default values.

#### Primary cortical neuron culture

PCN were prepared from embryonic brains (E14) of C57BL/6J mice. The cortices were carefully dissected, meninges were removed, and the neurons separated by trituration. Cells were plated on poly-D-lysine pre-coated plates at a density of  $1.2 \times 10^5$  cells/well (96

well plates). Neurobasal medium supplemented with 2% (v/v) B27-supplement, 0.5 mM glutamine and 1% (v/v) penicillin/ streptomycin was used as a culture medium. After 48 h, neurons were treated with 10  $\mu$ M cytosine arabinoside for another 48 h to inhibit non-neuronal cell growth. Subsequently, the medium was completely exchanged, and, after 6 days of *in vitro* culture, the neurons were used for experiments.

#### Treatment of cells

Possible toxicity of LPYFDa, its control peptide scrP, and A $\beta$ <sub>42</sub> oligomers was determined by incubating neuronal cultures for 24 h with different concentrations of the peptide solutions. The neuroprotective effect of LPYFDa was assessed by incubating neurons (cultured in 96 well plates) for 24 h with 20  $\mu$ M oligomeric A $\beta$  in the presence or absence of different concentrations of LPYFDa or control peptide. After the treatment, the medium was completely exchanged, and 24 h later, the cell viability was determined by an MTT-assay (Fig. 1C). All treatments were performed in triplicates and the experiments were repeated at least two times.

### Determination of cell viability by MTT-assay

Neuronal viability was determined by the colorimetric MTT [3-(4,5-dimethylthiazol-2-yl)-2,5-diphenyltetrazolium bromide] assay as described previously [44]. 1.25 mg/ml MTT solution was added to each well of a 96 well plate. After 2 h of incubation, cells were lysed in acidic propan-2-ol solution (37% HCl/ propan-2-ol: 1/166). The absorbance of each well was measured with an automated ELISA plate reader (BioRad, Munich, Germany) at 595 nm with a reference filter at 630 nm.

### Animals

Behavioral experiments were performed with 9–12 weeks old male C57Bl/6J mice (Harlan, Horst, The Netherlands). Individually housed mice were maintained on a 12 h light/dark cycle (lights on at 7.00 a.m.) with food (Hopefarms, standard rodent pellets) and water *ad libitum*. A layer of sawdust served as bedding. The animals were allowed to adapt to the housing conditions for 1–2 weeks before the experiments started. The procedures concerning animal care and treatment were in accordance with the regulations of the Ethical Committee for the use of experimental animals of the University of Groningen (DEC4668C).

### Animal surgery

Double guide cannulae type C235 (Plastics One, Roanoke, USA) were implanted in the brain using a Kopf stereotactic instrument during Hypnorm/Midazolam (10 ml/kg, i.p.) anesthesia under aseptic conditions as previously described [45] with anteroposterior (AP) coordinates zeroed at Bregma directed toward both dorsal hippocampi (i.h.), AP -1.5 mm, lateral 1 mm, depth 2 mm [46]. Each double guide cannula with inserted dummy cannula and dust cap was fixed to the skull with dental cement (3M ESPE AG, Seefeld, Germany). Administration of 1 mg/ml finadyne (2.5 mg/kg s.c.) before the surgery served as analgesic. The animals were allowed to recover for 6–7 days before the behavioral measurements started.

### Intrahippocampal injections

Bilateral i.h. injections were performed under short isofluran anesthesia using a Hamilton microsyringe fitted to a syringe pump unit (TSE systems, Bad Homburg, Germany) at a constant rate of 0.3  $\mu$ l/min (final volume: 0.3  $\mu$ l per side). The amount of injected A $\beta$ <sub>42</sub> was of 15, 30, or 60 pmol and LPYFDa as well as the control peptide scrP in an amount of 150 pmol into the dorsal hippocampus. PBS (pH 7.5) served as vehicle. One hour after the injection the animals were subjected to a training session in a fear conditioning paradigm (Fig. 1D). The number of animals per group varied from 5 to 9.

### Fear conditioning

Fear conditioning was performed in a plexiglas cage (44  $\times$  22  $\times$  44 cm) with constant illumination (12 V, 10W halogen lamp, 100–500 lux). The training (conditioning) consisted of a single trial. Before each individual mouse entered the box, the box was cleaned with 70% ethanol. The mouse was exposed to the conditioning context for 180 s followed by a scrambled footshock (0.7 mA, 2 s, constant current) delivered through a stainless steel grid floor. The mouse was removed from the fear conditioning box 30 s after shock termination to avoid an aversive association with the handling procedure. Memory tests were performed 24 h after fear conditioning. Contextual memory was tested in the fear conditioning box for 180 s without footshock presentation. Freezing, defined as the lack of movement except for respiration and heart beat, was assessed as the behavioral parameter of the defensive reaction of mice by a time-sampling procedure every 10 s throughout memory tests. In addition, mean activity of the animal during the training and retention test was measured with the Ethovision system (Noldus, Wageningen, The Netherlands).

### Histology

Immediately after the behavioral test, mice were injected i.h. with methylene blue solution during sodium-pentobarbital anesthesia (0.1 ml/ 10 g, i.p.). Brains were removed and serially sectioned at 50  $\mu$ m. Sections were stained on glass for 5 min in 0.1% nuclear fast red solution. To identify the location of the injection, sections were analyzed using light microscopy. Only data from animals in which the proper intrahippocampal site of injection was confirmed, were evaluated (Fig. 1E).

### Statistical analysis

Behavioral data were analyzed by analysis of variance (ANOVA) followed by the Bonferroni post-hoc test to determine statistical significance. For statistical analysis of the MTT assays, an unpaired Student's *t* test with unequal variance was used. A *p*-value < 0.05 was considered to be statistically significant. Data are presented as mean value  $\pm$  standard error of the mean (SEM).

## RESULTS

### Characterization of the oligomeric A $\beta_{42}$

The state of aggregation of the oligomeric A $\beta_{42}$  preparation was determined by Western blot analysis. The results confirmed that the A $\beta_{42}$  preparation consisted of a mixture of small molecular weight A $\beta_{42}$  oligomers from monomeric to tetrameric A $\beta_{42}$  (Fig. 1A). In addition, we used CD spectrometry to characterize the secondary structure of A $\beta_{42}$  in solution. We could show that our oligomeric A $\beta_{42}$  preparation consists of 43.02%  $\beta$ -sheets, 5.40%  $\alpha$ -helix, and 51.58% random-coil conformation (Fig. 1B), which shows a good correlation to the conformation behavior of A $\beta_{42}$  aggregates observed by Masman et al. [40].

### Molecular modeling and stochastic conformational search. EDMC calculations

To have a better view at the molecular level, it is crucial to assess the conformational behavior of the pentapeptides in solution. Therefore, LPYFDa and scrP were selected for energy calculations to determine the biologically relevant conformations. The results of the theoretical calculations are summarized in Table 1. Calculations yielded a large set of conformational families for each peptide studied. The total number of conformations generated was 62515 and 65056, for LPYFDa and scrP respectively, whereof 5000 conformations for each pentapeptide were accepted. In the clustering procedure, an R.M.S.D (Root Mean Square Deviation) of 0.75 Å and a  $\Delta E$  of 30 kcal mol<sup>-1</sup> were used. The number of families after clustering was 220 and 323, for LPYFDa and scrP, respectively. The total number of families accepted with a relative population higher than 0.50% was 10 and 25, for LPYFDa and scrP, respectively, that sum up to *ca* 90% of all conformations. All low-energy conformers of pentapeptides studied here

Table 1

Conformational search and clustering results for LPYFDa and scrP optimized at the EDMC/SRFOPT/ECCEP/3 level of theory. Total ( $E_{tot}$ , kcal mol<sup>-1</sup>) and relative ( $\Delta E$ , kcal mol<sup>-1</sup>) energies are also shown. All conformational families shown here have relative population (%PF) higher than 0.5%

LPYFDa	Electrostatic	Random	Thermal	Total
Generated <sup>a</sup>	4233	58242	40	62515
Accepted <sup>b</sup>	535	4431	34	5000
Family	NF <sup>c</sup>	%PF <sup>d</sup>	$E_{tot}$	$\Delta E$
1	2502	50.04	-70.79	0.00
2	768	15.36	-70.76	0.03
3	370	7.40	-69.43	1.36
4	262	5.24	-70.12	0.66
5	261	5.22	-69.31	1.47
6	247	4.94	-70.25	0.54
7	62	1.24	-69.37	1.42
8	47	0.94	-70.13	0.66
9	35	0.70	-69.75	1.03
10	30	0.60	-68.45	2.34
scrP	Electrostatic	Random	Thermal	Total
Generated <sup>a</sup>	4288	60708	60	65056
Accepted <sup>b</sup>	362	4595	43	5000
Family	NF <sup>c</sup>	%PF <sup>d</sup>	$E_{tot}$	$\Delta E$
1	1146	22.92	-49.71	1.18
2	635	12.70	-50.16	0.73
3	478	9.56	-49.95	0.93
4	329	6.58	-50.88	0.00
5	272	5.44	-49.66	1.22
6	250	5.00	-49.94	0.94
7	190	3.80	-50.19	0.69
8	116	2.32	-49.71	1.17
9	114	2.28	-50.57	0.31
10	101	2.02	-49.44	1.44
11	97	1.94	-49.63	1.26
12	88	1.76	-50.23	0.65
13	60	1.20	-50.25	0.64
14	53	1.06	-49.47	1.41
15	51	1.02	-49.81	1.07
16	48	0.96	-49.39	1.50
17	45	0.90	-48.58	2.30
18	39	0.78	-48.78	2.10
19	39	0.78	-48.22	2.66
20	38	0.76	-48.97	1.91
21	37	0.74	-49.23	1.65
22	32	0.64	-49.74	1.14
23	30	0.60	-48.90	1.98
24	27	0.54	-49.03	1.86
25	26	0.52	-49.07	1.81

<sup>a</sup>Number of conformations generated electrostatically, randomly and thermally during the conformational search.

<sup>b</sup>Number of conformations accepted from those generated electrostatically, randomly and thermally during the conformational search.

<sup>c</sup>NF represents the total number of conformational families as result of the clustering run.

<sup>d</sup>%PF represents the percent relative population based on a total of 5000 accepted conformations.

were then compared to each other. The comparison involved the spatial arrangements, relative energy, and populations. The LPYFDa evaluation showed that the

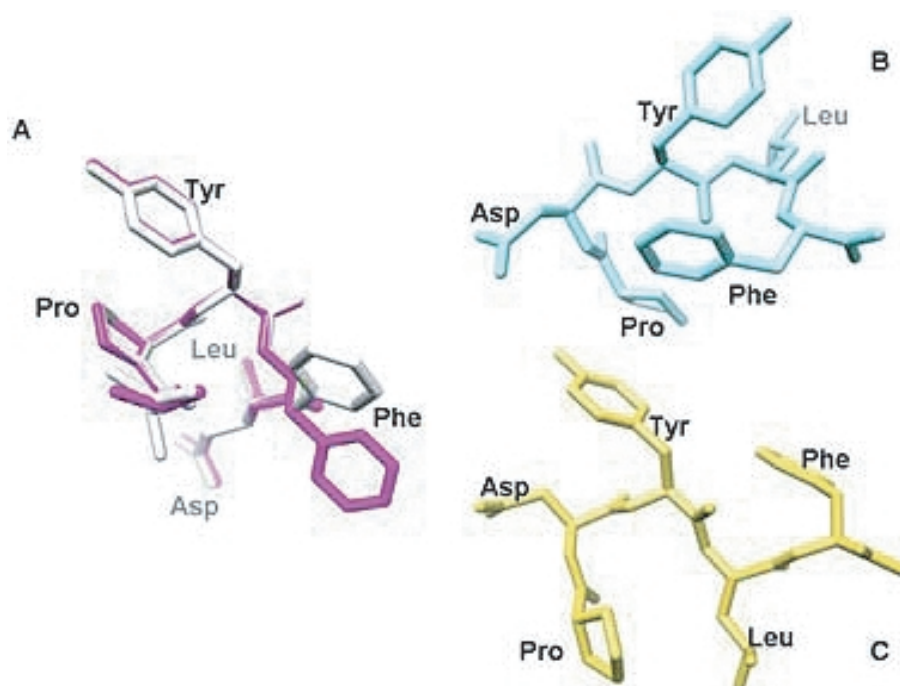


Fig. 2. Stereoview of selected conformations for LPYFDa and scrP optimized at EDMC/SRFOPT/ECCEP/3 level of theory. A) overlapping of the two most populated and energetically preferred families of LPYFDa, family 1 ( $\Delta E = 0.00$  kcal.mol $^{-1}$ , white) and family 2 ( $\Delta E = 0.03$  kcal.mol $^{-1}$ , pink). B) Family 4 with a relative energy ( $\Delta E$ ) of 0.00 kcal.mol $^{-1}$  and C) Family 1 with an  $\Delta E = 1.18$  kcal.mol $^{-1}$  of scrP. All hydrogen atoms have been deleted for more clarity.

most populated family (50.04%) is also the energetically preferred one, while its second most populated family (15.36%) has a relative energy of 0.03 kcal mol $^{-1}$  above the global minimum. This small energetic difference is due to a slight reorientation of the side-chain of the residue Phe (see Fig. 2A), while the rest of the structure showed approximately the same orientation. On the other hand, the most populated family of scrP (22.92%) showed a relative energy of 1.18 kcal mol $^{-1}$  above the global minimum and a relative population of 6.38%. It was observed that LPYFDa is conformationally, generally more restricted than scrP, with a preference to form folded structures, while scrP tended to form semi-extended or fully-extended conformations. Spatial views of selected conformations, for LPYFDa and scrP are shown in Fig. 2.

#### Docking studies

##### Monomeric model

Two potential binding sites were found by using a single blind docking run (results not shown) on the monomeric A $\beta_{42}$  molecule (PDB code 1IYT), which comprises two  $\alpha$ -helix moieties (residues 8–25 and 29–

39) connected by a loop (residues 26–28). Site I encompasses the residues 21–26 containing Glu<sup>22</sup> and Asp<sup>23</sup>, which were previously identified as residues for aggregation of the oligomers [40,47]. Site II includes residues 6–12 located in the portion of the molecule that loses all structural organization after oligomer formation, thus forming the so-called disordered region. In Table 2 the two most populated families of the complexes of LPYFDa and scrP with the monomeric A $\beta_{42}$  are summarized. LPYFDa showed lower binding energies, while site II was in general energetically preferred over site I but families on site II poorly populated. In general it can be concluded that LPYFDa binds stronger to the monomeric A $\beta_{42}$  than scrP.

##### Pentameric model

As previously reported by Masman et al. [40], the A $\beta_{42}$  aggregates contain two  $\beta$ -sheet moieties ( $\beta_1$ , residues 18–26 and  $\beta_2$ , residues 31–42) organized into a parallel interchain orientation, which were proposed as intermolecular binding sites for the pentameric conformation. Moreover, a third possible site for interactions with ligand molecules was postulated, which involves the  $\beta_1$  and  $\beta_2$  portions of the chain located at



Table 2

The two most populated families of LPYFDa and scrP found by docking simulations on the monomeric and pentameric A $\beta_{42}$  peptide and the corresponding binding energies ( $E_B$ ) of the complexes. The binding constant ( $K_B$ ) and the relative populations (%P) are also shown

		LPYFDa			scrP			
		$E_B$ (kcal mol <sup>-1</sup> )	$K_B^a$ (M)	%P	$E_B$ (kcal mol <sup>-1</sup> )	$K_B^a$ (M)	%P	
Monomeric A $\beta_{42}$	Site I	1	-4.42	$5.78 \times 10^{-4}$	13.6	-3.67	$2.05 \times 10^{-3}$	4.80
		2	-4.35	$6.49 \times 10^{-4}$	8.00	-3.18	$4.66 \times 10^{-3}$	4.00
	Site II	1	-4.95	$2.35 \times 10^{-4}$	6.40	-4.10	$9.89 \times 10^{-4}$	3.20
		2	-4.66	$3.85 \times 10^{-4}$	3.20	-3.96	$1.24 \times 10^{-3}$	2.00
Pentameric A $\beta_{42}$	TOP	1	-5.67	$6.99 \times 10^{-5}$	5.60	-4.50	$5.03 \times 10^{-4}$	5.20
		2	-5.04	$2.02 \times 10^{-4}$	3.60	-4.73	$3.39 \times 10^{-4}$	3.60
	$\beta 1$	1	-8.19	$9.88 \times 10^{-7}$	8.80	-6.17	$3.00 \times 10^{-5}$	5.20
		2	-7.05	$6.75 \times 10^{-6}$	6.80	-5.01	$2.11 \times 10^{-4}$	4.40
	$\beta 2$	1	-4.75	$3.32 \times 10^{-4}$	6.00	-4.68	$3.69 \times 10^{-4}$	2.80
		2	-4.77	$3.20 \times 10^{-4}$	3.20	-4.92	$2.48 \times 10^{-4}$	2.40

<sup>a</sup> $K_B$  is calculated in with the equation  $K_B = \exp(\Delta G * 1000.) / (Rcal * TK)$ , where  $\Delta G$  is the docking energy, Rcal is 1.98719 and TK is 298.15.

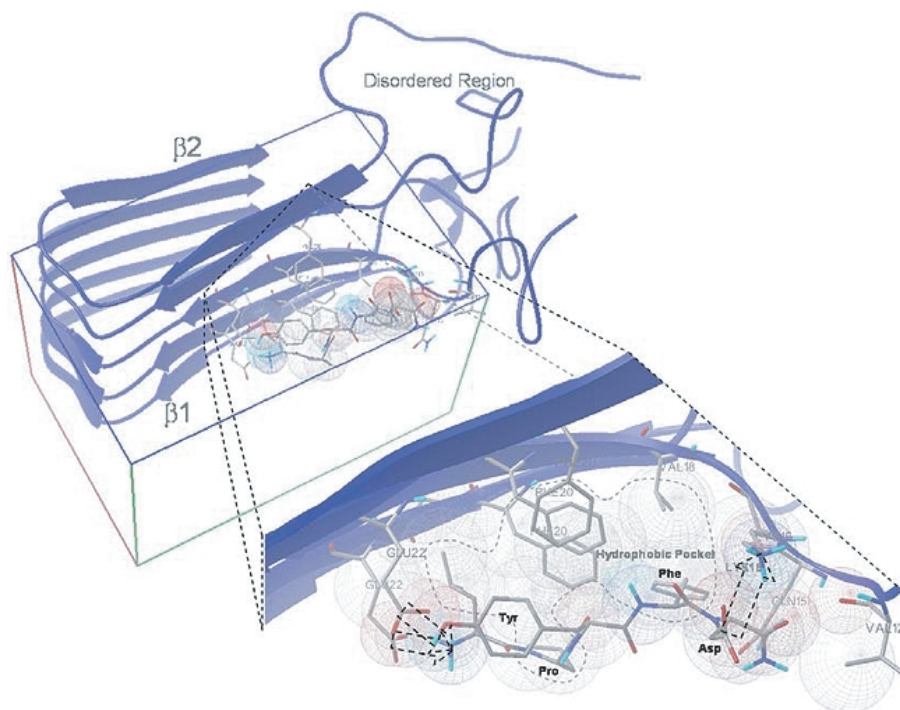


Fig. 3. A steric view of binding between the pentameric A $\beta_{42}$  model and LPYFDa. Salt bridges are signaled with block-arrows. All the ligand-target contacts are depicted as wireframe spheres.

the edge of the aggregate. This site is orientated into axis of the oligomers, in the same direction where the oligomers grows by aggregation. Table 2 shows the two most populated families of the complexes of LPYFDa and ScrP with the pentameric A $\beta_{42}$ . For all the sites proposed, LPYFDa showed lower binding energies than scrP. Interestingly, both pentapeptide LPYFDa and scrP, revealed an energetic preference for site

$\beta 1$ . LPYFDa was designed on the basis of Soto's pentapeptide LPFFD, which derives from the amino acid sequence Leu<sup>17</sup>-Val-Phe-Phe-Ala<sup>21</sup> of A $\beta_{42}$ , being the  $\beta 1$  portion of the aggregate. Figure 3 shows the atomic details of the interactions of the best complex (family  $\beta 1$  1, in Table 2) found between LPYFDa and the pentameric A $\beta_{42}$ . It can be appreciated that the N-terminal of LPYFDa formed a double salt bridge with the Glu<sup>22</sup>s



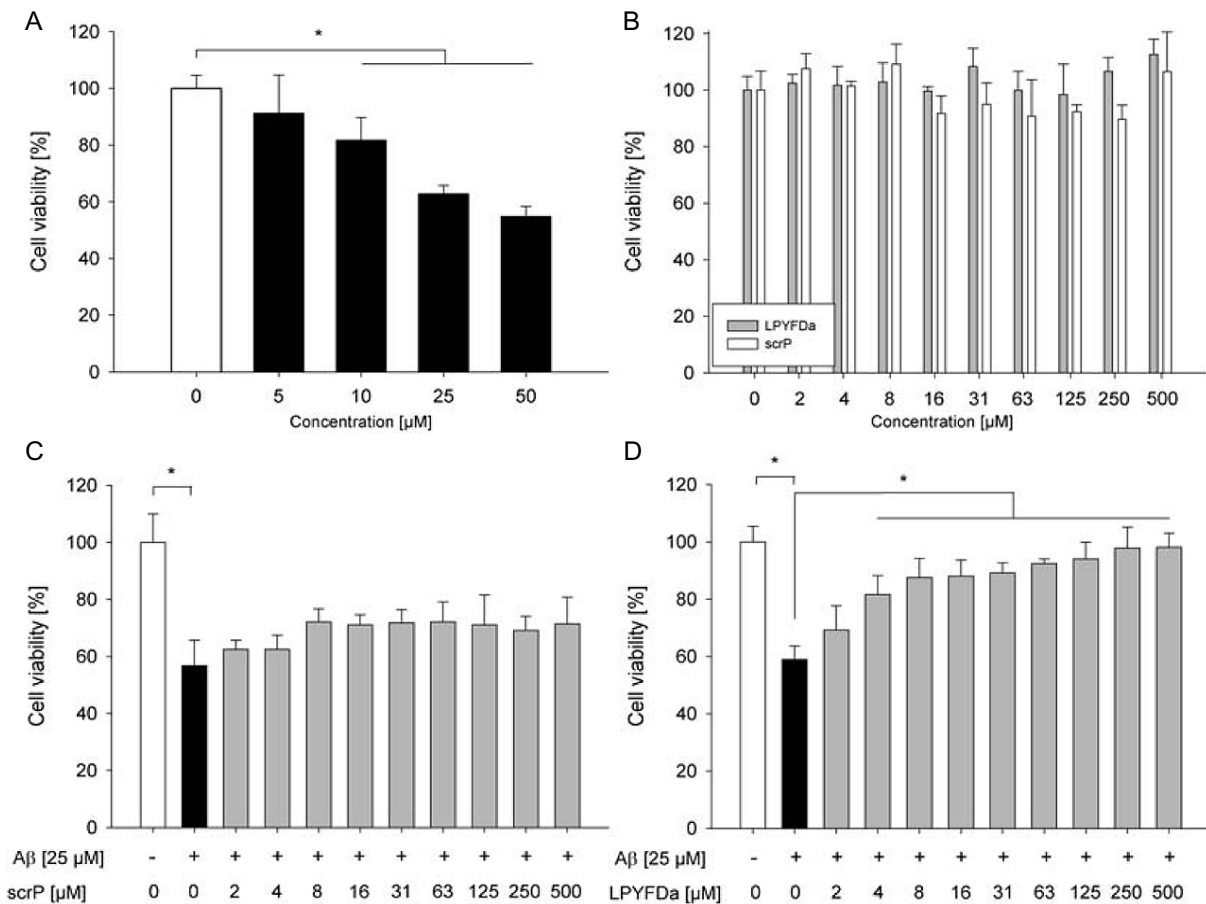


Fig. 4. Cell viability of PCN as determined by an MTT-assay. Neurons treated with increasing concentrations of A) A $\beta$ <sub>42</sub> or B) pentapeptides LPYFDa and scrP incubated for 24 hours. Neuroprotection by C) scrP or D) LPYFDa was determined by co incubating increasing concentrations of the pentapeptides with 25  $\mu$ M A $\beta$ <sub>42</sub> for 24 hours. Bars indicate the mean cell viability in % relative to untreated controls  $\pm$  SEM. (\* = significant at  $p < 0.05$ ).

of the second and third chain of the aggregate. Also, a second salt bridge links the Lys16 to the Asp residue of LPYFDa. All salt bridges, indicated with a block-arrow that points to the positive member of the interaction, revealed an interacting distance of approximately 3.5 Å. All the ligand-target contacts are depicted as wireframe spheres. An important hydrophobic pocket was formed between the residues Phe<sup>20</sup> and Val<sup>18</sup> of the aggregate, and the residues Leu, Pro and Phe of the pentapeptide LPYFDa. This hydrophobic pocket is indicated with a dashed line.

#### LPYFDa is neuroprotective against oligomeric A $\beta$ <sub>42</sub> *in vitro*

Part of our study was to assess the neuroprotective potential of the  $\beta$ -sheet breaker LPYFDa against A $\beta$ -

induced toxicity. Therefore, we first determined the toxic effect of the A $\beta$ <sub>42</sub> oligomer preparation *in vitro* on cultured PCN. Neuronal cultures were exposed to increasing concentrations of oligomerized A $\beta$ <sub>42</sub> for 24 h, followed by an MTT-reduction assay to assess cell viability. The results showed a clear A $\beta$ -induced, dose dependent decrease in cell survival reaching significance at concentrations higher than 10  $\mu$ M (Fig. 4A). For the subsequent experiments we used oligomeric A $\beta$ <sub>42</sub> at a concentration of 25  $\mu$ M as a toxic stimulus.

Second, we investigated if LPYFDa or the control peptide scrP exhibited any toxicity to PCN and whether the  $\beta$ -sheet breaker peptides were capable to overcome the toxic effect of oligomeric A $\beta$ <sub>42</sub>. For this purpose PCN were exposed to different concentrations of LPYFDa or scrP alone, A $\beta$ <sub>42</sub> alone (25  $\mu$ M) or  $\beta$ -sheet breaker peptides and A $\beta$ <sub>42</sub> together for 24 h. The results showed that LPYFDa and scrP alone were not

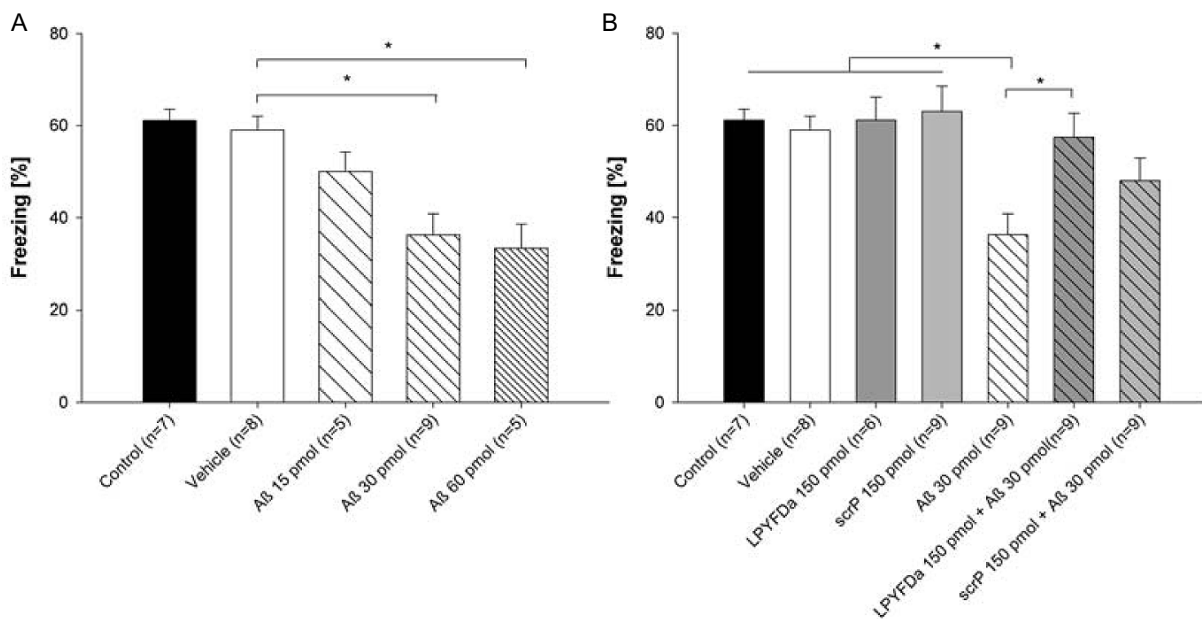


Fig. 5. Effect of A $\beta$ <sub>42</sub> and LPYFDa on contextual fear conditioning. A) A single i.h. injection of oligomeric A $\beta$ <sub>42</sub> led to a dose dependent significant decrease in conditioned fear when compared to a vehicle injection. B) Co-injection of A $\beta$ <sub>42</sub> with LPYFDa prevented the A $\beta$ -induced memory impairment significantly, whereas the non-specific control peptide scrP failed to revert memory deficits. Bars indicate the mean relative freezing score in %  $\pm$  SEM. Differences were determined by ANOVA (\* = significant at  $p < 0.05$ ).

toxic to PCN at any tested concentration (Fig. 4B). Furthermore, the control peptide scrP was not able to protect the neurons from A $\beta$ -induced toxicity (Fig. 4C). In contrast, we could demonstrate a dose dependent neuroprotective effect of LPYFDa against A $\beta$ -induced toxicity, reaching significance at 4  $\mu$ M LPYFDa and higher (Fig. 4D).

#### *A single intrahippocampal injection of oligomeric A $\beta$ <sub>42</sub> induces cognitive deficits in contextual fear conditioning*

One hour prior to the training session in a contextual fear conditioning paradigm C57BL/6J mice received a single injection of oligomeric A $\beta$ <sub>42</sub> (15, 30, or 60 pmol) or vehicle. Injections did not affect locomotion or the shock reaction during training (data not shown). The vehicle injected animals displayed an average relative freezing behavior of 58.9  $\pm$  2.9%, which did not differ from untreated control animals (61.1  $\pm$  2.4%). The mice injected with A $\beta$ <sub>42</sub> showed a dose dependent decrease in freezing behavior (Fig. 5A). 15 pmol A $\beta$ <sub>42</sub> caused an average relative freezing of 50.0  $\pm$  4.2%, which was not significantly different from the vehicle-injected animals. However, the mice injected with 30 pmol and 60 pmol of A $\beta$ <sub>42</sub> had significantly reduced

freezing scores compared to the vehicle group (36.2  $\pm$  4.6%;  $p = 0.024$  and 33.3  $\pm$  5.3%;  $p = 0.037$ ).

Next, we investigated whether LPYFDa is able to revert the A $\beta$ -induced memory deficits. Therefore, we injected mice with 150 pmol LPYFDa or 150 pmol of the non specific control peptide scrP in the presence or absence of 30 pmol oligomerized A $\beta$ <sub>42</sub> into the hippocampus. The LPYFDa and the scrP injected mice showed an average freezing of 61.1  $\pm$  5.0% and 63.0  $\pm$  5.5% which did not significantly differ from the untreated (61.1  $\pm$  2.4%) or vehicle injected group (58.9  $\pm$  2.9%).

However, LPYFDa co-injected with A $\beta$ <sub>42</sub> was able to abolish the A $\beta$ <sub>42</sub> oligomer-induced memory impairment (57.4  $\pm$  5.2% versus 36.2  $\pm$  4.46%;  $p = 0.039$ ). Co-injection of A $\beta$  with the control peptide scrP, which resulted in an average freezing score of 48.0  $\pm$  4.9%, did not significantly reverse the A $\beta$ -induced memory deficits (Fig. 5B).

These results indicate that LPYFDa can reverse the detrimental effects of A $\beta$ <sub>42</sub> oligomers and subsequent impaired memory performance.

## DISCUSSION

In the present study, we could show that A $\beta$ <sub>42</sub> oligomers are toxic to primary cortical neurons in cul-

ture in a dose-dependent manner (Fig. 4A). These results are in line with studies by Dahlgren and colleagues, who reported that the oligomeric form of A $\beta_{42}$  is 10 fold more toxic when compared to the fibrillar form [26]. These and our present findings support the growing general view that, in particular, oligomeric A $\beta_{42}$  peptides contribute to the progressive neuronal loss and the associated memory impairment observed in AD patients. Indeed, several studies showed that elevated levels of soluble oligomeric A $\beta$  correlate strongly with cognitive decline in AD patients [6,7]. Walsh and colleagues observed that a low-n oligomeric assembly of naturally secreted human A $\beta$  alters hippocampal synaptic plasticity by inhibiting LTP [48]. Also the number of dendritic spines was dramatically decreased when neurons were incubated with A $\beta$  oligomers, but not with monomers [48]. However, the loss in spines could be reverted by treating neurons with an anti-A $\beta$  antibody [14].

A possibility to counteract the injurious effects of oligomeric A $\beta$  is by modulating its aggregation. Crucial for the aggregation process of the A $\beta$  molecule are the hydrophobic residues (amino acids 17–21: LVFFA) within the internal region of the A $\beta$  peptide. Experiments by Hilbich and colleagues revealed that replacement of those hydrophobic residues by hydrophilic residues results in impaired fibril formation [49]. These and other findings eventually led to the concept of  $\beta$ -sheet breakers as therapeutic strategy for AD as proposed by Soto et al. [50,51]. The initially synthesized compounds were peptides of 11 to 5 amino acids targeting the center region of the A $\beta$  peptide and evolved to compounds like LPFFD (iA $\beta$ 5) and/or LPYFDa. These pentapeptides are partially homologous to this hydrophobic center region and bind with a relatively high affinity to A $\beta$  [52–54] by similar intermolecular interactions, leading to a competitive replacement of A $\beta$  molecules. A major drawback with peptide drugs for neurological disorders is their rapid degradation *in vivo* by proteolytic enzymes and their poor blood-brain permeability [55]. These issues were overcome by chemical modifications, like C-terminal amidation and N-terminal carboxylation, which resulted in increased half life *in vivo* and rapid brain uptake [54]. Although our knowledge of the biochemistry in respect to catabolism and brain uptake of certain aggregation inhibitor peptides has developed greatly in recent years, the detailed mechanisms of action are still poorly understood. Therefore, it is essential to elucidate and study the three dimensional structure of the A $\beta$  peptide/aggregation inhibiting peptide complex to

gain more insight into the molecular dynamics of the A $\beta$  aggregation process.

We used computational modeling and docking experiments to address this question. Interestingly our docking results showed that LPYFDa binds preferably to the  $\beta$ 1 portion of the aggregate (Table 2 and Fig. 3), which has a good correlation with the design of this pentapeptide, since LPYFDa derives from the wild-type sequence Leu<sup>17</sup>-Val-Phe-Phe-Ala<sup>21</sup> of A $\beta_{42}$ , which is contained in this portion of the aggregate. Our docking results did not show any binding preference of LPYFDa (nor scrP) for the monomeric or the pentameric A $\beta$ .

In the present study, we showed that the pentapeptide LPYFDa can protect cultured neurons from oligomeric A $\beta$ -induced cell death. Datki and colleagues reported similar results on neuronal-like cell lines, e.g., SHSY-5Y cells. They could show that a 5-fold molar excess of LPYFDa protects these cells from toxic effects of fibrillar A $\beta$  [24,56]. In our study we could confirm that a molar excess of LPYFDa can prevent A $\beta_{42}$  mediated neurotoxicity. Moreover, we demonstrated a dose-dependent protective effect of LPYFDa and that this pentapeptide already has significant neuroprotective properties even with a 6-fold molar excess of oligomeric A $\beta_{42}$ . Our results are also in agreement with other studies reporting protection by LPYFDa against the rapid neuromodulatory action of fibrillar A $\beta_{42}$  demonstrated by *in vitro* and *in vivo* electrophysiology [23].

We found that a single bilateral intrahippocampal injection of oligomeric A $\beta_{42}$  impairs memory formation if applied 1 h before the training session in a contextual fear conditioning paradigm. These findings are in line with several other studies, which consistently report on memory deficits after intracerebral injections of A $\beta_{42}$  peptides, although the experimental conditions vary in terms of the injected peptide, injection procedure, and behavioral tasks employed [57–62]. It should be noted that these injections obviously lead to A $\beta$  levels beyond the basal levels necessary for proper synaptic functioning. Garcia-Osta showed that neutralizing endogenous A $\beta$  by an anti-A $\beta$  antibody resulted in memory impairment which implies that physiological soluble A $\beta$  levels are required for proper memory function [17], which was recently confirmed by a study of Morley et al. [63].

The peptide LPFFD, which was designed by the Soto group, was able to prevent fibrillogenesis in a rat brain model [64] and to reduce A $\beta$  deposition a transgenic AD mouse model [54]. Most interestingly, iA $\beta$ 5p was shown to reverse the memory impairment caused by

intrahippocampal injections of A $\beta$  fibrils in rats [65]. However, these studies did not reveal whether impairment of learning and memory after oligomeric A $\beta$  injections could be counteracted by such compounds. A novelty of our study is that we used A $\beta$  oligomers instead of the less effective A $\beta$  fibrils. Therefore, an important aim of our study was to establish if a compound like LPYFDa is able to prevent A $\beta$  oligomer-induced learning and memory deficits. We showed that a 5-fold molar excess of LPYFDa to A $\beta$  could overcome the detrimental effects of A $\beta$  oligomers on memory. Thus, we provide evidence that so-called  $\beta$ -sheet breaker peptides such as LPYFDa bear therapeutic potential against A $\beta$ -induced memory impairment. Moreover, it was recently demonstrated that intraperitoneally administered LPYFDa is able to cross the blood brain barrier and protects synapses against excitatory action of fibrillar A $\beta$  [22].

The mechanism of how these pentapeptides exert their protective effects on cell death and behavior is not yet fully understood. However, it should be noted that the two actions of A $\beta$  reported here, namely, the neuronal degeneration following application of A $\beta$  oligomers *in vitro* and memory loss following injections of A $\beta$  oligomers *in vivo* may be unrelated. In hippocampal tissue extracted one hour after A $\beta$  injection, we were unable to detect any caspase-3 cleavage which would indicate apoptotic cell death (data not shown). Furthermore, there are no studies so far that show toxic effects of oligomeric A $\beta$  on neurons *in vivo*. Therefore, the effects on memory following an hour post-injection may not have a direct correlation with neuronal degeneration, but could simply reflect the effects of A $\beta$  on synaptic integrity. It is well documented that the main effects of A $\beta$  on synapses are inhibition of LTP [9,66] and elimination of postsynaptic glutamate receptors [8, 67,68]. Remarkably, the A $\beta$ -induced synaptic dysfunction occurs rather rapidly, starting 20 minutes after application, and does not need chronic exposure [69–72]. Furthermore, it is likely that the injected oligomeric A $\beta$  does not remain unchanged in terms of its conformation, and the effects on memory may be due to changes of A $\beta$  to other conformations. The importance of the A $\beta$  conformation on memory was demonstrated by Lesne and collaborators [73], who showed that only specific A $\beta$  protein assemblies in the brain are able to impair memory [73].

It remains elusive whether aggregation inhibiting peptides like LPYFDa directly bind to A $\beta$ , and thereby prevent possible interactions between A $\beta$  and neuronal membrane proteins, and in this way neutralize its toxic

effect. We could consider two options of interaction with A $\beta$ : 1) the pentapeptides bind to the monomeric A $\beta$ , thus preventing and/or retarding the formation of toxic oligomers; and 2) the pentapeptides bind the A $\beta$  oligomers already formed preventing and/or modulating, somehow, its neurotoxic properties. On the other hand, both above mentioned possibilities might act simultaneously comprising a third possible way of action of this peptide toward its neuroprotective effects.

Being aware of the many possible biological pathways that these peptides might follow while inducing neuroprotection, it is interesting to see whether these peptides show a preference to bind the monomeric A $\beta$  or its soluble oligomers. Previous studies using CD spectrometry and molecular docking studies have been carried out on LPYFDa and other so-called  $\beta$ -sheet breaker peptides [24,52,74,75] but none of them so far have demonstrated proof at the molecular level of the  $\beta$ -sheet breaking properties of these peptides. We also might consider the possibility that these peptides might act as “glue” that promote elongation to biologically inert larger aggregates, or conversely, bind to the monomeric A $\beta$  and this way inhibits oligomer formation. By either of these actions, or both, the neurotoxicity of A $\beta$  is decreased or reverted.

In summary, our findings provide evidence on how and where LPYFD interacts with A $\beta$  mono- and oligomers, that LPYFDa neutralizes the neurotoxic activity of soluble A $\beta$  oligomers, and in the present conditions can effectively prevent the oligomer-induced deficits in memory performance.

## ACKNOWLEDGMENTS

This work was supported by grants from the International Foundation for Alzheimer Research (ISAO), the Netherlands Brain Foundation (Hersenstichting Nederland), the Gratama Stichting, the EU-grant FP6 NeuroprMiSe LSHM-CT-2005-018637 and EC-grant FP-7 201 159 (Memoload). We thank Gea Schuurman-Wolters, Neele Mayer and Sepp R. Jansen for their excellent technical assistance. This work reflects only the author's views. The European Community is not liable for any use that may be made of the information herein.

Authors' affiliations are available online (<http://www.j-alz.com/disclosures/view.php?id=170>).

## REFERENCES

- [1] Haass C, Selkoe DJ (2007) Soluble protein oligomers in neurodegeneration: lessons from the Alzheimer's amyloid beta-peptide. *Nat Rev Mol Cell Biol* 8, 101-112.

- [2] Wisniewski T, Ghiso J, Frangione B (1997) Biology of A beta amyloid in Alzheimer's disease. *Neurobiol Dis* **4**, 313-328.
- [3] Forman MS, Mufson EJ, Leurgans S, Pratico D, Joyce S, Leight S, Lee VM, Trojanowski JQ (2007) Cortical biochemistry in MCI and Alzheimer disease: lack of correlation with clinical diagnosis. *Neurology* **68**, 757-763.
- [4] Naslund J, Haroutunian V, Mohs R, Davis KL, Davies P, Greengard P, Buxbaum JD (2000) Correlation between elevated levels of amyloid beta-peptide in the brain and cognitive decline. *JAMA* **283**, 1571-1577.
- [5] Lue LF, Kuo YM, Roher AE, Brachova L, Shen Y, Sue L, Beach T, Kurth JH, Rydel RE, Rogers J (1999) Soluble amyloid beta peptide concentration as a predictor of synaptic change in Alzheimer's disease. *Am J Pathol* **155**, 853-862.
- [6] McLean CA, Cherny RA, Fraser FW, Fuller SJ, Smith MJ, Beyreuther K, Bush AI, Masters CL (1999) Soluble pool of Abeta amyloid as a determinant of severity of neurodegeneration in Alzheimer's disease. *Ann Neurol* **46**, 860-866.
- [7] Wang J, Dickson DW, Trojanowski JQ, Lee VM (1999) The levels of soluble versus insoluble brain Abeta distinguish Alzheimer's disease from normal and pathologic aging. *Exp Neurol* **158**, 328-337.
- [8] Chang EH, Savage MJ, Flood DG, Thomas JM, Levy RB, Mahadomrongkul V, Shirao T, Aoki C, Huerta PT (2006) AMPA receptor downscaling at the onset of Alzheimer's disease pathology in double knockin mice. *Proc Natl Acad Sci U S A* **103**, 3410-3415.
- [9] Chapman PF, White GL, Jones MW, Cooper-Blacketer D, Marshall VJ, Irizarry M, Younkin L, Good MA, Bliss TV, Hyman BT, Younkin SG, Hsiao KK (1999) Impaired synaptic plasticity and learning in aged amyloid precursor protein transgenic mice. *Nat Neurosci* **2**, 271-276.
- [10] Wasling P, Daborg J, Riebe I, Andersson M, Portelius E, Blennow K, Hanse E, Zetterberg H (2009) Synaptic retrogenesis and amyloid-beta in Alzheimer's disease. *J Alzheimers Dis* **16**, 1-14.
- [11] Walsh DM, Selkoe DJ (2007) A beta oligomers - a decade of discovery. *J Neurochem* **101**, 1172-1184.
- [12] Shankar GM, Li S, Mehta TH, Garcia-Munoz A, Shepardson NE, Smith I, Brett FM, Farrell MA, Rowan MJ, Lemere CA, Regan CM, Walsh DM, Sabatini BL, Selkoe DJ (2008) Amyloid-beta protein dimers isolated directly from Alzheimer's brains impair synaptic plasticity and memory. *Nat Med* **14**, 837-842.
- [13] Hsieh H, Boehm J, Sato C, Iwatsubo T, Tomita T, Sisodia S, Malinow R (2006) AMPAR removal underlies Abeta-induced synaptic depression and dendritic spine loss. *Neuron* **52**, 831-843.
- [14] Shankar GM, Bloodgood BL, Townsend M, Walsh DM, Selkoe DJ, Sabatini BL (2007) Natural oligomers of the Alzheimer amyloid-beta protein induce reversible synapse loss by modulating an NMDA-type glutamate receptor-dependent signaling pathway. *J Neurosci* **27**, 2866-2875.
- [15] Pearson HA, Peers C (2006) Physiological roles for amyloid beta peptides. *J Physiol* **575**, 5-10.
- [16] Puzzo D, Privitera L, Leznik E, Fa M, Staniszewski A, Palmeri A, Arancio O (2008) Picomolar amyloid-beta positively modulates synaptic plasticity and memory in hippocampus. *J Neurosci* **28**, 14537-14545.
- [17] Garcia-Osta A, Alberini CM (2009) Amyloid beta mediates memory formation. *Learn Mem* **16**, 267-272.
- [18] Harkany T, Abraham I, Konya C, Nyakas C, Zarandi M, Penke B, Luiten PG (2000) Mechanisms of beta-amyloid neurotoxicity: perspectives of pharmacotherapy. *Rev Neurosci* **11**, 329-382.
- [19] Schenk D, Barbour R, Dunn W, Gordon G, Grajeda H, Guido T, Hu K, Huang J, Johnson-Wood K, Khan K, Kholodenko D, Lee M, Liao Z, Lieberburg I, Motter R, Mutter L, Soriano F, Shopp G, Vasquez N, Vandeventer C, Walker S, Wogulis M, Yednock T, Games D, Seubert P (1999) Immunization with amyloid-beta attenuates Alzheimer-disease-like pathology in the PDAPP mouse. *Nature* **400**, 173-177.
- [20] Orgogozo JM, Gilman S, Dartigues JF, Laurent B, Puel M, Kirby LC, Jouanny P, Dubois B, Eisner L, Flitman S, Michel BF, Boada M, Frank A, Hock C (2003) Subacute meningoencephalitis in a subset of patients with AD after Abeta42 immunization. *Neurology* **61**, 46-54.
- [21] Hock C, Konietzko U, Streffer JR, Tracy J, Signorell A, Muller-Tillmanns B, Lemke U, Henke K, Moritz E, Garcia E, Wollmer MA, Umbrecht D, de Quervain DJ, Hofmann M, Maddalena A, Papassotiropoulos A, Nitsch RM (2003) Antibodies against beta-amyloid slow cognitive decline in Alzheimer's disease. *Neuron* **38**, 547-554.
- [22] Juhasz G, Marki A, Vass G, Fulop L, Budai D, Penke B, Falkay G, Szegei V (2009) An intraperitoneally administered pentapeptide protects against Abeta (1-42) induced neuronal excitation *in vivo*. *J Alzheimers Dis* **16**, 189-196.
- [23] Szegei V, Fulop L, Farkas T, Rozsa E, Robotka H, Kis Z, Penke Z, Horvath S, Molnar Z, Datki Z, Soos K, Toldi J, Budai D, Zarandi M, Penke B (2005) Pentapeptides derived from Abeta 1-42 protect neurons from the modulatory effect of Abeta fibrils—an *in vitro* and *in vivo* electrophysiological study. *Neurobiol Dis* **18**, 499-508.
- [24] Datki Z, Papp R, Zadori D, Soos K, Fulop L, Juhasz A, Laskay G, Hetenyi C, Mihalik E, Zarandi M, Penke B (2004) *In vitro* model of neurotoxicity of Abeta 1-42 and neuroprotection by a pentapeptide: irreversible events during the first hour. *Neurobiol Dis* **17**, 507-515.
- [25] Zarandi M, Soos K, Fulop L, Bozso Z, Datki Z, Toth GK, Penke B (2007) Synthesis of Abeta[1-42] and its derivatives with improved efficiency. *J Pept Sci* **13**, 94-99.
- [26] Dahlgren KN, Manelli AM, Stine WB, Jr., Baker LK, Krafft GA, LaDu MJ (2002) Oligomeric and fibrillar species of amyloid-beta peptides differentially affect neuronal viability. *J Biol Chem* **277**, 32046-32053.
- [27] Stine WB, Jr., Dahlgren KN, Krafft GA, LaDu MJ (2003) *In vitro* characterization of conditions for amyloid-beta peptide oligomerization and fibrillogenesis. *J Biol Chem* **278**, 11612-11622.
- [28] Perez-Iratxeta C, Andrade-Navarro MA (2008) K2D2: estimation of protein secondary structure from circular dichroism spectra. *BMC Struct Biol* **8**, 25.
- [29] Liwo A, Tempczyk A, Oldziej S, Shenderovich MD, Hruby VJ, Talluri S, Ciarkowski J, Kasprzykowski F, Lankiewicz L, Grzonka Z (1996) Exploration of the conformational space of oxytocin and arginine-vasopressin using the electrostatically driven Monte Carlo and molecular dynamics methods. *Biopolymers* **38**, 157-175.
- [30] Ripoll DR, Scheraga HA (1988) On the multiple-minima problem in the conformational analysis of polypeptides. II. An electrostatically driven Monte Carlo method—tests on poly(L-alanine). *Biopolymers* **27**, 1283-1303.
- [31] Ripoll DR, Scheraga HA (1990) On the multiple-minima problem in the conformational analysis of polypeptides. IV. Application of the electrostatically driven Monte Carlo method to the 20-residue membrane-bound portion of melittin. *Biopolymers* **30**, 165-176.

- [32] Letoha T, Gaal S, Somlai C, Venkei Z, Glavinas H, Kusz E, Duda E, Czajlik A, Petak F, Penke B (2005) Investigation of penetratin peptides. Part 2. *In vitro* uptake of penetratin and two of its derivatives. *J Pept Sci* **11**, 805-811.
- [33] Nemethy G GK, Palmer KA, Yoon CN, Paterlini G, Zagari A, Rumsey S, Scheraga HA (1992) Energy parameters in polypeptides.10. improved geometrical parameters and non-bounded interactions for use in the ECEPP/3 algorithm, with application to proline-containing peptides. *J Phys Chem* **96**, 6472-6484.
- [34] Vila J, Williams RL, Vasquez M, Scheraga HA (1991) Empirical solvation models can be used to differentiate native from near-native conformations of bovine pancreatic trypsin inhibitor. *Proteins* **10**, 199-218.
- [35] Williams RL, Vila J, Perrot G, Scheraga HA (1992) Empirical solvation models in the context of conformational energy searches: application to bovine pancreatic trypsin inhibitor. *Proteins* **14**, 110-119.
- [36] Meadows RP, Olejniczak ET, Fesik SW (1994) A computer-based protocol for semiautomated assignments and 3D structure determination of proteins. *J Biomol NMR* **4**, 79-96.
- [37] Pohorille A, Pratt LR (1990) Cavities in molecular liquids and the theory of hydrophobic solubilities. *J Am Chem Soc* **112**, 5066-5074.
- [38] Masman MF, Rodriguez AM, Raimondi M, Zacchino SA, Luiten PG, Somlai C, Kortvelyesi T, Penke B, Enriz RD (2009) Penetratin and derivatives acting as antifungal agents. *Eur J Med Chem* **44**, 212-228.
- [39] Crescenzi O, Tomaselli S, Guerrini R, Salvadori S, D'Ursi AM, Temussi PA, Picone D (2002) Solution structure of the Alzheimer amyloid beta-peptide (1-42) in an apolar microenvironment. Similarity with a virus fusion domain. *Eur J Biochem* **269**, 5642-5648.
- [40] Masman MF, Eisel UL, Csizmadia IG, Penke B, Enriz RD, Marrink SJ, Luiten PG (2009) In Silico Study of Full-Length Amyloid beta 1-42 Tri- and Penta-Oligomers in Solution. *J Phys Chem B*. **113** (34), pp 11710-11719
- [41] Sanner MF (1999) Python: a programming language for software integration and development. *J Mol Graph Model* **17**, 57-61.
- [42] Pettersen EF, Goddard TD, Huang CC, Couch GS, Greenblatt DM, Meng EC, Ferrin TE (2004) UCSF Chimera—a visualization system for exploratory research and analysis. *J Comput Chem* **25**, 1605-1612.
- [43] Morris GM, Huey R, Lindstrom W, Sanner MF, Belew RK, Goodsell DS, Olson AJ (2009) AutoDock4 and AutoDockTools4: Automated docking with selective receptor flexibility. *J Comput Chem* **30**, 2785-2791.
- [44] Mosmann T (1983) Rapid colorimetric assay for cellular growth and survival: application to proliferation and cytotoxicity assays. *J Immunol Methods* **65**, 55-63.
- [45] Nijholt IM, Ostroveanu A, Scheper WA, Penke B, Luiten PG, Van der Zee EA, Eisel UL (2008) Inhibition of PKA anchoring to A-kinase anchoring proteins impairs consolidation and facilitates extinction of contextual fear memories. *Neurobiol Learn Mem* **90**, 223-229.
- [46] Franklin K, Paxinos G (1997) The Mouse Brain in Stereotaxic Coordinates. *Academic Press, San Diego*.
- [47] Buchete NV, Hummer G (2007) Structure and dynamics of parallel beta-sheets, hydrophobic core, and loops in Alzheimer's A beta fibrils. *Biophys J* **92**, 3032-3039.
- [48] Walsh DM, Klyubin I, Fadeeva JV, Cullen WK, Anwyl R, Wolfe MS, Rowan MJ, Selkoe DJ (2002) Naturally secreted oligomers of amyloid beta protein potently inhibit hippocampal long-term potentiation *in vivo*. *Nature* **416**, 535-539.
- [49] Hilbich C, Kisters-Woike B, Reed J, Masters CL, Beyreuther K (1992) Substitutions of hydrophobic amino acids reduce the amyloidogenicity of Alzheimer's disease beta A4 peptides. *J Mol Biol* **228**, 460-473.
- [50] Soto C, Kindy MS, Baumann M, Frangione B (1996) Inhibition of Alzheimer's amyloidosis by peptides that prevent beta-sheet conformation. *Biochem Biophys Res Commun* **226**, 672-680.
- [51] Soto C (1999) Plaque busters: strategies to inhibit amyloid formation in Alzheimer's disease. *Mol Med Today* **5**, 343-350.
- [52] Hetenyi C, Kortvelyesi T, Penke B (2002) Mapping of possible binding sequences of two beta-sheet breaker peptides on beta amyloid peptide of Alzheimer's disease. *Bioorg Med Chem* **10**, 1587-1593.
- [53] van Groen T, Kadish I, Wiesehan K, Funke SA, Willbold D (2009) *In vitro* and *in vivo* staining characteristics of small, fluorescent, Abeta42-binding D-enantiomeric peptides in transgenic AD mouse models. *Chem Med Chem* **4**, 276-282.
- [54] Permanne B, Adessi C, Saborio GP, Fraga S, Frossard MJ, Van Dorpe J, Dewachter I, Banks WA, Van Leuven F, Soto C (2002) Reduction of amyloid load and cerebral damage in a transgenic mouse model of Alzheimer's disease by treatment with a beta-sheet breaker peptide. *FASEB J* **16**, 860-862.
- [55] Adessi C, Soto C (2002) Converting a peptide into a drug: strategies to improve stability and bioavailability. *Curr Med Chem* **9**, 963-978.
- [56] Fulop L, Zarandi M, Datki Z, Soos K, Penke B (2004) Beta-amyloid-derived pentapeptide RIIGLa inhibits Abeta(1-42) aggregation and toxicity. *Biochem Biophys Res Commun* **324**, 64-69.
- [57] Christensen R, Marcussen AB, Wortwein G, Knudsen GM, Aznar S (2008) Abeta(1-42) injection causes memory impairment, lowered cortical and serum BDNF levels, and decreased hippocampal 5-HT(2A) levels. *Exp Neurol* **210**, 164-171.
- [58] Ammassari-Teule M, Middei S, Passino E, Restivo L (2002) Enhanced procedural learning following beta-amyloid protein (1-42) infusion in the rat. *Neuroreport* **13**, 1679-1682.
- [59] Harkany T, O'Mahony S, Keijsers J, Kelly JP, Konya C, Borostyankoi ZA, Gorcs TJ, Zarandi M, Penke B, Leonard BE, Luiten PG (2001) Beta-amyloid(1-42)-induced cholinergic lesions in rat nucleus basalis bidirectionally modulate serotonergic innervation of the basal forebrain and cerebral cortex. *Neurobiol Dis* **8**, 667-678.
- [60] Malin DH, Crothers MK, Lake JR, Goyarzu P, Plotner RE, Garcia SA, Spell SH, Tomsic BJ, Giordano T, Kowall NW (2001) Hippocampal injections of amyloid beta-peptide 1-40 impair subsequent one-trial/day reward learning. *Neurobiol Learn Mem* **76**, 125-137.
- [61] Nakamura S, Murayama N, Noshita T, Annoura H, Ohno T (2001) Progressive brain dysfunction following intracerebroventricular infusion of beta(1-42)-amyloid peptide. *Brain Res* **912**, 128-136.
- [62] O'Hare E, Weldon DT, Mantyh PW, Ghilardi JR, Finke MP, Kuskowski MA, Maggio JE, Shephard RA, Cleary J (1999) Delayed behavioral effects following intrahippocampal injection of aggregated A beta (1-42). *Brain Res* **815**, 1-10.
- [63] Morley JE, Farr SA, Banks WA, Johnson SN, Yamada KA, Xu L (2009) A physiological role for amyloid-beta protein: enhancement of learning and memory. *J Alzheimers Dis* **19**, 441-449.
- [64] Soto C, Sigurdsson EM, Morelli L, Kumar RA, Castano EM, Frangione B (1998) Beta-sheet breaker peptides inhibit fibril-

- logogenesis in a rat brain model of amyloidosis: implications for Alzheimer's therapy. *Nat Med* **4**, 822-826.
- [65] Chacon MA, Barria MI, Soto C, Inestrosa NC (2004) Beta-sheet breaker peptide prevents A $\beta$ -induced spatial memory impairments with partial reduction of amyloid deposits. *Mol Psychiatry* **9**, 953-961.
- [66] Kamenetz F, Tomita T, Hsieh H, Seabrook G, Borchelt D, Iwatsubo T, Sisodia S, Malinow R (2003) APP processing and synaptic function. *Neuron* **37**, 925-937.
- [67] Almeida CG, Tampellini D, Takahashi RH, Greengard P, Lin MT, Snyder EM, Gouras GK (2005) Beta-amyloid accumulation in APP mutant neurons reduces PSD-95 and GluR1 in synapses. *Neurobiol Dis* **20**, 187-198.
- [68] Ting JT, Kelley BG, Lambert TJ, Cook DG, Sullivan JM (2007) Amyloid precursor protein overexpression depresses excitatory transmission through both presynaptic and postsynaptic mechanisms. *Proc Natl Acad Sci U S A* **104**, 353-358.
- [69] Chen QS, Wei WZ, Shimahara T, Xie CW (2002) Alzheimer amyloid beta-peptide inhibits the late phase of long-term potentiation through calcineurin-dependent mechanisms in the hippocampal dentate gyrus. *Neurobiol Learn Mem* **77**, 354-371.
- [70] Chen QS, Kagan BL, Hirakura Y, Xie CW (2000) Impairment of hippocampal long-term potentiation by Alzheimer amyloid beta-peptides. *J Neurosci Res* **60**, 65-72.
- [71] Townsend M, Shankar GM, Mehta T, Walsh DM, Selkoe DJ (2006) Effects of secreted oligomers of amyloid beta-protein on hippocampal synaptic plasticity: a potent role for trimers. *J Physiol* **572**, 477-492.
- [72] Wang Q, Rowan MJ, Anwyl R (2004) Beta-amyloid-mediated inhibition of NMDA receptor-dependent long-term potentiation induction involves activation of microglia and stimulation of inducible nitric oxide synthase and superoxide. *J Neurosci* **24**, 6049-6056.
- [73] Lesne S, Koh MT, Kotilinek L, Kaye R, Glabe CG, Yang A, Gallagher M, Ashe KH (2006) A specific amyloid-beta protein assembly in the brain impairs memory. *Nature* **440**, 352-357.
- [74] Hetenyi C, Szabo Z, Klement E, Datki Z, Kortvelyesi T, Zarándi M, Penke B (2002) Pentapeptide amides interfere with the aggregation of beta-amyloid peptide of Alzheimer's disease. *Biochem Biophys Res Commun* **292**, 931-936.
- [75] Laczko I, Vass E, Soos K, Fulop L, Zarándi M, Penke B (2008) Aggregation of A $\beta$ (1-42) in the presence of short peptides: conformational studies. *J Pept Sci* **14**, 731-741.



Article

# Impact of Two Neuronal Sigma-1 Receptor Modulators, PRE084 and DMT, on Neurogenesis and Neuroinflammation in an A $\beta$ <sub>1-42</sub>-Injected, Wild-Type Mouse Model of AD

Emőke Borbély †, Viktória Varga †, Titanilla Szögi, Ildikó Schuster, Zsolt Bozsó, Botond Penke and Livia Fülöp \*

Department of Medical Chemistry, University of Szeged, Dóm Tér 8, H-6720 Szeged, Hungary; emokeborbely@gmail.com (E.B.); vargaviki666@gmail.com (V.V.); szogititi@gmail.com (T.S.); schuster.ildiko@med.u-szeged.hu (I.S.); bozso.zsolt@med.u-szeged.hu (Z.B.); penke.botond@med.u-szeged.hu (B.P.)

\* Correspondence: fulop.livia@med.u-szeged.hu; Tel.: +36-62-545-698

† These authors contributed equally to this work.

**Abstract:** Alzheimer's disease (AD) is the most common form of dementia characterized by cognitive dysfunctions. Pharmacological interventions to slow the progression of AD are intensively studied. A potential direction targets neuronal sigma-1 receptors (S1Rs). S1R ligands are recognized as promising therapeutic agents that may alleviate symptom severity of AD, possibly via preventing amyloid- $\beta$ -(A $\beta$ -) induced neurotoxicity on the endoplasmic reticulum stress-associated pathways. Furthermore, S1Rs may also modulate adult neurogenesis, and the impairment of this process is reported to be associated with AD. We aimed to investigate the effects of two S1R agonists, dimethyltryptamine (DMT) and PRE084, in an A $\beta$ -induced in vivo mouse model characterizing neurogenic and anti-neuroinflammatory symptoms of AD, and the modulatory effects of S1R agonists were analyzed by immunohistochemical methods and western blotting. DMT, binding moderately to S1R but with high affinity to 5-HT receptors, negatively influenced neurogenesis, possibly as a result of activating both receptors differently. In contrast, the highly selective S1R agonist PRE084 stimulated hippocampal cell proliferation and differentiation. Regarding neuroinflammation, DMT and PRE084 significantly reduced A $\beta$ <sub>1-42</sub>-induced astrogliosis, but neither had remarkable effects on microglial activation. In summary, the highly selective S1R agonist PRE084 may be a promising therapeutic agent for AD. Further studies are required to clarify the multifaceted neurogenic and anti-neuroinflammatory roles of these agonists.

**Keywords:** Alzheimer's disease; A $\beta$ <sub>1-42</sub>-induce mouse model; neurogenesis; neuroinflammation; sigma-1 receptor; dimethyltryptamine; PRE084

**Citation:** Borbély, E.; Varga, V.; Szögi, T.; Schuster, I.; Bozsó, Z.; Penke, B.; Fülöp, L. Impact of Two Neuronal Sigma-1 Receptor Modulators, PRE084 and DMT, on Neurogenesis and Neuroinflammation in an A $\beta$ <sub>1-42</sub>-Injected, Wild-Type Mouse Model of AD. *Int. J. Mol. Sci.* **2022**, *23*, 2514. <https://doi.org/10.3390/ijms23052514>

Academic Editors: Antonella Scorziello and Maria José Sisalli

Received: 21 December 2021

Accepted: 23 February 2022

Published: 24 February 2022

**Publisher's Note:** MDPI stays neutral with regard to jurisdictional claims in published maps and institutional affiliations.



**Copyright:** © 2022 by the authors. Licensee MDPI, Basel, Switzerland. This article is an open access article distributed under the terms and conditions of the Creative Commons Attribution (CC BY) license (<https://creativecommons.org/licenses/by/4.0/>).

## 1. Introduction

Alzheimer's disease (AD) is the most common form of dementia, characterized by progressive memory loss, impaired learning, and cognitive dysfunction. The main pathological hallmarks of AD are extracellular amyloid plaques and intracellular neurofibrillary tangles accumulated in the cerebral tissue [1], which first appear in the hippocampal and entorhinal regions of the brain, explaining the impairment of cognitive functions [2]. These changes are accompanied by the damage of synaptic connections, and neuronal death. The abnormal cleavage of amyloid precursor protein (APP) by  $\beta$ - and  $\gamma$ -secretases predominantly yields 40 to 43 amino acid long amyloid- $\beta$  (A $\beta$ ) peptides, which aggregate, and manifest as cerebral deposits. Besides forming plaques, these oligomeric forms of A $\beta$  are also thought to be neurotoxic [3–6]. These short oligomers might interfere with crucial intracellular mechanisms and signaling pathways. Thus, they may affect cell homeostasis, proliferation, differentiation, and survival [7–10]. Another significant symptom of AD is



neuroinflammation, which involves various inflammatory components, such as immune cells, cytokines, and chemokines. Neuroinflammation might significantly alter neurogenesis, as well as enhancing A $\beta$  production and plaque formation [11–13]. Currently, there is no cure for AD, and its progression cannot be prevented; at present, only symptomatic treatments of mild to moderate efficiency are available. Therefore, effective disease-modifying therapeutics that may halt the progression of AD and contribute to the protection of neuronal integrity are eagerly awaited. A potentially new direction of the research aiming to find novel disease-modulating agents targets the sigma receptors (SRs). SRs have received considerable attention for their potential role in the prevention of A $\beta$ -induced neurotoxicity, as well as in the regulation of the pathophysiology of AD. Furthermore, SRs may be essential for modulating neurogenesis in adulthood, and the stimulation of this process has been linked to AD. Thus, SR ligands are being recognized as promising therapeutic agents for treating or alleviating AD [6,14–16].

Two subtypes of SRs are distinguished, sigma-1 receptor (S1R) and sigma-2 receptor [17–19]. S1R is broadly expressed in the central nervous system (CNS), especially in the dentate gyrus (DG) region of the hippocampus (HC), both in neurons and glial cells. S1Rs are mainly located in a specific part of the cell where the endoplasmic reticulum (ER) and the mitochondria establish a tight interplay; this area is called the mitochondria-associated ER membrane (MAM) [16,20–23]. S1R is known to influence neuronal survival, proliferation, neurite growth, plasticity, as well as learning and memory functions [24–27]. It has been reported that the expression level of S1R decreases in patients with neurodegenerative diseases like AD [16,22,23,28–33].

S1R binds a diverse set of molecules, for example, antipsychotics, antidepressants, and neurosteroids [34–37]. A non-specific endogenous ligand of S1R is N,N-dimethyltryptamine (DMT), a hallucinogenic agent assumed to be produced in small quantities and accumulated in the CNS [16,38–40]. Previous studies have shown that the administration of DMT modulates many ion channels [39], protects against hypoxia-induced damage [41], alleviates neuroinflammation [42,43], increases the density of dendritic spines [44], as well as promotes neurogenesis and neuritogenesis [45–49]. However, DMT might also exert anxiogenic, neuro- and cytotoxic effects [47,50–52]. DMT is known to bind to several receptors with different affinities: 5-hydroxytryptamine (5-HT)<sub>1A-B</sub>, 5-HT<sub>1D</sub>, 5-HT<sub>2A-C</sub>, 5-HT<sub>5A</sub>, 5-HT<sub>6</sub>, 5-HT<sub>7</sub> receptors, S1R, SERT, dopamine (D)<sub>1-5</sub> receptors,  $\alpha_1$ AR, I<sub>1-3</sub>, TAAR, NMDA [53–55]. Several adverse effects of DMT are primarily associated with the stimulation of 5-HT<sub>2A</sub> receptors [47,50,51,53,56], while its positive impacts are rather related to the activation of S1Rs [40–44,46,49,50,52,57]. Moreover, the inflammation regulatory and plasticity promoting activities of DMT are also considered to result from its binding to both the S1Rs and 5-HT receptors. Identifying the valid contributor molecules and signaling pathways behind this assumption requires more convincing evidence.

Many exogenous ligands of S1R have been identified, including (+)-pentazocine, fluvoxamine, ANAVEX2-73, and 2-(4-morpholinethyl)-1-phenylcyclohexanecarboxylate (PRE084) [16,22,24,58]. The antidepressant and nootropic properties of PRE084 are also recognized [59]. Based on our current knowledge, PRE084 may promote neuroprotection and neurite growth by stimulating the expression of different neurotrophic factors, as well as by activating signaling pathways involved in cell survival [60–65]. Previous studies suggest that this S1R-agonist might positively impact learning and memory, as demonstrated in animal models of neurodegenerative diseases or traumatic brain injuries [63,64,66]. It is also reported that after the administration of A $\beta$ <sub>25-35</sub> infusion into the right lateral ventricle of mice, PRE084 administration has moderated the adverse behavioral effects of A $\beta$ <sub>25-35</sub> [27] via reducing neurotoxicity-induced cell death [32,64]. Moreover, PRE084 may also promote neurogenesis [9] and cell survival by attenuating excitotoxicity and reducing microglial activity, as well as diminishing the expression of proinflammatory factors [67,68].

As mentioned above, in addition to its ability to support cell survival under stress conditions, activated S1Rs may also stimulate the formation of new neurons, even in the

adult brain. In adulthood, mammalian neurogenesis is derived from neuronal stem cells (NSCs) located in the subgranular zone (SGZ) of the dentate gyrus (DG) in the hippocampus (HC), as well as from NSCs in the subventricular region of the lateral ventricles [69,70]. After differentiation and migration, these newly formed neurons can integrate into local neuronal circuits of the HC; thus, they might have a significant role in plasticity, cognitive functions, learning, and memory processes [71]. An optimal microenvironment is essential for the division, differentiation, migration, and maturation of NSCs. Physiologically, the activity of adult hippocampal neurogenesis decreases with aging, leading to a usually mild, age-associated cognitive decline. However, a growing body of evidence indicates that the extent of adult neurogenesis is sharply diminished in the early stages of AD, even before the appearance of senile plaques [72–78]. This finding raises the question of whether impaired neurogenesis may initiate and/or contribute to more severe cognitive deficits, thus mediating AD's pathogenesis. Furthermore, these findings suggest that the stimulation of neurogenesis might serve as a therapeutic target in AD, with a potential to improve cognitive functions and promote neural adaptability, thereby it might prevent or even treat AD.

In this study, two main objectives were addressed. First, to induce early acute AD-like impairments in neurogenesis and generate neuroinflammation in adult wild-type C57BL/6 mice by the intracerebroventricular (ICV) administration of  $A\beta_{1-42}$  oligomers. In this experimental paradigm, we followed the administration protocol described by Li et al., who examined the effects of  $A\beta_{25-35}$  on the same processes [9]. They reported that  $A\beta_{25-35}$  stimulated the proliferation of neuronal progenitor cells, while enhancing the death of newly formed neurons and impaired neurite growth. Secondly, we attempted to restore the normal functioning of adult neurogenesis and reduce neuroinflammation by activating S1Rs with two different ligands, PRE084 and DMT. The intraperitoneally-(IP-)-injected compounds were tested in wild-type mice, either treated with  $A\beta_{1-42}$ -oligomers or injected with vehicle (phosphate buffered saline (PBS)) as a control. Based on previously published articles on the beneficial effects of these S1R modulators, we expected to detect an obvious positive impact of the tested agents on the  $A\beta_{1-42}$ -induced impairments in adult neurogenesis and neuroinflammation [41–43,49,52,57,60–64,79].

## 2. Results

### 2.1. Effects of PRE084 and DMT on Adult Neurogenesis in $A\beta_{1-42}$ and Vehicle-Treated Mice

$A\beta_{1-42}$  and DMT impair, while PRE084 promotes the survival of progenitor cells in DG.

Proliferating cells were labeled by three IP injections of 5-Bromo-2'-Deoxyuridine (BrdU) with a 6 h interval, which was administered 24 h after the stereotaxic surgery. BrdU is a synthetic thymidine analog, which incorporates into the DNA strand, and can be detected by specific antibodies. We counted BrdU+ cells 14 days after the surgery. According to our results, the quantity of BrdU+ stem cells in the SGZ of the DG significantly differed among the six groups (ANOVA:  $p \leq 0.0001$ ).  $A\beta_{1-42}$  infusion significantly reduced the number of progenitor cells compared to the respective control group (PBS-PBS vs.  $A\beta_{1-42}$ -PBS  $p = 0.001$ ). Interestingly, significantly more severe negative changes were detected in animals treated with DMT. In those co-treated with both  $A\beta_{1-42}$  and DMT, hardly any BrdU+ stem cells were detected in the SGZ ( $A\beta_{1-42}$ -DMT vs. PBS-PBS  $p \leq 0.0001$ , vs.  $A\beta_{1-42}$ -PBS  $p = 0.005$ , vs.  $A\beta_{1-42}$ -PRE084  $p \leq 0.0001$ ; PBS-DMT vs. PBS-PBS  $p = 0.001$ , vs. PBS-PRE084  $p \leq 0.0001$ ). PRE084 treatment increased the amount of BrdU+ cells; the difference between the  $A\beta_{1-42}$ -infused groups was significant ( $A\beta_{1-42}$ -PBS vs.  $A\beta_{1-42}$ -PRE084  $p \leq 0.0001$ ) (Figure 1).

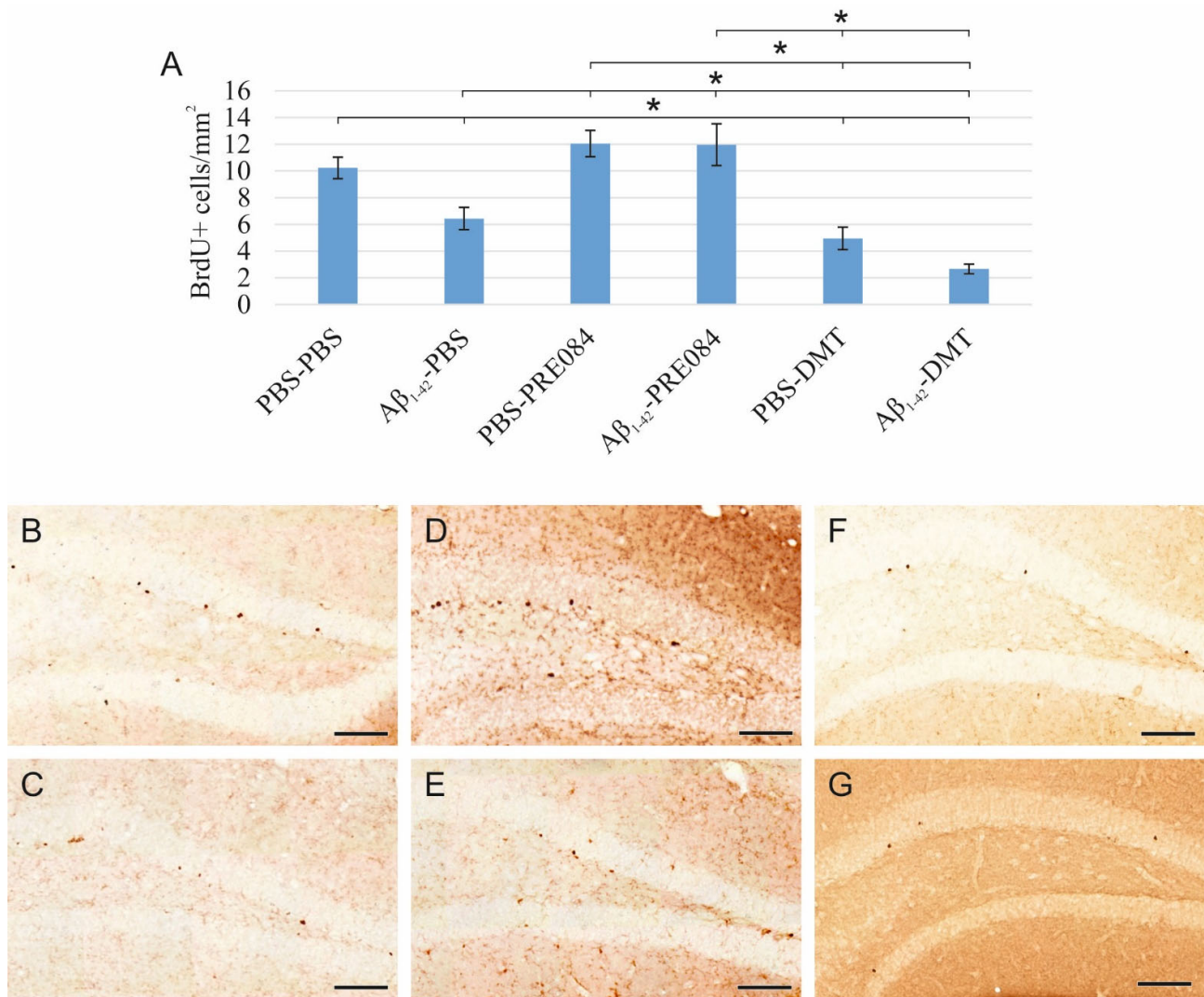


**Figure 1.** (A) Results for 5-Bromo-2'-Deoxyuridine (BrdU) immunolabeling. We observed significant differences in the quantity of stem cells between the six groups (ANOVA:  $p \leq 0.0001$ ). Significantly fewer BrdU+ cells were detected in the A $\beta_{1-42}$ -PBS, PBS-DMT, and in the A $\beta_{1-42}$ -DMT treated animals compared to the PBS-PBS group (PBS-PBS vs. A $\beta_{1-42}$ -PBS  $p = 0.001$ , vs. PBS-DMT  $p = 0.001$ , vs. A $\beta_{1-42}$ -DMT  $p \leq 0.0001$ ). The difference between the A $\beta_{1-42}$ -PBS and A $\beta_{1-42}$ -DMT treatment groups was also significant ( $p = 0.005$ ). PRE084-treatment increased the number of stem cells detected in the SGZ; this change was significant in the A $\beta_{1-42}$ -administered group compared to its vehicle-treated control (A $\beta_{1-42}$ -PBS vs. A $\beta_{1-42}$ -PRE084  $p \leq 0.0001$ ). The differences between the following groups in pairwise comparisons also reached significance: PBS-PRE084 vs. A $\beta_{1-42}$ -PBS  $p \leq 0.0001$ , vs. PBS-DMT  $p \leq 0.0001$ , vs. A $\beta_{1-42}$ -DMT  $p \leq 0.0001$ ; A $\beta_{1-42}$ -PRE084 vs. PBS-DMT  $p \leq 0.0001$ , vs. A $\beta_{1-42}$ -DMT  $p \leq 0.0001$ . (B–G) Representative images of BrdU staining: (B) PBS-PBS, (C) A $\beta_{1-42}$ -PBS, (D) PBS-PRE084, (E) A $\beta_{1-42}$ -PRE084, (F) PBS-DMT, (G) A $\beta_{1-42}$ -DMT. Scale bars represent 100  $\mu$ m. \*:  $p \leq 0.05$

A $\beta_{1-42}$  and PRE084 increase the number of premature cells, while DMT does not affect their quantity.

To understand the effects of PRE084 and DMT on the maturation of granule cells, we quantified immature neurons in the SGZ of DG. To label premature cells, we stained a microtubule-associated protein called doublecortin (DCX), which is expressed specifically in migrating neuronal precursors. The measured DCX densities were significantly different among the six groups (ANOVA:  $p \leq 0.0001$ ). In those treated with A $\beta_{1-42}$ -PBS and PBS-

PRE084, the number of immature neurons was significantly higher compared to the control group (PBS-PBS vs.  $A\beta_{1-42}$ -PBS  $p = 0.037$ , vs. PBS-PRE084  $p \leq 0.0001$ , vs.  $A\beta_{1-42}$ -PRE084  $p \leq 0.0001$ ). We also detected a significant difference between the  $A\beta_{1-42}$ -PBS and  $A\beta_{1-42}$ -PRE084 mice groups ( $p = 0.007$ ). DMT administration did not affect the number of premature neurons compared to PBS-PBS mice (Figure 2).

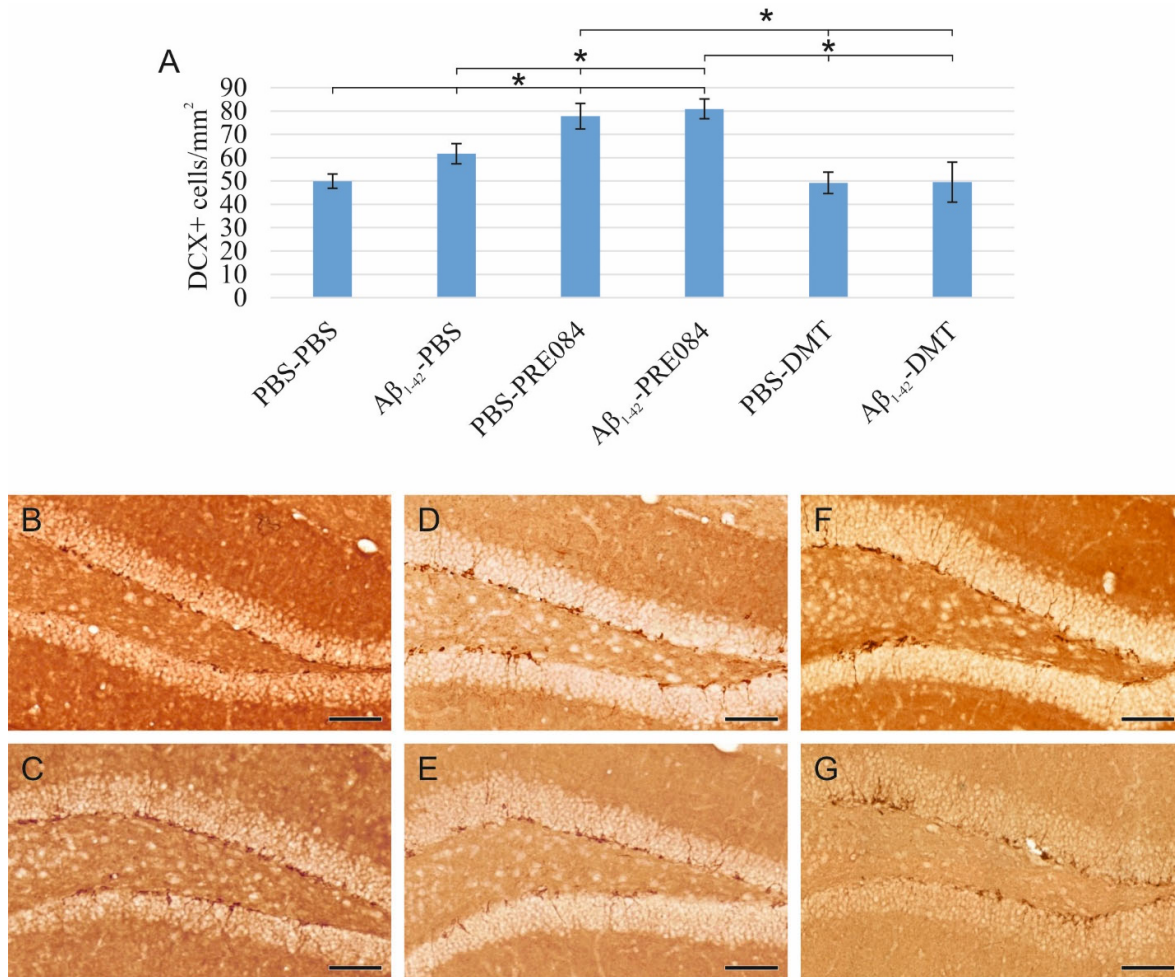


**Figure 2.** (A) Results for doublecortin (DCX) immunostaining. Detected DCX densities significantly differed among the six groups (ANOVA:  $p \leq 0.0001$ ). Compared to the control (PBS-PBS) animals, a significantly higher amount of DCX+ cells were detected in the  $A\beta_{1-42}$ -PBS, PBS-PRE084 and  $A\beta_{1-42}$ -PRE084-treated groups (PBS-PBS vs.  $A\beta_{1-42}$ -PBS  $p = 0.037$ , vs. PBS-PRE084  $p \leq 0.0001$ , vs.  $A\beta_{1-42}$ -PRE084  $p \leq 0.0001$ ). Similarly, a significant difference was detected between the groups treated with  $A\beta_{1-42}$ -PBS and  $A\beta_{1-42}$ -PRE084 ( $p = 0.007$ ). DMT treatment did not alter the number of immature neurons in the SGZ. Furthermore, significant differences were found when the groups were compared to the PBS-PRE084-treated group: PBS-PRE084 vs.  $A\beta_{1-42}$ -PBS  $p = 0.023$ , vs. PBS-DMT  $p = 0.001$ , vs.  $A\beta_{1-42}$ -DMT  $p = 0.001$ . Additional significant results were detected:  $A\beta_{1-42}$ -PRE084 vs. PBS-DMT  $p \leq 0.0001$ , vs.  $A\beta_{1-42}$ -DMT  $p \leq 0.0001$ . (B–G) Representative images of DCX immunolabeling: (B) PBS-PBS, (C)  $A\beta_{1-42}$ -PBS, (D) PBS-PRE084, (E)  $A\beta_{1-42}$ -PRE084, (F) PBS-DMT, (G)  $A\beta_{1-42}$ -DMT. Scale bars represent 100  $\mu$ m. \*:  $p \leq 0.05$

The density of mature granule cells is unaffected by  $A\beta_{1-42}$  or PRE084 administration, while DMT induces a decrease in neuronal density.

To detect and evaluate mature granule cells in the HC, we performed neuronal nuclei (NeuN) immunostaining (Figure 3). Again, significant differences were observed among the groups (ANOVA:  $p = 0.001$ ). In DMT-treated animals, significantly lower NeuN+ cell



densities were evident in the HC compared to the PBS-PBS and A $\beta_{1-42}$ -PBS group (PBS-PBS vs. PBS-DMT  $p = 0.001$ , vs. A $\beta_{1-42}$ -DMT  $p = 0.022$ ; A $\beta_{1-42}$ -PBS vs. PBS-DMT  $p \leq 0.0001$ , vs. A $\beta_{1-42}$ -DMT  $p = 0.003$ ).

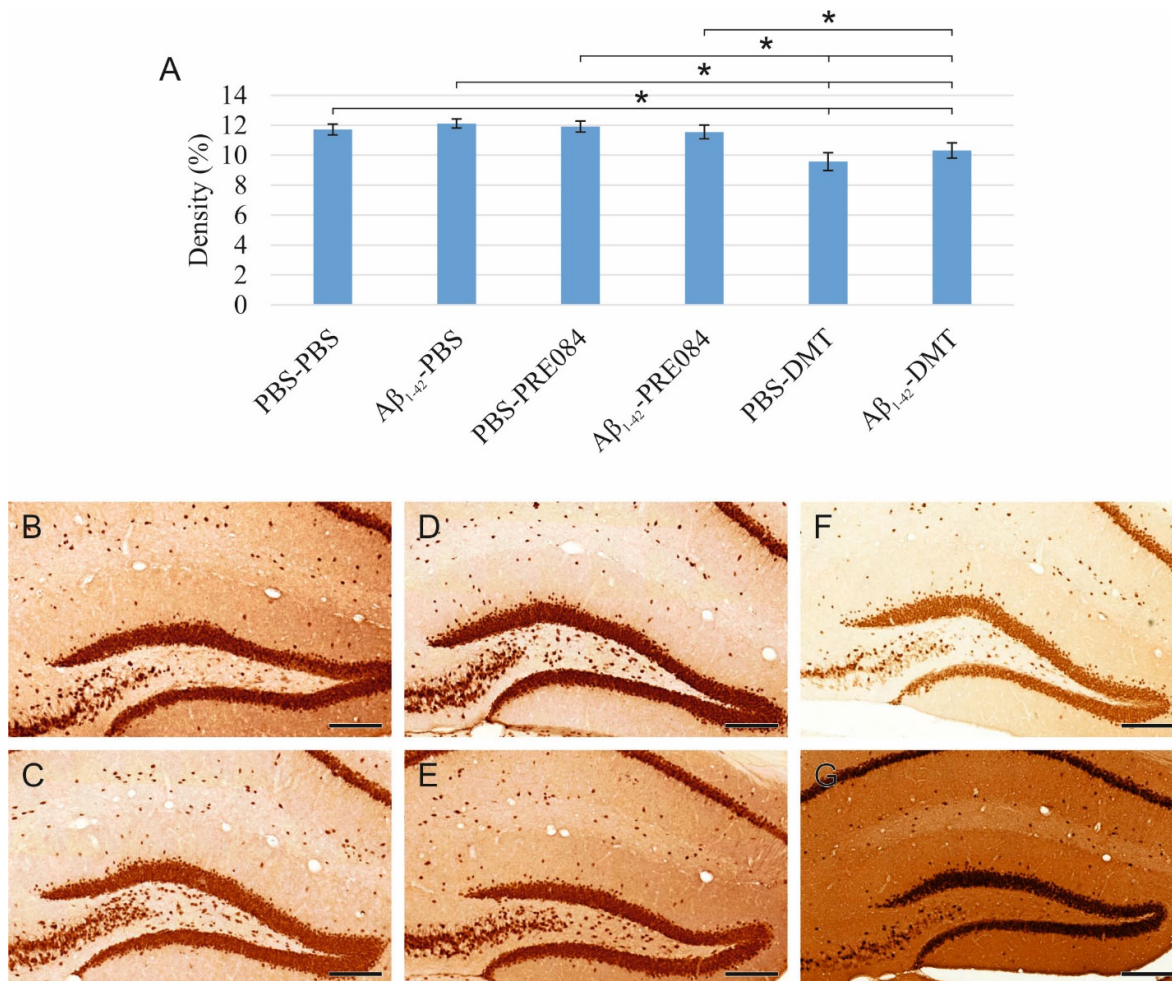


**Figure 3.** (A) Results for neuronal nuclei (NeuN) immunostaining. Significant differences were detected among the groups as follows (ANOVA:  $p = 0.001$ ): in DMT-treated animals, significantly lower NeuN densities were evident compared to the PBS-PBS and A $\beta_{1-42}$ -PBS groups (PBS-DMT vs. PBS-PBS  $p = 0.001$ , vs. A $\beta_{1-42}$ -PBS  $p \leq 0.0001$ ; A $\beta_{1-42}$ -DMT vs. PBS-PBS  $p = 0.022$ , vs. A $\beta_{1-42}$ -PBS  $p = 0.003$ ). Furthermore, significant differences were found when the groups were compared to the PBS-DMT-treated group: PBS-DMT vs. PBS-PRE084  $p = 0.001$ , vs. A $\beta_{1-42}$ -PRE084  $p = 0.006$ ; A $\beta_{1-42}$ -DMT vs. PBS-PRE084  $p = 0.024$ . (B–G) Representative photomicrographs of NeuN immunolabeling: (B) PBS-PBS, (C) A $\beta_{1-42}$ -PBS (D) PBS-PRE084, (E) A $\beta_{1-42}$ -PRE084, (F) PBS-DMT, (G) A $\beta_{1-42}$ -DMT. Scale bars represent 200  $\mu\text{m}$ . \*:  $p \leq 0.05$

## 2.2. Effects of PRE084 and DMT on Neuroinflammation Induced by A $\beta_{1-42}$

A $\beta_{1-42}$  stimulates microglia activation, and neither PRE084, nor DMT alleviate this effect, while DMT alone significantly decreases microglial density.

Neuroinflammation results from the activation of an immune response in the CNS, mediated by microglia and astrocytes. This process is induced by infective agents, neurodegenerative diseases, or injuries. To identify activated microglia in the HC, we stained ionized calcium-binding adapter molecule 1 (Iba1), expressed explicitly by monocyte-derived and resident macrophages, including microglia. Our results showed a significant difference in the density of Iba1+ microglia among the groups (ANOVA:  $p = 0.002$ ). A $\beta_{1-42}$  administration significantly increased the density of activated microglia compared to the

vehicle-treated control groups (PBS-PBS vs.  $A\beta_{1-42}$ -PBS  $p = 0.015$ ; PBS-PRE084 vs.  $A\beta_{1-42}$ -PRE084  $p = 0.035$ ; PBS-DMT vs.  $A\beta_{1-42}$ -DMT  $p = 0.039$ ). In the PBS-DMT group, the density of Iba1+ microglia was significantly reduced compared to PBS-PBS-treated animals (PBS-PBS vs. PBS-DMT  $p = 0.031$ ). Still, none of the treatments were found to be able to alleviate the proinflammatory effect of  $A\beta_{1-42}$  (Figure 4).

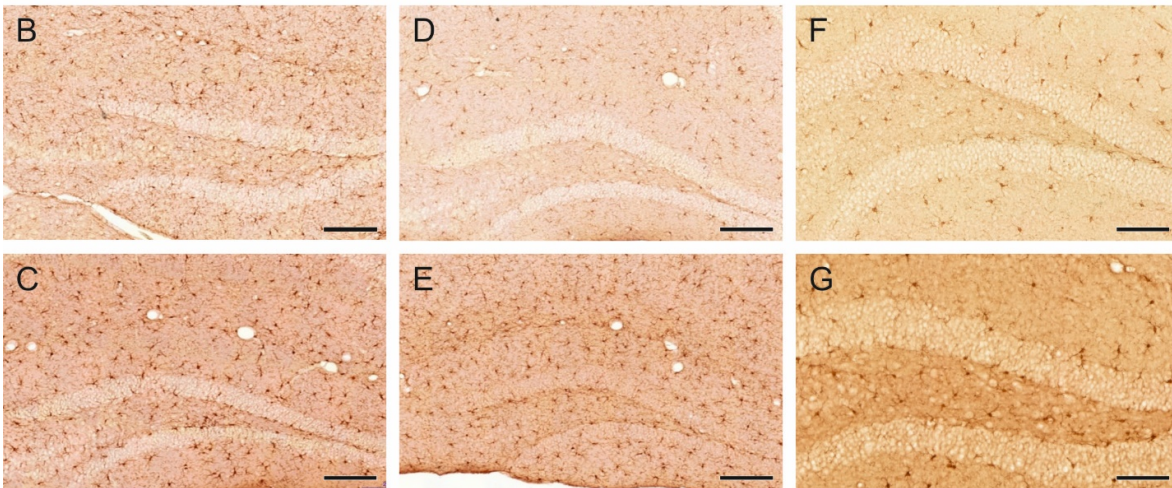
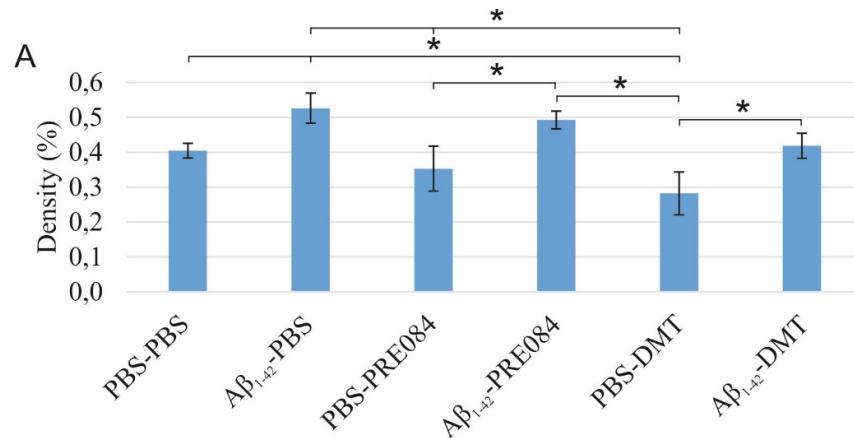


**Figure 4.** (A) Results for ionized calcium-binding adapter molecule 1 (Iba1) immunolabeling. Significant differences were observed among the groups (ANOVA:  $p = 0.002$ ).  $A\beta_{1-42}$  increased the density of Iba1+ microglia significantly compared to PBS-PBS, PBS-PRE084, and PBS-DMT treated mice, respectively (PBS-PBS vs.  $A\beta_{1-42}$ -PBS  $p = 0.015$ ; PBS-PRE084 vs.  $A\beta_{1-42}$ -PRE084  $p = 0.035$ ; PBS-DMT vs.  $A\beta_{1-42}$ -DMT  $p = 0.039$ ). The difference between the PBS-PBS and PBS-DMT groups was also significant (PBS-PBS vs. PBS-DMT  $p = 0.031$ ). Moreover, significant differences were detected between the following groups:  $A\beta_{1-42}$ -PBS vs. PBS-PRE084  $p = 0.005$ , vs. PBS-DMT  $p \leq 0.0001$ ;  $A\beta_{1-42}$ -PRE084 vs. PBS-DMT  $p = 0.002$ . (B–G) Representative images of Iba1 immunostaining: (B) PBS-PBS, (C)  $A\beta_{1-42}$ -PBS, (D) PBS-PRE084, (E)  $A\beta_{1-42}$ -PRE084, (F) PBS-DMT, (G)  $A\beta_{1-42}$ -DMT. Scale bars represent 100  $\mu\text{m}$ . \*:  $p \leq 0.05$

$A\beta_{1-42}$  stimulates astrocyte reactivation, while the administration of DMT or PRE084 reduces this effect.

Reactive astrocytes were immunostained for glial fibrillary acidic protein (GFAP), an intermediate filament protein expressed by different cell types, mainly reactive astrocytes, in the CNS. Significantly different GFAP+ cell densities were detected in the HC of the different groups (ANOVA:  $p = 0.002$ ). A significant increase in the rate of reactivated astrocytes was detected in the  $A\beta_{1-42}$ -PBS group compared to PBS-PBS-treated mice ( $p \leq 0.0001$ ). Furthermore, GFAP+ cell densities were significantly lower in all other groups



compared to A $\beta_{1-42}$ -PBS-treated mice (A $\beta_{1-42}$ -PBS vs. PBS-PRE084  $p = 0.013$ , vs. A $\beta_{1-42}$ -PRE084  $p = 0.013$ , vs. PBS-DMT  $p \leq 0.0001$ , vs. A $\beta_{1-42}$ -DMT,  $p = 0.001$ ). The stimulatory effect of A $\beta_{1-42}$  on astrocyte reactivation was alleviated by PRE084 and DMT administration (Figure 5).

The activation of inflammatory processes was assessed by the determination of certain proinflammatory cytokines (IL1 $\beta$  and TNF $\alpha$ ). The levels of both pro-IL1 $\beta$  and soluble IL1 $\beta$ , as well as membrane-bound TNF $\alpha$  and soluble TNF $\alpha$ , were determined by western blot analyses (see Supplement Figure S1). These results corroborate our findings regarding the activation of the glial immunodefense system in response to the A $\beta_{1-42}$  stimulus. The production of the active cytokine forms could be modulated by DMT-treatment; however, only the change in TNF $\alpha$ -level was significant.

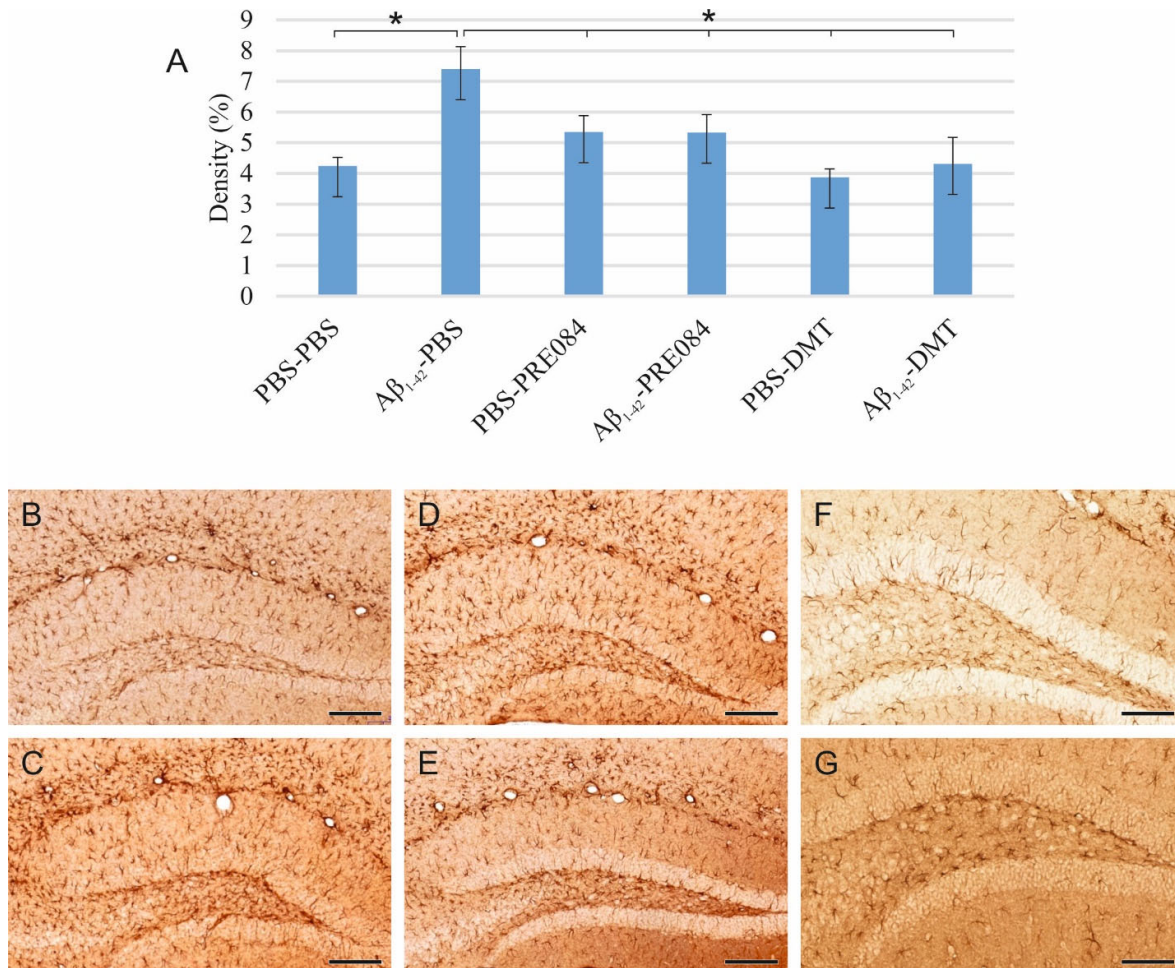


**Figure 5.** (A) Results of glial fibrillary acidic protein (GFAP) immunostaining. The densities of GFAP+ astrocytes differed among the groups (ANOVA:  $p \leq 0.0001$ ). A significantly higher GFAP+ density was detected in the A $\beta_{1-42}$ -PBS group compared to those treated with PBS-PBS ( $p \leq 0.0001$ ), PBS-PRE084 ( $p = 0.013$ ), A $\beta_{1-42}$ -PRE084 ( $p = 0.013$ ), PBS-DMT ( $p \leq 0.0001$ ), and A $\beta_{1-42}$ -DMT ( $p = 0.001$ ). (B–G) Representative images of GFAP immunolabeling: (B) PBS-PBS, (C) A $\beta_{1-42}$ -PBS, (D) PBS-PRE084, (E) A $\beta_{1-42}$ -PRE084, (F) PBS-DMT, (G) A $\beta_{1-42}$ -DMT. Scale bars represent 100  $\mu\text{m}$ . \*:  $p \leq 0.05$

### 2.3. S1R Protein Level Is Elevated by $A\beta_{1-42}$ Treatment, as Well as by the Co-Administration of $A\beta_{1-42}$ and PRE084 or DMT

To determine the effects of  $A\beta_{1-42}$  and PRE084 or DMT on the expression of S1R, a western blot (WB) analysis using GAPDH loading control was performed on HC and cerebral cortex samples of three animals per group. Our findings revealed a significant difference in the S1R levels among the groups (ANOVA:  $p \leq 0.0001$ ). S1R protein levels were significantly elevated in all groups, except in PBS-DMT-treated animals, as compared to control subjects (PBS-PBS vs.  $A\beta_{1-42}$ -PBS  $p \leq 0.0001$ , vs. PBS-PRE084  $p = 0.018$ , vs.  $A\beta_{1-42}$ -PRE084  $p \leq 0.0001$ , vs. PBS-DMT  $p = 0.540$ ; vs.  $A\beta_{1-42}$ -DMT  $p \leq 0.0001$ , respectively). In comparison with  $A\beta_{1-42}$ -PBS-treated mice, the  $A\beta_{1-42}$ -PRE084 ( $p = 0.004$ ) and  $A\beta_{1-42}$ -DMT ( $p = 0.673$ ) groups showed higher protein levels, while significantly lower levels of S1R were detected in PBS-PRE084 ( $p = 0.032$ ) and PBS-DMT ( $p = 0.001$ ) treated mice. As expected, the co-administration of  $A\beta_{1-42}$  and either of the S1R agonists increased the S1R protein level compared to the respective control group ( $A\beta_{1-42}$ -PRE084 vs. PBS-PRE084  $p \leq 0.0001$ ;  $A\beta_{1-42}$ -DMT vs. PBS-DMT  $p = 0.015$ ). Notably, the expression of S1R was significantly increased in  $A\beta_{1-42}$ -PRE084-treated animals compared to the  $A\beta_{1-42}$ -DMT group ( $p \leq 0.0001$ ). (Figure 6).

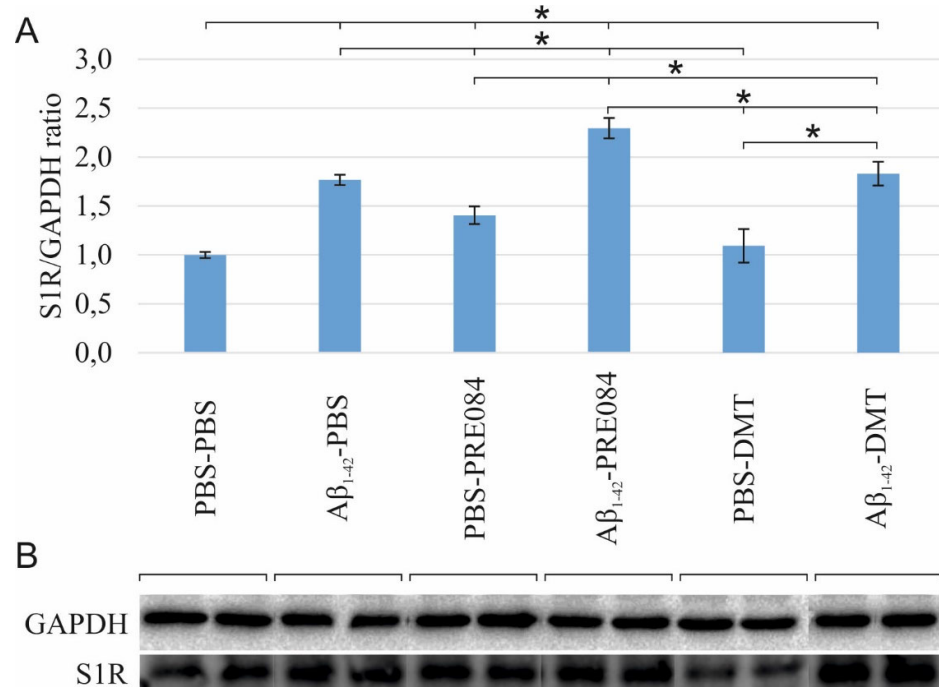


**Figure 6.** (A) Results for the western blot (WB) analysis. Significant differences were observed in the S1R levels among the groups (ANOVA:  $p \leq 0.0001$ ). Compared to PBS-PBS-treated mice, the S1R protein levels were significantly elevated in the  $A\beta_{1-42}$ -PBS ( $p \leq 0.0001$ ), PBS-PRE084 ( $p = 0.018$ ),  $A\beta_{1-42}$ -PRE084 ( $p \leq 0.0001$ ), and  $A\beta_{1-42}$ -DMT ( $p \leq 0.0001$ ) groups. In PBS-DMT-treated mice, the S1R protein expression remained close to the control level ( $p = 0.540$ ), while S1R levels were somewhat higher in the PRE084-treated groups (PBS-PBS vs. PBS-PRE084  $p = 0.018$ ;  $A\beta_{1-42}$ -PBS vs.  $A\beta_{1-42}$ -PRE084  $p = 0.004$ ; PBS-PRE084 vs.  $A\beta_{1-42}$ -PRE084  $p \leq 0.0001$ ). In contrast, the co-administration of  $A\beta_{1-42}$  and DMT induced a significant increase in the quantity of S1R (PBS-DMT vs.  $A\beta_{1-42}$ -DMT  $p \leq 0.0001$ ). Furthermore, significant differences were detected in the S1R expression upon the pairwise comparisons of the following groups:  $A\beta_{1-42}$ -PBS vs. PBS-PRE084  $p = 0.032$ , vs. PBS-DMT  $p = 0.001$ ;  $A\beta_{1-42}$ -PRE084 vs. PBS-DMT  $p \leq 0.0001$ , vs.  $A\beta_{1-42}$ -DMT  $p \leq 0.0001$ , respectively. (B) WB gel electrophoresis images of S1R and GAPDH lines of the experimental groups. \*:  $p \leq 0.05$



### 3. Discussion

During neurogenesis in adulthood, new neurons continuously develop and differentiate from hippocampal stem cells, and are integrated into existing neuronal networks to maintain plasticity of the CNS, and thereby preserve learning and memory functions. It has been recognized that the formation of new neurons reduces with age, manifesting in impaired cognitive functions [80]. In certain neurodegenerative diseases this cluster of mental symptoms is much more pronounced due to a decreased rate of neurogenesis, increased destruction of mature neurons, and enhanced neuroinflammatory responses. The most prevalent disease of this kind is AD, characterized by progressive dementia. Early alternations in adult neurogenesis and neuroinflammation may appear several years or even a decade before the diagnosis of AD, and probably contributes to the onset of neurological symptoms. It is hypothesized that an intensive stimulation of hippocampal neurogenesis and the reduction in neuroinflammation in adulthood could slow down the rate of decline of cognitive skills. Moreover, the uniquely structured S1R protein, functioning as a ligand-operated chaperone, is known to play a major role in both neurogenesis and neuroinflammation. Thus, it is assumed that the activation of S1Rs may be a promising therapeutic strategy to stimulate adult neurogenesis and alleviate neuroinflammatory processes.

The first objective of our study was to model these early alternations appearing in AD. Our experimental paradigm was based on the work of Li et al., in a modified way: instead of  $A\beta_{25-35}$ , we injected  $A\beta_{1-42}$  ICV to induce early AD-like changes [9]. The reason for this modification is that  $A\beta_{25-35}$  is a non-natural, truncated sequence, and although it is prone to aggregation, its kinetics for aggregation differ from that of the native  $A\beta_{1-42}$  peptide. Therefore, using this latter peptide should yield biologically more relevant findings [81]. In the work of Li et al., neurogenesis was assessed 14 and 28 days after the peptide injections, and significant differences were detected on day 28 in neurogenic markers compared to baseline (reduced proliferation and neurite growth, increased death of newly formed cells) [9]. In our experimental model, AD-like cerebral neurogenic and neuroinflammatory changes could be detected as early as two weeks after the administration of  $A\beta_{1-42}$ . We demonstrated that a single administration of  $A\beta_{1-42}$ , directly into the lateral ventricles, significantly impaired the proliferation and increased the number of immature cells in mice. The effects of  $A\beta$  on neurogenesis are highly controversial in the literature. Numerous reports indicate that  $A\beta$  significantly decreases the formation of new neurons, possibly by impairing their ability to divide, as well as by diminishing the survival of neuronal stem cells in DG [7–9,75–77,82]. However, some research groups have published that  $A\beta$  can induce the initial proliferation step of neuron formation in different transgenic mouse strains [9,78,83–85] or in cellular models of AD [86–91]. In our experiments, an increase in the number of differentiating immature neurons was observed in  $A\beta_{1-42}$ -treated animals, which may be explained by a compensatory cerebral mechanism [77,92]. Specifically, this enhancement of neuronal cell differentiation may be a response to the disturbed homeostasis resulting from the decrease in the stem cell population, aiming to restore the balance within the CNS. As we expected, in our experimental model, no significant reduction was detected in the density of mature, functional neurons in HC two weeks after the administration of  $A\beta_{1-42}$ , indicating that the existing neuronal system may remain unaffected. Regarding neuroinflammation, we found that a single administration of  $A\beta_{1-42}$  stimulated neuroinflammatory processes, causing a significant increase in the densities of activated microglia and hyperreactive astrocytes. In line with our observations, several *in vivo* experiments have demonstrated the neuroinflammation-inducing effects of  $A\beta$  fibrils and oligomers injected into the brain tissue in different experimental models [93–95]. This neuroinflammatory environment may affect adult neurogenesis either positively or negatively [11,12,96–101]. It is known that cytokines and chemokines produced by activated microglia and astrocytes play an important role in neuroinflammatory processes. Certain anti-(IL-4, IL-10) and proinflammatory (IL-6, TNF- $\alpha$ ) factors substantially influence neurogenesis, e.g., they can diminish proliferation and cell survival, while they may

also stimulate cell differentiation [13]. Thus, beyond its direct effects on immature neurons, A $\beta$ <sub>1-42</sub> may also affect neurogenesis by generating a relatively mild, but chronic neuroinflammatory environment. Further research is needed to clarify the relative contribution of these two processes (direct and indirect) to the final decline of adult neurogenesis in AD.

Since the S1R protein plays a major role in neurogenesis and neuroinflammation, and changes in S1R expression levels have not been studied in exogenous A $\beta$ -induced AD models, we examined the expression levels of this protein. In our case, the expression of S1R increased after a single administration of A $\beta$ <sub>1-42</sub>. This finding may contradict some literature data, which report on the down-regulation of S1R in the early stage of human AD [24]. In the reported cases, both the amount and the binding potential of S1R were found to be decreased, presumably as a consequence of hippocampal neuronal death [24,102–105]. In contrast, other studies indicate that AD-related ER-stress can lead to an up-regulation of S1R [16,29,106,107], which, serving as a chaperon, modulates the canonical unfolded protein response (UPR) pathways (PERK, IRE1a, ATF6) [16,108]. In our study, the observed elevation of the level of S1R may be a consequence of the cytotoxic effect of A $\beta$ <sub>1-42</sub>, which induces ER stress, and thus activates the UPR pathways and upregulates S1R expression.

To date, the biological effects of DMT and PRE084 have not been studied in an A $\beta$ -induced model of early AD with demonstrated changes in neurogenesis and S1R expression levels, as well as neuroinflammation. Therefore, we aimed to assess whether the modulation of S1Rs with selected ligands can restore A $\beta$ <sub>1-42</sub>-induced alternations in adult neurogenesis and reduce neuroinflammation.

In our study, DMT significantly reduced the number of neuronal stem cells and densities of neurons. Similar to this finding, another tryptamine, psilocybin (4-phosphoryloxy-N, N-dimethyltryptamine) with a chemical structure close to that of DMT and a high binding affinity to 5-HT<sub>2A</sub> receptors (K<sub>d</sub> = 6 nM), was also found to impair synaptic growth and neurogenesis (proliferation and neuronal survival) [109]. However, the neuroprotective and neurogenesis stimulating effects of DMT and its analog, 5-methoxy-DMT, exerted via S1Rs, were also described in *in vitro* cell cultures and in a wild-type rodent model [44,46,49,54]. In our study, DMT was administered at a concentration of 1 mg kg<sup>-1</sup>, thus it is supposed to have occupied both receptor types, so their mixed effects could have been observed. Comparison of the K<sub>d</sub> values (DMT-S1R K<sub>d</sub> = 14.75  $\mu$ M, DMT-5-HT<sub>2A</sub> receptor K<sub>d</sub> = 130 nM) indicates that DMT binds to the 5-HT<sub>2A</sub> receptor with higher affinity than to S1R; thus, it is more likely to act on the 5-HT<sub>2A</sub> receptors than on S1R [39,53]. Therefore, we suppose that DMT exerted its negative effect on neurogenesis via the 5-HT<sub>2A</sub> receptors. The results of our WB analysis support this hypothesis, since the expression of the S1R protein was only slightly elevated after DMT treatment.

Regarding the relation of DMT and neuroinflammation, conflicting findings are published in the literature. Some of them support the theory that DMT can alleviate neuroinflammatory processes, thus it may reduce the density of reactive astrocytes [41–43,52,57]. This effect may be related to the ability of DMT to bind to S1R [41–43,52], but the serotonergic receptors may also have roles in this process [110]. Morales-Garcia et al. reported that DMT induces a significant increase in the density of GFAP<sup>+</sup> astrocytes via the activation of S1Rs, but these researchers conclude that this elevated GFAP level promotes neurogenesis [49]. In our experiments, DMT treatment was found to exert a positive effect on activated microglia and hyperreactive astrocytes against the A $\beta$ <sub>1-42</sub>-induced neurotoxicity, but it was not detected to promote neurogenesis.

These contradictory results may be explained by the application of different protocols (injection and doses of BrdU and DMT, different survival times). It is also known that although DMT can penetrate the blood-brain barrier, upon exogenous administration its concentration in the CNS is elevated for a relatively short time only (elimination half-life ~15 min [44]). Therefore, it is also possible that in our model, the concentration of DMT in the CNS after IP administration was not sufficient to exert its effects on S1R as Morales-

Garcia reported [49]. Further experiments are required to elucidate the exact mode of action of DMT regarding neurogenesis and neuroinflammation.

To study the effect of an exogenous S1R agonist on neurogenesis and neuroinflammation, we applied PRE084 ( $K_d = 2.2$  nM, [111]). Similarly, as Li et al. reported in an  $A\beta_{25-35}$ -induced mouse model of AD, we have demonstrated that PRE084 promotes neurogenesis upon treatment with  $A\beta_{1-42}$ , as it is indicated by the quantitative increase in stem cells and immature neurons after PRE084 administration. Furthermore, PRE084 *per se* activates cell proliferation, possibly by stimulating S1R.

Regarding neuroinflammation, the density of hyperreactive astrocytes and the degree of  $A\beta_{1-42}$ -induced astrogliosis were reduced by the administration of PRE084. However, the substance neither *per se*, nor in combination with  $A\beta_{1-42}$  could impair microglial activation. It is known that in case of CNS tissue damage, activated microglia may behave either neurotoxic or neuroprotective, depending on their morphological and functional states. According to the literature, PRE084 can stimulate the proliferation of the anti-inflammatory type of microglia (M2), while it suppresses pro-inflammatory M1 microglia, thus it maintains the delicate balance between functional restorative and inflammatory glial phenotypes [62,112]. As we did not analyze the distribution and morphology of the microglia, we assume that the apparent ineffectiveness of PRE084 treatment on microglial activation may result from the above mentioned two mutual processes.

PRE084 binds to S1R with high affinity, either alone (compared to PBS and DMT controls) and when co-administered with  $A\beta_{1-42}$  (compared to  $A\beta_{1-42}$ -PBS or  $A\beta_{1-42}$ -DMT animals), and significantly induces the expression of this receptor protein. These results may confirm that PRE084 activates the S1R receptors effectively, so its neurogenic impact is more pronounced than that of DMT.

## 5. Materials and Methods

### 5.1. Animals

Male C57BL/6 wild-type mice ( $n = 80$ ) from in-house breeding, weighing 23–28 g and aged 12 weeks at the beginning of the study, were used for the experiments. All animals, divided into groups, were kept under constant circumstances, including constant temperature ( $23 \pm 0.5$  °C), lighting (12:12 h light/dark cycle, lights on at 7 a.m.), and humidity (~50%). Standard mouse chow and tap water were supplied *ad libitum*. All behavioral experiments were performed in the light period. Handling was executed daily, at the same time, started one week before the experiments. All efforts were made to minimize the number of animals used, and their suffering throughout the experiments.

All experiments were performed in accordance with the European Communities Council Directive of 22 September 2010 (2010/63/EU on protecting animals used for scientific purposes). The experimental protocols were approved by the National Food Chain Safety and Animal Health Directorate of Csongrad County, Hungary (project license: XXVI./3644/2017). Formal approval to conduct the experiments was obtained from the Animal Welfare Committee of the University of Szeged (project No. I-74-16/2017, 04.07.2017).

### 5.2. Preparation and Structure Analysis of $A\beta_{1-42}$ Peptide Oligomers

The iso- $A\beta_{1-42}$  peptide was synthesized in the solid phase using tert-butyloxycarbonyl (Boc)-chemistry in-house, as reported earlier [113]. A stock solution of this peptide was prepared using distilled water, to yield a concentration of 1 mg/mL (200  $\mu$ M, pH = 7), and it was sonicated for 3 min. The solution was incubated for 10 min at room temperature (RT), then the pH level was adjusted (pH = 11), and it was further incubated for 2 h. After a 3-min-long sonication process, the  $A\beta_{1-42}$  solution was diluted in phosphate buffer (PBS, 20 mM) to a final peptide concentration of 50  $\mu$ M (26.67 mM phosphate, 1.2% NaCl, pH = 7.4). The solution was stored at 4 °C until further use on the same day.

The oligomeric state of the A $\beta$  peptide was verified by a transmission electron microscope (JEM-1400, JEOL USA Inc., Peabody, MA, USA) operating at 120 kV. Images were taken by an EM-15300SXV system, routinely at a magnification of 25,000 and 50,000, and were processed by the SightX Viewer Software (EM-15300SXV Image Edit Software, JEOL Ltd., Tokyo, Japan).

### 5.3. Surgery, Solutions, and Drug Administration

Mice were anesthetized by an IP injection of a mixture of ketamine (10.0 mg/0.1 kg) and xylazine (0.8 mg/0.1 kg). The animals were then placed into a stereotaxic apparatus (David Kopf Instruments, Tujunga, CA, USA; Stoelting Co., Wood Dale, IL, USA), a mid-line incision of the scalp was made, the skin and muscles were carefully retracted to expose the skull, and a hole was drilled above the target area. A single intracerebroventricular injection of either A $\beta$ <sub>1-42</sub> (50  $\mu$ M) or PBS (20 mM) was administered at the right side using a Hamilton syringe (32 G), injected at a rate of 0.5  $\mu$ L/min. The following coordinates were used (from Bregma point): AP: -0.3; ML: -1.0; DV: -2.5. All animals were treated with antibiotics and analgesics after the surgery.

To detect stem cells, the animals were injected IP with BrdU (50 mg kg<sup>-1</sup>; Sigma-Aldrich, Saint Louis, MO, USA) dissolved in physiological saline, 3 times, 24 h after the surgery as described previously by Li et al. [9].

PRE084 (1 mg kg<sup>-1</sup>, Sigma-Aldrich, Saint Louis, MO, USA) and DMT (1 mg kg<sup>-1</sup>, Lipomed AG, Arlesheim, Switzerland) were also administered IP on a daily basis between postsurgery days 7–12. Both substances were dissolved in PBS (sterile-filtered, 20 mM) complemented with 1% dimethyl sulfoxide (DMSO, Sigma-Aldrich, Saint Louis, MO, USA).

Six groups of animals (with 18 mice in the control group, whereas 11 mice per group in the other groups) were developed to represent a control for each of the A $\beta$ <sub>1-42</sub>-treated groups (i.e., those PBS-treated after the development of AD-like symptoms of impaired neurogenesis and neuroinflammation and those treated with DMT or PRE084 after the induction of neurogenic and neuroinflammatory changes). In the nomenclature of the groups, the first term refers the ICV administered solution (PBS or A $\beta$ <sub>1-42</sub>), while the second one indicates the IP injected agent with potential disease-modifying activity (PBS again as a control, or PRE084 or DMT). Based on this nomenclature, the six groups were the following:

ICV: PBS-IP: PBS (PBS-PBS, i.e., PBS-treated, non-diseased control; n = 18),

ICV: A $\beta$ <sub>1-42</sub>-IP: PBS (A $\beta$ <sub>1-42</sub>-PBS, i.e., A $\beta$ <sub>1-42</sub>-treated, PBS-treated control; n = 18),

ICV: PBS-IP: PRE084 (PBS-PRE084, i.e., PRE084-treated, non-diseased control; n = 11),

ICV: A $\beta$ <sub>1-42</sub>-IP: PRE084 (A $\beta$ <sub>1-42</sub>-PRE084, i.e., A $\beta$ <sub>1-42</sub>-treated, PRE084-treated group; n = 11),

ICV: PBS-IP: DMT (PBS-DMT, i.e., DMT-treated, non-diseased control; n = 11),

ICV: A $\beta$ <sub>1-42</sub>-IP: DMT (A $\beta$ <sub>1-42</sub>-DMT, i.e., A $\beta$ <sub>1-42</sub>-treated, DMT-treated group; n = 11).

### 5.4. Immunohistochemistry

Two weeks after the surgery, mice (n = 8-8 from the PRE084- and DMT-treated, and n = 15-15 from the control groups) were anesthetized with chloral hydrate (1 mg kg<sup>-1</sup>) and were perfused transcardially with PBS, followed by 4% paraformaldehyde (PFA, Sigma-Aldrich, St. Louis, MO, USA). All procedures after perfusion, including the post-fixation and the preparation of the slides, were executed the same way as described previously [114].

Immunohistochemical analysis was carried out on 20  $\mu$ M formalin fixed cryosections. All immunohistochemical procedures were performed according to Szogi et al. [114]. All chemicals used in the immunohistochemical procedures, except the antibodies (Ab), were purchased from Sigma-Aldrich (St. Louis, MO, USA). Briefly, for BrdU staining, the sections were incubated in 2 M HCl for 2 h at RT to denature DNA. For the evaluation of BrdU-stained and NeuN-positive cells, the sections were blocked in a mixture

of 8% normal goat serum, 0.3% bovine serum albumin (BSA), and 0.3% Triton X-100 in PBS for 1 h at RT. For DCX, Iba1 and GFAP labeling, the sections were blocked in a mixture of 0.1% BSA and 0.3% Triton X-100 in PBS for 1 h at RT. After this step, the slices were incubated at 4 °C overnight with primary antibodies added to the samples in the following dilutions: mouse anti-BrdU Ab (1:800; Santa Cruz Biotechnology, Dallas, TX, USA), goat anti-DCX Ab (1:4000; Santa Cruz Biotechnology, Dallas, TX, USA), mouse anti-NeuN Ab (1:500; Merck Millipore, Darmstadt, Germany), rabbit anti-Iba1 Ab (1:3600; Wako Chemicals GmbH, Neuss, Germany), and mouse anti-GFAP Ab (1:1500; Santa Cruz Biotechnology, Dallas, TX, USA). For BrdU, DCX, and NeuN stainings, the sections were treated with a polymer-based HRP-amplifying system (Super Sensitive™ One-Step Polymer-HRP Detection System, BioGenex, Fremont, CA, USA), according to the manufacturer's instructions. For Iba1 and GFAP labeling, the slices were incubated with the corresponding secondary antibodies: biotinylated goat anti-rabbit Ab (1:400; Jackson ImmunoResearch, West Grove, PA, USA), and biotinylated goat anti-mouse Ab (1:400; ThermoFisher Scientific, Waltham, MA, USA) for 60 min. Next, the sections were rinsed 3 times in PBS, and were incubated with avidin-biotin-complex (ABC Elite Kit; Vector Laboratories, Burlingame, CA, USA) for Iba1 in 1:1000 and for GFAP stainings in 1:1500, for 60 min at RT. The peroxidase immunolabeling was developed in 0.5 M Tris-HCl buffer (pH 7.7) with 3,3'-diaminobenzidine (10 mM) at RT in 30 min. The sections were mounted with dibutyl phthalate xylene onto the slides and were coverslipped.

#### 5.5. Quantification of the Immunohistochemical Data

Slides were scanned by a digital slide scanner (Mirax Midi, 3DHistech Ltd., Budapest, Hungary), equipped with a Panoramic Viewer 1.15.4, a CaseViewer 2.1 program and a QuantCenter, HistoQuant module (3DHistech Ltd., Budapest, Hungary). For quantifications, all sections derived from each animal were analyzed. In DG and HC, the regions of interest (ROI) were manually outlined. Antibody-positive cell types were counted and quantified from ROIs. The number of stem cells (BrdU+) and neuroblasts (DCX+) were assessed by the observers. The densities (%) of neurons (NeuN+), microglia (Iba1+), and astrocytes (GFAP+) were calculated by the quantification software. To assess cell densities, we divided the total number of counted cells per animal with the DG/HC area, and represented them as cells/mm<sup>2</sup> (BrdU+, DCX+) or % (NeuN+, Iba+, GFAP+).

#### 5.6. Western Blot Analysis

To determine the effects of A $\beta$ <sub>1-42</sub> and PRE084 or DMT on the expression of S1R, the receptor protein samples of 3 animals per group (n = 18) were identically prepared, separated, and transferred to nitrocellulose membranes. The membranes were washed and treated as described by Szogi et al. [54]. The levels of S1R (mouse S1R antibody, Santa Cruz, Dallas, TX, USA, 1:1000) were analyzed in each group. For the analysis, we used glyceraldehyde 3-phosphate dehydrogenase (GAPDH, rabbit GAPDH antibody, Cell Signaling, Danvers, MA, USA, 1:200,000) as the loading control.

#### 5.7. Statistical Analysis

The data obtained from the immunohistochemistry analyses were evaluated with a one-way ANOVA, followed by Fisher's LSD post hoc tests. The WB data did not follow normal distribution; thus, they were analyzed with Kruskal-Wallis nonparametric tests, followed by Mann-Whitney U tests for multiple comparisons. Data were analyzed with the SPSS software (IBM SPSS Statistics 24), and the results were expressed as mean  $\pm$  (SEM). Statistical significance was set at  $p \leq 0.05$ .

## 4. Conclusions

Adult neurogenesis is essential for CNS plasticity. In early AD, neurogenic impairment can be observed, accompanied by hyperreactive astrogliosis. During the treatment

of AD, neurogenesis should be promoted, while neuroinflammation should be suppressed. S1R plays a role in both processes. In our experiments, we established a model of early AD induced by A $\beta$ <sub>1-42</sub>, in which acute neuroinflammation, impaired neurogenesis and elevated S1R levels were detected. In this model, two S1R agonists were tested. DMT, binding moderately to S1R but with a high affinity to 5-HT receptors, negatively influenced neurogenesis in the A $\beta$ <sub>1-42</sub>-induced rodent model, probably explained by its acting on the latter receptor class. In contrast, the highly selective S1R agonist, PRE084 improved the proliferation and differentiation of hippocampal stem cells, manifesting in a quantitative increase in progenitor cells and immature neurons. Further experiments are required to investigate the main molecular pathways targeted by DMT, through which it affects neurogenesis and the survival of mature neurons. Moreover, DMT and PRE084 were found to significantly reduce A $\beta$ <sub>1-42</sub>-induced hyperreactive astrogliosis. However, none of these ligands had a remarkable effect on microglial activation. Therefore, further studies are needed to clarify the role of DMT and PRE084 in neuroinflammatory processes induced by A $\beta$ <sub>1-42</sub>, resembling the changes characteristic of AD.

**Supplementary Materials:** The following supporting information can be downloaded at: [www.mdpi.com/article/10.3390/ijms23052514/s1](http://www.mdpi.com/article/10.3390/ijms23052514/s1), Figure S1: Figure S1. Results for the Western Blot (WB) analyses and representative gel images.

**Author Contributions:** Conceptualization: L.F. and B.P.; methodology: V.V., E.B., T.S., and I.S.; statistical analysis: E.B.; investigation: V.V., E.B., and T.S.; preparation and structure analysis of A $\beta$ <sub>1-42</sub> peptide oligomers: Z.B. and T.S.; resources: L.F. and B.P.; data curation: T.S. and E.B.; writing/original draft preparation: V.V. and E.B.; writing/review/editing: L.F.; visualization: E.B.; supervision: L.F.; funding acquisition: L.F. and B.P. All authors have read and agreed to the published version of the manuscript.

**Funding:** This project was supported by the National Research, Development, and Innovation Office (GINOP-2.3.2-15-2016-00060) and by the Hungarian Brain Research Program I and II—Grant No. KTIA\_13\_NAP-A-III/7, and 2017-1.2.1-NKP-2017-00002. Support by the Ministry of Innovation and Technology of Hungary from the National Research, Development and Innovation Fund (TKP2021-EGA-32) is acknowledged.

**Institutional Review Board Statement:** The study was conducted according to the guidelines of the Declaration of Helsinki, and approved by the Institutional Review Board (or Ethics Committee) of University of Szeged (project license: XXVI./3644/2017).

**Informed Consent Statement:** Not applicable.

**Data Availability Statement:** Not applicable.

**Acknowledgments:** The technical assistance of Szilvia Dénes and Péter Sütő is greatly acknowledged. The authors thank Dora Bokor, for proofreading the manuscript.

**Conflicts of Interest:** The authors declare no conflicts of interest. The funders had no role in the design of the study, nor in the collection, analyses, or interpretation of data, nor in the writing of the manuscript, nor in the decision to publish the results.

## Abbreviations

5-HT	5-hydroxytryptamine
AD	Alzheimer's disease
APP	amyloid precursor protein
A $\beta$	amyloid- $\beta$
BrdU	5-Bromo-2'-Deoxyuridine
BSA	bovine serum albumin
CNS	central nervous system
DCX	doublecortin
DG	dentate gyrus
DMT	N,N-dimethyltryptamine
ER	endoplasmic reticulum
GAPDH	glyceraldehyde 3-phosphate dehydrogenase

GFAP	glial fibrillary acidic protein
HC	hippocampus
Iba1	ionized calcium-binding adapter molecule 1
ICV	intracerebroventricular
IP	intraperitoneal injection
MAM	mitochondria-associated ER membrane
NeuN	neuronal nuclei
NMDA	N-methyl-d-aspartate receptor
NSC	neuronal stem cell
PFA	paraformaldehyde
PRE084	2-(4-morpholinethyl)-1-phenylcyclohexanecarboxylate
SR	sigma receptor
S1R	sigma-1 receptor
SGZ	subgranular zone
UPR	unfolded protein response
WB	western blot analysis

## References

- Alzheimer, A.; Stelzmann, R.A.; Schnitzlein, H.N.; Murtagh, F.R. An English translation of Alzheimer's 1907 paper, "Über eine eigenartige Erkrankung der Hirnrinde". *Clin. Anat.* **1995**, *8*, 429–431.
- Karlawish, J. *2017 Alzheimer's Disease Facts and Figures*; Alzheimer's Association: Chicago, IL, USA, 2017; p. 88.
- Mu, Y.; Gage, F.H. Adult hippocampal neurogenesis and its role in Alzheimer's disease. *Mol. Neurodegener.* **2011**, *6*, 85.
- Winner, B.; Winkler, J. Adult neurogenesis in neurodegenerative diseases. *Cold Spring Harb. Perspect. Biol.* **2015**, *7*, a021287.
- Weintraub, S.; Wicklund, A.H.; Salmon, D.P. The neuropsychological profile of Alzheimer disease. *Cold Spring Harb. Perspect. Med.* **2012**, *2*, a006171.
- Penke, B.; Bogár, F.; Fülöp, L.  $\beta$ -Amyloid and the Pathomechanisms of Alzheimer's Disease: A Comprehensive View. *Molecules* **2017**, *22*, 1692.
- Ramírez, E.; Mendieta, L.; Flores, G.; Limón, I.D. Neurogenesis and morphological-neural alterations closely related to amyloid  $\beta$ -peptide (25-35)-induced memory impairment in male rats. *Neuropeptides* **2018**, *67*, 9–19.
- Zheng, M.; Liu, J.; Ruan, Z.; Tian, S.; Ma, Y.; Zhu, J.; Li, G. Intrahippocampal injection of A $\beta$ 1-42 inhibits neurogenesis and down-regulates IFN- $\gamma$  and NF- $\kappa$ B expression in hippocampus of adult mouse brain. *Amyloid* **2013**, *20*, 13–20.
- Li, L.; Xu, B.; Zhu, Y.; Chen, L.; Sokabe, M. DHEA prevents A $\beta$ 25-35-impaired survival of newborn neurons in the dentate gyrus through a modulation of PI3K-Akt-mTOR signaling. *Neuropharmacology* **2010**, *59*, 323–333.
- Russo, I.; Caracciolo, L.; Tweedie, D.; Choi, S.H.; Greig, N.H.; Barlati, S.; Bosetti, F. 3,6'-Dithiothalidomide, a new TNF- $\alpha$  synthesis inhibitor, attenuates the effect of A $\beta$ 1-42 intracerebroventricular injection on hippocampal neurogenesis and memory deficit. *J. Neurochem* **2012**, *122*, 1181–1192.
- Minter, M.R.; Taylor, J.M.; Crack, P.J. The contribution of neuroinflammation to amyloid toxicity in Alzheimer's disease. *J. Neurochem.* **2016**, *136*, 457–474.
- Sung, P.S.; Lin, P.Y.; Liu, C.H.; Su, H.C.; Tsai, K.J. Neuroinflammation and Neurogenesis in Alzheimer's Disease and Potential Therapeutic Approaches. *Int. J. Mol. Sci.* **2020**, *21*, 701.
- Fuster-Matanzo, A.; Llorens-Martín, M.; Hernández, F.; Avila, J. Role of neuroinflammation in adult neurogenesis and Alzheimer disease: Therapeutic approaches. *Mediat. Inflamm.* **2013**, *2013*, 260925.
- Fish, P.V.; Steadman, D.; Bayle, E.D.; Whiting, P. New approaches for the treatment of Alzheimer's disease. *Bioorg. Med. Chem. Lett.* **2019**, *29*, 125–133.
- Ma, W.H.; Chen, A.F.; Xie, X.Y.; Huang, Y.S. Sigma ligands as potent inhibitors of A $\beta$  and A $\beta$ O<sub>s</sub> in neurons and promising therapeutic agents of Alzheimer's disease. *Neuropharmacology* **2020**, *190*, 108342.
- Penke, B.; Fulop, L.; Szucs, M.; Frecska, E. The Role of Sigma-1 Receptor, an Intracellular Chaperone in Neurodegenerative Diseases. *Curr. Neuropharmacol.* **2018**, *16*, 97–116.
- Bowen, W.D.; Hellewell, S.B.; McGarry, K.A. Evidence for a multi-site model of the rat brain sigma receptor. *Eur. J. Pharm.* **1989**, *163*, 309–318.
- Hellewell, S.B.; Bowen, W.D. A sigma-like binding site in rat pheochromocytoma (PC12) cells: Decreased affinity for (+)-benzomorphans and lower molecular weight suggest a different sigma receptor form from that of guinea pig brain. *Brain Res.* **1990**, *527*, 244–253.
- Hellewell, S.B.; Bruce, A.; Feinstein, G.; Orringer, J.; Williams, W.; Bowen, W.D. Rat liver and kidney contain high densities of sigma 1 and sigma 2 receptors: Characterization by ligand binding and photoaffinity labeling. *Eur. J. Pharm.* **1994**, *268*, 9–18.
- Schmidt, H.R.; Zheng, S.; Gurpinar, E.; Koehl, A.; Manglik, A.; Kruse, A.C. Crystal structure of the human  $\sigma$ 1 receptor. *Nature* **2016**, *532*, 527–530.
- Yang, K.; Wang, C.; Sun, T. The Roles of Intracellular Chaperone Proteins, Sigma Receptors, in Parkinson's Disease (PD) and Major Depressive Disorder (MDD). *Front. Pharm.* **2019**, *10*, 528.

22. Hayashi, T.; Su, T.P. An update on the development of drugs for neuropsychiatric disorders: Focusing on the sigma 1 receptor ligand. *Expert Opin. Ther. Targets* **2008**, *12*, 45–58.
23. Tesei, A.; Cortesi, M.; Zamagni, A.; Arienti, C.; Pignatta, S.; Zanoni, M.; Paolillo, M.; Curti, D.; Rui, M.; Rossi, D.; et al. Sigma Receptors as Endoplasmic Reticulum Stress “Gatekeepers” and their Modulators as Emerging New Weapons in the Fight Against Cancer. *Front. Pharm.* **2018**, *9*, 711.
24. Jin, J.L.; Fang, M.; Zhao, Y.X.; Liu, X.Y. Roles of sigma-1 receptors in Alzheimer’s disease. *Int. J. Clin. Exp. Med.* **2015**, *8*, 4808–4820.
25. Maurice, T.; Meunier, J.; Feng, B.; Ieni, J.; Monaghan, D.T. Interaction with sigma(1) protein, but not N-methyl-D-aspartate receptor, is involved in the pharmacological activity of donepezil. *J. Pharm. Exp. Ther.* **2006**, *317*, 606–614.
26. Maurice, T.; Privat, A. SA4503, a novel cognitive enhancer with sigma1 receptor agonist properties, facilitates NMDA receptor-dependent learning in mice. *Eur J. Pharm.* **1997**, *328*, 9–18.
27. Meunier, J.; Ieni, J.; Maurice, T. The anti-amnesic and neuroprotective effects of donepezil against amyloid beta25-35 peptide-induced toxicity in mice involve an interaction with the sigma1 receptor. *Br. J. Pharm.* **2006**, *149*, 998–1012.
28. Su, T.P.; Su, T.C.; Nakamura, Y.; Tsai, S.Y. The Sigma-1 Receptor as a Pluripotent Modulator in Living Systems. *Trends Pharm. Sci* **2016**, *37*, 262–278.
29. Hayashi, T.; Su, T.P. Sigma-1 receptor chaperones at the ER-mitochondrion interface regulate Ca(2+) signaling and cell survival. *Cell* **2007**, *131*, 596–610.
30. Maurice, T.; Gogvadze, N. Role of  $\sigma$ . *Adv. Exp. Med. Biol.* **2017**, *964*, 213–233.
31. Maurice, T.; Gogvadze, N. Sigma-1 ( $\sigma$  1) Receptor in Memory and Neurodegenerative Diseases. *Handb. Exp. Pharm.* **2017**, *244*, 81–108.
32. Ruscher, K.; Wieloch, T. The involvement of the sigma-1 receptor in neurodegeneration and neurorestoration. *J. Pharm. Sci* **2015**, *127*, 30–35.
33. Tsai, S.A.; Su, T.P. Sigma-1 Receptors Fine-Tune the Neuronal Networks. *Adv. Exp. Med. Biol.* **2017**, *964*, 79–83.
34. Krogmann, A.; Peters, L.; von Hardenberg, L.; Bödeker, K.; Nöhles, V.B.; Correll, C.U. Keeping up with the therapeutic advances in schizophrenia: A review of novel and emerging pharmacological entities. *CNS Spectr.* **2019**, *24* (Suppl. S1), 38–69.
35. Maurice, T.; Su, T.P.; Privat, A. Sigma1 (sigma 1) receptor agonists and neurosteroids attenuate B25-35-amyloid peptide-induced amnesia in mice through a common mechanism. *Neuroscience* **1998**, *83*, 413–428.
36. Urani, A.; Romieu, P.; Portales-Casamar, E.; Roman, F.J.; Maurice, T. The antidepressant-like effect induced by the sigma(1) (sigma(1)) receptor agonist igmesine involves modulation of intracellular calcium mobilization. *Psychopharmacology* **2002**, *163*, 26–35.
37. Van Waarde, A.; Ramakrishnan, N.K.; Rybczynska, A.A.; Elsinga, P.H.; Ishiwata, K.; Nijholt, I.M.; Luiten, P.G.; Dierckx, R.A. The cholinergic system, sigma-1 receptors and cognition. *Behav. Brain Res.* **2011**, *221*, 543–554.
38. Nichols, D.E. N,N-dimethyltryptamine and the pineal gland: Separating fact from myth. *J. Psychopharmacol.* **2018**, *32*, 30–36.
39. Fontanilla, D.; Johannessen, M.; Hajipour, A.R.; Cozzi, N.V.; Jackson, M.B.; Ruoho, A.E. The hallucinogen N,N-dimethyltryptamine (DMT) is an endogenous sigma-1 receptor regulator. *Science* **2009**, *323*, 934–937.
40. Barker, S.A. N, N-Dimethyltryptamine (DMT), an Endogenous Hallucinogen: Past, Present, and Future Research to Determine Its Role and Function. *Front. Neurosci.* **2018**, *12*, 536.
41. Szabo, A.; Kovacs, A.; Riba, J.; Djurovic, S.; Rajnavolgyi, E.; Frecska, E. The Endogenous Hallucinogen and Trace Amine N,N-Dimethyltryptamine (DMT) Displays Potent Protective Effects against Hypoxia via Sigma-1 Receptor Activation in Human Primary iPSC-Derived Cortical Neurons and Microglia-Like Immune Cells. *Front. Neurosci* **2016**, *10*, 423.
42. Szabo, A.; Kovacs, A.; Frecska, E.; Rajnavolgyi, E. Psychedelic N,N-dimethyltryptamine and 5-methoxy-N,N-dimethyltryptamine modulate innate and adaptive inflammatory responses through the sigma-1 receptor of human monocyte-derived dendritic cells. *PLoS ONE* **2014**, *9*, e106533.
43. Szabo, A.; Frecska, E. Dimethyltryptamine (DMT): A biochemical Swiss Army knife in neuroinflammation and neuroprotection? *Neural Regen Res.* **2016**, *11*, 396–397.
44. Ly, C.; Greb, A.C.; Cameron, L.P.; Wong, J.M.; Barragan, E.V.; Wilson, P.C.; Burbach, K.F.; Soltanzadeh Zarandi, S.; Sood, A.; Paddy, M.R. et al. Psychedelics Promote Structural and Functional Neural Plasticity. *Cell Rep.* **2018**, *23*, 3170–3182.
45. Lima da Cruz, R.V.; Moulin, T.C.; Petiz, L.L.; Leão, R.N. Corrigendum: A Single Dose of 5-MeO-DMT Stimulates Cell Proliferation, Neuronal Survivability, Morphological and Functional Changes in Adult Mice Ventral Dentate Gyrus. *Front. Mol. Neurosci.* **2019**, *12*, 79.
46. Lima da Cruz, R.V.; Moulin, T.C.; Petiz, L.L.; Leão, R.N. A Single Dose of 5-MeO-DMT Stimulates Cell Proliferation, Neuronal Survivability, Morphological and Functional Changes in Adult Mice Ventral Dentate Gyrus. *Front. Mol. Neurosci.* **2018**, *11*, 312.
47. Cameron, L.P.; Benson, C.J.; DeFelice, B.C.; Fiehn, O.; Olson, D.E. Chronic, Intermittent Microdoses of the Psychedelic. *ACS Chem Neurosci* **2019**, *10*, 3261–3270.
48. Dakic, V.; Minardi Nascimento, J.; Costa Sartore, R.; Maciel, R.M.; de Araujo, D.B.; Ribeiro, S.; Martins-de-Souza, D.; Rehen, S.K. Short term changes in the proteome of human cerebral organoids induced by 5-MeO-DMT. *Sci Rep.* **2017**, *7*, 12863.
49. Morales-Garcia, J.A.; Calleja-Conde, J.; Lopez-Moreno, J.A.; Alonso-Gil, S.; Sanz-SanCristobal, M.; Riba, J.; Perez-Castillo, A. N,N-dimethyltryptamine compound found in the hallucinogenic tea ayahuasca, regulates adult neurogenesis in vitro and in vivo. *Transl Psychiatry* **2020**, *10*, 331.
50. Carbonaro, T.M.; Gatch, M.B. Neuropharmacology of N,N-dimethyltryptamine. *Brain Res. Bull.* **2016**, *126* (Pt 1), 74–88.



51. Simão, A.Y.; Gonçalves, J.; Gradillas, A.; García, A.; Restolho, J.; Fernández, N.; Rodilla, J.M.; Barroso, M.; Duarte, A.P.; Cristóvão, A.C.; et al. Evaluation of the Cytotoxicity of Ayahuasca Beverages. *Molecules* **2020**, *25*, 5594.
52. Frecska, E.; Szabo, A.; Winkelman, M.J.; Luna, L.E.; McKenna, D.J. A possibly sigma-1 receptor mediated role of dimethyltryptamine in tissue protection, regeneration, and immunity. *J. Neural Transm.* **2013**, *120*, 1295–1303.
53. Keiser, M.J.; Setola, V.; Irwin, J.J.; Laggner, C.; Abbas, A.L.; Hufeisen, S.J.; Jensen, N.H.; Kuijter, M.B.; Matos, R.C.; Tran, T.B. et al. Predicting new molecular targets for known drugs. *Nature* **2009**, *462*, 175–181.
54. Inserra, A. Hypothesis: The Psychedelic Ayahuasca Heals Traumatic Memories via a Sigma 1 Receptor-Mediated Epigenetic-Mnemonic Process. *Front. Pharm.* **2018**, *9*, 330.
55. Rickli, A.; Moning, O.D.; Hoener, M.C.; Liechti, M.E. Receptor interaction profiles of novel psychoactive tryptamines compared with classic hallucinogens. *Eur. Neuropsychopharmacol.* **2016**, *26*, 1327–1337.
56. Cameron, L.P.; Olson, D.E. Dark Classics in Chemical Neuroscience: N, N-Dimethyltryptamine (DMT). *ACS Chem. Neurosci.* **2018**, *9*, 2344–2357.
57. Szabó, Í.; Varga, V.; Dvoráckó, S.; Farkas, A.E.; Körmöczy, T.; Berkecz, R.; Kecskés, S.; Menyhárt, Á.; Frank, R.; Hantosi, D.; Cozzi, N.V.; Frecska, E.; et al. N,N-Dimethyltryptamine attenuates spreading depolarization and restrains neurodegeneration by sigma-1 receptor activation in the ischemic rat brain. *Neuropharmacology* **2021**, *192*, 108612.
58. Christ, M.G.; Huesmann, H.; Nagel, H.; Kern, A.; Behl, C. Sigma-1 Receptor Activation Induces Autophagy and Increases Proteostasis Capacity In Vitro and In Vivo. *Cells* **2019**, *8*, 211.
59. Entrena, J.M.; Sanchez-Fernandez, C.; Nieto, F.R.; Gonzalez-Cano, R.; Yeste, S.; Cobos, E.J.; Baeyens, J.M. Sigma-1 Receptor Agonism Promotes Mechanical Allodynia After Priming the Nociceptive System with Capsaicin. *Sci Rep.* **2016**, *6*, 37835.
60. Francardo, V.; Bez, F.; Wieloch, T.; Nissbrandt, H.; Ruscher, K.; Cenci, M.A. Pharmacological stimulation of sigma-1 receptors has neurorestorative effects in experimental parkinsonism. *Brain* **2014**, *137* (Pt 7), 1998–2014.
61. Penas, C.; Pascual-Font, A.; Mancuso, R.; Forés, J.; Casas, C.; Navarro, X. Sigma receptor agonist 2-(4-morpholinethyl)1 phenylcyclohexanecarboxylate (Pre084) increases GDNF and BiP expression and promotes neuroprotection after root avulsion injury. *J. Neurotrauma* **2011**, *28*, 831–840.
62. Peviani, M.; Salvaneschi, E.; Bontempi, L.; Petese, A.; Manzo, A.; Rossi, D.; Salmona, M.; Collina, S.; Bigini, P.; Curti, D. Neuroprotective effects of the Sigma-1 receptor (S1R) agonist PRE-084, in a mouse model of motor neuron disease not linked to SOD1 mutation. *Neurobiol. Dis.* **2014**, *62*, 218–232.
63. Xu, Q.; Ji, X.F.; Chi, T.Y.; Liu, P.; Jin, G.; Gu, S.L.; Zou, L.B. Sigma 1 receptor activation regulates brain-derived neurotrophic factor through NR2A-CaMKIV-TORC1 pathway to rescue the impairment of learning and memory induced by brain ischemia/reperfusion. *Psychopharmacology* **2015**, *232*, 1779–1791.
64. Koshibu, K. Nootropics with potential to (re)build neuroarchitecture. *Neural Regen. Res.* **2016**, *11*, 79–80.
65. Brimson, J.M.; Safrany, S.T.; Qassam, H.; Tencomnao, T. Dipentylammonium Binds to the Sigma-1 Receptor and Protects Against Glutamate Toxicity, Attenuates Dopamine Toxicity and Potentiates Neurite Outgrowth in Various Cultured Cell Lines. *Neurotox Res.* **2018**, *34*, 263–272.
66. Maurice, T. Beneficial effect of the sigma(1) receptor agonist PRE-084 against the spatial learning deficits in aged rats. *Eur. J. Pharm.* **2001**, *431*, 223–227.
67. Griesmaier, E.; Posod, A.; Gross, M.; Neubauer, V.; Wegleiter, K.; Hermann, M.; Urbanek, M.; Keller, M.; Kiechl-Kohlendorfer, U. Neuroprotective effects of the sigma-1 receptor ligand PRE-084 against excitotoxic perinatal brain injury in newborn mice. *Exp. Neurol.* **2012**, *237*, 388–395.
68. Sánchez-Blázquez, P.; Pozo-Rodríguez, A.; Merlos, M.; Garzón, J. The Sigma-1 Receptor Antagonist, S1RA, Reduces Stroke Damage, Ameliorates Post-Stroke Neurological Deficits and Suppresses the Overexpression of MMP-9. *Mol. Neurobiol.* **2018**, *55*, 4940–4951.
69. Altman, J.; Das, G.D. Autoradiographic and histological evidence of postnatal hippocampal neurogenesis in rats. *J. Comp. Neurol.* **1965**, *124*, 319–335.
70. Altman, J. Autoradiographic and histological studies of postnatal neurogenesis. IV. Cell proliferation and migration in the anterior forebrain, with special reference to persisting neurogenesis in the olfactory bulb. *J. Comp. Neurol.* **1969**, *137*, 433–457.
71. Ming, G.L.; Song, H. Adult neurogenesis in the mammalian central nervous system. *Annu Rev. Neurosci.* **2005**, *28*, 223–250.
72. Choi, S.H.; Tanzi, R.E. Is Alzheimer's Disease a Neurogenesis Disorder? *Cell Stem Cell* **2019**, *25*, 7–8.
73. Moreno-Jiménez, E.P.; Flor-García, M.; Terreros-Roncal, J.; Rábano, A.; Cafini, F.; Pallas-Bazarra, N.; Ávila, J.; Llorens-Martín, M. Adult hippocampal neurogenesis is abundant in neurologically healthy subjects and drops sharply in patients with Alzheimer's disease. *Nat. Med.* **2019**, *25*, 554–560.
74. Tobin, M.K.; Musaraca, K.; Disouky, A.; Shetti, A.; Bheri, A.; Honer, W.G.; Kim, N.; Dawe, R.J.; Bennett, D.A.; Arfanakis, K.; et al. Human Hippocampal Neurogenesis Persists in Aged Adults and Alzheimer's Disease Patients. *Cell Stem Cell* **2019**, *24*, 974–982.e3.
75. Verret, L.; Jankowsky, J.L.; Xu, G.M.; Borchelt, D.R.; Rampon, C. Alzheimer's-type amyloidosis in transgenic mice impairs survival of newborn neurons derived from adult hippocampal neurogenesis. *J. Neurosci.* **2007**, *27*, 6771–6780.
76. Demars, M.; Hu, Y.S.; Gadadhar, A.; Lazarov, O. Impaired neurogenesis is an early event in the etiology of familial Alzheimer's disease in transgenic mice. *J. Neurosci. Res.* **2010**, *88*, 2103–2117.
77. Hamilton, A.; Holscher, C. The effect of ageing on neurogenesis and oxidative stress in the APP(swe)/PS1(deltaE9) mouse model of Alzheimer's disease. *Brain Res.* **2012**, *1449*, 83–93.

78. Unger, M.S.; Marschallinger, J.; Kaindl, J.; Höfling, C.; Rossner, S.; Heneka, M.T.; Van der Linden, A.; Aigner, L. Early Changes in Hippocampal Neurogenesis in Transgenic Mouse Models for Alzheimer's Disease. *Mol. Neurobiol.* **2016**, *53*, 5796–5806.
79. Dos Santos, R.G.; Valle, M.; Bouso, J.C.; Nomdedéu, J.F.; Rodríguez-Espinosa, J.; McIlhenny, E.H.; Barker, S.A.; Barbanj, M.J.; Riba, J. Autonomic, neuroendocrine, and immunological effects of ayahuasca: A comparative study with d-amphetamine. *J. Clin. Psychopharmacol.* **2011**, *31*, 717–726.
80. Eriksson, P.S.; Perfilieva, E.; Björk-Eriksson, T.; Alborn, A.M.; Nordborg, C.; Peterson, D.A.; Gage, F.H. Neurogenesis in the adult human hippocampus. *Nat. Med.* **1998**, *4*, 1313–1317.
81. Chen, G.F.; Xu, T.H.; Yan, Y.; Zhou, Y.R.; Jiang, Y.; Melcher, K.; Xu, H.E. Amyloid beta: Structure, biology and structure-based therapeutic development. *Acta Pharm. Sin.* **2017**, *38*, 1205–1235.
82. Hu, Y.S.; Xu, P.; Pigino, G.; Brady, S.T.; Larson, J.; Lazarov, O. Complex environment experience rescues impaired neurogenesis, enhances synaptic plasticity, and attenuates neuropathology in familial Alzheimer's disease-linked APP<sup>swe</sup>/PS1<sup>DeltaE9</sup> mice. *FASEB J.* **2010**, *24*, 1667–1681.
83. Jin, K.; Peel, A.L.; Mao, X.O.; Xie, L.; Cottrell, B.A.; Henshall, D.C.; Greenberg, D.A. Increased hippocampal neurogenesis in Alzheimer's disease. *Proc. Natl. Acad. Sci. USA* **2004**, *101*, 343–347.
84. Jin, K.; Galvan, V.; Xie, L.; Mao, X.O.; Gorostiza, O.F.; Bredesen, D.E.; Greenberg, D.A. Enhanced neurogenesis in Alzheimer's disease transgenic (PDGF-APP<sup>Sw</sup>,Ind) mice. *Proc. Natl. Acad. Sci. USA* **2004**, *101*, 13363–13367.
85. López-Toledano, M.A.; Shelanski, M.L. Increased neurogenesis in young transgenic mice overexpressing human APP(Sw, Ind). *J. Alzheimers Dis.* **2007**, *12*, 229–240.
86. Itokazu, Y.; Yu, R.K. Amyloid  $\beta$ -peptide 1-42 modulates the proliferation of mouse neural stem cells: Upregulation of fucosyltransferase IX and notch signaling. *Mol. Neurobiol.* **2014**, *50*, 186–196.
87. Chen, Y.; Dong, C. Abeta40 promotes neuronal cell fate in neural progenitor cells. *Cell Death Differ.* **2009**, *16*, 386–394.
88. Fonseca, M.B.; Solá, S.; Xavier, J.M.; Dionísio, P.A.; Rodrigues, C.M. Amyloid  $\beta$  peptides promote autophagy-dependent differentiation of mouse neural stem cells: A $\beta$ -mediated neural differentiation. *Mol. Neurobiol.* **2013**, *48*, 829–840.
89. Bernabeu-Zornoza, A.; Coronel, R.; Palmer, C.; Monteagudo, M.; Zambrano, A.; Liste, I. Physiological and pathological effects of amyloid- $\beta$  species in neural stem cell biology. *Neural Regen. Res.* **2019**, *14*, 2035–2042.
90. López-Toledano, M.A.; Shelanski, M.L. Neurogenic effect of beta-amyloid peptide in the development of neural stem cells. *J. Neurosci.* **2004**, *24*, 5439–5444.
91. Heo, C.; Chang, K.A.; Choi, H.S.; Kim, H.S.; Kim, S.; Liew, H.; Kim, J.A.; Yu, E.; Ma, J.; Suh, Y.H. Effects of the monomeric, oligomeric, and fibrillar Abeta42 peptides on the proliferation and differentiation of adult neural stem cells from subventricular zone. *J. Neurochem.* **2007**, *102*, 493–500.
92. Perry, E.K.; Johnson, M.; Ekonomou, A.; Perry, R.H.; Ballard, C.; Attems, J. Neurogenic abnormalities in Alzheimer's disease differ between stages of neurogenesis and are partly related to cholinergic pathology. *Neurobiol. Dis.* **2012**, *47*, 155–162.
93. Calvo-Flores Guzmán, B.; Elizabeth Chaffey, T.; Hansika Palpagama, T.; Waters, S.; Boix, J.; Tate, W.P.; Peppercorn, K.; Dragunow, M.; Waldvogel, H.J.; Faull, R.L.M. et al. The Interplay Between Beta-Amyloid 1-42 (A $\beta$ <sub>1-42</sub>)-Induced Hippocampal Inflammatory Response, p-tau, Vascular Pathology, and Their Synergistic Contributions to Neuronal Death and Behavioral Deficits. *Front. Mol. Neurosci.* **2020**, *13*, 522073.
94. Mudò, G.; Frinchi, M.; Nuzzo, D.; Scaduto, P.; Plescia, F.; Massenti, M.F.; Di Carlo, M.; Cannizzaro, C.; Cassata, G.; Cicero, L.; et al. Anti-inflammatory and cognitive effects of interferon- $\beta$ 1a (IFN $\beta$ 1a) in a rat model of Alzheimer's disease. *J. Neuroinflammation* **2019**, *16*, 44.
95. Dhawan, G.; Floden, A.M.; Combs, C.K. Amyloid- $\beta$  oligomers stimulate microglia through a tyrosine kinase dependent mechanism. *Neurobiol. Aging* **2012**, *33*, 2247–2261.
96. Hansen, D.V.; Hanson, J.E.; Sheng, M. Microglia in Alzheimer's disease. *J. Cell Biol.* **2018**, *217*, 459–472.
97. Edler, M.K.; Mhatre-Winters, I.; Richardson, J.R. Microglia in Aging and Alzheimer's Disease: A Comparative Species Review. *Cells* **2021**, *10*, 1138.
98. Heneka, M.T.; Kummer, M.P.; Latz, E. Innate immune activation in neurodegenerative disease. *Nat. Rev. Immunol.* **2014**, *14*, 463–477.
99. Frost, G.R.; Li, Y.M. The role of astrocytes in amyloid production and Alzheimer's disease. *Open Biol.* **2017**, *7*, 463–477.
100. Leng, F.; Edison, P. Neuroinflammation and microglial activation in Alzheimer disease: Where do we go from here? *Nat. Rev. Neurol.* **2021**, *17*, 157–172.
101. González-Reyes, R.E.; Nava-Mesa, M.O.; Vargas-Sánchez, K.; Ariza-Salamanca, D.; Mora-Muñoz, L. Involvement of Astrocytes in Alzheimer's Disease from a Neuroinflammatory and Oxidative Stress Perspective. *Front. Mol. Neurosci.* **2017**, *10*, 427.
102. Yin, J.; Sha, S.; Chen, T.; Wang, C.; Hong, J.; Jie, P.; Zhou, R.; Li, L.; Sokabe, M.; Chen, L. Sigma-1 ( $\sigma$ <sub>1</sub>) receptor deficiency reduces  $\beta$ -amyloid(25-35)-induced hippocampal neuronal cell death and cognitive deficits through suppressing phosphorylation of the NMDA receptor NR2B. *Neuropharmacology* **2015**, *89*, 215–224.
103. Ryskamp, D.A.; Korban, S.; Zhemkov, V.; Kraskovskaya, N.; Bezprozvanny, I. Neuronal Sigma-1 Receptors: Signaling Functions and Protective Roles in Neurodegenerative Diseases. *Front. Neurosci.* **2019**, *13*, 862.
104. Mishina, M.; Ohyama, M.; Ishii, K.; Kitamura, S.; Kimura, Y.; Oda, K.; Kawamura, K.; Sasaki, T.; Kobayashi, S.; Katayama, Y.; et al. Low density of sigma1 receptors in early Alzheimer's disease. *Ann. Nucl. Med.* **2008**, *22*, 151–156.
105. Jansen, K.L.; Faull, R.L.; Storey, P.; Leslie, R.A. Loss of sigma binding sites in the CA1 area of the anterior hippocampus in Alzheimer's disease correlates with CA1 pyramidal cell loss. *Brain Res.* **1993**, *623*, 299–302.

106. Meunier, J.; Hayashi, T. Sigma-1 receptors regulate Bcl-2 expression by reactive oxygen species-dependent transcriptional regulation of nuclear factor kappaB. *J. Pharm. Exp. Ther.* **2010**, *332*, 388–397.
107. Maurice, T. Bi-phasic dose response in the preclinical and clinical developments of sigma-1 receptor ligands for the treatment of neurodegenerative disorders. *Expert Opin. Drug Discov.* **2021**, *16*, 373–389.
108. Mori, T.; Hayashi, T.; Hayashi, E.; Su, T.P. Sigma-1 receptor chaperone at the ER-mitochondrion interface mediates the mitochondrion-ER-nucleus signaling for cellular survival. *PLoS ONE* **2013**, *8*, e76941.
109. Catlow, B.J.; Song, S.; Paredes, D.A.; Kirstein, C.L.; Sanchez-Ramos, J. Effects of psilocybin on hippocampal neurogenesis and extinction of trace fear conditioning. *Exp. Brain Res.* **2013**, *228*, 481–491.
110. Szabo, A. Psychedelics and Immunomodulation: Novel Approaches and Therapeutic Opportunities. *Front. Immunol.* **2015**, *6*, 358.
111. Wang, J.; Xiao, H.; Barwick, S.R.; Smith, S.B. Comparison of Sigma 1 Receptor Ligands SA4503 and PRE084 to (+)-Pentazocine in the rd10 Mouse Model of RP. *Invest. Ophthalmol Vis. Sci.* **2020**, *61*, 3.
112. Jia, J.; Cheng, J.; Wang, C.; Zhen, X. Sigma-1 Receptor-Modulated Neuroinflammation in Neurological Diseases. *Front. Cell Neurosci.* **2018**, *12*, 314.
113. Bozso, Z.; Penke, B.; Simon, D.; Laczkó, I.; Juhász, G.; Szegedi, V.; Kasza, A.; Soós, K.; Hetényi, A.; Wéber, E.; et al. Controlled in situ preparation of A beta(1-42) oligomers from the isopeptide “iso-A beta(1-42)”, physicochemical and biological characterization. *Peptides* **2010**, *31*, 248–256.
114. Szögi, T.; Schuster, I.; Borbély, E.; Gyebrovszki, A.; Bozsó, Z.; Gera, J.; Rajkó, R.; Sántha, M.; Penke, B.; Fülöp, L. Effects of the Pentapeptide P33 on Memory and Synaptic Plasticity in APP/PS1 Transgenic Mice: A Novel Mechanism Presenting the Protein Fe65 as a Target. *Int. J. Mol. Sci.* **2019**, *20*, 3050.